UAB
Universitat Autònoma de Barcelona

Dissection of the innate immune response in porcine epidemic diarrhea virus (PEDV) infected pigs

Carlos López Figueroa

Dissection of the innate immune response in porcine epidemic diarrhea virus (PEDV) infected pigs

Carlos López Figueroa

PhD Thesis

Bellaterra (Barcelona), Spain, 2025

Dissection of the innate immune response in porcine epidemic diarrhea virus (PEDV) infected pigs

Doctoral thesis presented by **Carlos López Figueroa** to obtain the Doctoral degree under the program of Animal Medicine and Health at the Faculty of Veterinary medicine from the *Universitat Autònoma de Barcelona*, under the supervision of **Joaquim Segalés** and **Júlia Vergara-Alert.**

Bellaterra, 2025

Joaquim Segalés, catedràtic del Departament de Sanitat i d'Anatomia Animals de la Facultat de Veterinària de la Universitat Autònoma de Barcelona i investigador adscrit al Centre de Recerca en Sanitat Animal de l'Institut de Recerca i Tecnologia Agroalimentàries (IRTA-CReSA), i Júlia Vergara-Alert, investigadora de l'IRTA-CReSA,

Certifiquem:

Que la memòria titulada "**Dissection of the innate immune response in porcine epidemic diarrhea virus (PEDV) infected pigs**", presentada per Carlos López Figueroa per a l'obtenció del grau de Doctor en Medicina i Sanitat Animals, s'ha realitzat sota la nostra direcció i tutoria, i n'autoritzem la seva presentació a fi de ser avaluada per la comissió corresponent.

I perquè així consti i tingui els efectes que corresponguin, signen el present certificat a Bellaterra (Barcelona), XXX de XXXX de 2025.

Dr. Joaquim Segalés	Dr. Júlia Vergara-Alert	Carlos López Figueroa
Director	Director	Doctorand

This work has been financially supported by the PORCOPROTECT project (PID2019-110260RB-I00) of the Ministerio de Ciencia, Innovación y Universidades from the Spanish government.

Carlos López Figueroa has a predoctoral fellowship funded by the crowdfunding initiative “yomecorono.com” (https://www.yomecorono.com/).

“Las personas no deciden su futuro,

deciden sus hábitos

y son sus hábitos los

que deciden su futuro”

F.M Alexander

Table of Contents

List of abbreviations

3CLpro	3C-like proteinase
6-HB	6 helix bundle
aa	Amino acid
ADAR	Adenosine deaminases acting on RNA
AEN	Apoptosis-enhancing nuclease
AIM2	Absent in melanoma 2
AkT	Protein kinase B
ALI	Air-liquid interface
ALR	AIM2-like receptors
AMPK	Adenosine monophosphate-activated protein kinase
AP	Adaptor proteins
AP1	Activator protein 1
APN	Aminopeptidase N
ATF6	Activating transcription factor 6
ATG	Autophagy-related genes
BAL	Bronchoalveolar lavage
BCL2	B-cell lymphoma 2
BECN1	Beclin 1
BSA	Bovine serum albumin
BST2	Bone marrow stromal cell antigen 2
BtCoV	Bat CoV
CARDIF	Caspase activation recruitment domain adaptor inducing IFN-B
CASP	Caspase
CARDs	CASP-recruitment domains
CBP	CREB-binding protein
CCL	CC chemokine ligand
CCN1	Cell communication network factor 1
CDCD	Cesarian-derived, colostrum-derived
cDNA	Complementary DNA
CECoV	Canine enteric CoV
cGAS	Cyclic GMP-AMP synthase
CLN	Claudin
CMs	Convoluted membranes
C-NEG	Negative control
COE	Core neutralizing epitope
COP1	Constitutive photomorphogenesis protein 1
CoVs	Coronaviruses
CP	Cytoplasmic domain
CPE	Cytopathic effect
CREB	cAMP response element-binding protein
CSF	Colony stimulating factor
CTD	C-terminal domain
CTL	Cytotoxic T Lymphocytes
CXCL	C-X-C motif chemokine ligand
CyP40	Cyclophilin 40
DAB	Diaminobenzidine

DCs	Dendritic cells
DC-SIGN	DC-specific ICAM-3-grabbing non-integrin
DDX24	DEAD-box RNA helicase 24
DEGs	Differentially expressed genes
DMVs	Double-membrane vesicles
DNA	Deoxyribonucleic acid
dpi	Days post inoculation
DR	Death receptor
dsRNA	Double sense RNA
DUB	Deubiquitinase
E	Envelope protein
EGFR	Epidermal growth factor receptor
EGR1	Growth response gene 1
eIF3L	Eukaryotic translation initiation factor 3 subunit L
eIF4F	Eukaryotic translation initiation factor 4F
ELS	Endolysosomal compartment
EndoU	Endoribonuclease
ER	Endoplasmic reticulum
ERB	ER bodies
ERGIC	ER-Golgi intermediate compartments
ERK	Extracellular signal-regulated kinase
ExoN	Exoribunuclease
FBXW7	F-Box and WD repeat domain-containing 7
Fc	Fold change
FCoV	Feline CoV
FIPV	Feline infectious peritonitis virus
Fos	Proto-oncogene c-Fos
FP	Fusion peptide
FUBP3	Far upstream element-binding protein 3
G3BP	Ras GTPase-activating protein-binding protein 1
GRP78	ER chaperone glucose-regulated protein 78
GSDMD	Gasdermin D
H&E	Hematoxylin & eosin
H2BE	Histone cluster 2
HCoV-NL63	Human CoV NL63
HDACs	Histone deacetylases
HEL	Helicase
HERC5	HECT and RLD domain containing E3 ubiquitin protein ligase 5
hnRNPA1	Heterogeneous nuclear ribonucleoprotein A1
HPF	High-power field
HR	Heptad repeat regions
HS	Heparan sulfate
HSP	Heat shock protein
HSPA	HSP family A
IBV	Infectious bronchitis virus
IECs	Intestinal epithelial cell
IF	Immunofluoerescence
IFIT	IFN-induced protein with tetratricopeptide
IFITM	IFN-induced transmembrane
IFN	Interferon

IFNAR	IFN α/β receptor
IFNLR1	IFN lambda receptor 1
IKKs	IkB kinase
IL	Interleukin
IL-1RA	IL 1 receptor antagonist
INDEL	Insertion and deletion
IPEC	Small intestine porcine epithelial cell
IPS-1	IFN-β promoter stimulator-1
IRAK	IL-1 receptor-associated kinase
IRE1	Inositol-requiring transmembrane kinase/endonuclease 1
IRF	IFN regulatory factor
ISGF3	IFN-stimulated gene factor 3
ISGs	IFN- stimulated genes
ISRE	IFN-stimulated response element
IVCs	Irregular vesicle clusters
JAK	Janus kinase
JNK	Jun N-terminal kinase
KPNA	Karyopherin subunit α
LAMP	Lysosomal-associated membrane protein
LC3	Microtubule-associated protein 1A/1B-light chain 3
LCM	Laser capture microdissection
LGP2	Laboratory of genetics and physiology 2
L-SIGN	Lymph node-SIGN
LTBR	Lymphotoxin β receptor
LVCV	Large virion-containing vacuoles
M	Membrane protein
MAPK	Mitogen-activated protein kinase
MARCH8	Membrane associated ring-CH-type finger 8
MAVS	Mitochondrial antiviral signaling protein
MDA5	Melanoma differentiation-associated protein 5
MERS-CoV	Middle east respiratory syndrome CoV
MFPE	Methacarn-fixed paraffin-embedded tissue
MHV	Mouse hepatitis virus
MLN	Mesenteric lymph node
MOI	Multiplicity of infection
mRNA	messenger RNA
MSPL	Mosaic serine protease large-form 1
MTase	Methyltransferase
mTOR	Mammalian target of rapamycin
MxA (MX1 and MX2)	Myxovirus resistance A
MyD88	Myeloid differentiation primary response 88
N	Nucleocapsid protein
nAbs	Neutralizing antibodies
NDP52	Nuclear domain 10 protein 52
NECs	Nasal epithelial cells
NEMO	NF-kβ essential modulation
NF-kβ	Nuclear factor kappa β

NF-kβIA	NF-kβ inhibitor
NHE3	Sodium-hydrogen exchanger 3
NK	Natural killer cells
NLR	Nucleotide-binding oligomerization domain-like receptors
NPM1	Nucleophosmin 1
NQ	Normalized quantity
nsp	non-structural protein
NTD	N-terminal domain
NTO	Nasal turbinate organoid
OASL	Oligoadenylate synthetase-directed RNaseL
OCN	Occludin
ORFs	Open reading frames
PABPC1	Poly(A) binding protein cytoplasmic 1
PAMPs	Pathogen-associated molecular patterns
PAMs	Porcine alveolar macrophages
PBS	Phosphate-buffered saline
PCBP	Poly(C) binding protein 2
PCoVs	Porcine CoVs
PCR	Polymerase chain reaction
PCV2	Porcine circovirus 2
PDCoV	Porcine deltaCoV
pDCs	Plasmacytoid DCs
PEAV	Porcine enteric alphaCoV
PED	Porcine epidemic diarrhea
PEDV	PED virus
PEN	Polyethylene naphthalate
PERK	Pancrearic ER eIF2a kinase
PFA	Paraformaldehyde
pfd	Post-farrowing day
PHEV	Porcine hemagglutinating encephalomyelitis virus
PI3K	Phosphatidylinositol 3 kinase
PLpro	Papain-like proteinase
pp1a	Polyprotein 1a
pp1ab	Polyprotein 1ab
PPID	Peptidyl-prolyl cis-trans isomerase D
PRCV	Porcine respiratory CoV
PRPF19	Pre-mRNA processing factor 19
PRRs	Pattern recognition receptors
PRRSV	Porcine reproductive and respiratory syndrome virus
PRV-A	Porcine rotavirus A
PTBP1	Polypyrimidine tract-binding protein 1
PTEN	Phosphatase and tensin homolog
PTGS2	Prostaglandin E2
qPCR	Quantitative PCR
RALY	RNA-binding protein associated with lethal yellow mutation
RBD	Receptor binding domain
RdRp	RNA-dependent RNA polymerase
RIG-I	Retinoic acid-inducible genes-I
RLR	RIG-I-like receptors
RNA	Ribonucleic acid

RNP	Ribonucleoprotein
ROS	Reactive oxygen species
RS	Rectal swab
RSAD2	Radical S-adenosyl methionine domain containing 2
RT	Room temperature
RTC	Replication and transcription complex
RT-qPCR	Reverse transcription-qPCR
S	Spike protein
S1	S subunit 1
S2	S subunit 2
SA	Sialic acid
SADS-CoV	Swine acute diarrhea syndrome CoV
SAP18	Sin3-associated protein 18
SARS-CoV	Severe acute respiratory syndrome CoV
SD	Study day
SeACoV	Swine enteric alphaCoV
SEC	Serotonin-positive enterochromaffin-like cells
SeCoV	Swine enteric CoV
SG	Stress granules
sg mRNA	subgenomic mRNA
SOCS1	Suppressor of cytokine signaling 1
SP	Signal peptide
Sp1	Specificity protein 1
ssRNA	Single sense RNA
STAT	Signal transducer and activator of transcription protein
STING	Stimulator of IFN genes
SV	Secretion vesicles
TAK1	Mitogen-activated protein kinase 7
TARDBP	Trans-active response DNA binding protein
TBK1	TANK-binding kinase 1
TCID50	50% tissue culture infectious dose
TEER	TransEpithelial electrical resistance
TEM	Transmission electron microscopy
TF	Transcription factors
TfR1	Transferrin receptor 1
TGEV	Transmissible gastroenteritis virus
TGF	Transforming growth factor
TIR	Toll/interleukin-1 receptor
TLR	Toll-like receptors
TM	Transmembrane domain
TMPRSS2	Transmembrane protease serine 2
TNF	Tumor necrosis factor
TNFRSF10B	Tumor necrosis factor receptor superfamily 10B
TRADD	Tumor necrosis factor receptor type 1-associated DEATH domain
TRAF	TNF-receptor associated factor
TRIF	TIR domain-containing adapter-inducing IFN-β
TRIM	Tripartite motif-containing protein
TYK2	Tyrosine kinase 2

UPR	Unfolded protein response
UTR	Untranslated regions
VH:CD	Villus-height-to-crypt-depth
VISA	Virus induced signaling adaptor
VPS36	Vacuolar protein-sorting-associated protein 36
VWD	Vomiting and wasting disease
YBX1	Y-box binding protein 1
YTHDC1	YTH domain-containing protein 1
ZO	Zonula occludens

Abstract

Porcine epidemic diarrhea (PED) virus (PEDV) causes a major swine gastrointestinal disease globally. Current outbreaks have been attributed to emerging viral strains that originated after 2010 through genetic recombination. Among these, non-S INDEL strains are associated with most severe clinical cases, while S INDEL strains result in milder disease outcomes. Nevertheless, both strains exhibit reduced virulence after multiple cell passages, driven by poorly understood mechanisms.

This PhD thesis investigated whether PEDV virulence loss correlates with genomic alterations from repeated cell passages. Study I examined genome mutations alongside clinical, pathological, and virological profiles of wild-type and cell-adapted S INDEL and non-S INDEL strains in newborn piglets. Results confirmed that virulence decreases with an increasing number of cell passages. Additionally, cell-adapted PEDV strain prevented intestinal damage and the disease onset in suckling piglets. In contrast, comparative analysis of non-S INDEL and S INDEL strains revealed that the severity of the disease correlated with the extent of intestinal damage, which was more pronounced in suckling piglets inoculated with non-S INDEL strains, suggesting strain-dependent clinical outcomes. Furthermore, specific mutations in the genomic regions of non-structural proteins (nsp)-2, 3, 4, 12, and 15, as well as the N-terminal domain (NTD) of the S1 domain, HR1 and HR2 of the S2 domain, open reading frame (ORF) 3, and N, were identified in cell-adapted S INDEL strain and may have contributed to the lesser virulence. In conclusion, genomic differences between both strains might have accounted for strain-dependent clinical outcomes.

Piglet age also influences PEDV severity, with newborn piglets exhibiting the most severe clinical signs, while older piglets remain asymptomatic. This age-dependent difference may be attributed to variations in intestinal development and innate immune responses of the intestinal mucosa. Study II explored these differences by characterizing intestinal expression of type I and III interferons (IFNs) and pro-inflammatory cytokines in suckling and weaned piglets inoculated with S INDEL and non-S INDEL strains. Both strains caused comparable intestinal atrophy, viral replication, and fecal viral loads in all piglets. However, weaned piglets mounted a stronger antiviral response, including enhanced expression of type I and III IFNs, Th1- and Th17-related pro-inflammatory cytokines, and widespread upregulation of IFN-stimulated genes (ISGs) in the intestinal mucosa. In contrast, suckling piglets showed weaker innate immune responses,

correlating with more severe clinical signs. These findings suggest that IFNs, ISGs, and pro-inflammatory cytokines play a role in mitigating PEDV severity.

PEDV primarily targets enterocytes in the small intestine, but emerging evidence suggests potential involvement of other cells, such as alveolar macrophages and nasal epithelial cells, indicating potential pulmonary replication. Although the role of these cells in the pathogenesis of the disease remains unclear, it has been suggested that the spike (S) protein might facilitate the adaptation of PEDV to other cells and influence shifts in viral tropism. In study II, both PEDV strains were also inoculated via the intranasal route in suckling and weaned piglets to explore this possible alternative transmission pathway. Although viral RNA was detected in the nasal turbinate and lungs of some animals (Study II), no respiratory disease or further digestive complications were observed. Study III, analyzed *in vitro* different macrophagic cell lines, such as porcine alveolar macrophages (PAMs), 3D4/21, and nasal epithelial cells, and revealed PEDV internalization but no evidence of active viral replication or activation of inflammatory or antiviral responses. These findings suggest that, while alternative cell types may internalize PEDV, their role in pathogenesis is limited. However, genomic variations in domains such as the receptor-binding domain (RBD), S1/S2 cleavage site, fusion peptide (FP), heptad repeated (HR)1, and HR2 suggest that the S protein may be involved in PEDV tropism and its potential pulmonary invasion.

Resumen

El virus de la diarrea epidémica porcina (PEDV, por sus siglas en inglés) es un importante patógeno gastrointestinal a nivel mundial. Los brotes recientes se asocian a cepas emergentes que surgieron después de 2010 debido a recombinación genética. Mientras que las cepas no-S INDEL se asocian con cuadros clínicos más graves, las cepas S INDEL generan brotes más leves. Sin embargo, ambas cepas pierden virulencia tras múltiples pases celulares, un proceso impulsado por mecanismos moleculares aún desconocidos.

Dada la hipótesis de que la pérdida de virulencia de PEDV podría estar relacionada con alteraciones genómicas adquiridas durante varios pases celulares, el objetivo del Estudio I fue correlacionar las mutaciones en el genoma de cepas S INDEL y no-S INDEL con los perfiles clínicos, patológicos y virológicos observados en lechones recién nacidos. Los resultados mostraron que la virulencia disminuye conforme aumentan los pases celulares. Además, la cepa adaptada a células previno el daño intestinal y la aparición de la enfermedad en lechones lactantes. Por otro lado, los lechones inoculados con cepas virulentas no-S INDEL presentaron un daño intestinal más severo, lo que confirma que la gravedad de la enfermedad depende de la cepa. Asimismo, se identificaron mutaciones específicas en las regiones genómicas de las proteínas no estructurales (nsp)-2, 3, 4, 12 y 15, así como el dominio N terminal (NTD, por sus siglas en inglés) del dominio S1, HR1 y HR2 del dominio S2, el marco de lectura abierta (ORF3, por sus siglas en inglés) y N de la cepa S INDEL adaptada a células, lo que podría haber contribuido a la menor virulencia. Las diferencias genómicas observadas entre las cepas no-S INDEL y S INDEL podrían explicar los resultados clínicos dependientes de la cepa.

La edad de los lechones también influye en la gravedad de los brotes. Si bien los lechones recién nacidos son más vulnerables, los lechones mayores permanecen asintomáticos. Esta diferencia podría deberse a variaciones en el desarrollo intestinal y en la respuesta inmune innata de la mucosa intestinal. En el Estudio II se caracterizó la expresión intestinal de interferones (IFN) de tipo I y III, y citocinas proinflamatorias en relación con la progresión de la enfermedad en lechones lactantes y destetados inoculados con cepas S INDEL y no-S INDEL. Ambas cepas causaron atrofia intestinal, replicación y cargas virales fecales similares en todos los lechones. Sin embargo, los lechones destetados desarrollaron una respuesta antiviral más robusta, con mayor expresión de IFN tipo I y III, citocinas proinflamatorias relacionadas con Th1 y Th17, y genes estimulados por interferones (ISGs, por sus siglas en inglés) en la mucosa intestinal. Por el contrario, los lechones lactantes mostraron respuestas inmunitarias innatas más

débiles, lo que se asoció con síntomas clínicos más graves. Esto sugiere que los IFNs, ISGs y las citocinas proinflamatorias son clave para mitigar la gravedad del PEDV.

Aunque PEDV infecta principalmente enterocitos del intestino delgado, evidencias recientes sugieren que otras células, como macrófagos alveolares y células epiteliales nasales, podrían estar involucradas en una posible replicación pulmonar. El papel de estas células en la patogénesis sigue sin esclarecerse, pero se ha planteado que la proteína spike (S) podría facilitar la adaptación viral a diferentes células e influir en el tropismo viral. En el Estudio II, se inocularon ambas cepas de PEDV por vía intranasal en lechones lactantes y destetados para evaluar esta posible vía alternativa de transmisión. Aunque se detectó ARN viral en cornetes nasales y pulmones (Estudio II), no se observaron signos de enfermedad respiratoria ni complicaciones digestivas adicionales. En el Estudio III, se analizaron líneas celulares, como macrófagos alveolares porcinos (PAMs, por sus siglas en inglés), células 3D4/21 y epiteliales nasales, para evaluar su susceptibilidad a PEDV. Si bien se detectó internalización viral en estas células, no se observó replicación activa ni activación de respuestas inflamatorias o antivirales. Por lo tanto, no se pudo determinar un papel específico de estas células. Sin embargo, variaciones en dominios como el RBD, S1/S2, FP, HR1 y HR2, sugieren que la proteína S podría estar involucrada en el tropismo del PEDV y en su potencial invasión pulmonar.

Resum

El virus de la diarrea epidèmica porcina (PEDV, per les sigles en anglès) és un important patogen gastrointestinal a nivell mundial. Els brots recents s'associen a soques emergents que van sorgir després del 2010 a causa de recombinació genètica. Mentre que les soques no-S INDEL s'associen amb quadres clínics més greus, les S INDEL generen brots més lleus. Tot i això, les dos soques perden virulència després de múltiples passades cel·lulars, un procés impulsat per mecanismes moleculars encara desconeguts.

Atesa la hipòtesi que la pèrdua de virulència de PEDV podria estar relacionada amb alteracions genòmiques adquirides durant diverses passades cel·lulars, l'objectiu de l'Estudi I va ser correlacionar les mutacions al genoma de soques S INDEL i no-S INDEL amb els perfils clínics, patològics i virològics observats en garrins nadons. Els resultats van mostrar que la virulència disminueix a mesura que augmenten els passos cel·lulars. A més, la soca adaptada a cèl·lules va prevenir el dany intestinal i l'aparició de la malaltia en garrins lactants. D'altra banda, els garrins inoculats amb la soca no-S INDEL van presentar un dany intestinal més sever, cosa que confirma que la gravetat de la malaltia depèn de la soca. Així mateix, es van identificar mutacions específiques a les regions genòmiques de les proteïnes no estructurals (nsp)-2, 3, 4, 12 i 15, així com el domini N terminal (NTD, per les sigles en anglès) del domini S1, HR1 i HR2 del domini S2, el marc de lectura oberta (ORF3, per les sigles en anglès) i N de la soca S INDEL adaptada a cèl·lules, cosa que podria haver contribuït a la menor virulència. Les diferències genòmiques observades entre els ceps non-S INDEL i S INDEL podrien explicar els resultats clínics dependents de la soca.

L'edat dels garrins també influeix en la gravetat dels brots. Si bé els garrins nadons són més vulnerables, els garrins adults romanen asimptomàtics. Aquesta diferència podria ser deguda a variacions en el desenvolupament intestinal i en la resposta immune innata de la mucosa intestinal. A l'Estudi II es va caracteritzar l'expressió intestinal d'interferons (IFN) de tipus I i III, i citocines proinflamatòries en relació amb la progressió de la malaltia en garrins lactants i deslletats inoculats amb soques S INDEL i no-S INDEL. Ambdós soques van causar atròfia intestinal, replicació i càrregues virals fecals similars en tots els garrins. No obstant això, els garrins deslletats van desenvolupar una resposta antiviral més robusta, amb més expressió d'IFN tipus I i III, citocines proinflamatòries relacionades amb Th1 i Th17, i gens estimulats per interferons (ISGs, per les sigles en anglès) a la mucosa intestinal. Per contra, els garrins lactants van mostrar respostes immunitàries innates més febles, cosa que es va associar amb símptomes

clínics més greus. Això suggereix que els IFNs, ISGs i les citocines proinflamatòries són clau per mitigar la gravetat del PEDV.

Encara que PEDV infecta principalment enteròcits de l'intestí prim, evidències recents suggereixen que altres cèl·lules, com macròfags alveolars i cèl·lules epitelials nasals, podrien estar involucrades en una possible replicació pulmonar. El paper d'aquestes cèl·lules a la patogènesi continua sense aclarir-se, però s'ha plantejat que la proteïna spike (S) podria facilitar l'adaptació viral a diferents cèl·lules i influir en el tropisme viral. A l'Estudi II, es van inocular les dos soques de PEDV per via intranasal en garrins lactants i deslletats per avaluar aquesta possible via alternativa de transmissió. Tot i que es va detectar ARN viral en cornets nasals i pulmons (Estudi II), no es van observar signes de malaltia respiratòria ni complicacions digestives addicionals. A l'Estudi III, es van analitzar línies cel·lulars, com macròfags alveolars porcins (PAMs, per les sigles en anglès), cèl·lules 3D4/21 i epitelials nasals, per avaluar-ne la susceptibilitat a PEDV. Tot i que es va detectar internalització viral en aquestes cèl·lules, no es va observar replicació activa ni activació de respostes inflamatòries o antivirals. Per tant, no s'ha pogut determinar un paper específic d'aquestes cèl·lules. No obstant això, variacions en dominis com el RBD, S1/S2, FP, HR1 i HR2 suggereixen que la proteïna S podria estar involucrada en el tropisme del PEDV i en la seva potencial invasió pulmonar.

PART I

General introduction
Hypothesis and objectives

CHAPTER 1

General introduction

1.1 Porcine coronaviruses (PCoVs)

1.1.1 Nomenclature, taxonomy, epidemiology and distribution

Coronaviruses (CoVs) are the largest positive-sense, single-stranded RNA (+RNA) viruses known (1). They belong to the family *Coronaviridae* within the order *Nidovirales* and are classified into two subfamilies, *Coronavirinae* and *Torovirinae*. The *Coronavirinae* subfamily is further divided into four genera, namely *Alphacoronavirus, Betacoronavirus, Gammacoronavirus*, and *Deltacoronavirus*. To date, seven porcine CoVs (PCoVs) have been identified and causally associated with disease in pigs, belonging to the *Alphacoronavirus, Betacoronavirus*, and *Deltacoronavirus* genera (2). Notably, no *Gammacoronaviruses* have been identified in pigs. The taxonomy and classification of swine coronaviruses is illustrated in Figure 1.1.

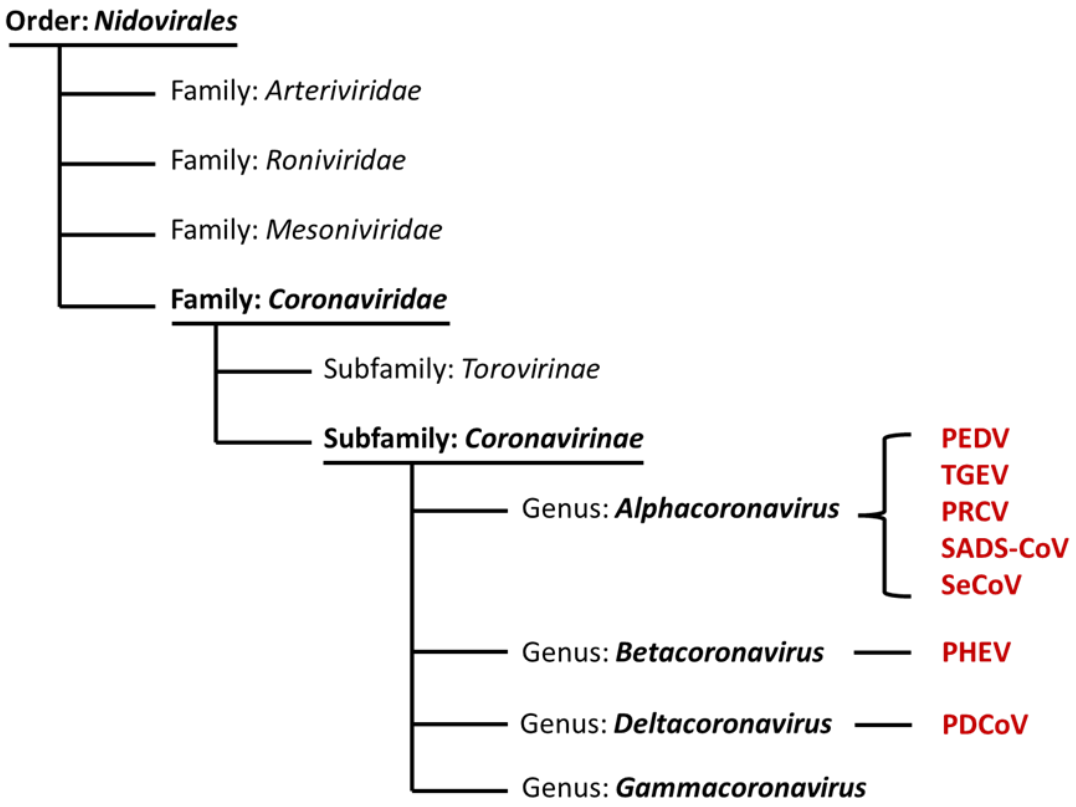

Figure 1.1. **Schematic diagram showing the taxonomic classification of PCoVs**. The seven known PCoVs are marked in red. Abbreviations: PEDV, porcine epidemic diarrhea virus; TGEV, transmissible gastroenteritis virus; PRCV, porcine respiratory coronavirus; SeCoV, swine enteric coronavirus; SADS-CoV, swine acute diarrhea syndrome coronavirus; PHEV, porcine hemagglutinating encephalomyelitis virus; and PDCoV, porcine deltacoronavirus.

The most epidemiologically significant PCoVs belong to the *Alphacoronavirus* and *Deltacoronavirus* genera, including porcine epidemic diarrhea virus (PEDV), transmissible

gastroenteritis virus (TGEV) and porcine deltacoronavirus (PDCoV). These viruses have recently emerged or re-emerged, causing substantial economic losses in the global swine industry (3). Among them, PEDV is a virus causing a significant emerging disease in the USA and a re-emerging virus in Asia and Europe, currently co-circulating with TGEV in some parts of the world (4). PDCoV, a newly emerging virus originated in Asia, has not yet been reported in Europe (4).

TGEV, porcine respiratory coronavirus (PRCV), and porcine hemagglutinating encephalomyelitis virus (PHEV) are worldwide distributed and have been circulating for decades in swine (4). TGEV was first described in 1946 in USA swine herds by Doyle and Hutchings (5), although the first outbreak consistent with TGE was reported a decade before (4). With the intensification of global pig farming, TGEV became a major concern for pork producers, with cases reported worldwide (2,6). The emergence of PRCV in 1984 led to a decrease in TGEV infections due to cross-protection from PRCV, complicating the global assessment of TGEV (7–9). While current epidemiological data on TGEV prevalence are scarce, it appears to be globally endemic but nearly absent in Europe. In the USA, its prevalence ranges from 3.8 to 6.8%, often co-circulating with PRCV, PEDV, and rotaviruses (2). Recent reports from China describe a highly virulent TGEV strain resulting from a natural recombination between the Miller M6 and Purdue 115 strains (10,11). PHEV, the only *Betacoronavirus* infecting swine, was first described in 1957 in nursery pigs exhibiting vomiting and encephalomyelitis in Ontario, Canada, although it was not isolated until 1962 (12–14). A similar outbreak was later reported in England, affecting suckling pigs with vomiting and wasting disease (VWD) (15–17). PHEV is widespread in swine herds globally, with high pig seroprevalence rates (53.35% in the USA), and a herd seroprevalence of 96.15% (18). Although it typically causes subclinical infections, clinical outbreaks may occur in litters from non-immune sows, particularly first-parity ones (19). Therefore, PHEV is not considered a significant pathogen associated with pig diarrhea (2).

RNA viruses like CoVs exhibit high mutation rates and a tendency for recombination, potentially leading to new emerging viruses (20–24). These novel CoVs may eventually cause more severe diseases, alter cellular and tissue tropism, or cross host species barriers, indicating a risk of cross-species transmission among different PCoVs (4,25). For example, PRCV emerged due to a significant deletion in the N-terminal region of the TGEV Spike (S) protein, conferring greater affinity for the respiratory tract compared to TGEV and PEDV, both of which are clinically indistinguishable and major causes of enteric disease (26–28). The global situation of PCoVs continues evolving, with the emergence of novel PCoV variants, such as swine enteric coronavirus (SeCoV), which is a recombinant virus with a TGEV backbone and a PEDV S protein gene (29).

SeCoV has circulated in Spain since 1993 and was recently detected in Italy, Germany, and Central and Eastern Europe (30–32). Although this chimeric enteric virus causes a disease similar to PEDV and TGEV, there is limited data on its overall impact, suggesting that its effects on pig health are limited (4). In contrast, swine acute diarrhea syndrome coronavirus (SADS-CoV), also referred as porcine enteric alphacoronavirus (PEAV) or swine enteric alphacoronavirus (SeACoV), was initially identified in diarrheic pigs in China between 2016 and 2017 (33–35). Since then, its prevalence in the Guangdong province has decreased (36). However, recent outbreaks suggest ongoing transmission and evolution of SADS-CoV in China (37,38). PDCoV, the only member of its genus affecting swine, was first detected in China in 2012 and later in the USA in 2014 (39–42). PDCoV has been reported in several countries, including Canada, South Korea, mainland China, Southeast Asia, and Peru, despite not in other regions of the world where research efforts are limited (43,44). Both SADS-CoV and PDCoV generally cause sporadic outbreaks of severe diarrhea in piglets from seronegative herds, similar to other PCoVS (4,45). While the prevalence and virulence of PDCoV are considered lower than those of PEDV, co-infection with PEDV can exacerbate disease severity in piglets (46–48). Limited data are available on the virulence of SADS-CoV compared to other PCoVs, but its incidence rate is relatively low (10%) (49).

1.1.2 Interspecies transmission and zoonotic potential of PCoVs

The origins of various PCoVs, including PEDV, TGEV, SADS-CoV, and PDCoV, are debated, but cross-species transmission has been suggested. TGEV is biologically, antigenically, and genetically closely related to canine enteric CoV (CECoV) and feline CoV (FCoV), suggesting a possible common ancestor and potential for interspecies transmission (6,25,50). These viruses share over 90% amino acid (aa) identity, and their S proteins have more than 80% identical aa (25). Additionally, cross-infection can occur among pigs, dogs, cats, and foxes, as each species sheds the virus in feces for varying durations. Virus shed by dogs has been shown to infect pigs, and feline infectious peritonitis virus (FIPV) causes diarrhea and intestinal lesions in neonatal piglets similar to those caused by TGEV (2,51,52). Molecular analysis of the common cell receptor aminopeptidase N (APN) for these alpha CoVs showed 78% identity, indicating that these viruses utilize evolutionarily conserved host cell components as receptors, thereby enhancing the potential for cross-species (25).

Moreover, genomic analysis demonstrated a high degree of similarity between PEDV and a bat alphacoronavirus (BtCoV/512/2005) (53). It has been suggested interspecies transmission

from bats to pigs, potentially through an intermediate host, which may account for the emergence of PEDV in the 1970s (42,54). PEDV can replicate in various cell lines, including those from swine, bats, ducks, and human and non-human primates, raising concerns about its potential zoonotic nature (55,56). Similarly, gene sequencing analysis of SADS-CoV revealed a high similarity (>95% nucleotide identity) to bat coronavirus HKU2, and ability to infect a broad range of species (35,57,58), posing a zoonotic potential (59). Regarding PDCoV, molecular analyses suggest that interspecies transmission occurred relatively recently, likely due to interactions between birds and mammals (42). The ancestors of PDCoV are believed to originate from avian species, such as quails and sparrows (60). PDCoV has been found to infect a variety of species, including chickens, turkey poults, mice, and calves, as well as multiple cell culture lines, particularly those derived from bats and non-human primates (43,61–63). Furthermore, PDCoV was reported to infect three Haitian children, suggesting also potential for zoonotic transmission (64). The ability of PDCoV to bind to the APN receptor may facilitate direct transmission to non-reservoir species, including humans, reflecting a possible mechanism by which PDCoV crossed the species barrier between birds and mammals (60). In contrast, there are no reported instances of cross-species transmission regarding the origin of PHEV, although this possibility cannot be entirely ruled out.

1.2. Porcine epidemic diarrhea virus (PEDV)

1.2.1 PEDV genome organization and viral proteins

PEDV is a single-stranded, positive-sense RNA virus with a genome length of approximately 28 kb (53,65). The genome includes 5’ cap and 3’ polyadenylated tails at both ends, along with untranslated regions (UTRs). It encodes at least seven open reading frames (ORFs) designated as ORF1a, ORF1b, and ORF2 to 6 (53). The two large ORFs, 1a and 1b, occupy the 5’-proximal two-thirds of the PEDV genome. Translation of ORF1a produces the replicase polyprotein (pp) 1a, while ORF1b extends the C-terminus of pp1a to generate pp1ab. Internal proteases post-translationally cleave these pp1a and pp1ab into 16 nonstructural proteins (nsp 1-16). The remaining ORFs in the 3’-proximal region of the genome encode one accessory protein (ORF3) and four structural proteins: the S protein (180–220 kDa), envelope (E) protein (7 kDa), membrane (M) protein (27–32 kDa), and nucleocapsid (N) protein (55–58 kDa) (66–70). The genome structure is shown in Figure 1.2.

The S protein is a type I transmembrane glycoprotein, comprising an N-terminal signal peptide, a large extracellular domain, a transmembrane domain, and a short cytoplasmic tail

(71). The extracellular domain comprises the N-terminal S1 subunit (19-726 aa), responsible for receptor binding, and the C-terminal S2 subunit (727-1388 aa), responsible for membrane fusion (55,69,72). The S1 subunit contains a signal peptide (SP) (1–18 aa) and two receptor-binding domains (RBDs): the N-terminal domain (NTD) (19–233 aa) and C-terminal domain (CTD) (499–638 aa), which are responsible for interacting with receptors (sialic acid and APN, respectively) to facilitate viral attachment (73,74). In contrast, the S2 subunit includes four key domains: a fusion peptide (FP at 891–908 aa), two heptad repeat regions (HR1 at 978–1117 aa and HR2 at 1274–1313 aa) a transmembrane domain (TM) at 1328–1350 aa and a cytoplasmic domain (CP, 1351–1386 aa) (75).

The main functions of each viral protein are summarized in the table 1.1.

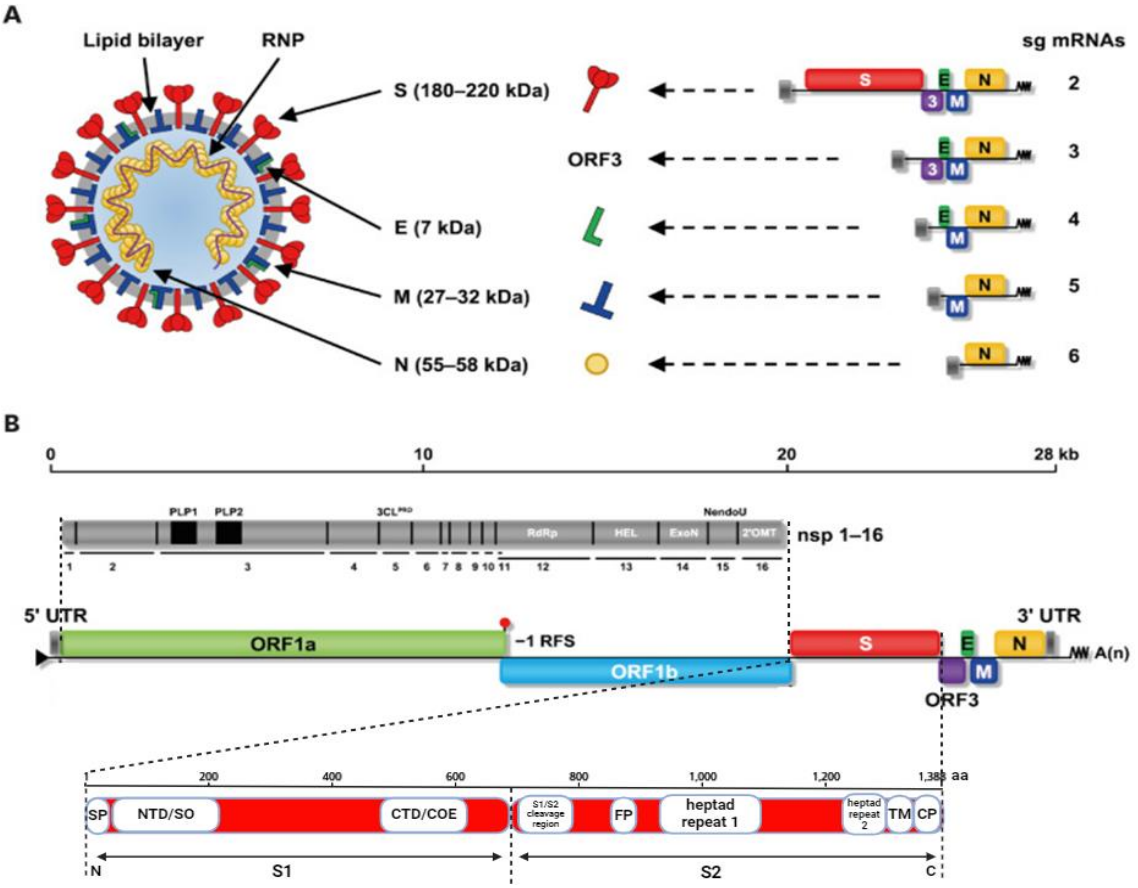

Figure 1.2. **Structure and genome organization of PEDV**. (A) Schematic representation of the PEDV virion. (B) Diagram of the PEDV genome, illustrating its organization into structural proteins—spike (S), envelope (E), membrane (M), and nucleocapsid (N)—along with accessory protein (ORF3) and non-structural proteins (nsp1-16). Key nsp include papain-like proteinase (PLpro), 3C-like proteinase (3CLpro), RNA-dependent RNA polymerase (RdRp), helicase (HEL), exoribonuclease (ExoN), endoribonuclease (EndoU), and 2'-O-methyltransferase (2'-O-MTase). The S protein comprises a signal peptide (SP), N-terminal domain (NTD), C-terminal domain/core neutralizing epitope (CTD/COE), fusion peptide (FP), heptad repeat domains (HR1, HR2), transmembrane domain (TM), and cytoplasmic domain (CP, 1351–1386 aa). Adapted from (76), using Biorender.com

Table 1.1. Viral proteins involved in PEDV infection.

Classification	Viral proteins	Role in PEDV Infection	References
Structural proteins	S	Essential for receptor binding (S1), membrane fusion (S2), and neutralizing antibody induction. Its receptor interactions affect cell tropism, pathogenic mechanisms, and interspecies transmission, serving as an important indicator of PEDV genetic diversity. It is essential for attenuation and adaptation *in vitro*	(55,66,69,73,77–83)
	E	Unknown specific function in PEDV infection but is essential for inducing membrane curvature, facilitating virion morphogenesis, assembly, and budding in other coronaviruses	(84–86)
	M	Aids in the complete viral assembly by interacting with the E and S proteins	(83,87–89)
	N	Forms the ribonucleoprotein (RNP) complex. Is crucial for packaging RNA into the helical nucleocapsid and assembling viral particles with the M protein. It enhances viral transcription by promoting mRNA cyclization through interactions with poly(A) binding protein cytoplasmic 1 (PABPC1) and eukaryotic initiation factor 4F (eIF4F) proteins	(90–95)
Accessory protein	ORF3	Potassium ion channel which regulates virion release. Promotes viral adaptation and attenuation *in vitro*. It prolongs the cellular S-phase, facilitates the formation of virion-transporting vesicles, and enhance the binding of the S protein to cell receptors	(96–103)
Nonstructural proteins	These proteins form the viral replication and transcription complex (RTC), which regulates viral genome		(85)
	nsp3 and nsp5	The PLpro (nsp3) and 3CLpro (nsp5) enzymes cleave the pp1a and pp1ab polyprotein precursors to generate mature nsp	(104–106)
	nsp7, nsp9 and nsp12	Assemble into the replication and transcription complex	(85)
	nsp9	Essential RNA-binding protein for viral RNAs stabilization	(107,108)
	nsp10	Acts as a regulator in viral RNA synthesis by enhancing the activities of nsp14 and nsp16	(85)
	nsp12	Acts as an RNA-dependent RNA polymerase (RdRp)	(109)
	nsp13	Functions as a nucleic acid helicase (HEL)/NTPase/ATPase. Bind and efficiently unwind both dsRNA and dsDNA substrates in a 5’-to-3’ direction	(85)
	nsp14	Has a N7-methyltransferase (N7-MTase) and exoribonuclease (ExoN) activity, which is involved in the replicative mismatch repair system	(110–112)
	nsp15	Acts as an endoribonuclease (EndoU)	(113)
	nsp16	Act as a 2’-O-MTase along with nsp14	(114)

1.2.2 Cellular receptor

The interaction between viruses and their specific receptors significantly influences cell and tissue tropism. In this context, the S protein of CoVs plays a major role as it mediates interactions with host factors to facilitate viral attachment and entry into target cells (115). Accordingly, the S protein of PEDV determines adaptability to different cell lines, highlighting its decisive role in cell tropism (116).

It has been reported that, depending on the density, APN serves as a functional receptor for PEDV (117,118), with the APN binding domain residing within the C-terminal half of the PEDV S1 protein (residues 477-629) (67). Several studies support its role in PEDV infection: (1) APN is highly expressed on the apical membrane of mature enterocytes, the primary target cells for PEDV (119,120); (2) antibodies against porcine APN (pAPN) inhibit viral infection *in vitro* (55,117,121); (3) overexpression of APN in non-permissive cell lines renders them susceptible to PEDV infection (118); (4) PEDV infection occurs successfully in transgenic mice expressing pAPN (122); and (5) the PEDV S1 protein interacts with both soluble and cell surface-expressed APN, as demonstrated by dot-blot and FACS assay (55,67). Moreover, PEDV can also infect cell lines from species other than pigs, including bats, ducks, and primates (both human and non-human) (123). In fact, PEDV has been shown to interact with and utilize human APN as a functional receptor. This ability to infect cells from multiple species indicates that PEDV utilizes evolutionarily conserved host cell components as receptors, enhancing the potential for cross-species transmission (56,69). However, studies have shown that PEDV can still infect APN-knockout pig and human cell cultures, as well as transgenic pigs, suggesting that APN is not the sole receptor for PEDV infection (124–127). Notably, Vero cells, which are commonly used for PEDV isolation and propagation, do not express APN (70,117). Therefore, pAPN's ability to facilitate PEDV cell entry appears to be primarily associated with its peptidase activity rather than functioning solely as a receptor (128). Also, APN is a recognized receptor for other swine CoVs such as TGEV, PRCV, and PDCoV (25,60,129,130).

In addition to APN, other receptors involved in PEDV pathogenesis by interacting with the S protein are summarized in Table 1.2 (115).

Table 1.2. Receptors involved in PEDV pathogenesis

Receptor	PEDV-Binding Domain	Role in PEDV pathogenesis	Other PCoVs using the receptor
Aminopeptidase N (APN)	S1 protein (67)	Attachment and internalization (117)	TGEV, PRCV, and PDCoV (25,60)
Sialic acid (SA)	N-terminal of the S1 protein (residues 1-249) (131)	Co-receptor (132). Enhance hemagglutination activity and viral adherence to mucin (55,69,132,133)	TGEV, SADS-CoV, PDCoV and PHEV (55,67,69,134–138)
N-Glycans	O- and *N*-linked glycosylation (S protein) (139)	Viral entry in IPEC-J2 cells (139)	SADS-CoV and PDCoV (134,140)
Alpha-1 Na+/K+-ATPase	S1 protein (141)	Involved in PEDV attachment (141)	Not described
Epidermal growth factor receptor (EGFR)	S1 protein (142)	Co-receptor for PEDV invasion in IPEC-J2 (142)	TGEV, SADS-CoV and PDCoV (143–146)
DC-SIGN/L-SIGN	Mannose carbohydrate residues (S protein) (147)	Uncertain. Possible co-receptor mediating the cell entry and dissemination (148)	Not described
Heparan sulfate (HS)	*N*- and *O*-linked sulfate groups of HS with S protein (149)	Attachment receptor in Vero Cells (149,150)	PDCoV, SADS-CoV and PHEV (135,138,151,152)
Transmembrane protease serine 2 (TMPRSS2) and mosaic serine protease large-form 1 (MSPL)	S1/S2 cleavage region (115)	Viral fusion, entry, and release of viral particles in Vero cells following proteolytic cleavage of the S1/S2 (70,153,154)	SADS-CoV and PDCoV (134,138,155)
Heat shock protein family A member 5 (HSPA5)	N-terminal domain of the S protein (156)	Regulates viral attachment and internalization (156)	Not described
Transferrin receptor 1 (TfR1)	S1 protein (157)	Involved in PEDV entry into Caco-2 and HEK 293T cells (157)	TGEV (158)
Death receptor (DR) 5 or TNFRSF10B	Unknown	Uncertain. Enhance viral entry and replication in Vero cells (159)	Not described
Integrin (αvβ3)	Four different integrin recognition motifs in the S protein (160)	Potential co-receptor for PEDV attachment and entry, functioning in synergy with pAPN (160,161)	Not described
Occludin (OCN)	Unknown	Co-receptor for late entry events through a macropinocytosis-like process (162,163)	TGEV (163)

1.2.3 Replication cycle

The replication cycle of PEDV involves several key stages, which are represented in Figure 1.3: (1) attachment and entry, (2) translation of viral replication enzymes, (3) genome transcription and replication, (4) translation of structural proteins, and (5) virion assembly and release. The process begins with the attachment of the PEDV S1 subunit protein to its receptor, pAPN (85). PEDV internalization occurs via clathrin-mediated endocytosis or via a macropinocytosis-like process involving microfilaments, following the proteolytic cleavage of the S1/S2 site by host-derived serine or furin proteases (3,153,162–164). Additionally, lysosomal cysteine proteases like cathepsin L and cathepsin B contribute to PEDV entry by activating the S protein (72). Like other CoVs, upon activation, the S2 subunit undergoes a conformational change that exposes the FP, enabling fusion with the plasma membrane (3,165). The HR1 and HR2 regions subsequently interact to form a six-helix bundle (6-HB), resulting in the complete fusion between the viral envelope and the host cell membrane, enabling viral entry into the cytoplasm (166,167).

Once PEDV enters the cell, the viral genome is released into the cytosol, where translation of the two major ORFs (ORF1a and ORF1b) begins, producing two replicase polyproteins, pp1a and pp1ab. These polyproteins are subsequently cleaved into 16 nsp by viral proteases (168). The nsp, comprising nsp1 to nsp16, constitute the RTC, which plays a pivotal role in subgenomic (sg) mRNA transcription and viral genomic RNA synthesis (85,107). Mechanistically, the RTC first synthesizes negative-strand RNA using positive-strand genomic RNA as a template. Both full-length and sg negative strands are produced, which are then used to synthesize full-length genomic RNA and 3'-coterminal sg mRNAs, respectively. Each sg mRNA is translated into proteins encoded by the ORFs 2 to 6, producing the structural (S, E, M, N) and the accessory protein (ORF3) of PEDV (76). As with other CoVs, transcriptional regulatory sequences (TRSs), located at the start of each structural or accessory gene, are essential for the discontinuous transcription process of each of these genes, guiding subgenomic mRNA synthesis during replication (169). While uncertainties remain regarding this critical aspect of CoV replication, evidence suggests that the primary factor responsible for this process is RdRp (nsp12). The envelope proteins S, E, and M are inserted into the endoplasmic reticulum (ER) and subsequently anchored in the Golgi apparatus, while the N protein interacts with newly synthesized genomic RNA to form RNP complexes (168). Progeny virions containing these RNPs, are assembled within the ER-Golgi intermediate compartments (ERGIC) and are finally released from the cell via exocytosis-like fusion of smooth-walled vesicles containing virions with the plasma membrane (85,168).

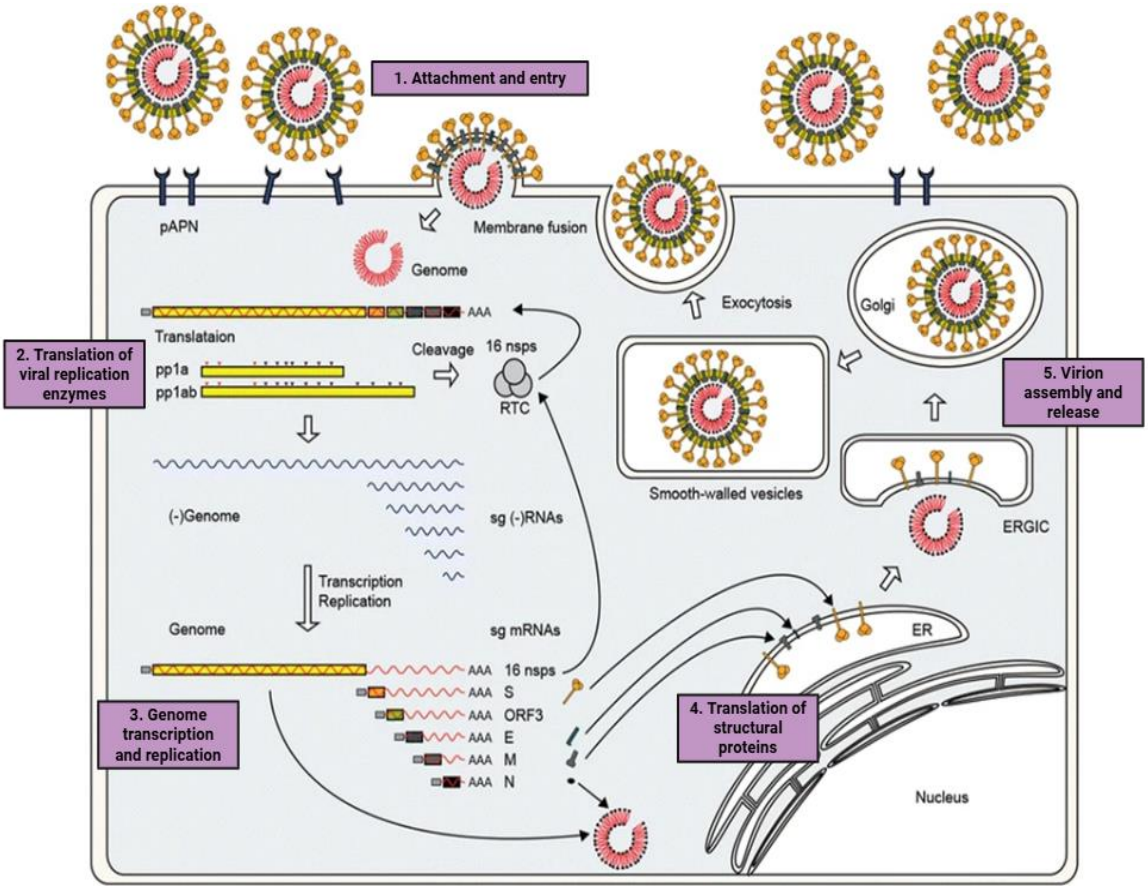

Figure 1.3. Overview of the PEDV replication cycle. PEDV binds to pAPN via its spike protein, leading to virus-cell fusion at the plasma membrane and the entry of the viral genome into the cytoplasm. Subsequently, ORF1a and ORF1b are translated into polyproteins (pp1a and pp1ab), which are cleaved into 16 nsps that form the replication and transcription complex (RTC). Then, full- and subgenomic (sg)-length minus strands are synthesized, followed by the production of full-length genomic RNA and sg mRNAs. The resultant N protein binds with genomic RNA to form helical RNP complexes, while the envelope proteins S, E, and M are inserted into the ER and moved to the ERGIC, where they assemble with RNP to form new virions. After maturation in the Golgi, the virus is transported in smooth-walled vesicles and released via exocytosis-like fusion with the plasma membrane. Adapted from (168), using Biorender.com.

1.3 PEDV epidemiology and transmission

1.3.1 Historical relevance of PEDV

PEDV has been a significant concern in the European and Asian pig industries for the past 50 years, with the first reports of the virus emerging in England in 1971 (170). In 1978, the etiologic agent of PED was identified in Belgium as a novel CoV and was designated as PEDV, with the prototype strain named CV777 (65). Over the following two decades, PEDV spread widely and became endemic within pig populations, although serological surveys revealed a low to moderate prevalence of PEDV across European herds (171,172). Then, PEDV prevalence in Europe declined significantly for reasons that remain unclear, with limited outbreaks reported in

the Netherlands (173), Belgium (172), Hungary (174), the Czech Republic (175) and England (176). However, a notable epidemic occurred in Italy between 2005 and 2006 (177). Although PEDV prevalence in Europe was reduced, the virus persisted endemically in pig populations (178,179).

In Asia, PEDV was first detected in China during the 1980s, and subsequently spread to other Asian countries, including Japan and South Korea, where it has since become endemic (180,181). These “classical” Eurasian PEDV strains are genetically similar to the CV777 prototype, with some insertions and deletions in the S protein gene (182,183). The global landscape of PED changed in 2010 with the emergence of highly virulent strains in China, leading to a devastating outbreak with almost 100% mortality in neonatal piglets, resulting in the loss of over one million piglets within a single year despite the use of CV777-based inactivated vaccines (184,185). These outbreaks involved both classical European/Asian strains and novel PEDV variants that differed genetically from the CV777 prototype (186–189). The virulent strains quickly spread to other Asian countries, including South Korea, Japan, Vietnam, and Thailand (190–192).

Later, PEDV outbreaks were reported for the first time in the United States, affecting over 5,000 farms across 25 states, resulting in significant economic losses ranging from 900 million to 1.8 billion dollars, and the death of more than 7 million pigs between 2013 and 2014 (193,194). Since its introduction, PEDV spread rapidly across the USA, Canada, and Mexico, generating high rates of piglet mortality and substantial economic losses (195–198). Sequence analyses revealed that the initial USA PEDV strains were genetically similar (>99% identity) to certain Chinese PEDV strains (China/2012/AH2012) circulating between 2011 and 2012 (54,194,199). Furthermore, Canadian and Mexican PEDV strains were 99% and 99.8% identical, respectively, to highly virulent PEDV isolates from the USA (OH851) and China (CH/HBQX/10) (200,201). These findings, along with the timing of the introduction of PEDV into these countries, suggest that the outbreaks in Canada and Mexico may be linked to the PEDV emergence in the USA, which possibly spread from Asia (4).

Since 2010, the emergence of highly virulent PEDV strains in China and the USA has led to the re-emergence of PEDV in Europe, with cases reported between 2014 and 2016, first in Germany and subsequently in Austria, Belgium, France, and Italy (32,202–206). However, only a few European Union countries have recently reported PED clinical cases and/or PEDV-seropositive animals. It remains to be answered why the clinical outcome and impact of European strains are less severe compared to those in Asia and the USA, where PEDV continues to be one of the main pathogens in the swine industry (4,193).

1.3.2 Emergence of non-S INDEL and S INDEL PEDV strains

Global PEDV strains exhibit significant genetic diversity. The initial PEDV strains (from 1970 to 2010) are referred to as classical PEDV strains (CV777-linage), while strains identified since 2010 are referred to emerging PEDV strains (2,207). Based on the nucleotide sequence of the S gene, PEDV strains are currently classified into two main genogroups (G): GI, which contains multiple insertions and deletions (INDEL) within the S1 subunit of the S protein, and GII. Genogroups GI and GII can be further subdivided into two clades each: GIa (classical strains, CV777), GIb (S INDEL strains), GIIa (variant strain), and GIIb (non-S INDEL recombinant strains) (54,208). Recently, new recombinant variants (GIc and GIIc) were identified within the GI and GII genogroups, respectively (209–211). Additionally, a new classification system based on the nucleocapsid gene has been proposed, organizing PEDV strains into three main genogroups (N1, N2, N3) and further dividing N3 into two sub-genogroups (N3a and N3b) (212). Consequently, Lin et al (2016) proposed categorizing global PEDV strains into Classical, S INDEL, emerging North American non-S INDEL, and emerging Asian non-S INDEL strains (207).

The first outbreak of PEDV in the USA in 2013 was caused by highly virulent non-S INDEL (GIIb) strains closely related to GIIb PEDV strains that emerged in China (China/2012/AH2012) between 2011 and 2012 (194). Emerging S INDEL (GIb) strains, likely resulting from recombination between the GIa CV777-lineage and GII strains, were detected in China in 2010 and spread to Japan (2013) and South Korea (2014) (2,182). In January 2014, a novel GIb strain was detected in the USA, causing milder PED outbreaks (201). This strain (USA/OH851/2014) clustered closely with Chinese strains HBQX-2010 or CH/ZMZDY/11, suggesting that potential recombination events with Chinese strains may have contributed to rapid PEDV evolution and variant emergence in the USA (178,201). By the end of 2016, both non-S INDEL and S INDEL PEDV strains had spread throughout North and South America and Asia. While highly virulent GII strains remain predominant in both continents, GIb strains continue circulating, although less frequently diagnosed (41,183,201,207,213). In contrast, for reasons that remain unclear, Europe has primarily reported S INDEL strains over the past decade, leading to clinical PED cases or seropositive animals in several countries (Austria, Belgium, France, Germany, Italy, the Netherlands, Portugal, Ukraine, Spain and Slovenia) (214). The viruses identified in these European countries resembled milder S INDEL USA variants (USA/OH851/2014 and USA/Indiana12.83/2013) (214–217). In any case, there is no evidence of the non-S INDEL variant in Europe, except for a single Ukrainian isolate derived from the USA/Kansas29/2013 strain (202). This lack of highly virulent strains may explain the PEDV epidemiological scenario in Europe, where outbreaks tend to be isolated rather than endemic (2). The GIc variant was designed for

recombinant S INDEL strains from America (USA/OH851/2014), Europe (GER/L00862/2014), and Asia (OKY-1/JPN/2014) with high sequence similarity to Chinese strains CH5 and ZL29. This similarity suggests that the GIc S INDEL strains from Europe may have a common ancestral origin with the Chinese strains (210,211,216). However, the GIc strain (TW/Yunlin550/2018) showed recombination between an earlier Taiwanese GIIb strain and a wild-type PEDV GIa strain (210). On the other hand, GIIc subgroup evolved from a recombination event between S gene from GIa and GIIa genotypes (209,218).

1.3.3 Transmission of PEDV

PEDV infection among pigs primarily occurs via direct or indirect fecal-oral routes but can also happen through aerosol transmission (182,216). Nevertheless, the severity of PEDV infection, disease progression, and transmissibility depend on various factors, including the overall immunity and health status of the pig population, as well as the specific PEDV genogroup involved (182). In general, the transmission rate of PEDV, whether through direct contact or aerosol, is higher in pigs infected with non-S INDEL strains compared to those infected with S INDEL strains (219). Table 1.3 summarizes the potential transmission routes of PEDV.

Table 1.3. Routes of PEDV transmission.

Direct contact transmission	**Fecal-oral route** (most relevant)	Feces and vomit of infected pigs (182)
	Fecal–nasal route	Aerosol transmission: PEDV can infect respiratory epithelium (220,221) and alveolar macrophages (222)
	Potential vertical transmission	Contaminated milk or colostrum (184,185,223). RT-qPCR detected PEDV in semen, testicles, and umbilical cords; however, no infectious virus was identified in the semen (224–226)
Indirect contact transmission	Fecal-oral/Fecal-nasal route	Contaminated fomites: transport trailers (227), farm workers' clothing (228), feed and additives including spray dried porcine plasma (229–231) Aerosol transmission: pig-to-pig or farm-to-farm transmission (232)
	Mechanical vectors, reservoirs, and carriers	Carriers: Subclinically PEDV infected older pigs, due to prolonged viral shedding (178,219,233) Reservoir/Mechanical vector: no reported cases of non-porcine animals acting as reservoirs or mechanical vectors for PEDV. However, wild boar could be a potential reservoir for PEDV, as they have been shown to harbor PEDV in their feces (234)

1.4 *In vitro* models for PEDV infection

The first successful *in vitro* propagation of PEDV was achieved in 1988 using Vero cells, which are derived from kidney epithelial cells of the African green monkey (235). Vero cells supplemented with trypsin have been widely used in PEDV research. However, repeated passaging of field isolates in Vero cells requires adaptation for efficient replication resulting in the loss of infectivity over time (199). While permissive to PEDV replication and propagation, these cells lack the type I interferon (IFN) gene cluster, limiting their suitability for pathogenesis studies, especially in areas regarding innate immune response modulation (236,237).

As a result, various traditional and newly established cell lines have been evaluated for their ability to support PEDV replication and pathogenesis studies while minimizing adaptation to cell culture. These tested cell lines have been previously reviewed (123) and are summarized in Table 1.4. Additionally, newly developed porcine enteroids, consistent with piglet intestinal organoids, support PEDV replication and are valuable for studying pathogenicity, immunology, and drug and vaccine toxicity (238–240).

1.5 Pathogenesis of PEDV infection

1.5.1 Tissue tropism

The primary targets of PEDV are epithelial cells in the small intestinal villi (enterocytes), as these cells express the functional APN receptor (182). Nevertheless, PEDV-positive cells are also detected in epithelial cells from the intestinal crypts, goblet cells, and scattered cells in Peyer's patches (178). Over the past decade, several studies have detected PEDV in extraintestinal tissues, raising the question of whether the virus can replicate in non-intestinal tissues and reach the intestine through systemic dissemination. Li et al. (2018) demonstrated that nasal epithelial cells can support PEDV replication following intranasal infection and suggested that systemic spread might be facilitated by nasal dendritic cells (DCs) and subepithelial CD3+ T cells (220). Moreover, *in vivo* and *in vitro* studies indicate that DCs and macrophages, including primary alveolar macrophages (PAMs) and the 3D4/21 cell line, are susceptible to PEDV, pointing to a potential role in the dissemination process (222,241–244).

Table 1.4. Cell lines used in PEDV studies. Cells tested and confirmed to be permissive to *in vitro* propagation of PEDV are indicated in black.

Cell line name	Cell type	Description	References
Vero cell	Epithelial	African green monkey kidney cell line	(55,116,125,199,235,242,245–248)
Vero C1008 (clone E6)	Epithelial	African green monkey kidney cell line	(249–257)
TMPRSS2 and MSPL	Epithelial	Vero cells expressing TMPRSS2 or MSPL	(70,154,258)
MARC-145	Epithelial	African green monkey kidney cell line (MA-104)	(138,259–265)
LLC-PK1, IB-RS-2, PK15, **PK15-APN**	Epithelial	Pig kidney cell line, exogenously expressing human or porcine APN	(55,116,259,266–273)
KSEK6	Epithelial	Pig epithelial cell line	(273)
IECs	Epithelial	Swine small intestine epithelial cells	(94,161,245,249–251,274,275)
IPEC-J2	Epithelial	2-day old derived porcine small intestine epithelial cells	(247,254,263,276–282)
IPEC-DQ	Epithelial	IPEC-J2 sub-cloned	(112,263,283–286)
IPI-2I and IPI-FX	Epithelial	Porcine intestinal epithelial cells	(287)
PAMs, 3D4/21	Macrophage	Primary and continuous porcine alveolar macrophage cell line, respectively	(222,243)
ST	Epithelial	Pig testis cell line	(55,125,259,288)
MDCK-APN	Epithelial	Canine kidney cells exogenously expressing human or porcine APN	(55,125)
Bovine cells	Mesenchymal	Primary bovine renal and cardiac cells	(289)
MK-DIEC	Epithelial	Duck intestinal epithelial cells	(290)
Tb1-Lu	Epithelial	Bat lung cell line	(55)
IEC-6	Epithelial	Rat crypt epithelial cells	(291)
L929 and LR7	Mesenchymal	Mouse fibroblast	(292–294)
EpH4-Ev	Epithelial	Mouse mammary epithelium	(223)
FHs 74	Epithelial	Human small intestinal epithelial cells	(56)
MRC-5	Epithelial	Human lung cell line	(55)
Huh-7, HepG2, Hep3B217, SNU387	Epithelial	Human liver cell line	(55,125,295)
HEK293	Epithelial	Human embryonic kidney 293	(103,125,242,248,252,253,282,294,296)

However, the significance of this alternative route in the pathogenesis of the disease is debatable. While some studies suggest PEDV does not replicate effectively in these respiratory cells (222), others indicate that PAMs and 3D4 cells modulate viral infectivity through GAS6 via an m6A-YTHDF2-dependent mechanism (243). Moreover, the possibility of systemic spread remains controversial. Viremia can be detected as early as the incubation stage, peaking during the acute phase before gradually declining, with a lower viral load in the serum compared to the intestine (297–299). Viremia may result from the diffusion of replicated PEDV from the acutely infected intestine into the bloodstream, but it is important to determine whether circulating PEDV or PEDV-loaded CD3+ T cells reach and infect extra-intestinal cells, as well as the enterocytes at the villous-crypt interface (220). These immature enterocytes are thought to be the initial site of PEDV replication (Figure 1.4), although the exact reason is still unclear. It has been suggested that PEDV can access them due to their close proximity to the blood vessels in the submucosa (299). Additionally, despite this short viremic phase, PEDV antigens have not been detected in key organs such as the liver, spleen, tonsils, or kidneys (182), indicating that further investigation is necessary to clarify this mechanism.

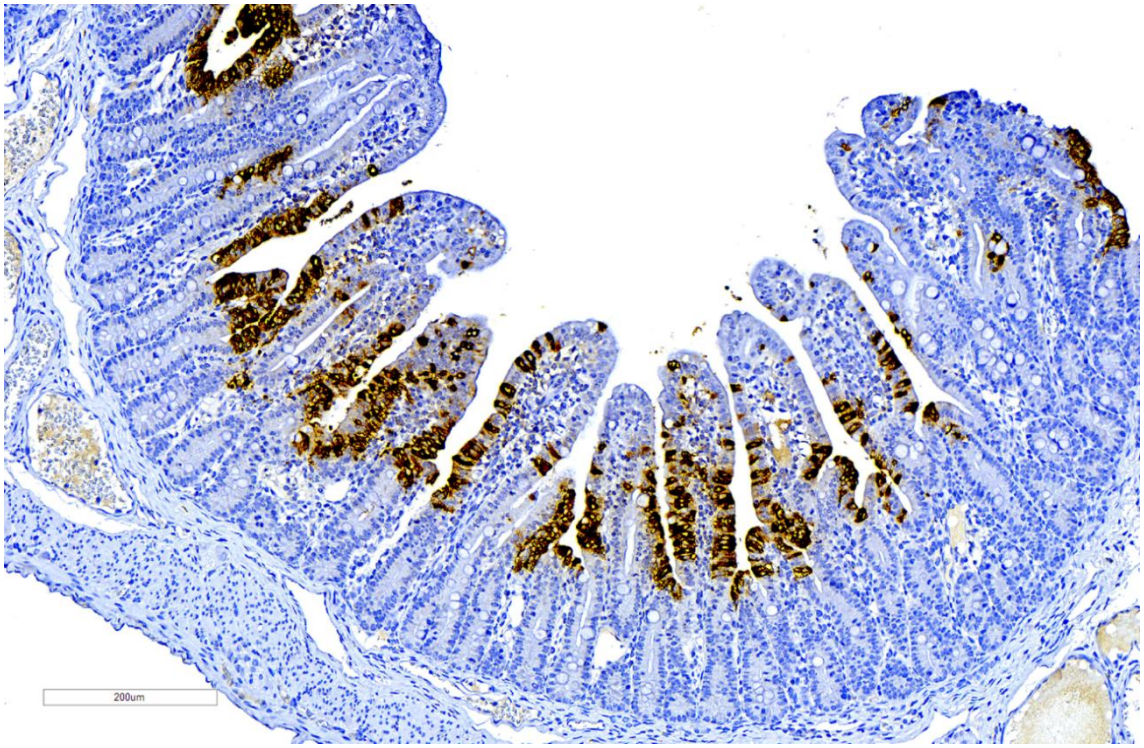

Figure 1.4. Immunohistochemistry on the jejunum of a 5-day-old piglet inoculated with the PEDV-USA strain (non-S INDEL) from Study II, detailed in Chapter 4. PEDV antigen-positive cells located in the cytoplasm of enterocytes at the villus-crypt interface of the small intestine, with no signs of villous atrophy.

1.5.2 Factors involved in PEDV's pathogenesis

The virulence of PED outbreaks is influenced by several factors, including host-dependent factors (e.g., pig age and innate immune response), virus-dependent factors (e.g., PEDV strain, infectious dose, and immune evasion capabilities), and environmental factors (e.g., inoculation route and herd immune status). Among these, pig age and viral strain are the most significant factors influencing PEDV pathogenesis, while additional factors are summarized in Table 1.5.

1.5.2.1 Age-dependent virulence

Although PEDV can infect pigs of all ages, disease severity and mortality rates are inversely correlated to pig age (2,168,300). Acute and severe clinical signs were observed at 1 day post-inoculation (dpi) in infected gnotobiotic, cesarean-derived, colostrum-deprived (CDCD), or conventional lactating piglets from 1-10 days of age (297,301–304). Dehydration and electrolyte imbalance are often fatal, leading to an average mortality rate of 50%, and sometimes reaching 100% in 1-3 day-old piglets (168). In contrast, 26-day-old weaned pigs exhibited milder clinical signs, reduced fecal virus shedding, and fewer intestinal lesions compared to 9-day-old pigs (305). Consequently, mortality rates drop significantly in adult pigs, including weaners and finishers (168). Additionally, weaned pigs display a longer incubation period before exhibiting fecal virus shedding (by 1 dpi) and developing diarrhea and lesions (by 2 dpi) compared to suckling piglets. They also excrete viral RNA in feces for longer durations (15–48 dpi, depending on used strain and inoculation route) compared to suckling piglets (14 dpi). Therefore, adult piglets are epidemiologically significant, as they serve as primary carriers of PEDV and the leading source of recurring epidemics (219,233,302).

The increased susceptibility of piglets up to 1 week of age is not fully understood, although it may be related to: (1) slower turnover of villous enterocytes in neonatal piglets (5–7 days) compared to 3-week-old pigs (2–3 days) (305), (2) proliferation of intestinal stem cells and renewal of crypt cells occur later in neonatal piglets (3 dpi) compared to weaned pigs (1 dpi) (305), (3) suckling pigs have weaker innate immunity compared to weaned pigs, as evident by a functional defect in natural killer cells (NK) (306), and (4) neonatal piglets have a higher gastric pH (4–6) compared to older pigs (pH 2–3), which allows PEDV to stay longer in the stomach in the younger animals (182).

1.5.2.2 PEDV strain-dependent virulence

In general, the CV777 prototype and S INDEL PEDV strains exhibit lower infectivity compared to non-S INDEL strains (182). Nonetheless, the pathogenesis and age-dependent resistance to the emerging non-S INDEL PEDV strains were similar to those of the classical and S INDEL PEDV strains (2).

According to *in vivo* studies, suckling piglets inoculated with the CV777 or S INDEL strains (TTR-2 or TC-PC177) had lower mortality rates, milder villous atrophy, less PEDV antigen in the small intestine, reduced fecal shedding and duration of diarrhea (2-7 days) compared to those inoculated with non-S INDEL strains (7-8 days of diarrhea) (207,301,307–312). Similarly, diarrhea appeared 1-3 days delay in piglets inoculated with S INDEL compared with non-S INDEL strains, indicating a longer incubation period for S INDEL PEDV (219,308). In contrast, the duration of diarrhea in weaned to feeder pigs was 6 days, regardless of the PEDV strain, and the prolonged fecal viral shedding was similar for both S INDEL (15–18 days) and non-S INDEL strains (15–26 days) (182). Nevertheless, if infected sows have compromised immune, nutritional, or health conditions, the S INDEL strain may still cause severe disease in offspring, with mortality rates and peak fecal PEDV RNA titers comparable to non-S INDEL strains (182,308,313).

1.5.2.3 Vero cell-adapted PEDV strain-reduced virulence

PEDV strains passaged at least 70 times to Vero cells (using trypsin or glycochenodeoxycholic acid) generally demonstrate reduced infectivity, replication, and immunogenicity in the intestines of pigs compared to their virulent counterparts (182). While the exact mechanism of attenuation is unclear, mutations during replication, such as truncated nsp, S, M and ORF3 variants, may play a role (103,314,315).

Reduced clinical signs, lesions, and fecal viral RNA shedding were observed in both lactating and adult pigs exposed to S INDEL and non-S INDEL cell-adapted PEDV strains. For example, little to no fecal viral RNA shedding and mild villous atrophy were observed in 1- to 4-day-old pigs inoculated with GIIb PEDV 8aa (70th–105th passage) and PC22A (140th–160th passage) isolates (316,317). Similarly, 6-day-old pigs inoculated with the GIIb PEDV CT strain (120th passage) showed mild diarrhea, moderate fecal viral RNA shedding, and mild villous atrophy (318). Intermittent fecal viral RNA shedding was also noted in 10- to 12-day-old pigs inoculated with GIa PEDV 83P-5 (100th passage) and GIIb PEDV YN (144th passage) isolates; however, intestinal PEDV antigen was detected only in the latter (319,320).

Table 1.5. Factors involved in PEDV pathogenesis other than age, strain and cell-adaptation.

	Factors	Role in PEDV pathogenesis	References
Host factors	Intestinal microbiota	Prevent infection by improving intestinal barrier	(321–332)
	Nucleophosmin 1 (NPM1)	Supports viral replication by inhibiting PEDV N protein proteolytic cleavage. Promotes cell survival by increasing resistance to apoptosis	(333)
	Heterogeneous nuclear ribonucleoprotein A1 (hnRNPA1)	Activates autophagy and promotes N protein degradation and the formation of the viral replication-transcription complex	(334,335)
	Growth response gene 1 (EGR1)	Degrades the PEDV N protein and suppress viral replication	(336)
	Bone marrow stromal cell antigen 2 (BST2); Far upstream element-binding protein 3 (FUBP3); Trans-active response DNA binding protein (TARDBP); Polypyrimidine tract–binding protein 1 (PTBP1); Pre-mRNA processing factor 19 (PRPF19); RNA-binding protein associated with lethal yellow mutation (RALY)	Enhance N protein degradation via membrane associated ring-CH-type finger 8 (MARCH8) and nuclear domain 10 protein 52 (NDP52)-selective autophagy	(337–341)
	Histone deacetylases (HDACs)	Modulates the interaction between PEDV N protein and host transcription factor Sp1	(342)
	Eukaryotic translation initiation factor 3 subunit L (eIF3L); Peptidyl-prolyl *cis-trans* isomerase D (PPID) or CyP40	Interacts with the PEDV M protein to negatively regulate viral replication	(343,344)
	Sodium-hydrogen exchanger 3 (NHE3) (SLC9A3)	Promotes PEDV invasion under EGFR regulation	(142,345,346)
	Vacuolar protein-sorting-associated protein 36 (VPS36)	Interacts with ORF3 to impede PEDV replication	(97)
	Mitogen-activated protein kinase (MAPK), extracellular signal-regulated kinase (ERK) 1/2, c-Jun N-terminal kinase (JNK)/p38, janus kinase (JAK)/signal transducer and activator of transcription proteins (STAT), phosphatidylinositol-3 kinase (PI3K)/protein kinase B (Akt)/mammalian	Signaling pathways used by PEDV to enhance viral replication	(115,347–352)

	target of rapamycin (mTOR), nuclear factor kappa B (NF-kB) signaling		
	Apoptosis, ER stress, pyroptosis, autophagy	Cell damage-related pathways involved in PEDV pathogenesis	(353,354)
	Membrane transporters and aquaporins; Mucin production; Tight and adhesion junctions like zonula occludens (ZO), claudin (CLN), OCN and E-Cadherin	Epithelial barrier components altered by PEDV	(115,162,163, 355–360)
	Dynein and kinesin-1	Facilitates PEDV internalization and transport along microtubules	(361,362)
	Intestinal innate immunity	Type I and III IFNs play essential antiviral roles in combating PEDV	(75,363)
Viral factors	Viral dose	The minimum infectious dose of PEDV varies with age	(303,304)
	Structural, nsp and accessory viral proteins	Strategies involved in evading innate immunity (IFNs) and controlling cell damage-related pathways (detailed in table 8)	(75,85,115,354,363–368)

1.6 Clinical outcome, lesions, and fecal virus shedding

The clinical progression of PEDV infection correlates with the severity of lesions and fecal virus shedding, both of which gradually develop based on the stage of infection, influenced by the distribution and replication of PEDV in various sections of the intestine (168,299). An overview of these clinical stages and associated findings is summarized in Table 1.6.

During the incubation period, most piglets exhibit no clinical signs other than vomiting, and intestinal damage or fecal viral shedding is not observed (182). Vomiting may be triggered by decreased serotonin-positive enterochromaffin-like cells (SEC) in the intestinal crypts, which return to normal levels as vomiting ceases (299). In contrast, intestinal lesions and the most severe clinical signs are observed during the acute phase, correlating with the PEDV replication peak and the detection of viral RNA in feces and serum (182). During this phase, PED is characterized by acute watery diarrhea, vomiting, cachexia, dehydration, and death, similar to other enteric PCoV (213). In suckling piglets, diarrhea begins at 1 dpi when exposed to non-S INDEL strains but is delayed by 1–3 days with S INDEL strains. In weaned piglets, diarrhea typically starts later, between 1 and 4 dpi (182). Once PEDV replicates in enterocytes, these cells undergo necrosis or apoptosis, causing villous atrophy and fusion. This is characterized by a reduction in the villus-height-to-crypt-depth (VH:CD) ratio from the normal 7:1 to ≤4:1 (2). Gross lesions include a distended stomach with undigested milk curd and thin, transparent intestines filled with yellowish fluid and gas. Histology reveals atrophic villi with swollen enterocytes, cytoplasmic vacuolization, flattened epithelium, and occasional necrotic or apoptotic enterocytes shed into the lumen (168). The lamina propria appears contracted and is accompanied by few inflammatory cells (178). Based on electron microscopy, these degenerated enterocytes are characterized by cytoplasmatic loss of electron-density and significant mitochondrial degeneration (178). Watery diarrhea arises from malabsorption and maldigestion due to the extensive loss and functional disruption of infected enterocytes (182). This impairment of water and electrolytes reabsorption leads to dehydration, further aggravated by vomiting, which is responsible for the acute death of infected piglets (178,182). Malabsorption and maldigestion occur due to a series of pathophysiological mechanisms:

- maldigestion caused by the loss of brush border membrane-bound digestive enzymes, including disaccharidases, alkaline phosphatase, and leucine aminopeptidase
- impaired gut integrity resulting from abnormal tight junction and adherent protein expression and decreased transepithelial resistance, leading to osmotic diarrhea and facilitating bacterial uptake

- loss of bicarbonate in feces leading to hypernatremia, hyperkalemia, and hyperchloremia, resulting in acidosis and impaired cardiac contractility
- reduction in mucin production due to the extensive loss of infected goblet cells, disrupting the first line of defense against intestinal microbes and promoting bacterial colonization.

Clinical signs persist in the mid and late infection stages, marked by extensive villous atrophy and numerous PEDV-infected enterocytes (299). However, the fecal viral titer significantly decreases during this stage and then titers remained low followed by at least one recurrent peak, possibly due to PEDV reinfection of regenerating enterocytes during the recovery stage of infection (178,182). The duration of diarrhea in suckling piglets ranges from 2 to 8 dpi, depending on the PEDV strain, and up to 6 dpi in weaned piglets. However, it resolves during the recovery phase, as gut integrity and digestive function are restored (14 days in suckling piglets and 6 days in weaned pigs) (182). However, fecal viral RNA shedding can continue for at least 14 dpi in suckling piglets and longer period in weaned-feeder pigs (15-26 dpi) extending up to 48 dpi in cases of direct contact or aerosol transmission. Although the duration of clinical signs in the herd typically ranges from 3 to 4 weeks, it varies significantly among suckling, weaned, and feeder pigs, as well as piglets infected with S INDEL or non-S INDEL strains (168).

1.7 PEDV immunology

1.7.1 Innate immune responses against PEDV infection

An effectively functioning immune cell system rapidly identify harmful agents and initiate an antiviral immune response. This initial response not only limits the spread of infection but also facilitates the activation of the adaptive immune response, which ultimately eliminates pathogens from the host (369). The first line of defense against viral infections is the host innate immune system, a complex network of signaling pathways and cellular processes that result in the production of multiple antiviral proteins, including IFNs, IFN-stimulated genes (ISGs), and proinflammatory cytokines (370).

Generally, monocytes, macrophages, DCs, cytotoxic lymphocytes (CTLs), NK and epithelial cells activate the antiviral innate immune response through three sequential stages: (1) recognition of pathogen-associated molecular patterns (PAMPs) by pattern recognition receptors (PRRs), (2) synthesis of type I and III IFNs and proinflammatory cytokines by infected cells, and (3) expression of numerous antiviral ISGs that promote an antiviral state (369–372).

1.7.1.1 Sensing of RNA viruses via PRRs

The main PRRs responsible for viral detection include both RNA and DNA sensors. Retinoic acid-inducible gene (RIG)-I-like receptors (RLRs) detect viral RNA within the cytoplasm, while toll-like receptors (TLRs), found on both the cell membrane and endosomes, can recognize both RNA and DNA (370,373). Nucleotide-binding oligomerization domain-like receptors (NLRs), located in the cellular cytoplasm, function as DNA and RNA sensors (374). Additionally, stimulator of IFN genes (STING), cyclic GMP-AMP synthase (cGAS) and absent in melanoma 2 (AIM2)-like receptors (ALRs) are DNA sensors located in the cellular cytoplasm or nucleus (375–377). After PEDV invades and replicates within the host cell, its viral RNA genome is primarily recognized by RLR and TLR sensors, triggering antiviral responses as illustrated in Figure 1.5 (364). Nevertheless, different NLRs have been proved to play essential roles in intestinal antiviral responses against other important CoVs such as severe acute respiratory syndrome CoV-2 (SARS-CoV-2) and middle east respiratory syndrome CoV (MERS-CoV) (378–380). Activation of these receptors ultimately results in the synthesis of type I and III IFNs and proinflammatory cytokines, albeit via distinct adaptor proteins (APs) to initiate their signaling cascade (365,370,373).

<u>RLR signaling pathway</u>

RLRs are cytoplasmic RNA helicases, including RIG-I (DDX58), melanoma differentiation-associated protein 5 (MDA5), and laboratory of genetics and physiology 2 (LGP2), that detect viral dsRNA and interact with downstream caspase-recruitment domains (CARDs) (381,382). In a resting state, RIG-I remains inactive, with its CARD domains blocked. After PEDV infection, RIG-I and MDA5 are activated by recognizing viral dsRNA, exposing their CARD regions, and initiating ubiquitination via tripartite motif containing protein 25 (TRIM25). This process facilitates oligomerization and translocation to the mitochondria, where the mitochondrial adaptor IFN-β promoter stimulator-1 (IPS-1) is recruited and activated, also known as mitochondrial antiviral signaling protein (MAVS), caspase activation recruitment domain adaptor inducing IFN-β (CARDIF), or virus induced signaling adaptor (VISA) (382,383). Subsequently, tumor necrosis factor receptor type 1-associated DEATH domain (TRADD) interaction activates TANK-binding kinase 1 (TBK1) and IκB Kinase (IKKs) (IKKα/β/γ/ε) via TNF-receptor associated factors 6, 2, and 3 (TRAF6, TRAF2, and TRAF3) through both NF-kB essential modulation (NEMO)-dependent and NEMO-independent pathways (384). Additionally, MAVS is recruited and activated in peroxisomes, where it triggers IFN signaling through an alternative mechanism (385).

Table 1.6. PEDV replication and intestinal distribution are correlated with clinical outcomes, lesions, and fecal virus shedding at various stages of the disease.

	Incubation period	**Acute phase**	**Mid and Late phase**	**Recovery phase**
Duration	< 16 hours post-inoculation (hpi)	16-48 hpi	Mid: 3 days post-inoculation (dpi) Late: 5 dpi	SP: 14 dpi WP/FP: 6 dpi
Viremia **SP: 100%; WP: 55%**	Started at 12hpi	Peak (24-72hpi): non-S INDEL: 1-5 dpi; S INDEL: 3 dpi	Progressively reduced	Ceased at 14-21 dpi
PEDV replication within intestine segments	First replication (12-18 hpi) in Jejunum (mid) and Ileum >>> jejunum (proximal-distal), duodenum and colon	Replication peak (24-36 hpi) in Jejunum (mid) and Ileum >>> jejunum (proximal-distal), duodenum and colon	Reduced replication in Jejunum (mid) and Ileum (mid and late phase) >>> colon (only mid phase)	No PEDV intestinal replication
PEDV Ag distribution	Villus-crypt interface of the jejunum and ileum >>> apical enterocytes	100% of the apical enterocytes. Also, colonic enterocytes, cryptal cells, goblet cells and DC-like cells	100% of the apical enterocytes of the jejunum and ileum. In the colon (only in mid phase)	
Clinical signs	Vomiting	Vomiting and a severe watery diarrhea starting in SP: 1 dpi (non-S INDEL); 2-3 dpi (S INDEL); WP/FP: 1-4 dpi	Less severe watery diarrhea. No vomiting	Diarrhea disappears in SP at 2-7 dpi (S INDEL) and 7-8 dpi (non-S INDEL); WP/FP: 6dpi. No vomiting
Pathology	No villous atrophy. Reduction in serotonin-positive enterochromaffin-like cells (SEC)	Severe villous atrophy and reduced SEC	Severe villous atrophy and normal SEC	Gut integrity and digestive function are restored
Fecal viral shedding (FVS) and viral titre (VT)	No PEDV RNA in feces	24 hpi: PEDV RNA 1rst detection in feces. 24-72 hpi: peak VT in feces	Low VT in feces	Recurrent peak. Low VT in feces. SP: FVS until 14 dpi; WP/FP: FVS until 15-18 (S INDEL); up to 26 dpi (non-S INDEL)

*hpi, hours post-inoculation; dpi, days post-inoculation; SP, suckling pigs; WP, weaned pigs; FP, fattening pigs; Ag, antigen; SEC, serotonin-positive enterochromaffin-like cells; FVS, fecal viral shedding; VT, viral titre

TLR signaling pathway

Among the TLRs involved in the recognition of PEDV (TLR2, TLR3, TLR4, TLR7, TLR8, and TLR9), the endosomal receptors (TLR3, TLR7, and TLR8) play a crucial role in PED pathogenesis in porcine IECs, Vero cells, IPEC-J2 and MARC-145 (249,262,386–390). This suggests that the virus uses its surface glycoproteins and nucleic acids within endosomes to initiate innate immune responses. TLR3 dimerizes upon binding viral dsRNA, while TLR7 and TLR8 dimerize when binding viral ssRNA (371,391). The activation of the resulting IFN-related signaling pathways depends on the recruitment of specific downstream APs by different TLRs. TLR3 engages the toll/interleukin-1 receptor (TIR) domain-containing adapter-inducing IFN-β (TRIF) pathway, recruiting TRAF3, TRAF6, TBK1, and IKKε. In contrast, TLR7 and TLR8 recruit and activate Interleukin-1 receptor-associated kinase 1 and 4 (IRAK1 and IRAK4), TRAF3, TRAF6, mitogen-activated protein kinase 7 (TAK1), and IKKa via myeloid differentiation primary response 88 (MyD88) (364,368,392).

1.7.1.2 Induction of type I and III IFNs by PEDV

Upon viral infection, the host rapidly responds by producing IFNs, which establish an antiviral state in both infected and neighboring uninfected cells. There are three types of IFNs: type I (IFN-α/β), type II (IFN-γ), and type III (IFN-λ1/3) (393–396). While the induction of IFN-α and IFN-β has traditionally been the hallmark of host innate immune responses against PEDV infection, it is now widely recognized that type III IFNs (IFN-λ) are also generated upon PEDV infection under *in vivo* and *in vitro* conditions, including when infecting intestinal organoids (238,240,364,365,397,398).

Although the induction of type I and III IFN pathways involves significant overlap in the RLRs/TLRs signaling cascade, their production pathways differ (365). Specifically, the IFN regulatory factors (IRFs) IRF3 and IRF7 predominantly control type I IFN expression, whereas type III IFN expression is regulated by the NF-kB pathway and IRF1-dependent signaling from peroxisomes (75,385,399). As illustrated in Figure 1.5, regardless of whether activated via RLRs/MAVS or TLR pathways, the APs TRAF3, TRAF6, TBK1, IRAK1 and IKK complex are fundamental for the activation of IRF1, IRF3, IRF7, and NF-κB. TRIM56 induces an increase of TRAF3 protein level, significantly activating downstream IRF3 and NF-κB signaling (262). Once phosphorylated, these transcription factors (TFs) dimerize and translocate to the nucleus, where they bind to the cAMP response element-binding protein (CREB)-binding protein (CBP), leading to the induction of type I and III IFNs as well as proinflammatory cytokines (75,391,400,401).

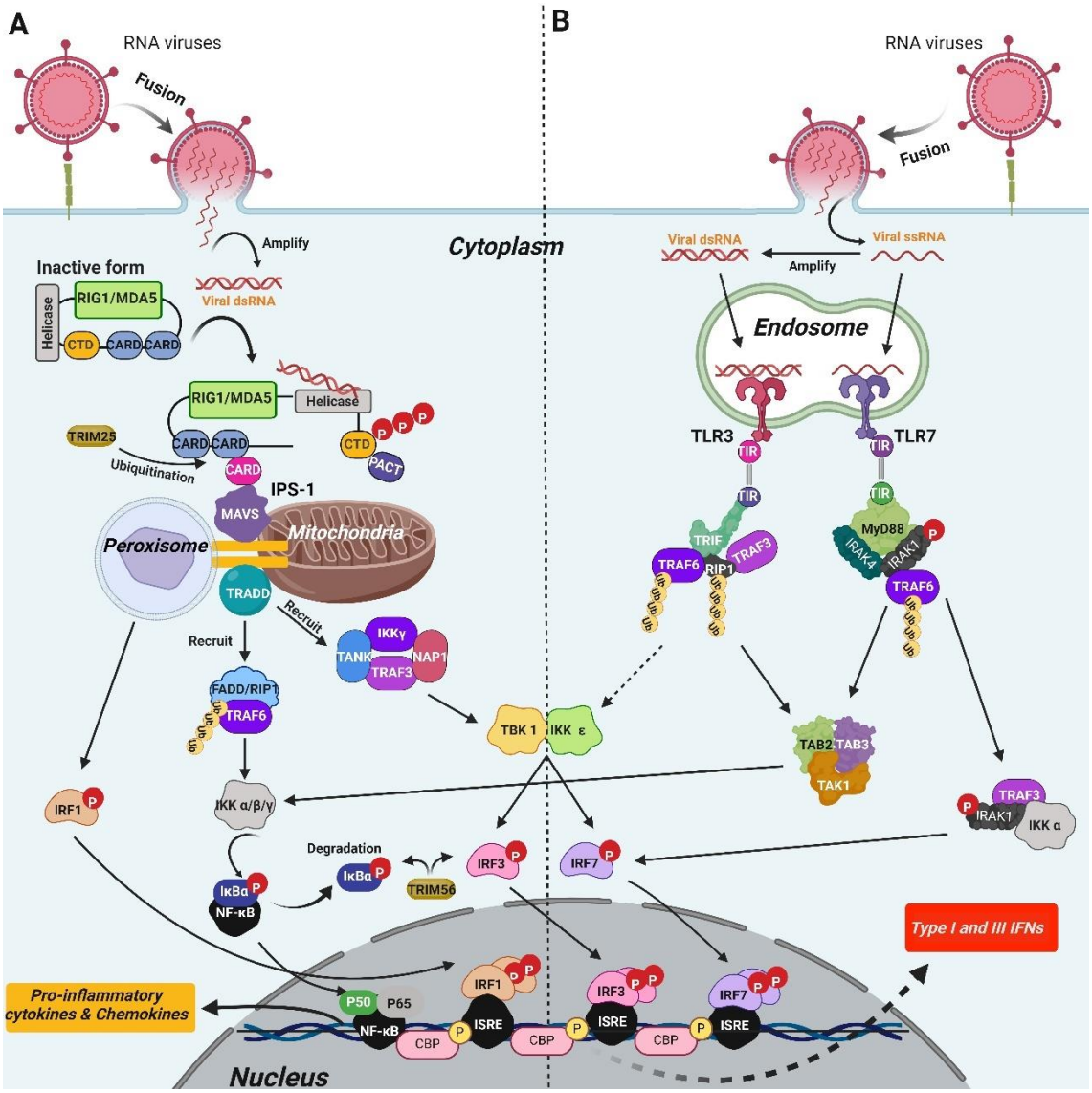

Figure 1.5. Mechanisms of type I and III IFN activation and inflammation triggered by RLR (A) and TLR (B) pathways in response to PEDV detection. The IFN signaling pathway activated upon RNA virus detection involves various components including PRRs (RIG-I/MDA5, TLR3, and TLR7); APs such as MAVS, TRIM-25, TRIM-56, FADD/RIP-1, TRAF6, TRAF3, TANK, TBK1, TRIF, MyD88, IRAK1, IRAK4, TAK1, and the IKK complex (α/β/γ/ε); and TFs including NF-kB, IRF1, IRF3, IRF7. These TFs translocate to the nucleus, where they bind with CBP to induce IFN synthesis. Modified from Te Nigeer's PhD thesis using BioRender.com.

Previous *in vitro* and *in vivo* studies have shown that both type I and III IFNs are co-produced in response to viral infections, sharing similar antiviral functions (365). However, IFN-λ plays a more crucial role in protecting mucosal barriers against various viruses, including norovirus, reovirus, rotavirus, adenovirus, murine cytomegalovirus, influenza A virus, and hepatitis B and C viruses (402–404). Specifically, type III IFNs have shown to inhibit PEDV replication more effectively than type I IFNs (398,405). This difference is attributed to the

distribution of their receptors (Table 1.7), as studies have demonstrated that IFNLRs (interleukin (IL)28R1) are more highly expressed than IFNAR1/2 in IECs and IPEC-J2 cells (398,406,407). These findings indicate a compartmentalized IFN response in the gut, wherein epithelial cells primarily respond to IFN-λ, while other cells within the gut rely on IFN-α/β for antiviral defense (406).

Table 1.7. Type I, II and III IFN receptors: distribution, cell source and function.

IFN type	Subtype	Receptor	Receptor distribution	Cellular source	Antiviral function
Type I IFN	IFN- α IFN-β IFN-ε IFN-κ IFN-ω	IFNAR1 and IFNAR2	Nearly all nucleated cells	IFN-β: all nucleated cells. IFN-α: leukocytes and plasmacytoid dendritic cells (pDCs)	Potent antiviral activity
Type II IFN	IFN-γ	IFNGR1 and IFNGR2	Broad tissue distribution	NK, CD4+ and CD8+ T-cells, Macrophages and DCs	Critical in cellular and cytotoxic proinflammatory reaction but also modest antiviral activity
Type III IFN	IFN-λ1 (IL-29) IFN-λ2 (IL-28A) IFN-λ3 (IL-28B) IFN-λ4	IL-10R2 and IFNLR1 (IL28R1)	IL-10R2: multiple cell types IFNLR1 (IL28R1): restricted to epithelial cells	Epithelial cells from mucosal barrier. Less common: hematopoietic cells	Crucial role in protecting mucosal barriers against infections

1.7.1.3 Production of ISGs in response to PEDV

The synthesis of ISGs is regulated by the JAK/STAT signaling pathway, which is activated by both type I and III IFNs (408) (Figure 1.6). Various APs, such as tyrosine kinase 2 (TYK2), JAK1, and JAK2, are involved in ISG transcription, along with TFs like the STAT1-STAT2 heterodimer, which binds to IRF9 to form the interferon stimulated gene factor 3 (ISGF3) complex that translocates to the nucleus (368,408–410). In PEDV infection, STAT-1 degradation has been shown to inhibit the IFN signaling pathway (411). Additionally, upregulation of ISGs and IFN-stimulated response element (ISRE) occur through p53-dependent IFN signaling (253).

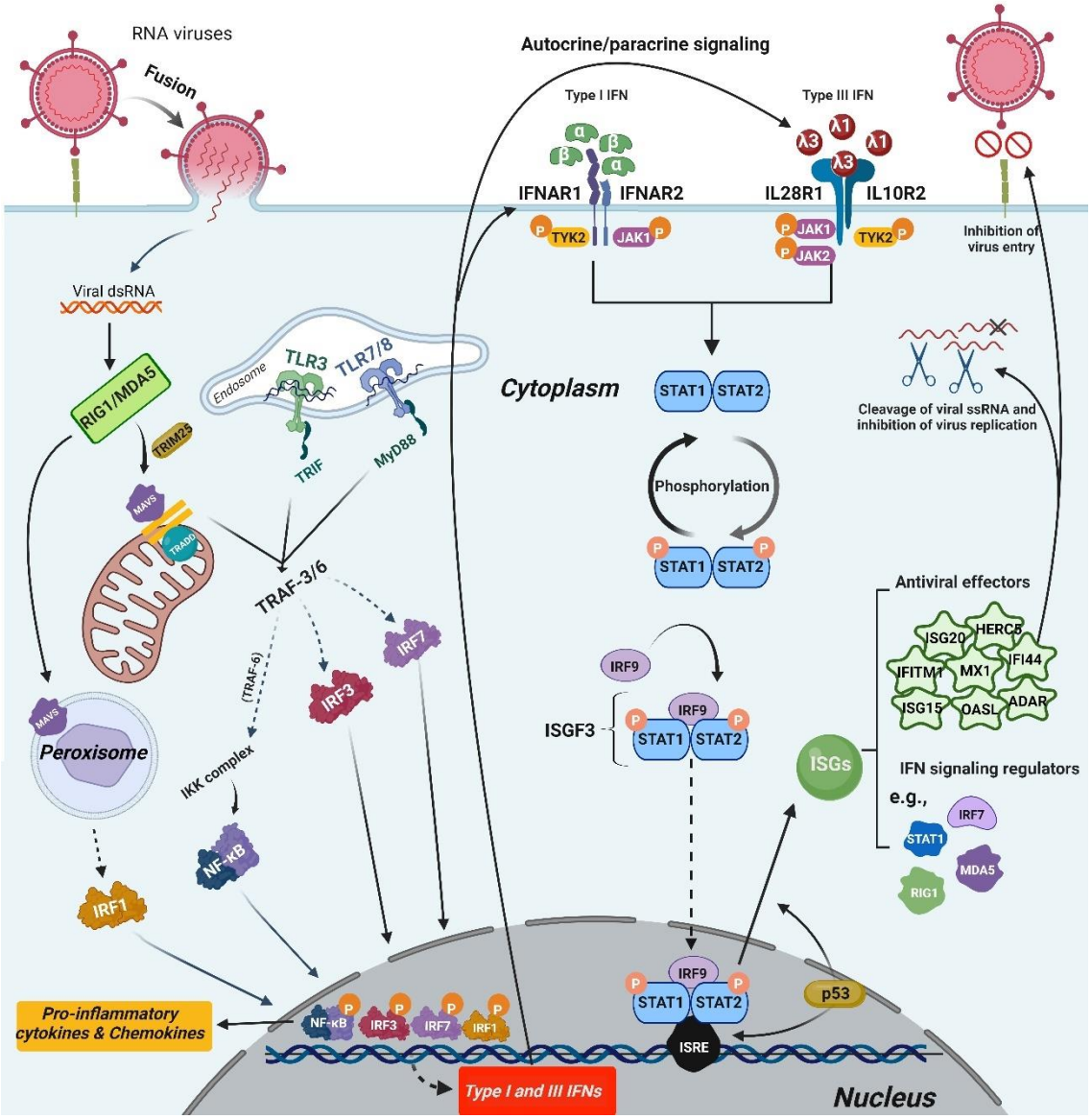

Figure 1.6. Synthesis of antiviral ISGs induced by type I and type III IFNs following PRRs (RLRs and TLRs) RNA viral sensing. After the synthesis of both IFNs, they bind to their respective receptors in autocrine and paracrine manner, activating the JAK/STAT pathway and the ISGF3 transcription factor complex. Once ISGF3 translocate to the nucleus, it induces the expression of various ISGs. Modified from Te Nigeer's PhD thesis using BioRender.com.

ISGs are powerful antiviral molecules that disrupt viral replication at multiple stages (412). ISGs can block viral entry, cleave viral ssRNA, and regulate IFN signaling, establishing a feedback loop that boosts IFN and ISG production, which leads to viral resistance and aid the activation of the adaptive immune response (363). The induction and persistence of ISGs differ based on whether type I or type III IFNs activate them. Type III IFNs sustain ISG activity, while type I IFNs trigger a faster, transient response (413). Additionally, increased secretion of IFN-λ in PEDV-infected IEC and IPEC-J2 cells correlates with significantly higher transcription of ISGs,

including ISG15, interferon-induced transmembrane (IFITMs), myxovirus resistance A (MxA), and 2',5'-oligoadenylate synthetase-directed RNaseL (OASL), highlighting the stronger antiviral activity of IFN-λ compared to IFN-α against PEDV (398,414).

1.7.1.4. Regulation of the host innate immune response during PEDV infection: evasion of the antiviral response

Over the past decade, numerous studies have shown that PCoVs like PEDV, TGEV, PDCoV, and SADS-CoV have evolved mechanisms to counteract host innate immunity, optimizing viral adaptation and replication (363). These evasive strategies include: (1) inhibition of PRR-mediated IFN production pathways, (2) inhibition of TFs responsible for IFN induction, (3) disruption of IFN-induced signal cascades, (4) hiding its viral RNA to evade immune sensors, and (5) modulation of essential cellular processes, such as MAPK signaling, apoptosis, ER stress, the unfolded protein response (UPR), pyroptosis, and autophagy pathways, all essential components of innate immunity during viral infections (3,75,85,115,268,353,354,363–368).

PEDV innate immune evasion strategies are summarized in Table 1.8 and illustrated in Figures 1.7 (IFNs) and Supplementary Figures 1-3 (apoptosis, pyroptosis, ER stress and UPR and autophagy). These strategies are primarily regulated by viral-encoded structural, nsp, and ORF3, and their interactions with host proteins (75,216,415). Numerous virus-host interactions have been identified, involving proteins such as TRIM21, DEAD-box RNA helicase 24 (DDX24), Ras GTPase-activating protein-binding protein 1 (G3BP) stress granule (SG) assembly factor 1, YTH domain-containing protein 1 (YTHDC1), nucleolin, Y-box binding protein 1 (YBX1), vimentin, hnRNP A2/B1, karyopherin subunit alpha 1 (KPNA1), apoptosis-enhancing nuclease (AEN), E3 ubiquitin ligase constitutive photomorphogenesis protein 1 (COP1), lymphotoxin beta receptor (LTβR), and heat shock proteins (HSP), including HSP27, HSP70, and HSP90, as demonstrated in both *in vivo* and *in vitro* studies (156,252,260,276,286,351,414,416–419). In addition, ribosomal proteins, oxidative phosphorylation (ROS), phosphatase and tensin homolog (PTEN), cell communication network factor 1 (CCN1), BST2, autophagy-related genes (ATG)5/ATG12, lysosomal-associated membrane protein (LAMP)1/LAMP2, microtubule-associated protein 1A/1B-light chain 3 (LC3) and Beclin 1 (BECN1) modulates apoptosis and autophagy in PEDV infection. Key signaling pathways, including 5' adenosine monophosphate-activated protein kinase (AMPK), JNK and PI3K/AKT/mTOR, play crucial roles in the antiviral response within IPEC-J2 and IPEC-DQ cells (265,285,349,420–423). Of the 16 nsp of PEDV, nsp1 has been found to be the most effective NF-κB and IFN antagonist, significantly influencing the host immune response during the early stages of infection (272).

Table 1.8. Main functions of PEDV proteins regarding viral replication, host's immunity evasion and the regulation of the main pathways of cell death.

Viral protein	Host innate immune evasion	Apoptosis, pyroptosis, autophagy and ER stress regulation
S protein	Impairs IFN activity by EGFR signaling activation (424)	S1 protein has the strongest ability to induce apoptosis (425)
M protein	Suppresses IFN and various ISGs by disrupting IRF7/IRF3 promoter *in vitro* (264,426). Enhances PEDV replication by interacting with HSP70 and eIF3L (343,417). Induces cell cycle arrest at the S-phase *in vitro* (89)	
N protein	Inhibits IFN and ISGs by disrupting IRF3, TBK1 and IPS-1 (264,427). Regulates NF-kB activation and translocation (249,428). Promotes the degradation of the antiviral factor p53 (252) inducing cell cycle prolongation at the S-phase (92,94). Upregulates MyD88, TRAF3, TRAF6, TBK1, and IRF3 by interacting with HnRNP K and PTBP1 (339,429). And upregulates IRAV by interacting with EGR1 (336–338,340,421). Enhances PEDV replication by modulating specificity protein 1 (Sp1) and HDAC1 (342). TRIM21 regulates its proteasome degradation (430).	Modulates ER stress and apoptosis through ER chaperone glucose-regulated protein 78 (GRP78 or BiP), B-cell lymphoma 2 (Bcl2), NF-kB and IL-8 up-regulation (94). Induces mitophagy by interacting with TRIM28 and inhibiting the JAK/STAT1 pathway (431). N protein is degraded via MARCH8/NDP52-selective autophagy (334,336–340,421,429,432)
E protein	Inhibits the nuclear translocation of IRF3 *in vitro* (250,264,433,434). Blocks CD4+ T cell activation and antigen presentation (242)	Modulates ER stress and apoptosis through GRP78, Bcl2, NF-kB and IL-8 up-regulation (94). Triggers ER stress through the activation of the pancreatic ER eIF2α kinase (PERK/eIF2α) and activating transcription factor 6 (ATF6) pathway (435,436). KPNA2 promotes autophagy-mediated degradation of E protein (437)
ORF3	Suppresses IRF3 and modulates NF-κB and p65 translocation blocking IFN, ISGs, IL-6, and IL-8 (264,438–440). Prolongs the duration of the S-phase in the cell cycle (441).	Inhibits apoptosis, induces ER stress and autophagy through the PERK/eIF2α and promoting the conversion of LC3-I to LC3-II (292,422,442,443)
Nsp 1	Blocks NF-kB, p65, and IRF1 nuclear translocation, IκBα and STAT-1 phosphorylation and promote proteasomal degradation of CBP (263,264,272,444). Inhibits AEN (260). Counteracts the role of complement C3 in replication restriction (445)	

Nsp 2	Promotes the proteasome degradation of the F-box and WD repeat domain-containing 7 (FBXW7) (446)	
Nsp 3 (PLPro)	Suppresses IRF3 promoter activities (264). PLPro2 downregulates RIG-I and STING pathways by its deubiquitinase (DUB) activity (447). PLPro1 blocks IFN synthesis by interacting with poly(C) binding protein 2 (PCBP2) (448).	Suppresses Gasdermin D (GSDMD)-mediated pyroptosis (449). Potential role of PLPro2 in inhibiting apoptosis and inducing autophagy (420,450)
Nsp 4	Upregulates NF-κB pathway and proinflammatory cytokines expression (451)	
Nsp 5 (M3CL-pro)	Degrades NEMO and, possibly, STAT2 (269,452,453). Inhibits AEN (260)	Promotes apoptosis via MAVS or mitochondrial damage (454). Antagonizes pyroptosis by cleaving pore-forming p30 (455)
Nsp 6	It is not a direct INF antagonist, but modulates the antiviral response (75)	Induces autophagy through PI3K/Akt/mTOR axis inhibition and BECN1 upregulation (422)
Nsp 7	Blocks ISGF3 nuclear transport and inhibits STAT 1 and STAT 2 (456). Antagonize MDA5-mediated IFN production (457). Suppress IRF3 promoter activities (264).	
Nsp 8	Reduces IRF1 promoter activity (80)	
Nsp 9		Upregulates histone cluster 2 (H2BE) expression and suppress ER stress-induced apoptosis (261)
Nsp 10	Enhances the antiviral effect of nsp16 (458). Upregulate the expression of proinflammatory cytokines (459). Restricts PEDV replication by interacting with Sin3-associated protein 18 (SAP18) (460)	
Nsp 13	Impedes lactogenic protection *in vitro* by downregulating NF-κB-dependent neonatal Fc receptor expression (461)	
Nsp 14	Inhibits IKK complex and NF-κB p65 and suppresses the synthesis of proinflammatory cytokines (462). Suppress IRF3 promoter activities (264). G-N-7 MTase has a IFN antagonistic activity (284)	Suppresses ER stress directly inhibiting GRP78 (248)
Nsp 15	Degrades TBK1/IRF3 and their promoters (264,463,464). Inhibits several ISGs and chemokine (280). Blocks the formation of antiviral SGs (465)	
Nsp 16	IFN antagonist enhanced by nsp10. Downregulates RIG-I/MDA5 pathway, inhibits ISRE and reduces the expression of IFIT1, IFIT2, IFIT3 (458). Suppress IRF3 promoter activities (264)	

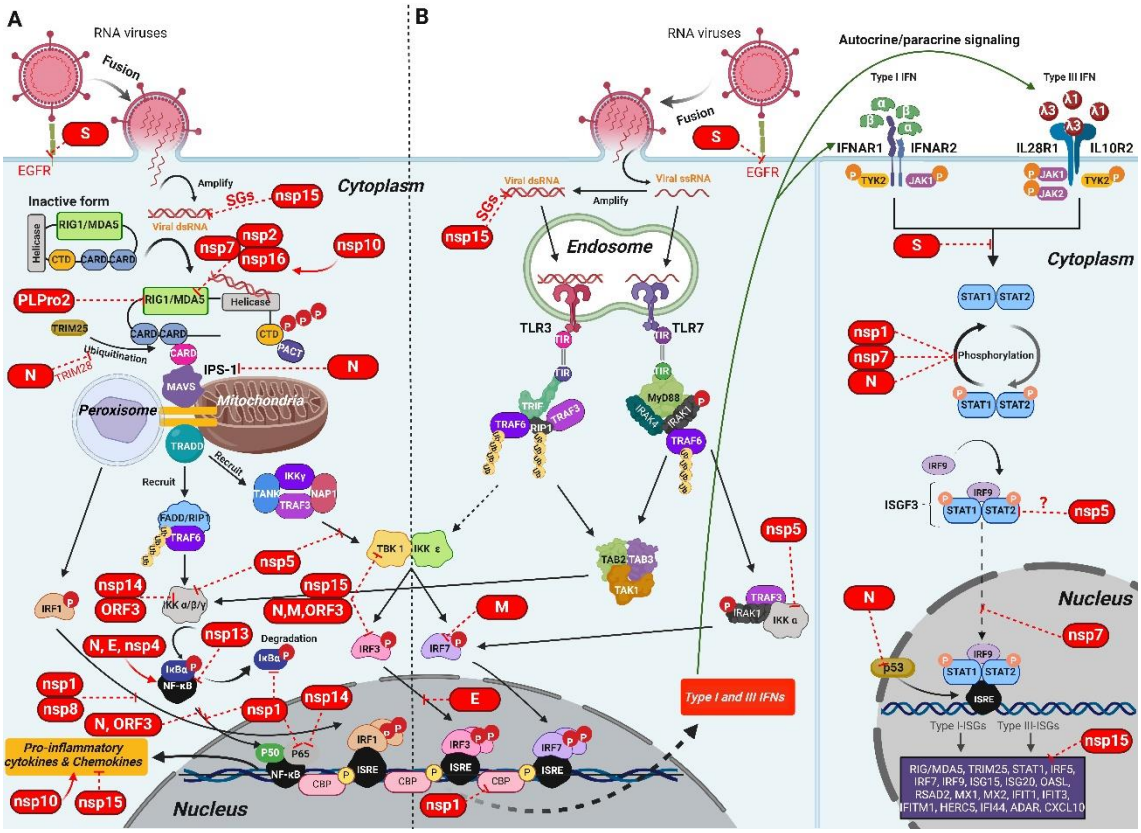

Figure 1.7. **Immune evasion strategies of PEDV against host innate immune signaling**. PEDV utilizes a range of mechanisms (shown in red) to counteract IFNs and ISGs, primarily mediated by its structural proteins (S, N, M, E), ORF3, and several nsps. The dashed line indicates inhibition, while the arrow indicates activation. Modified from Te Nigeer's PhD thesis using BioRender.com.

1.7.2 Acquired immune response against PEDV infection

The acquired immune response, encompassing both systemic and mucosal immunity, plays an essential role in protection against PEDV infection, with mucosal IgA production correlating with protection (466,467). PEDV infection in pigs triggers a strong humoral immune response, with neutralizing antibodies (nAbs) elicited between 7 and 14 dpi. Serum anti-PEDV IgM levels peak between 7 and 10 dpi, while IgG and IgA, detectable in serum and intestine as early as 5 dpi, reach their peak around 21 dpi (219,304,466,468,469). While IgM levels progressively decline, IgG and IgA in serum remain elevated between 35 and 40 dpi (469,470). However, pigs infected with S INDEL variants produce lower levels of IgG and nAbs compared to those infected with non-S INDEL strains (304,466,468). In 3-week-old pigs, serum IgG and IgA antibodies were detected against the structural proteins S and N. However, in 7-week-old piglets, antibodies also targeted the M protein but not the E protein (470,471).

Garber et al. (2016) reported that, at 7 dpi, approximately 40% of 10-day-old piglets had detectable serum IgG antibodies against PEDV, while only 10% had IgA antibodies. Upon

reinfection at 8 weeks of age, all pigs tested positive for both serum IgG and IgA antibodies, and over 50% showed detectable fecal secretory IgA (sIgA). Indeed, the number of PEDV-specific IgA antibody-positive pigs increased from 30% at reinfection to 70% within 3 days, showing a rapid secondary immune response after PEDV reinfection (302). By 14 dpi, IgG and IgA levels in both serum and feces in reinfected lactating piglets were comparable to those in first-time infected weaned piglets, with rising serum IgG and mucosal IgA, but declining serum IgA levels in both groups (302,469).

Notably, although PEDV-specific IgG, IgA, and nAbs are present in pigs reinfected 5 months after the initial challenge, this immune response does not completely prevent reinfection against homologous PEDV, as viral RNA was still detected in feces as described in previous experimental studies (469,472). However, viral shedding duration and load were significantly reduced in reinfected pigs. Interestingly, higher serum IgA levels were observed in pigs inoculated with a virulent non-S INDEL PEDV strain compared to those inoculated with the S INDEL strain; curiously, IgA production was not induced in pigs exposed to an attenuated strain (466,467). This suggests a possible link between IgA production and the severity of PEDV infection. PEDV-specific mucosal IgA antibodies of naturally infected sows wane approximately 1–2 months after infection, whereas serum IgA and IgG levels, along with antibody-secreting cells in intestinal and lymphoid tissues, persist for at least 6 months (473).

The relationship between PEDV strains and antibody responses has also been studied, focusing on cross-protection between emerging non-S INDEL and S INDEL strains. Both PEDV strains can cross-react and cross-neutralize *in vitro* and *in vivo*. Complete cross-protection was observed in weaned pigs immunized with the non-S INDEL strain before challenge with either the S INDEL or homologous non-S INDEL strain. In contrast, only partial protection occurred when pigs were initially immunized with the S INDEL strain and then challenged with the non-S INDEL strain (466,474). However, other *in vivo* studies have indicated incomplete cross-protection among different genetic strains of PEDV (308,468,475).

Although research on PEDV-specific cell-mediated immune responses is limited, studies have demonstrated that PEDV infection leads to an increase in CD4+ and CD8+ double-positive T cells in the mesenteric lymph nodes (MLN), while no significant increase is observed in the peripheral circulation, following a challenge in pigs previously exposed to the virus (469). The expansion of PEDV-specific effector memory cells in response to challenge highlights the importance of the local immune response rather than the systemic one. Understanding this mechanism can be beneficial in designing future mucosal vaccines against PEDV infection.

However, CD4+ and CD8+ T cell responses did not differ significantly between neonatal and weaned pigs (306).

1.7.3 Passive immune response (lactogenic immunity)

Robust lactogenic immunity is crucial to combat PED, especially given its global distribution and potential for reemergence. The identification of the intestine-mammary gland-sIgA axis in early studies of TGEV was a significant advancement in our understanding of passive protection for piglets (476–478). After PEDV infection, effector B cells or plasmablasts migrate from the gut-associated lymphoid tissue (GALT) to the mammary gland, where they secrete anti-PEDV sIgA antibodies into milk and colostrum (477,479). This concept highlights the critical role of sIgA in providing immunity through maternal milk, helping to safeguard piglets during their vulnerable early life, which is essential for effective PEDV outbreak management (480–484). Previous studies have demonstrated that sows exposed to mildly virulent PEDV strains develop lactogenic immunity, offering cross-protection to piglets against virulent PEDV strains (475). The strength of this passive immunity, however, depends on the route of exposure. For example, sows vaccinated orally with live-attenuated PEDV provide stronger passive immunity to piglets compared to those vaccinated intramuscularly (485,486). Additionally, the induction of a lactogenic immune response in pregnant sows is influenced by the stage of gestation; sows infected with PEDV during the second third of gestation provided complete protection, achieving 100% protection for nursing piglets (487).

Previous studies have identified nAbs in the colostrum and milk of PEDV-infected sows (488,489). PEDV-specific IgA and nAbs titers in sows infected three months before farrowing peak in colostrum on the first post-farrowing day (pfd) and then decline rapidly in milk by 3 pfd, followed by a more gradual decrease from 4 to 19 pfd (489). Likewise sows infected 3 to 4 months prior to farrowing and subsequently re-exposed to PEDV between 3 and 5 pfd showed progressive increase in PEDV-specific IgA-secreting cells in milk, peaking between 15 and 22 pfd (490). Furthermore, levels of nAbs and PEDV-specific IgG and IgA were elevated in the colostrum and milk of previously infected sows after vaccination with an inactivated PEDV vaccine given 5 and 2 weeks prior to farrowing. In contrast, naïve sows showed minimal or no responses in nAbs, IgG, or IgA antibodies in their colostrum and milk following the same vaccination (491).

While neonatal piglets are protected from PEDV by passive lactogenic immunity, this protection disappears after weaning, becoming susceptible to PEDV infection (2). Recurrence of PEDV in grower-finisher pigs can lead to intermittent diarrhea, viral persistence, and an endemic

situation on farms (177). This highlights the importance of inducing active immune responses as a critical protective mechanism in weaned piglets.

1.8 Prevention and control strategies against PEDV

Since PEDV is a highly contagious virus, the implementation of effective prevention strategies is crucial for global disease control. These strategies focus on three primary mechanisms of action aimed at preventing the entry and spread of the virus on farms and stimulating lactogenic immunity to protect suckling piglets (475,481,482,487,490). The mechanisms include strict sanitation and biosecurity protocols, as well as immunoprophylaxis measures such as vaccination and whole-herd feedback (2,168,182).

Strict biosecurity measures are among the most critical strategies for preventing PEDV introduction and spread into farms and minimizing direct or indirect transmission between farms. This includes stringent hygiene protocols for farm workers, thorough decontamination and disinfection of transport trailers and other potentially contaminated fomites, and ensuring the use of secure feed or feed additives (227–232). While various disinfectants, such as 0.5% Virkon S, 2.06% Clorox, super-oxidized water (pH 6.0), accelerated hydrogen peroxide, and peroxygen-based disinfectants, can inactivate PEDV, viral RNA may still be detectable (492–495).

More effectively, the implementation of immunoprophylaxis strategies serves as a promising practical tool for the prevention and control of PED, especially when combined with enhanced biosecurity measures and optimized farm management practices. Immunizing pregnant sows plays a vital role in controlling epidemic PED and reducing suckling piglet mortality by rapidly and artificially stimulating lactogenic immunity.

One historically widespread practice to achieve this goal is whole-herd feedback, which involves exposing sows to PEDV-contaminated material, such as feces or intestines from infected piglets (2,168,182). Although there is no standard feedback protocol, the most effective and safest timing of exposure is mid-gestation (days 57–59), particularly when gilts are orally inoculated with a virulent non-S INDEL PEDV strain (487). Gilts infected at this stage demonstrated stronger protective immunity, while those exposed earlier (days 19–22) or later (days 96–97) in gestation showed reduced immunity, with piglet survival rates of 87.2% and 55.9%, respectively. Following this protocol, infected gilts ceased fecal PEDV shedding before farrowing (313,487). However, several challenges must be considered before adopting this approach. Firstly, the circulation and transmission of other significant pathogens, such as porcine

reproductive and respiratory syndrome virus (PRRSV) or porcine circovirus 2 (PCV2), present in feces, along with the long-term persistence of PEDV on farms due to the spread of infectious virus in feces (182,496). Additionally, this practice often fails to induce adequate immunity in sows because the infectious material does not contain sufficient PEDV load (168). To address the frequent inefficiency and lack of safety, this immunoprophylactic strategy has been largely replaced using PEDV vaccines, particularly in the USA and Asia. However, in Europe, vaccination is not commonly implemented (2).

Vaccinating sows during gestation not only enhances lactogenic immunity by inducing high levels of protective antibodies in colostrum and milk but also sustains elevated levels of nAbs in the serum and colostrum of immunized sows (480–484,488,489). Since full protection against PEDV relies heavily on the presence of sIgA in the intestinal mucosa, active immunization (boosters) of weaner-to-finisher pigs may be essential for controlling endemic PEDV infections. The progression and current status of PEDV vaccines have been recently reviewed (497) and include various types: live attenuated, inactivated, subunit, virus-like particle, viral-vector, and nucleic acid vaccines. Historically used vaccines (CV777-attenuated or inactivated vaccines) have not been effective for controlling PED under field conditions. The low efficacy of these vaccines is attributed to antigenic, genetic (variability in S proteins), and phylogenetic (GI vs. GII) differences between vaccine strains and field epidemic strains (187,498–501). Therefore, in the future, the use of next-generation vaccines based on new platforms could play a crucial role in effectively controlling the disease, especially if they are based on PEDV strains that are phenotypically and genotypically similar or identical to the field strains responsible for PED epidemics worldwide or developing a pan-PEDV vaccine.

CHAPTER 2

Hypothesis and objectives

Hypothesis

PED is one of the most significant gastrointestinal diseases affecting pigs since its emergence in the 1970s. However, over the past decade, genetic modifications have led to the emergence of highly virulent strains with devastating consequences worldwide, creating an urgent need for action within the swine industry (4). The circulation of two genetically distinct strain types—non-S INDEL and S INDEL—further complicates the epidemiological landscape and presents significant challenges for the development of effective preventive measures to control the disease. Comprehensive studies have identified critical factors influencing the severity and outcomes associated with PEDV outbreaks. Among these, piglet age, PEDV strain, and innate immunity are particularly important (2,182). For this reason, understanding the mechanisms by which these factors modulate the disease is a crucial step towards developing new preventive strategies for disease control.

Evidence from *in vivo* studies suggest that infections caused by non-S INDEL strains result in more severe disease compared to those from S INDEL ones, as evidenced by clinical, pathological, and virological outcomes (301,305,309). Moreover, cell-adapted PEDV strains exhibit a reduced virulence in both PEDV genotypes (301,316–318). In the absence of comparative *in vivo* studies between cell-adapted and field strains of S INDEL and non-S INDEL PEDV, it is tempting to hypothesize that PEDV loss of virulence may be related to genomic alterations acquired through multiple cell passages.

On the other hand, numerous *in vivo* and *in vitro* studies provided evidence of newborns' increased susceptibility to PEDV, primarily attributed to key anatomical and physiological differences in intestinal development and NK cell activity compared to older pigs (305,306). Additionally, other research underscores the importance of innate immune effectors in controlling PEDV, revealing that mucosal production of type I and III IFNs and proinflammatory cytokines after infection establishes a protective antiviral state (238,364,365,397,398,502,503). Given these findings, it is reasonable to hypothesize that differences in the severity of PED outbreaks may arise from age-related and PEDV strain-specific variations in IFN and cytokine expression in the intestine. Therefore, understanding how the expression of these antiviral molecules changes with age and across different PEDV strains could be essential for developing targeted antiviral therapies against PEDV.

Finally, the detection of PEDV in the upper respiratory tract and alveolar macrophages suggests alternative mechanisms of transmission and replication (222,504,505), which, if

clarified, could further enhance understanding of the disease pathogenesis and shed light on the mechanisms involved in adaptation to new host tissues and cell types.

Objectives

Considering the abovementioned elements, the main objective of the present PhD thesis was to characterize the early immunopathogenesis of the infection by different PEDV strains (S INDEL and non-S INDEL) in piglets of different ages as well as in alternative models.

This general objective was approached through three specific objectives:

1- To identify potential determinants of virulence in PEDV by analyzing genomic differences between cell-adapted and wild-type PEDV strains using a neonatal pig model (Study I).
2- To characterize innate immune responses in piglets after PEDV infection in both suckling and weaned pigs, and to assess whether disease severity correlates with the level of these responses (Study II).
3- To examine alternative transmission routes of PEDV *in vivo* and assess the role of alveolar macrophages using *in vitro* studies (Studies II and III).

PART II

Studies

CHAPTER 3

Study I

Clinical, pathological, and virological outcomes of tissue-homogenate-derived and cell-adapted strains of porcine epidemic diarrhea virus (PEDV) in a neonatal pig model.

Viruses. 2023 Dec 27;16(1):44. doi: 10.3390/v16010044.

Introduction

PEDV is considered a re-emerging virus in Europe and Asia and emerging in the USA with reports from pig industries over the past 30 years (4,182). The global PEDV paradigm changed in 2010 when highly virulent PEDV strains re-emerged in China, and later, in 2013, emerge for the first time in USA resulting in devastating outbreaks and significant economic losses (185,193,194). Since then, new PEDV variants, known as S INDEL strains due to multiple insertions and deletions in the S gene, have been identified in PED outbreaks with milder clinical signs on U.S. farms and subsequently worldwide (183,201). Currently, S INDEL strains are responsible for ongoing PEDV outbreaks in Europe, while highly pathogenic non-S INDEL PEDV strains continue to pose significant economic challenges to the pig industry in the USA and Asia (4).

The severity of PEDV outbreaks is influenced by various host and viral factors. While the strain type (S INDEL or non-S INDEL) is the primary viral factor affecting disease outcome, the age of the piglets is the most significant host-associated risk factor, with neonatal piglets experiencing higher mortality rates than weaned or older pigs (182). The intestinal innate immune response activated against PCoVs is another relevant host factor alongside the ability of both PEDV strains evading antiviral type I and III IFN and modulating of key intracellular pathways involved in apoptosis, the ER stress response, and autophagy (354,363).

The loss of PEDV virulence following its adaptation in Vero cells has been described in previous experimental *in vivo* and *ex vivo* studies (182). Despite the thorough analysis and comparison of the complete genomic sequences of both cell-adapted or field strains, the molecular basis linked to the decreased virulence in the cell-adapted PEDV strains are yet to be fully understood (301). On the other hand, pathogenesis studies comparing PEDV strains from the USA in conventional neonatal piglets demonstrated that non-S INDEL strains are generally more pathogenic than S INDEL strains. Specifically, non-S INDEL isolates showed increased severity across all analyzed parameters, including clinical signs, fecal viral shedding, and gross as well as histopathological lesions (301). However, there is a lack of experimental comparative studies between global and European strains to understand why the pathogenesis and impact of European strains is limited considering the more severe scenarios of Asia and the USA (193).

Therefore, the aim of the present study was to compare the acute pathogenesis of European S INDEL and USA non-S INDEL PEDV isolates in a 1-week-old piglet model. Also, we compared the pathogenesis of the same European S INDEL strain coming from an intestine homogenate of an affected piglet with the corresponding PEDV isolate after several passages in

Vero cells. Finally, we discussed about the possible molecular bases that might be related to the loss of virulence of the cell-adapted isolate.

Materials and Methods

Ethics statement

Pig experiments were approved by the Animal Welfare Committee of the *Institut de Recerca i Tecnologia Agroalimentàries* (CEEA-IRTA, registration number CEEA 86/2022) and by the Ethical Commission of Animal Experimentation of the Government of Commission of Animal Experimentation of the Government of Catalonia (registration number 11560) and conducted by certified staff. Experiments with PEDV were performed at the Biosafety Level-2 (BSL-2) facilities at IRTA-Monells (Girona, Spain).

Viral inoculum

Isolation and characterization of the European GIb PEDV S-INDEL strain Calaf 2014 (GenBank accession number MT602520.1) have been described elsewhere (472). Briefly, the inoculum was obtained from four 3-day-old piglets intragastrically inoculated with 2 mL of the intestinal content of conventional piglets with confirmed PEDV infection and showing diarrhea. Small intestine content diluted 1/100 with 1x phosphate-buffered saline (PBS) solution was obtained at 48 hpi when animals were euthanized after developing severe diarrhea. This suspension, after filtration (Merck & Co., Darmstadt, Germany, SLGV013SL), was used directly as experimental inoculum and named CALAF-HOMOG. On the other hand, the same virus was subsequently isolated, adapted and passaged in Vero Cells (ATCC, CCL-81) with 10 µg/mL of trypsin following a previously described procedure (472). This inoculum was used in this study and named as CALAF-ADAP (viral titer of $10^{5.3}$ 50% tissue culture infectious dose ($TCID_{50}$)/mL, passage 22).

The isolation and characterization of the GIIb USA PEDV isolate USA/NC49469/2013 (GenBank accession number KM975737) have been reported elsewhere (301). This strain was kindly provided by Dr. J.Q. Zhang and D.M. Madson (Iowa State University Veterinary Diagnostic Laboratory, USA). Propagation of the virus on Vero cells (ATCC, CCL-81) yielded a virus to a viral titer of 10^6 $TCID_{50}$/mL (passage 8) and was used in this study as the PEDV-USA inoculum.

All PEDV inoculum used in this study were confirmed negative for TGEV, porcine rotavirus A (PRV-A) (both pathogens tested with Thermo Fisher Scientific, Carlsbad, CA, USA, 4486975),

PRRSV (Thermo Fisher Scientific, Carlsbad, CA, USA, A35751) and PCV2 (Thermo Fisher Scientific, Carlsbad, CA, USA, QPCV). For this purpose, inoculum samples were centrifuged at 2500 rpm at room temperature (RT), and RNA and DNA extraction was performed with the MagMAX pathogen RNA/DNA kit (Thermo Fisher Scientific, Carls-bad, CA, USA, 4462359) according to the manufacturer's instructions. The PEDV viral load (expressed as Ct value) of the CALAF-ADAP, CALAF-HOMOG, and PEDV-USA inocula were 13.37, 16.81, and 18.26, respectively.

Sequencing and phylogenetic analysis of the inocula

A comparison of complete genome sequences of the three inocula was carried out previously to the experimental phase. The complete sequence of the CALAF-HOMOG isolate was obtained from the GenBank database (MT602520.1). The complete sequence of the isolates CALAF-ADAP and PEDV-USA were subjected to genome sequencing. In addition, a comparison of the complete genome sequence was also carried out between the Vero cell-passed PEDV-USA inoculum and the original strain obtained from the GenBank database (KM975737). The sequencing procedure was carried out at the Institute of Biotechnology and Biomedicine (IBB) of the *Universitat Autònoma de Barcelona* (UAB) following a previously established protocol. Briefly, sequencing was performed using the Illumina Miseq Platform following RNA extraction using MagMAX pathogen RNA/DNA kit. RNA purification assessment was performed before sequencing using BioDrop µLite (Isogen Life Science, Utrecht, NL, 80-3006-51). The translation of the nucleotide to aa sequence was obtained with the Expasy program and the alignment of the nucleotide and aa sequences with the Clustal Omega command included in the unified bioinformatics toolkit Unipro UGENE (506). The graphics were obtained using the program Geneious Prime by Dotmatics (version 2023.1.2).

A phylogenetic analysis was carried out with PEDV sequences from inocula which were aligned together with a total of 53 PEDV complete genome sequences available in the GenBank database (Table 3.1) using the Clustal Omega software. The MEGA-X64 software was employed to determine the optimal substitution method, and the Seaview software was utilized to validate and rectify the alignment as well as to construct the phylogenetic tree along with iTOL program. Maximum Likelihood was used as the reconstruction method and the branch supports were calculated by using the Shimodaira–Hasegawa [SH]-approximate likelihood ratio test (aLRT) (507).

Table 3.1. Identification and classification of the selected 53 PEDV isolates for phylogenetic analysis. The PEDV strains used in this study are highlighted in black.

Global distribution	Genotype (G)	Name of the PEDV isolate	GenBank database	References
USA	IIa	Wisconsin74/2013	KJ645669	(183)
	IIa	Minnesota100/2013	KJ645691	(183)
	IIa	**NC/2013/49469**	**KM975737**	(301)
	IIb	NC35140/2013	KM975735	(301)
	IIb	Texas31/2013	KJ645639	(183)
	IIb	Minnesota94/2013	KJ645686	(183)
	Ib	Minnesota58/2013	KJ645655	(301)
	Ib	Indiana12.83/2013	KJ645635	(183)
	Ib	strainOH851/2014	KJ399978	(199)
ASIA	IIa	CHINA/strainJS-A/2017	MH748550	(199)
	IIa	CHINA/strainFL2013/2015	KP765609	(199)
	IIa	VIETNAM/strainHUA-14PED96/2014	KT941120	(199)
	IIa	SK/isolateKNU-1305/2014	KJ662670	(301)
	IIb	CHINA/strainLC/2011	JX489155	(299)
	IIb	JPN/strainOKN-1/JPN/2013	LC063836	(199)
	IIb	CHINA/strainNW8/2015	MF782687	(199)
	IIb	VIETNAM/cloneVN/JFP1013_1/2013	KJ960178	(301)

	IIb	CHINAstrainCH/SCZY44/2017	MH061338	(199)
	IIc	CHINA/isolateCH/JXJA/2017	MF375374	(199)
	IIc	CHINA/strainYC2014/2014	KU252649	(199)
	IIc	CHINA/strainCH/SCZG/2017	MH061337	(199)
	Ia	SK/strainVirulentDR13/2009	JQ023161	(301)
	Ia	CHINA/strain85-7/2013	KX839246	(199)
	Ia	KOREA/isolateSM98/1998	GU937797	(199)
	Ib	CHINA/strainCH/S/1986	JN547228	(199)
	Ib	CHINA/strainSD-M/2012	JX560761	(299)
	Ib	CHINA/isolateJS2008/2013	KC109141	(299)
	Ib	SK/isolateKNU-1406-1/2014	KM403155	(301)
EUROPE	Ia	CV777-Prototype	AF353511	(299)
	Ib	GER/L00721/GER/2014	LM645057	(202)
	Ib	GER_L01020-K01_15-10_2015	LT898413	(199)
	Ib	GER_L00919-K17_14-02_2014	LT898421	(204)
	Ib	BEL/15V010/BEL/2015	KR003452	(301)
	Ib	FRA/001/2014	KR011756	(301)
	Ib	FRA/FR2019001/2019	MN056942	(508)
	Ib	HUN/5031/2016	KX289955	(508)
	Ib	HUN/strainS236	MH593900	(508)

	Ib	SLOreBAS-2/2015	KY019624	(199)
	Ib	SLO/JH-11/2015	KU297956	(199)
	Ib	AUSTRIA_L01065-M10_15-04_2015	LT898418	(204)
	Ib	ROMANIA_L01329-K25_15-01_2015	LT898436	(204)
	IIb	Ukraine/Poltava01/2014	KP403954	(204)
	Ib	RUSSIA/PEDV/Belgorod/dom/2008	MF577027	(509)
	Ib	ITA/PEDV1842/2016	KY111278	(29,209)
	Ib	ITA/Italy/7239/2009	KR061458	(509)
	Ib	**ESP/PEDV/Pig-wt/Calaf-1/2014**	**MT602520**	(472)
	Ib	ESP/1931-1-Valladolid-Molpeceres/2017	MN692784	(29,209)
	Ib	ESP/2181-Castellon-Cati/2018	MN692790	(29,209)
	Ib	ESP/2098-1-Malaga-Casares/2018	MN692787	(29,209)
	Ib	ESP/H3-Barcelona-Vic/2019	MN692792	(29,209)
	Ib	ESP/1481-Pamplona-Tudela/2014	MN692774	(29,209)
	Ib	ESP/1776-Badajoz-Alburquerque/2016	MN692781	(29,209)
	Ib	ESP/1521-Segovia-Navas_de_Oro/2014	MN692776	(29,209)

Experimental design

A total of twenty 3-5-day-old piglets from 5 sows, negative by RT-qPCR for PEDV and TGEV in feces and with no antibodies against both viruses, were selected and transported to the experimental farm (IRTA-Monells, Girona, Spain). Sows were also negative against PRRSV and PCV2 in serum by RT-qPCR and qPCR, respectively. Upon arrival to the facilities, animals were weighed, and randomly distributed into four pens of 5 animals/pen, based on body weight, gender, and sow origin. Four experimental groups were considered attending to the inoculum administered: 1) S INDEL PEDV strain Calaf 2014 passaged in Vero cells (CALAF-ADAP), 2) S INDEL PEDV strain Calaf 2014 from intestine homogenate (CALAF-HOMOG), 3) non-S INDEL PEDV strain USA NC4969/2013 passaged in Vero cells (PEDV-USA), and 4) PBS (negative control group, C-NEG).

At study day (SD) 0, all animals were orogastrically inoculated with $5x10^{4,5}$ $TCID_{50}$ of each of the corresponding PEDV isolates in a 5 mL volume or with saline solution (C-NEG). Pigs were scored for clinical signs (rectal temperature and diarrhea) at 0 hpi before challenge and every 12 h until necropsy (at 48 hpi). Diarrhea severity was assessed using a scoring system: 0, normal feces; 1, soft and/or pastry feces; 2, liquid feces with some solid content; and 3, watery fecal content. Rectal temperature below 40ºC was considered normal and ≥40ºC was considered fever. Body weight and blood samples were recorded and collected at 0 hpi (before challenge) and repeated at necropsy (48 hpi). Rectal swabs (RS) were collected before challenge (0 hpi) and at 24 and 48 hpi in 500 µL of Minimum Essential Media, MEM (Thermo Fisher Scientific, Carlsbad, CA, USA, 21090022) supplemented with 1% penicillin/streptomycin (Thermo Fisher Scientific, Carlsbad, CA, USA, 15140122) to determine fecal PEDV shedding by RT-qPCR. Viral infectivity (expressed as log10 $TCID_{50}$/mL) was extrapolated from the Ct values of the jejunum content using standard curve, as previously described (510).

Nucleic acid extraction and RT-PCR/PCR for detection of viral pathogens

Viral RNA extraction from feces and swabs at 0, 24 and 48 hpi, and from small intestinal (jejunum) content at 48 hpi were done following the procedure previously described (472). Briefly, RS and feces were diluted with PBS supplemented with 1% penicillin/streptomycin (feces were diluted 1/10) and, after vortexing the samples, RNA extraction was performed with the MagMAX pathogen RNA/DNA kit described previously according to the manufacturer's instructions. Detection and quantification of PEDV, TGEV and PRV-A were performed with the commercial qPCR kits described previously. Also, PRRSV and PCV2 were ruled out in serum from

all pigs at 0 hpi by means of the previously mentioned RT-qPCR and qPCR methods, respectively. Results were expressed as Ct values as expression of the viral load in serum and/or resuspended feces/swabs.

ELISA tests

Presence of antibodies against PEDV and TEGV in serum at 0 hpi were tested using commercial ELISAs Ingezim PEDV (Ingenasa, Madrid, Spain, 11.PED.K1) and Ingezim TGEV 2.0 (Ingenasa, Madrid, Spain, 11.TGE.K3) kits, respectively according to the manufacturer's instructions. Results were expressed as mean S/P titers. For PEDV, the kit employs an indirect ELISA, with results classified as positive (>0.35) or negative (<0.35). For TGEV, the kit uses a capture blocking ELISA, categorizing results as positive (<1.0008), negative (>1.1676), or doubtful (1.0008–1.1676).

PEDV genome sequencing

Jejunal contents at 48 hpi of all experimentally inoculated animals were subjected to viral sequencing at the IBB of the UAB following the procedure described above. One animal from each group (the one with the lowest Ct value) was selected to compare the complete genomic sequences between the different PEDV strains recovered at 48 hpi with the corresponding inoculum.

Pathological analyses and immunohistochemistry (IHC)

All pigs were euthanized at 48 hpi with an overdose of pentobarbital. Complete necropsies were performed, and the small intestine (jejunum and ileum), caecum, colon, and MLN were examined for gross lesions by European College of Veterinary Pathologists (ECVP)-certified veterinary pathologists, blinded to the treatment groups. Intestinal wall findings were scored as: 0, normal; 1, thin-walled or gas-distended; 2, presence of both. Contents of small intestine, caecum and colon were examined and scored following the scoring system: 0, normal; 1, pastry; or 2, watery content.

Small intestine, colon and MLN were collected in 10% neutral-buffered formalin and embedded in paraffin. Tissues were processed and stained with hematoxylin and eosin (H&E) using standard laboratory procedures. Villus lengths and crypt depths were measured from ten

representative villi and crypts of middle jejunum per animal (353). VH:CD ratio was calculated as the quotient of the mean villus length divided by the mean crypt depth.

An IHC technique to detect PEDV nucleoprotein using a rabbit monoclonal antibody (Medgene Labs, Brookings, SD, USA, SD6-29) at dilution 1/5000 was performed on selected tissues (jejunum, ileum, colon, and MLN). After deparaffinization and hydration of the samples, peroxidase blocking was performed with methanol 3% H_2O_2 for 30 min at RT. Antigen retrieval with citrate buffer pH6 (Dako/Agilent Technologies, Santa Clara, CA, USA, S169984-2) at 98ºC for 20 min plus 30 min at RT was performed after washing the samples with PBS. The primary antibody was added after blocking the specific binding with PBS-Tween 20% and 2% Bovine Serum Albumin (BSA). After overnight incubation with the primary antibody at 4ºC, the CRF-Anti-polyvalent HRP Polymer/ScyTeck (Quimigen, Madrid, Spain, ABZ125) and 3,3'-diaminobenzidine (DAB) (Sigma-Aldrich/Merck & Co, Darmstadt, Germany, D5637) were added as secondary antibody and chromogen substrate, respectively. Finally, slides were counterstained with hematoxylin.

For intestinal tissues, the amount of viral antigen was semiquantitatively scored from 0 to 3. Score 0 was assigned to tissues with no PEDV staining. Scores 1, 2, and 3 were assigned to tissues with less than 30%, 30–60%, or more than 60% of PEDV-immunolabeled enterocytes, respectively. The evaluation was performed in 10 high-power fields (HPF; magnification, 400×). The IHC scoring in MLN, also from 0 to 3, was assigned to tissue with a lack of immunolabeled cells (0), and the detection of 10–30, 30–50 and more than 50 PEDV-immunolabeled cells received scorings of 1, 2 and 3, respectively.

Statistical analyses

Comparisons between groups and times of body weight, temperature and VH:CD ratio were calculated using ANOVA. The analysis of diarrhea, gross findings and histopathological data was performed using a generalized linear model with a binary response. The Ct values of the PEDV RT-qPCR of the RS and jejunum contents were compared among groups using the Kruskal–Wallis Test. In all tests, *p*-values for pairwise comparisons were adjusted for multiplicity using Tukey's correction for parametric tests and Bonferroni's correction for nonparametric tests. Statistical analyses were performed with the SAS system version 9.4 (SAS Institute Inc., Cary, NC, USA). Graphics were generated using GraphPad Prism 8. In all analyses, a p-value < 0.05 was considered statistically significant.

Results

Both CALAF inocula had similar genomes and showed more variation in their sequences when compared to the PEDV-USA one

The CALAF-ADAP inoculum showed a high nucleotide identity compared to CALAF-HOMOG, displaying a consistent 99.91% similarity between their sequences. Likewise, the PEDV-USA strains (original and cell-passaged) exhibited 99.98% similarity. In contrast, the CALAF-HOMOG and cell-passaged PEDV-USA genomes were only 98.7% identical, revealing 356 discrepancies in their nucleotide sequences. These variations were notably concentrated within the aa sequence of the S protein, followed by the ORF1ab, N, ORF3, and M viral proteins across all PEDV inocula. The aa sequence differences between both CALAF inocula were primarily concentrated in Nsp-2, -3 (PLPro), -4, -12 (RdRp), and -15 (NendoU), within the NTD/SO and RBD sequences of S1, and within HR1 and HR2 of S2. Remarkably, this investigation unveiled the exceptional conservation of the E protein across various PEDV strains, with no alterations observed even after extensive cell-culture passaging.

The complete genomes of the CALAF-HOMOG and PEDV USA strains were compared to a total of 53 global PEDV strains sourced from GenBank (Figure 3.1). Our results confirmed that both PEDV strains belong to distinct genogroups, specifically, S INDEL and non-S INDEL, respectively.

The phylogenetic analysis revealed that European PEDV strains re-emerging since 2010 belong to the S INDEL genogroup, primarily within the GIb clade, except for the 2014 Ukraine strain. This latter strain clusters within the GIIb clade alongside non-S INDEL strains from America and Asia, consistent with prior findings (202). The close alignment of the Calaf 2014 strain with most European strains from 2014–2015 implies a common origin for PEDV reintroduction into Europe in 2014. Notably, American and Asian S INDEL strains within the G1b clade (Indiana12.83/2013, Strain OH851/2014, Minnesota58/2013, and SK/KNU-1406/2014) show relative proximity to European S INDEL strains from 2014–2015, suggesting potential origins for re-emerging PEDV strains in Europe as proposed (204,217). Conversely, the non-S INDEL USA strain (NC/2013/49469) closely aligns with other American PEDV strains from 2013–2014, all falling within the GIIa clade, indicating widespread dissemination of PEDV in the United States since its introduction in 2013. Spanish S INDEL strains exhibit distinct subgroups within separate branches, with strains from 2013-2015 displaying a more branched pattern and strains from 2016-2019 showing high sequence conservation.

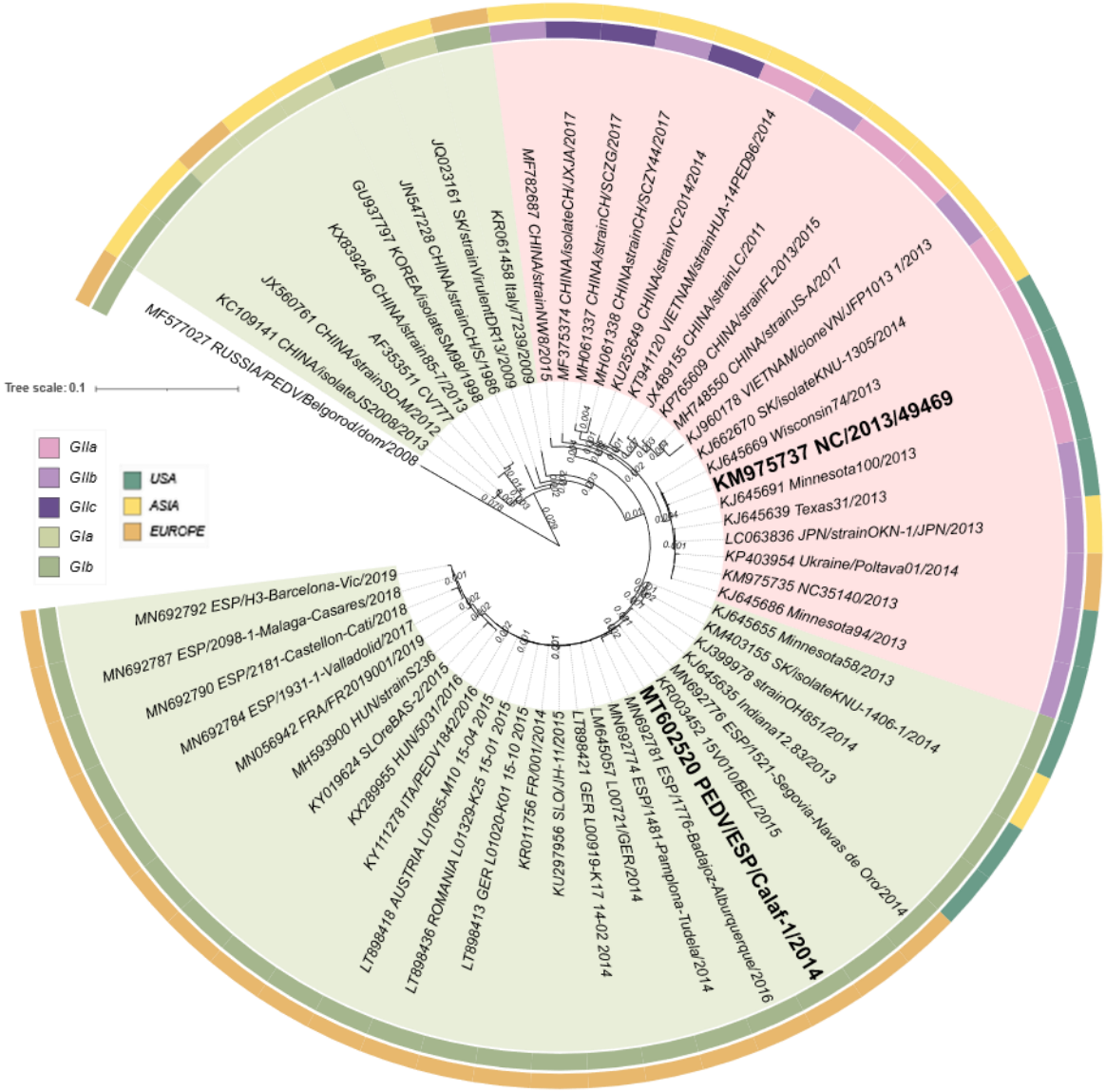

Figure 3.1. Phylogenetic analysis of PEDV strains in Europe (orange), USA (dark green) and Asia (yellow). The selected 53 PEDV isolates are categorized as S INDEL (light green, inner circle) or non-S INDEL strains (pale pink, inner circle). They are further classified into genotypes: GIa (green, middle circle), GIb (olive green, middle circle), GIIa (pink, middle circle), GIIb (purple, middle circle), and GIIc (dark purple, middle circle). The internal numbers represent branch distances. Tree scale: 0.1.

Clinical outcome varies depending on the PEDV isolate

Compared to starting weight (0 hpi), PEDV-USA-inoculated piglets showed a significant weight loss (p<0.05) at 48 hpi, while no major weight variation was observed in CALAF-HOMOG piglets, and animals from PEDV-ADAP and C-NEG groups significantly gained weight (p<0.05) (Figure 3.2A). Weight at 48 hpi was significantly different among groups, with the lower weight for the PEDV-USA inoculated piglets followed by the CALAF-HOMOG ones and the remaining two

groups; no significantly different weight at 48 hpi was observed between piglets that received CALAF-ADAP or PBS (Figure 3.2B).

All three groups inoculated with PEDV isolates developed diarrhea (Figure 3.2C), which varied between average scores 1 and 2. Diarrhea was first detected at 24 hpi with a score of 1 (pasty diarrhea) in both the PEDV-USA and CALAF-HOMOG groups and evolved to liquid (score of 2) only in the PEDV-USA group at 48 hpi. Regarding PEDV-ADAP, diarrhea had a slower and milder course, characterized by soft feces (score of 1) at 48 hpi. Even so, no significant differences were observed between the PEDV-USA, CALAF-HOMOG and CALAF-ADAP groups in terms of mean diarrhea scoring (p<0.05). No vomiting or fever was observed in any piglet throughout the study.

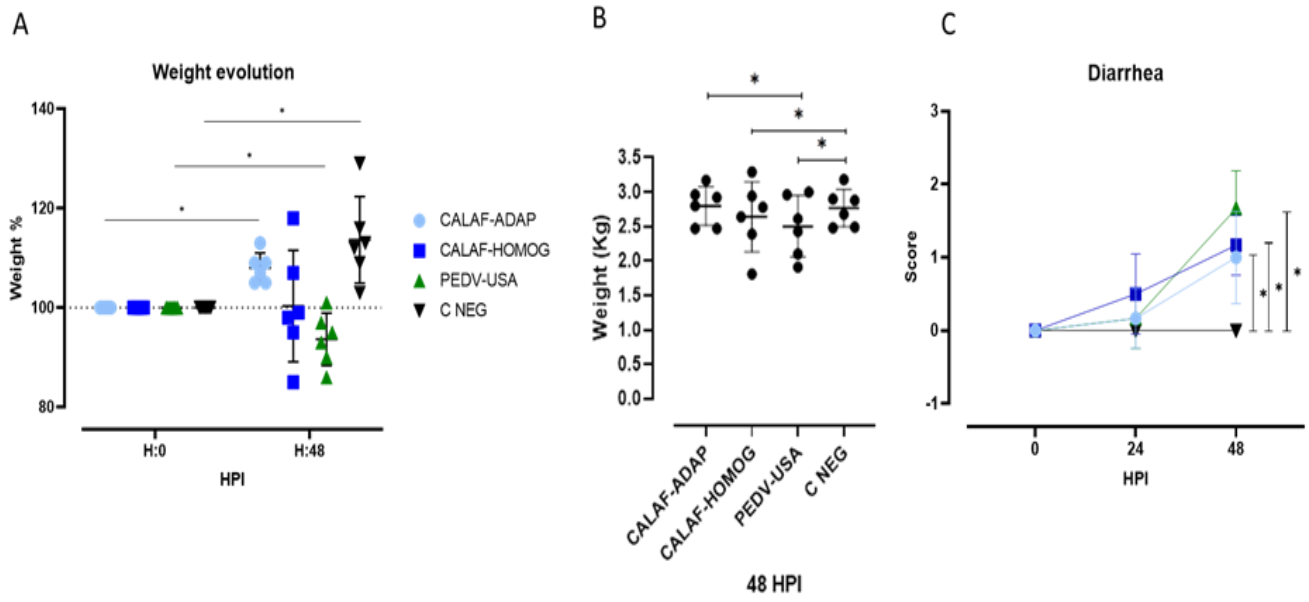

Figure 3.2. (A) Individual and average weight (represented in % with respect to the initial weight) of the experimental groups at 0 and 48 hpi. While piglets inoculated with the PEDV-USA strain showed weight loss at 48 hpi, piglets inoculated with CALAF-ADAP and those from C-NEG gained weight (p<0.05). No significant differences in weight were observed in the CALAF-HOMOG group between 0–48 hpi. (B) Individual (dots) and average (line) weight (in kg) of studied piglets within each experimental group at 48 hpi. The PEDV-USA strain caused a significant weight reduction compared to the rest of the groups, but no significant differences were observed between the different study groups. (C) Evolution of diarrhea from all experimental groups until the end of the study (48 hpi). Score for diarrhea: 0 = Normal stools; 1 = Soft and/or pasty feces; 2 = Liquid with some solid content and 3 = Watery feces. Pasty diarrhea started at 24 hpi in both the PEDV-USA and CALAF-HOMOG groups, but the CALAF-ADAP strain caused mild (pasty) diarrhea later than the other groups (48 hpi). At 48 hpi, the PEDV-USA group showed severe watery diarrhea compared to the CALAF-HOMOG group. No differences were observed between the CALAF-HOMOG and CALAF-ADAP groups at the end of the study. Asterisk means significant difference between groups (p<0.05).

PEDV antigen was present in the jejunum and ileum, but only the PEDV-USA and CALAF-HOMOG isolates caused intestinal damage

The summary of individual scores related to intestinal wall and digestive contents is displayed in Figure 2. At 48 hpi, both the PEDV-USA and CALAF-HOMOG strains caused similar lesions in the enteric tract regarding the studied parameters (Figure 3.3A); interestingly, the intestinal wall and content scores caused by the PEDV-ADAP were significantly lower ($p < 0.05$). In the PEDV-USA and CALAF-HOMOG groups, the intestinal wall was thin and transparent, distended by gas (score 2) and with yellowish watery contents (score 2) (Figure 3.3B). On the other hand, the CALAF-ADAP strain caused no or mild lesions in the intestinal wall characterized by mildly thin or gas-distended walls (score 1) with pasty contents (score 1), which were similar to the C-NEG group.

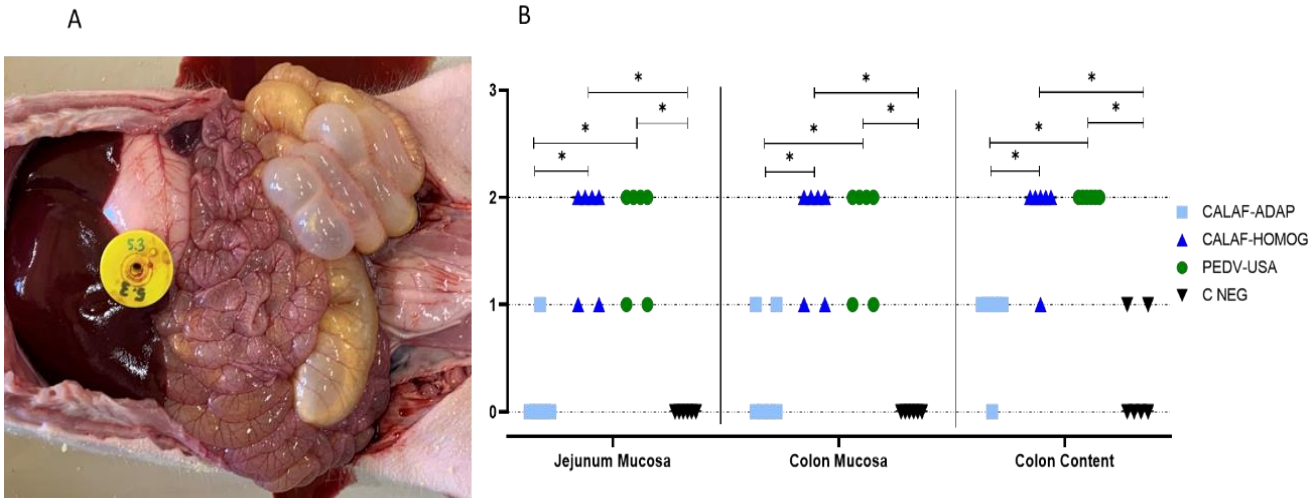

Figure 3.3. Gross pathological findings at 48 hpi after inoculation of the PEDV-USA strain. (A) Severe form of the disease characterized by marked dilation of the intestinal loops with large amounts of gas and fluid content in both the small and large intestines. (B) Damage to the mucosa (wall) of the jejunum and colon at 48 hpi (ranging from normal (0) to thin-walled and gas-distended wall (2)) and content of the colon at 48 hpi (solid (0); pasty (1) and watery (2) content). Both PEDV-USA and CALAF-HOMOG strains caused similar severe wall lesions in the jejunum and colon at 48 hpi, characterized by thin and gas distended-walls. However, no significant lesions were observed in the jejunum and colon wall in CALAF-ADAP and negative control group. Furthermore, both PEDV strains (PEDV-USA and CALAF-HOMOG) caused severe watery diarrhea in the large intestine at 48 hpi compared to the CALAF-ADAP strain, which caused pasty diarrhea ($p<0.05$). Asterisk means significant difference between groups ($p<0.05$).

Histological intestinal lesions in PEDV inoculated piglets consisted of enterocyte swelling and villous fusion and atrophy (Figure 3.4A–D) and were severe in jejunum and ileum in all piglets from PEDV-USA and CALAF-HOMOG groups at 48 hpi. Intestinal atrophy and fusion were characterized by a marked reduction in intestinal VH, causing a decreased VH:CD ratio (Figure

3.4E), which was significantly (p<0.05) more severe in the PEDV-USA-inoculated pigs compared to the ones of the CALAF-HOMOG group (mean VH:CD ratio of 1.52 and 3, respectively). No intestinal lesions were observed in piglets from the PEDV-ADAP group, which showed a similar VH:CD ratio than C-NEG animals (mean VH:CD ratio of 5.5) (Figure 3.4E).

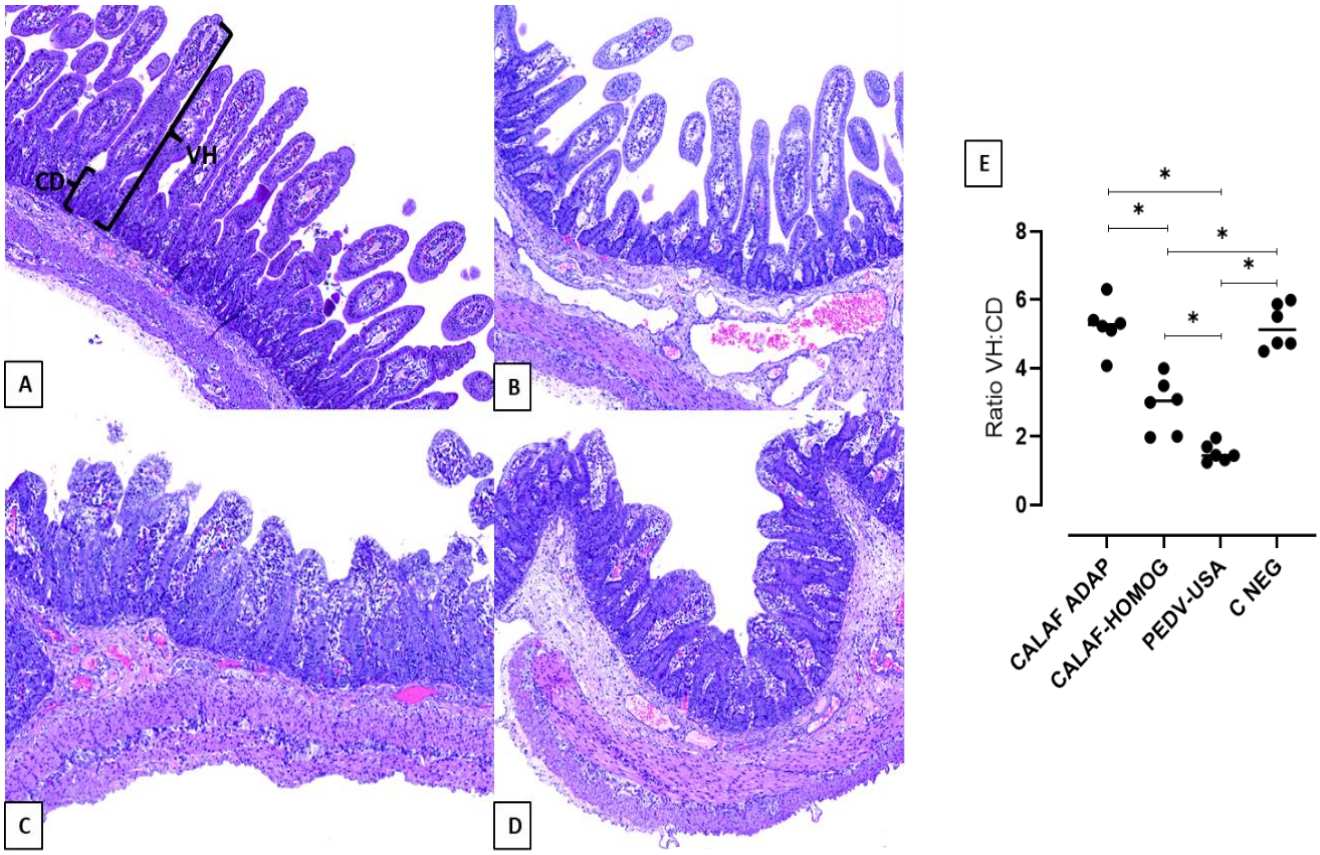

Figure 3.4. Jejunum at 48 hpi from the negative control (A), CALAF-ADAP (B), CALAF-HOMOG (C) and PEDV USA (D) stained with hematoxylin and eosin (H&E). While no histological damage was observed in groups A and B, similar severe villous atrophy and fusion were observed in both C and D groups. (E) The degree of intestinal damage was measured by the villus-height-to-crypt- depth ratio (VH:CD). PEDV-USA caused a higher degree of atrophy and fusion of villi at 48 hpi, followed by PEDV-HOMOG. However, PEDV-ADAP did not cause epithelial damage (p<0.05). Asterisk means significant difference between groups (p<0.05).

In addition, atrophic enterocytes observed in piglets from PEDV-USA and CALAF-HOMOG groups showed cytoplasmic vacuolation (enterocyte degeneration), cell hypereosinophilia, cell retraction and nuclear pyknosis (enterocyte necrosis) and epithelial attenuation in the apical villi (Figure 3.5). None of these features were observed in small intestine sections of animals inoculated with the CALAF-ADAP isolate or in piglets that received PBS.

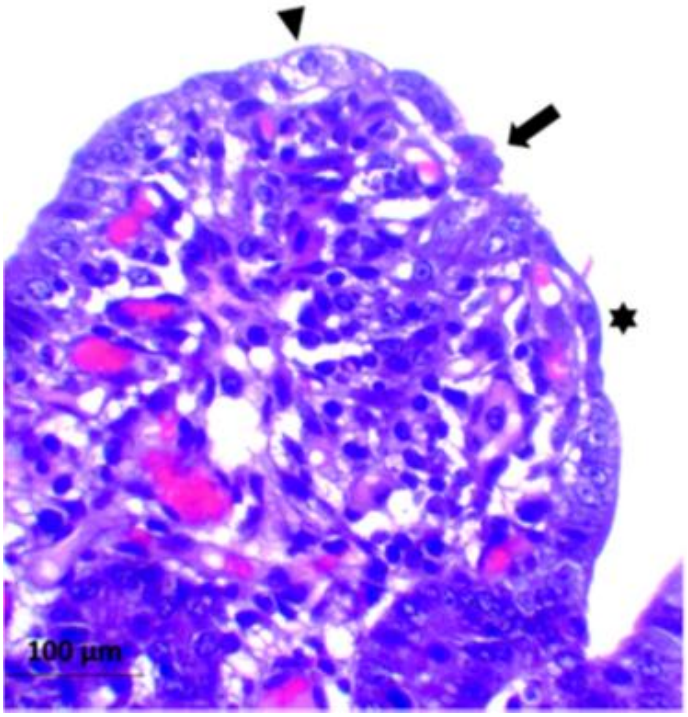

Figure 3.5. Epithelial damage and degeneration in PEDV-infected enterocytes at 48 hpi, stained with Hematoxylin and Eosin (H&E). The apical portion of the atrophic and fused villi is lined by either vacuolated cuboidal epithelium (degeneration, arrowhead) or attenuated epithelium (asterisk), showing cellular retraction with cytoplasmic hypereosinophilia and nuclear pyknosis (necrosis, arrow).

PEDV antigen showed diffuse and granular staining patterns and was mainly located in the cytoplasm of the enterocytes of the apical part of the villi of the jejunum (Figure 3.6A–D) and ileum. While few PEDV-immunolabeled apical enterocytes were observed in the CALAF-ADAP-inoculated pigs, it was detected widespread in the cytoplasm of enterocytes in both PEDV-HOMOG and PEDV-USA piglets, coinciding with the areas of atrophy and fusion of villi.

PEDV antigen was also observed in few colonic apical enterocytes only in the case of PEDV-USA and CALAF-HOMOG inoculated piglets and in dendritic-like cells of the MLN in all PEDV inoculated animals (Figure 3.6E and Figure 3.6F, respectively). Although differences in viral detection by IHC were observed in the small and large intestines and in MLN among the three PEDV strains, these were not statistically significant (Figure 3.6G). Nevertheless, a notable trend emerged when comparing the CALAF-ADAP strain with the other two strains in the jejunum sections ($p<0.05$). Furthermore, the PEDV antigen detection in the MLN was greater in the PEDV-

USA strain when contrasted with both CALAF strains in terms of mean IHC scoring (mean of 3 in PEDV-USA group and 1.5 in both CALAF groups).

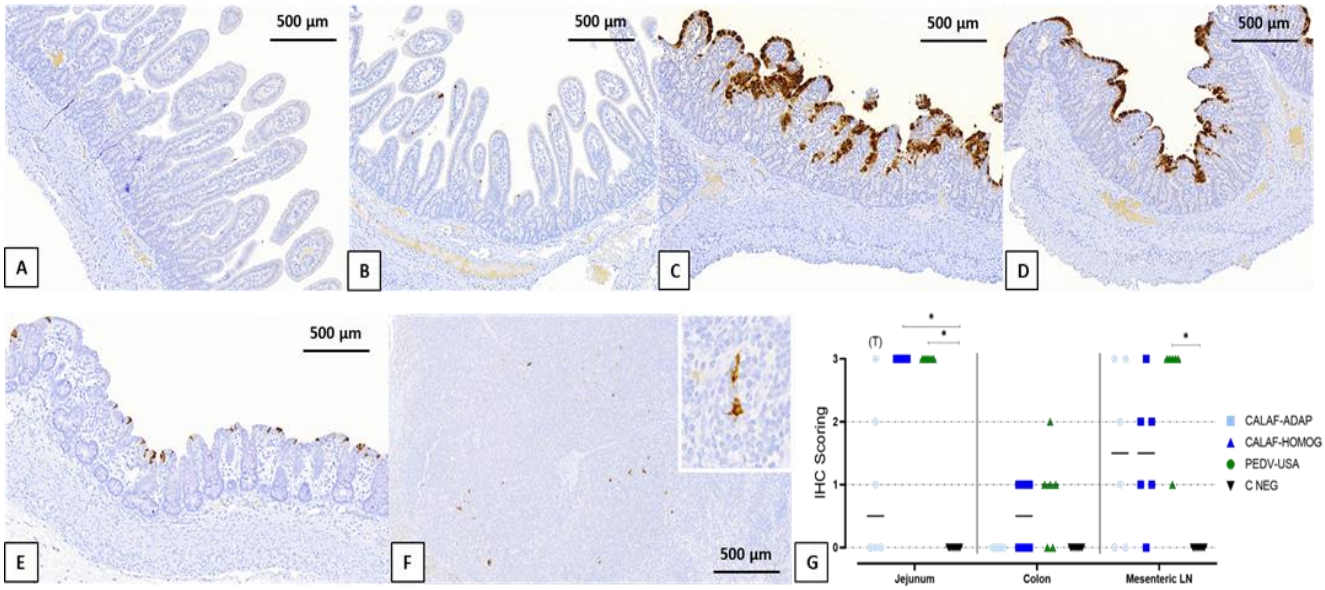

Figure 3.6. Detection of PEDV by IHC in sections of jejunum at 48 hpi from the negative control (A), CALAF-ADAP (B), CALAF-HOMOG (C) and PEDV-USA (D). Scattered PEDV-immunolabeled apical enterocytes were observed in the PEDV-ADAP group, whereas it was detected as widespread in the cytoplasm of enterocytes from the apical part of atrophic and fused villi in both PEDV-HOMOG and PEDV-USA. Scattered PEDV-immunolabeled apical enterocytes were also observed in a few colonic apical enterocytes (E) and in dendritic-like cells of the MLN (F) from a piglet inoculated with PEDV-USA strain. (G) Detection of PEDV by IHC in the middle jejunum, colon, and MLN at 48 hpi. PEDV was mainly detected in the middle jejunum in a similar distribution both for the PEDV-USA and PEDV-HOMOG strains and, less frequently, in the colon. PEDV-ADAP was less observed in the middle jejunum compared with the other strains. PEDV labeled was observed for the three viral strains in the MLN at 48 hpi, but it was more frequent and constant in the PEDV-USA group. Asterisk means significant difference between groups (p<0.05).

Occasionally, in piglets from PEDV-USA and CALAF-HOMOG groups, viral antigen was also observed in the cytoplasm of epithelial cells of the crypts of Lieberkühn and in interstitial mononuclear cells (compatible with histiocytic cells or dendritic cells) widespread throughout the lamina propria (Figure 3.7A and Figure 3.7B, respectively).

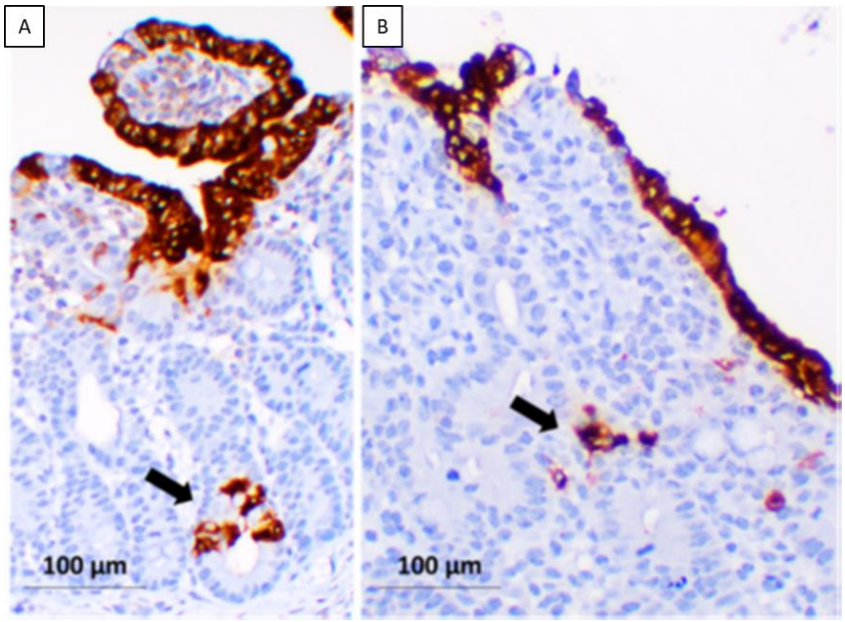

Figure 3.7. Scattered PEDV-immunolabeled cells were observed in a few intestinal glands (Crypts of Lieberkühn, arrow in A) and dendritic-like cells within the intestinal lamina propria (arrow in B).

All PEDV isolates replicated in the jejunum and were shed in feces at 48hpi with different viral loads depending on the isolate

The detection of PEDV RNA was analyzed by RT-qPCR in RS (0 and 48 hpi) and jejunal content (48 hpi) from all piglets. Viral inoculum, as well as all fecal samples throughout the whole study, were negative for TGEV and PRV-A, as determined by RT-qPCR. At 0 hpi, RS from all groups were negative for PEDV. However, the virus was detected in RS (Figure 3.8A) and jejunal contents (Figure 3.8B) at 48 hpi in all three viral inoculated groups, indicating that all PEDV isolates replicated and were shed in feces at that time post-inoculation. Although no significant differences were observed between the viral load of intestinal content or RS between the PEDV-USA and CALAF-HOMOG groups, their amounts were significantly higher than that of the CALAF-ADAP group (p<0.05). No PEDV RNA was detected in any C-NEG piglets.

Viral titers from jejunum content (extrapolated from Ct values) indicated that those of PEDV-USA strain were the highest ones, followed by the CALAF-HOMOG and the CALAF-ADAP isolates (viral titers of around 6, 4 and 2 log10 $TCID_{50}$/mL, respectively) (Figure 3.8C). Significant differences in viral titers among inoculated groups were only observed between the PEDV-USA and CALAF-ADAP strains (p<0.05).

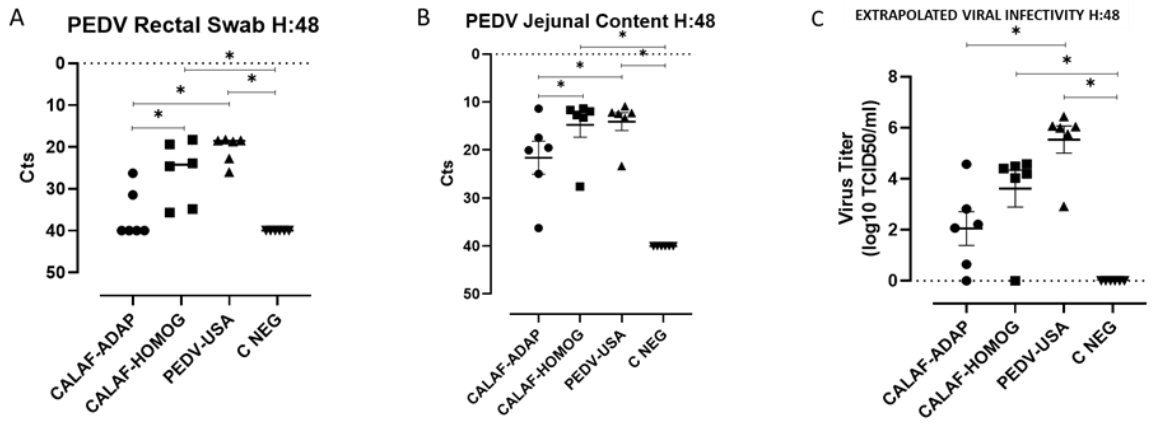

Figure 3.8. PEDV loads detectable in rectal swabs (A) and jejunal content (B) at 48 hpi. All PEDV isolates replicated in jejunal segments and were shed in faces at 48 hpi. No significant differences in viral load were observed between the CALAF HOMOG and PEDV-USA groups, but both were significantly higher than the CALAF-ADAP group. Estimated viral titer (C) (expressed as log10 $TCID_{50}$/mL) from jejunal content Ct values at 48 hpi. PEDV USA was the strain with the highest infectious virus titer, followed by the PEDV-HOMOG and PEDV-ADAP strains. Asterisk means significant difference between groups (p<0.05).

Sequences of inocula and viruses recovered from intestinal contents at 48 hpi were highly conserved

After 48 hpi, the PEDV sequences retrieved from the jejunal contents from inoculated piglets had a high degree of genomic similarity nucleotide identity with the consensus sequences of the PEDV-ADAP, CALAF-HOMOG, and PEDV-USA inocula (100%, 99.91%, and 99.98%, respectively).

Discussion

The present work focused on elucidating the early pathogenesis and severity of the clinical disease in a newborn piglet model for PEDV using different isolates. Specifically, we compared the clinical, pathological, and virological outcomes of cell-passaged USA non-S INDEL (PEDV-USA) and European S INDEL (CALAF-HOMOG), an intestine homogenate from a piglet inoculated with intestinal content of piglets infected with PEDV, as well as its cell culture adapted isolate (CALAF-ADAP).

Upon comparing the sequences of different inocula, notable distinctions among the three PEDV isolates were observed in the sequences of the nsp and S proteins, followed by N, M and ORF3 proteins. These viral proteins have been previously demonstrated to counteract host antiviral mechanisms through diverse molecular pathways, enhancing the virus's ability to evade innate immunity and promoting viral replication (75,115,132,365). The role of these viral

proteins in the clinical, pathological, and virological differences between PEDV S INDEL and non-S INDEL strains requires comprehensive studies, such as reverse genetics, mutagenesis or pseudovirus assays, to further investigate this hypothesis and obtain more robust conclusions. The sequencing analysis of fecal samples of inoculated piglets revealed the preservation of the PEDV genome at 48 hpi, remaining almost identical to the initial inoculum across all three PEDV isolates. This implies that viral variation within the first 48 hpi is limited; the short period of time is probably not enough to accumulate significant mutations.

Globally, the results obtained in this study aligned with previous studies (182,301), demonstrating two major issues. First, the adaptation of PEDV in Vero cells (i.e., CALAF-ADAP isolate after 22 cell culture passages) attenuated the virulence of the original strain. In this study, the cell-adapted S INDEL isolate did not reproduce evident clinical signs or cause intestinal lesions when compared to the same strain derived from intestinal homogenate. Notably, the differences observed between the genomic sequences of different PEDV inocula could have arisen subsequently to cell passages, suggesting an important role in the attenuation of the cell-adapted PEDV strain. The differences between the two S INDELs inocula genomes in this study were exclusively located in nsp2, 3 (PLPro), 4, 12 (RdRp) and 15 (NendoU) genes, within the ORF1a/b, as well as RBD, HR1 and HR2 within the S gene. In many coronaviruses and other RNA viruses, HR1- and HR2-coded proteins progressively interact to form a 6-HB, facilitating viral entry into host cells and resulting in complete fusion between the viral envelope and the host cell membrane (75,166). These genomic differences suggested that the attenuation of cell-adapted PEDV strains after several cell passages may be related to abnormalities in the viral replication machinery and the production of IFN antagonists (regulated by nsp) or by preventing the fusion and entry of the virus into the cell (either due to a receptor alteration or an abnormal formation of the 6-HB). However, without detailed studies on these viral protein alterations, other factors could explain the phenotypic differences among the PEDV strains.

A second issue of the present study was the fact that the cell-passaged non-S INDEL isolate (PEDV-USA) caused more severe disease in newborn piglets compared to the cell-passaged S INDEL one (CALAF-ADAP). However, the tissue homogenate derived from a PEDV S INDEL (CALAF-HOMOG) exerted comparable effects to the cell-passaged non-S INDEL for most of the studied parameters. Virulence attenuation has also been reported in non-S INDEL strains after multiple cell passages in Vero cells (301,316–318). The non-S INDEL isolate used in this experiment was previously passed by CCL-81 Vero cells prior to the challenge (passage 8). Considering that cell-passaging tends to attenuate PEDV isolates (182), it is very likely that a putative non-S INDEL tissue homogenate would have caused an even more severe outcome

compared to the CALAF-HOMOG strain used in the present study. Noteworthy, the potential virulence attenuation by cell passaging of the non-S INDEL isolate was probably lower than the S INDEL one since the former one was subjected to eight passages while the latter one to 22. The obtained results further support a previous study showing that the adaptability and loss of virulence of PEDV to cells increases with the number of cell passages (318).

In fact, the higher virulence of non-S INDEL compared to S INDEL isolates has been widely demonstrated (182,301). Consistent with these investigations, the results of our comparative study indicate that non-S INDEL strains induced more pronounced intestinal villi atrophy and fusion in the jejunum and ileum segments compared to S INDEL strains. In general terms, the greater the degree of intestinal atrophy, the smaller the absorptive surface, causing greater malabsorptive diarrhea (511). Accordingly, the loss of pathogenicity of the cell-adapted S INDEL strain was linked to the lack of atrophy and fusion of the jejunal sections.

Noteworthy, non-S INDEL (PEDV-USA) and S INDEL (CALAF-HOMOG) antigens were located in the jejunum and ileum segments as previously reported during the initial (up to 24 hpi) stages of PEDV infection (2,182,301). However, the non-S INDEL had a greater ability to spread to the colon and MLN than the S INDEL CALAF-HOMOG strain by 48 hpi. The presence of viral antigen in the jejunum coincided with the areas of atrophy and fusion of villi, demonstrating that it is a direct viral-induced damage (299). Interestingly, the amount of viral antigen was similar in both PEDV-USA and CALAF-HOMOG strains regardless of the degree of atrophy and villous fusion since there were significant differences in VH:CD between both groups. These results could suggest that the degree of enterocyte damage is not strictly related to the amount of virus but depends on other factors. It has been recently demonstrated that different PCoV species, including PEDV, can modulate apoptosis, ER stress response and autophagy to favor a viral environment (354). In the present study, both the PEDV-USA and CALAF-HOMOG strains showed evidence of enterocyte degeneration and death coinciding with areas of villous atrophy and fusion and the presence of viral antigen. These results could suggest that both PEDV strains could induce programmed cell death of PEDV-infected enterocytes to evade the innate immune response. Even so, more precise pathophysiology studies are needed to evaluate the differences in PEDV-associated cell damage between non-S INDEL and S INDEL strains. On the other hand, PEDV-ADAP antigen was also identified in the small intestine sections, even in the absence of intestinal damage, as observed in previously reported cases with cell-adapted strains (301). Interestingly, the IHC results of the cell-adapted S INDEL strain showed an increased ability of this strain to infect segments of the ileum rather than the middle jejunum, which differs from what has been previously described (182).

In addition, there was discernible variation in PEDV antigen detection within the MLN between non-S INDEL and S INDEL strains. These findings could imply a potential connection between the disparities observed in both strains and the potential development of an immunological response, possibly influenced by the quantity of PEDV-immunolabeled dendritic-like cells, which could play a significant role in disease response and control. Nevertheless, more extensive studies are needed to validate this hypothesis.

The virological assessment demonstrated that non-S INDEL (PEDV-USA) and S INDEL (CALAF-HOMOG) strains had similar loads in the jejunum and that they were shed to the equivalent amount in feces at 48 hpi. Since viral load titration was estimated from the RT-qPCR Ct values from intestine contents, these values may not be accurate enough, so it was not possible to definitively assess if the replication capabilities of the two abovementioned strains were truly different. However, considering the amounts of antigen (PEDV nucleoprotein) detected by IHC were fairly similar between groups, it is very likely that replication levels were similar among both. On the other hand, the CALAF-ADAP strain had significantly higher Ct values by RT-qPCR compared to the other two isolates, indicating lower loads in the jejunum and feces. This finding aligns with prior research that suggested cell-adapted S INDEL strains exhibited reduced shedding and replication efficiency compared to the non-cell-adapted S INDEL strains (182).

Conclusion

In conclusion, the USA non-S INDEL cell-passaged isolate resulted in a disease outcome similar to that of the European S INDEL strain from tissue homogenate. However, both of these isolates displayed significant distinctions in clinical, pathological, and virological aspects when compared to the European S INDEL cell-passaged isolate.

CHAPTER 4

Study II

The role of innate immune responses against two strains of PEDV (S INDEL and non-S INDEL) in newborn and weaned piglets inoculated by combined orogastric and intranasal routes.

Submitted for publication

Introduction

PED poses a significant threat to newborn piglets by unknown reasons, but it is hypothesized that the immaturity of their gastrointestinal tract and a weaker innate immune response compared to weaned pigs may contribute to the increased mortality (306,512). In addition to age, disease severity also varies depending on the PEDV strain, with non-S INDEL strains being more virulent than S INDEL ones as observed in our previous study, among others (301,305,309,513).

Recent transcriptomic analyses have revealed changes in the expression profiles of numerous innate immunity-related genes following PEDV infection, both in the small intestinal mucosa and *in vitro* cell cultures. Accordingly, the acute onset of diarrhea coincided with differentially expressed genes (DEGs) primarily associated with IFNs and proinflammatory cytokines (278,280,350) in IPEC-J2 cells and intestinal mucosa. However, other essential components of innate immunity, such as those involved in maintaining epithelial barrier integrity, goblet cell function, and the modulation of signaling pathways like MAPK (ERK1/2 and JNK/p38), JAK/STAT, PI3K-AKT/mTOR, and NF-kB, also show significant transcriptional changes upon PEDV infection in both the intestinal mucosa and various *in vitro* cell types (163,350,352,355–357). Additionally, biological processes including apoptosis, ER stress, and autophagy are also involved in the innate antiviral response against PEDV (353,354). These findings emphasize the importance of the mucosal innate immune response in PEDV pathogenesis.

The host innate immunity, a key part of mucosal defense, is crucial against PCoVs (363). During PEDV infection, IFNs and proinflammatory cytokines synthesized upon recognition by PRRs serve as primary effectors of innate immunity (75,364,365,368). Several studies have demonstrated significant alterations in the expression of proinflammatory cytokines following PEDV infection, including IL-1α, IL-1β, IL-6, IL-8, IL-10, IL-11, IL-12B, IL-18, IL-22, IL-27, CC chemokine ligands (CCL)2, CCL3, CCL4, CCL5 (RANTES), C-X-C motif chemokine ligand (CXCL)2, CXCL10, tumor necrosis factor (TNF)-α, transforming growth factor (TGF)-β, and IFN-γ (247,350,514). Notably, certain cytokines such as IL-11, IL-18, and IL-22 suppress PEDV replication, while IL-6 and IL-8 may contribute to viral persistence (275,439,502,503,515). On the other hand, both type I (IFN-α/β) and type III (IFN-λ) IFNs are generated upon PEDV infection (364,398,405) with type III IFN demonstrating greater effectiveness in inhibiting viral replication (398,406). Both type I and III interferons activate the JAK/STAT pathway to stimulate the expression of ISGs, which provide antiviral defense by inhibiting viral replication and strengthening adaptive immunity (408,412).

Previous studies investigating the innate immune response to PEDV have primarily utilized cell lines (such as Vero cells and IPEC-J2) or pigs (247,350,352,514,516). Nevertheless, comparative *in vivo* studies involving piglets of different ages are absent. Therefore, the objective of the present study was to compare early pathogenesis of PEDV infection and analyze the role of the innate immune responses in two different age groups, suckling, and weaned piglets, inoculated with either non-S INDEL or S INDEL PEDV isolates.

Materials and Methods

Ethics statement

Pig experiments were approved by IRTA-Committee and Ethical Commission of the Government of Catalonia such as study I (registration number CEEA 86/2022 and 11560, respectively). The experimental phase was also conducted at the BSL-2 facilities at IRTA-Monells.

Viral inocula

We used the same S INDEL (PEDV CALAF) and non-S INDEL PEDV isolates (PEDV USA) as in Study I. In study II, both inocula were prepared from jejunal contents and small intestine homogenates collected from one of the 5-day-old piglets intragastrically inoculated with each strain in Study I. For inocula preparation, original samples were diluted 1:5 with 1× PBS supplemented with 1% penicillin/streptomycin to a final volume of 90 mL. The mixture was centrifuged for 10 minutes at 800 g and subsequently stored at -80ºC until further use. RNA extraction, RT-qPCR, and viral titration were conducted in the same manner as in Study I, showing comparable viral RNA loads for both PEDV CALAF (Ct value of 12.65) and PEDV USA (Ct value of 11.30) isolates, with viral titers of 10^5 and 10^6 $TCID_{50}$/mL, respectively. Additionally, both inocula were confirmed negative for TGEV, PRV-A, PRRSV and PCV2 using the same kits than study I.

Experimental design

A total of eleven 5-day-old piglets from six sows, which tested negative for PEDV and TGEV in feces examined by RT-qPCR, and with no detectable antibodies against these viruses using commercial ELISAs (Ingenasa, Madrid, Spain, 11.PED.K1 and 11.TGE.K3, respectively), were selected and transported to the experimental farm at IRTA-Monells, Girona, Spain. The sows were also negative for PRRSV and PCV2 in serum, confirmed by RT-qPCR and qPCR, respectively.

Additionally, eleven 5-week-old piglets, also confirmed negative for the same pathogens, were selected and transported to the experimental facilities. Upon arrival, animals were weighed and randomly distributed to three physically separated rooms, with each room designated for a different inoculum: one for each PEDV strain (PEDV CALAF and PEDV USA) and one as a negative control. The experimental design consisted of six groups categorized by age and the type of inoculum administered: (1) 5-day-old piglets inoculated with S INDEL PEDV strain CALAF 2014 (PEDV CALAF 5d), (2) 5-week-old piglets inoculated with S INDEL PEDV strain CALAF 2014 (PEDV CALAF 5w), (3) 5-day-old piglets inoculated with non-S INDEL PEDV strain USA NC4969/2013 (PEDV USA 5d), (4) 5-week-old piglets inoculated with non-S INDEL PEDV strain USA NC4969/2013 (PEDV USA 5w), (5) 5-day-old piglets administrated with PBS (negative control group, CNEG 5d), and (6) 5-week-old piglets inoculated with PBS (negative control group, CNEG 5w). Groups 1–4 contained 4 piglets each, while groups 5 and 6 consisted of 3 piglets each. All had free access to water and were fed every six hours.

On SD 0, all animals were orogastrically inoculated with 5 mL of the corresponding PEDV isolate or saline solution (CNEG), and intranasally inoculated with 2 mL of the same inocula. Each animal received an equivalent viral titer (10^5 $TCID_{50}$/mL), irrespective of the PEDV isolate (510).

Pigs were monitored for clinical signs, including rectal temperature and diarrhea, at 0 hpi before challenge, and every 12 hours until necropsy at 48 hpi. Body weight was recorded and collected at 0 hpi (before challenge) and repeated at necropsy (48 hpi). RS were collected before challenge (0 hpi) and at necropsy, at 48 hpi for determining viral infectivity and fecal shedding by RT-qPCR. While all these parameters were obtained and analyzed in the same way as in Study I, diarrhea severity was assessed using a different scoring system (0: normal feces; 1: soft and/or pasty feces; 2: watery feces, with or without some solid content).

Nucleic acid extraction and RT-qPCR/PCR for detection of viral pathogens and detection of antibodies against PEDV and TGEV

Viral RNA/DNA extraction, along with the detection and quantification of various viral pathogens—such as PEDV, TGEV, PRV-A, PRRSV, and PCV2—and the detection of antibodies against PEDV and TGEV in serum samples from piglets and their dams, were performed using the same commercial kits as in Study I. For this study, PEDV RNA was obtained from RS, jejunal content, intestinal wall (jejunum and colon), nasal turbinate and lungs homogenate from inoculated piglets after 48 hpi and was expressed as Ct values.

Pathological analyses and immunohistochemistry

All pigs were euthanized at 48 hpi with an intravenous overdose of pentobarbital. Complete necropsies were performed, and the small intestine (jejunum and ileum), caecum, colon, MLN, nasal turbinates, and lung were examined for gross lesions by two ECVP-certified veterinary pathologists who were blinded to the treatment groups. These tissues were also selected for histological analysis (H&E staining and IHC) following the same procedures described in study I. Intestinal gross lesions, contents, jejunal VH:CD ratio, and IHC determination were assessed using the same score systems than study I.

Methacarn-fixed paraffin-embedded tissue (MFPE) specimens

The jejunum from each animal was selected for transcriptomic analysis. The intestine was fixed by immersion in methacarn at 48 hpi at 4ºC to ensure optimal RNA preservation (517). After 24 hours, tissues were embedded in paraffin, sectioned at 8 to 10 µm thickness and mounted on Arcturus RNase-free polyethylene naphthalate (PEN) membrane glass slides (Thermo Fisher Scientific, Carlsbad, CA, USA, #LCM0522).

Slides were air-dried for 30 minutes at 60ºC, deparaffinized using serial-based xylene and ethanol concentrations, and stained with 1% cresyl violet acetate (Sigma-Aldrich, Darmstadt, Germany, #MKCC0238) using standard laboratory procedures. After staining, samples were dehydrated in graded ethanol solutions prepared with RNase-free water, air-dried, and stored at -80ºC for at least 16 hours. All procedures were conducted under RNase-free conditions using DEPC-treated water (Thermo Fisher Scientific, Carlsbad, CA, USA, #AM9922) and RNaseZap (Thermo Fisher Scientific, Carlsbad, CA, USA, #AM9782) to prevent RNA degradation. After 24 hours, the methacarn-fixed paraffin-embedded (MFPE)-jejunal specimens were processed for laser capture microdissection (LCM) prior to RNA extraction. IHC was also performed on MFPE sections following the procedure described in Study I.

Lasser capture microdisection

For each animal, three consecutive sections from the same MFPE block containing jejunal specimens were cut and processed as described in the previous MFPE specimen section. One section underwent IHC for PEDV nucleoprotein detection to serve as a reference template for the subsequent two sections, which were subjected to LCM.

PEDV-infected enterocytes within the jejunal mucosa, identified by IHC in the reference template section, were outlined and micro-dissected using the Leica LMD6500 system (Leica AS LMD; Wetzlar, Germany) with 6.3× magnification, with settings of 115 power, and 10 speed, using the Laser Microdissection 6500 software version 6.7.0.3754. The specific areas microdissected from each cresyl violet-stained MFPE section were then placed into RNase-free 0.5 mL Eppendorf tubes containing 150 µL of buffer PKD from the miRNeasy FFPE Kit (Qiagen, Hilden, Germany, #217504) kept at 4ºC. The entire process was conducted under RNase-free conditions to prevent RNA degradation.

Total RNA isolation and cDNA synthesis

Total RNA was extracted from micro-dissected tissues following the protocol provided by the miRNeasy FFPE Kit (Qiagen, Hilden, Germany, #217504). Briefly, after treatment with proteinase K, RNA was concentrated through ethanol precipitation, purified using RNeasy MinElute spin columns, treated with DNase I for 15 minutes, and finally eluted with 15 µL of RNase-free water, utilizing components from the miRNeasy FFPE Kit. The entire process was conducted under RNase-free conditions. After total RNA extraction, the final RNA concentration was determined using a BioDrop µLite spectrophotometer (Biochrom, Cambridge, UK, #80-3006-55).

RNA samples were stored at -80ºC until they were sent to the Department of Health Technology at the Technical University of Denmark (DTU), where complementary DNA (cDNA) synthesis, preamplification, and qPCR analysis were conducted. cDNA was generated from 250 ng of total RNA/sample, following the manufacturer's instructions for the QuantiTect Reverse Transcription Kit (Qiagen, Hilden, Germany, #205311). Briefly, RNA (250 ng/sample) was diluted with RNase-free water to a final volume of 12 µL. Subsequently, 2 µL of gDNA buffer was added, and the mixture was incubated at 42ºC to remove any genomic DNA contamination. Then, 6 µL of the master mix (containing reverse transcriptase, RT Primer mix, RT buffer, and RNase-free water) was added to each sample, and was then incubated for 15 minutes at 42ºC, followed by 3 minutes at 95ºC. For further pre-amplification and qPCR analysis, the cDNA was diluted 1:10 in low-EDTA TE buffer.

Transcriptomic analyses by microfluidic RT-qPCR

qPCR analysis was carried out using the high-throughput BioMark HD system (Fluidigm), using 96.96 Dynamic Array IFC chips (Fluidigm, South San Francisco, CA, USA, #BMK-M-96.96), which accommodate 96 samples in combination with 96 assays. cDNA pre-amplification was performed using TaqMan PreAmp Master Mix (Applied Biosystems, Waltham, MA, USA, #4391128), Low-EDTA TE buffer (Avantor, Radnor, PA, USA, #APLIA8569.0500), and Exonuclease I (New England Biolabs, Ipswich, MA, USA, #M0293L), following manufacturer's instructions. Briefly, 7.6 µL of the pre-amplification master mix was combined with 2.5 µL of the 1:10 diluted cDNA samples, as described above. The samples were then incubated for 10 minutes at 95ºC and pre-amplified through 18 cycles of 15 seconds at 95ºC and 4 minutes at 60ºC. Finally, 4 µL of Exonuclease I master mix was added, followed by incubation for 30 minutes at 37ºC, and 15 minutes at 80ºC, resulting in a final volume of 14 µL. The pooled undiluted pre-amplified, exonuclease-treated cDNA controls underwent serial dilution in low-EDTA TE buffer (1:2, 1:10, 1:50, 1:250, 1:1250) and were assayed in triplicate to establish relative standard curves and assess primer efficiencies. Additionally, each pre-amplified, exonuclease-treated cDNA sample was diluted 1:10 in low-EDTA TE buffer for later use in qPCR, and each sample was analyzed in duplicate.

The qPCR analysis of all pre-amplified cDNA samples, including both 10x diluted samples and undiluted standard curves, was performed using a mix composed of 2X TaqMan Gene Expression Mastermix (Applied Biosystems, Waltham, MA, USA, #4369016), 20X DNA binding dye (Fluidigm, South San Francisco, CA, USA, #100-0388), EvaGreen Dye 20X (Biotium, Fremont, CA, USA, #31000), and Low EDTA TE-Buffer. The individual assay mixes consisted of Assay Loading Reagent (Fluidigm, South San Francisco, CA, USA) and primer pairs (20 µM for each primer). Following the loading of samples into the wells of the 96.96 Chip (Fluidigm, South San Francisco, CA, USA, #BMK-M-96.96), it was placed in the HX IFC controller for 90 minutes. Subsequently, the chip was transferred to the Biomark HD system for sample quantification. The thermal cycle of the microfluidic qPCR was 600 seconds at 95ºC (Hot Start), followed by 35 cycles of 15 seconds at 95ºC (denaturation) and 60 seconds at 60ºC (amplification and data acquisition). Subsequently, a melting curve analysis was conducted to ensure specific amplification.

Selection of antiviral-related genes

Seventy-five genes were selected to study the gene expression and transcriptional regulation of the key canonical signaling pathways implicated in antiviral innate immunity and

inflammation during PEDV infection. The transcriptomic profiles included analyses of ISGs, type I, II, and III IFNs and their receptors, along with cytokines and chemokines involved in inflammatory responses. Additionally, we examined other innate immune-related genes, such as PRRs, APs and TFs associated with key PEDV-related signaling pathways. All primer pairs employed in the present study were designed in-house (DTU, Denmark) and purchased from Sigma-Aldrich (Darmstadt, Germany). However, the primer sequences specific for PEDV (targeting the N protein, forward primer at position 27313 and reverse primer at position 27453) were obtained from a previous study (518). Detailed information on the qPCR primer sequences and their amplification efficiencies is provided in Appendix Table 4.1. Whenever possible, primers pairs were designed to span intron/exon borders to minimize the risk of amplifying any contaminating genomic DNA.

Expression data (amplification curves, melting curves, and standard curves) of analyzed genes was collected with the Fluidigm Real-Time PCR analysis software 4.1.3 (Fluidigm Corporation, South San Francisco, CA, USA). The DAG expression software 1.0.5.6. (519) was used to calculate the relative expression of each gene using the relative standard curve method (refer to Applied Biosystems user bulletin #2). Multiple reference gene normalization was performed by using glyceraldehyde-3-phosphate dehydrogenase (GAPDH), Ribosomal protein L13a (RPL13A) and peptidylprolyl isomerase A (PPIA) as endogenous controls. R-squared values, PCR efficiencies and slope value for each assay are described in Appendix Table 4.1. The up- or down-regulated expression of each gene was expressed as mean fold change (Fc) values after dividing each individual normalized quantity (NQ) value with the calibrator (Supplementary table 4.1). The mean expression of the three pigs from CNEG 5d and CNEG 5w were used as the corresponding calibrator values to determine the NQ value for each assay.

Statistical analyses

The statistical analyses of the clinical, pathological, and virological results were conducted using SAS v9.4 software (SAS Institute Inc., Cary, NC, USA). Statistical significance was determined at a level of 0.05 ($p<0.05$). Quantitative variables (weight, temperature, RT-qPCR, viral titer, and VH:CD) were subjected to either parametric tests (ANOVA) or non-parametric tests (Kruskal-Wallis, K-W), depending on the normality and homogeneity of variances assessed through Shapiro-Wilk and Levene tests, respectively. In case of obtaining a significant result, type I error was corrected using Tukey or Bonferroni correction for ANOVA and K-W, respectively. Ordinal categorical variables (diarrhea, lesions, and intestinal content, and IHC) were analyzed

using a linear model considering binomial distribution, with P-values corrected using Tukey's Test. However, for comparing different post-inoculation times with hour 0 (in % weight, diarrhea evolution, and temperature), a linear model with binomial distribution was also applied, with P corrected using the Dunnett test in this case. Significance level was set at $p<0.05$.

Logarithmic 10 transformations were applied on Fc values provided by the gene expression data analyses to approach a log normal distribution. Thus, the parametric ordinary one-way ANOVA test corrected with Šídák's multiple comparisons test was used to compare the means of the logarithmic Fc obtained for each group of animals. Significant gene upregulation or downregulation was considered if they met the criteria of a relative Fc of ≥2-fold or ≤2-fold respectively with $p<0.05$.

All the graphs and heatmap, were created with Prism version 10 software (GraphPad Software Inc., La Jolla, CA).

Appendix Table 4.1. Detailed information on the F and R sequences, R-squared, PCR efficiencies and slope value of each primer used for gene expression analyses. Genes have been grouped in functional categories: Normalizer genes, IFNs, PRRs, transcription factors (TFs), ISGs, proinflammatory cytokines and chemokines, adaptor proteins (APs), signaling pathways enzymes (Sign Pathw), cellular receptors (MB recept) and, structural membrane proteins (Struct MB prot).

Gene symbol	Gene name	Classification based on primary function	Forward (F) primer sequence Reverse (R) primer sequence	Slope	R^2	PCR efficiency
IFNA1	Interferon alpha 1	Antiviral. Type I IFN	F: TTCCAGCTCTTCAGCACAGA R: AGCTGCTGATCCAGTCCAGT	3.282	0.975	1.020
IFNB	Interferon beta	Antiviral. Type I IFN	F: AGCACTGGCTGGAATGAAAC R: TCCAGGATTGTCTCCAGGTC	3.704	0.977	0.860
IFNL3	Interferon lambda 3	Antiviral. Type III IFN	F: CCTGGAAGCCTCTGTCATGT R: TCTCCACTGGCGACACATT	3.666	0.982	0.870
IFNL1	Interferon Lambda 1	Antiviral. Type III IFN	F: ATGGGCCAGTTCCAATCTC R: CTGCAGCTCCAGTTCTTCAGT	3.324	0.881	1.000
CASP1	Caspase 1	APs	F: GAAGGACAAACCCAAGGTGA R: TGGGCTTTCTTAATGGCATC	3.480	0.994	0.940
TRAF2	TNF receptor associated factor 2	APs	F: ACCAGAAGGTGACCCTGATG R: GGAAGGAGGACGAGCTCAC	3.113	0.923	1.100
TRAF6	TNF receptor associated factor 6	APs	F: CTGCCATGAAAAGATGCAGA R: GCGACTGGGTATTCTCTTGC	3.104	0.915	1.100
MAVS/IPS-1	IFN-β promoter stimulator 1 or mitochondrial antiviral signaling protein	APs	F: CGTCCTGAAAAGGAGACTCCAG R: AGCGGTCAGAGTTGCTGTCT	3.244	0.802	1.030
TBK1	TANK binding kinase 1	APs	F: TTTCCAGTTCTCAGGGAACAA R: CCTTCTTGATGGGTCCATGT	3.152	0.955	1.080
ISG15	Interferon-stimulated gene 15	ISG	F: AGTTCTGGCTGACTTTCGAGG R: GGTGCACATAGGCTTGAGGT	3.474	0.992	0.940
ISG20	Interferon-stimulated gene 20	ISG	F: AGATCCTGCAGCTCCTGAAA	3.568	0.964	0.910

			R: TGCTCATGTTCTCCTTCAGC			
OAS1	2'-5'-oligoadenylate synthetase 1	ISG	F: TGGTACCAGACGTGTAAGAAGAC R: CTGTTTTCCCGCTTCCTTGC	3.497	0.986	0.930
OASL	2'-5'-oligoadenylate synthetase like	ISG	F: TGGTACCTGAAGTACGTGAAAGC R: TACCCACTTCCCAGGCATAG	3.342	0.969	0.990
RSAD2	Radical S-adenosyl methionine domain containing 2	ISG	F: AAAGACGTGTCCTGCTTGGT R: GCCCGTTTCTACAGTTCAGG	3.713	0.982	0.860
IFIT1	Interferon induced protein with tetratricopeptide repeats 1	ISG	F: GGCCATTTTGTCTGAATGCT R: TCAGGGCAAAGAGAGCCTTA	3.516	0.987	0.930
IFIT3	Interferon induced protein with tetratricopeptide repeats 3	ISG	F: ACTGCAGCCCAACAGTCTTT R: TGATTTGCAGCTCCATTCTG	3.620	0.985	0.890
IFITM1	Interferon induced transmembrane protein 1	ISG	F: CACCACGGTGATCACCATCC R: GCACCAGTTCAGGAAGAGGG	3.360	0.992	0.980
MX1	Myxovirus resistance 1	ISG	F: GCCGAGATCTTTCAGCACCT R: CGGAGGATGAAGAACTGGATGA	3.509	0.992	0.930
MX2	Myxovirus resistance 2	ISG	F: ACCAAGGGCCTGAATATGCT R: ACGGGCTGTACAGGTTGTTC	3.084	0.885	1.100
HERC5	HECT And RLD Domain Containing E3 Ubiquitin Protein Ligase 5	ISG	F: TGAAGACGACGACTTTGGAA R: TGACGTCACTTCCATGAGGA	3.182	0.959	1.060
IFI44	Interferon-Induced Protein 44	ISG	F: ATTGCTCACTCACGTGGACA R: GCTTGAGTTTCACAGGCACA	3.559	0.983	0.910
ADAR	Adenosine Deaminases Acting on RNA	ISG	F: GAATTGTCCCGAGTCTCCAA R: CTGAGTAGGTCCCTGCGGTA	3.589	0.978	0.900
TRIM25	Tripartite Motif Containing 25	ISG	F: CGACCTGGAGAACAAGCTG R: GTTTAGCTCTCACGTCCTCCA	3.671	0.993	0.870
IFNLR1	Interferon lambda receptor 1	MB recept	F: TGTGTACCTGACGTGGCTTC	3.318	0.967	1.000

			R: GGGGTTGCTGAGCTTTGATA			
SIGLEC1	Sialic acid binding Ig like lectin 1	MB recept	F: ATGCCCAGGCTATGAGAGTG R: CCATACAAGGCAGGTCAGGT	3.464	0.947	0.940
SIGLEC5	Sialic acid binding Ig like lectin 5	MB recept	F: ACGCCTCGATCAAGGTCAC R: AGCTGAGTCTGAGGCTGGAG	3.345	0.980	0.990
IL10RB	Interleukin 10 receptor subunit beta	MB recept	F: TTCAAGTCCGAGCGTTTCTT R: GGTTTCGTCATTGGTCGTCT	3.497	0.983	0.930
IFNAR2	Interferon alpha and beta receptor subunit 2	MB recept	F: CCTTGATGACGACGATGATG R: CCCTTTACCACTGACCTCCA	3.137	0.946	1.080
TNFRSF1A	Tumor necrosis factor receptor 1	MB recept	F: AGTGAAATGTCCCAGGTGGA R: TTCTTTCTGCAGCCACACAC	3.522	0.984	0.920
CSF	Colony-stimulating factor	Other.	F: CCGAGGAAACTTCCTGTGAA R: GCAGTCAAAGGGGATGGTAA	3.155	0.963	1.070
HSP 14	Heat shock protein family A (Hsp70) member 14	Other.	F: CACTGGAAAAAGCAATATTCTGG R: AAATGTGTGCCTCCGATGTT	3.472	0.994	0.940
PTGS2	Prostaglandin-Endoperoxide Synthase 2, COX2	Other. Mediator of inflammation	F: AGGCTGATACTGATAGGAGAAACG R: GCAGCTCTGGGTCAAACTTC	3.608	0.934	0.890
CCL2	C-C Motif Chemokine Ligand 2	Pro-inflammatory chemokine	F: CTTCTGCACCCAGGTCCTT R: CGCTGCATCGAGATCTTCTT	2.937	0.916	1.190
CCL5 (RANTES)	C-C Motif Chemokine Ligand 5	Pro-inflammatory chemokine	F: CTCCATGGCAGCAGTCGT R: AAGGCTTCCTCCATCCTAGC	3.174	0.926	1.070
CXCL2	CXC motif chemokine ligand 2	Pro-inflammatory chemokine	F: GAAGATGCTAAACAAGAGCAGTG R: AGCCAAATGCATGAAACACA	2.952	0.973	1.180
IL1B	Interleukin 1, Beta	Pro-inflammatory cytokine	F: TCTCTCACCCCTTCTCCTCA R: GACCCTAGTGTGCCATGGTT	3.536	0.994	0.92
IL6	Interleukin 6	Pro-inflammatory cytokine	F: CCTCTCCGGACAAAACTGAA R: TCTGCCAGTACCTCCTTGCT	2.491	0.845	1.52
IL10	Interleukin 10	Pro-inflammatory cytokine	F: TACAACAGGGGCTTGCTCTT R: GCCAGGAAGATCAGGCAATA	2.598	0.920	1.430

IL12B	Interleukin 12 p40	Pro-inflammatory cytokine	F: GACCAGAAAGAGCCCAAAAAC R: AGGTGAAACGTCCGGAGTAA	3.498	0.956	0.930
IL1RN	Interleukin 1 Receptor Antagonist	Pro-inflammatory cytokine	F: TGCCTGTCCTGTGTCAAGTC R: GTCCTGCTCGCTGTTCTTTC	3.668	0.974	0.870
TNF	Tumor Necrosis Factor	Pro-inflammatory cytokine	F: CACGTTGTAGCCAATGTCAAAG R: GAGGTACAGCCCATCTGTCG	3.163	0.972	1.070
IFNG	Interferon gamma	Pro-inflammatory cytokine	F: CCATTCAAAGGAGCATGGAT R: TTCAGTTTCCCAGAGCTACCA	3.574	0.956	0.900
IL17A	Interleukin 17A	Pro-inflammatory cytokine	F: TCCAGCAAGAGATCCTGGTC R: AAGAAATATGGCGGACGATG	3.468	0.967	0.940
IL8	Interleukin 8	Pro-inflammatory cytokine	F: GAAGAGAACTGAGAAGCAACAACA R: TTGTGTTGGCATCTTTACTGAGA	3.516	0.990	0.930
IL18	Interleukin 18	Pro-inflammatory cytokine	F: CAATTGCATCAGCTTTGTGG R: TCCAGGTCCTCATCGTTTTC	3.311	0.968	1.000
IL22	Interleukin 22	Pro-inflammatory cytokine	F: GAAGTGCTGTTCCCCAACTC R: TACGGCATTGGCTTAGCTTT	3.229	0.934	1.040
IL27	Interleukin 27	Pro-inflammatory cytokine	F: GCCACTTTGCTGAATCACAC R: TGGAGAGGAAGCAGAGTCGT	3.559	0.906	0.910
IL33	Interleukin 33	Pro-inflammatory cytokine	F: AGGCATTCACCAACAAAAGG R: ACAGACCGTTCAAGGTGTCC	3.916	0.980	0.800
TGFB	Transforming growth factor beta 1	Pro-inflammatory cytokine	F: GCAAGGTCCTGGCTCTGTA R: TAGTACACGATGGGCAGTGG	3.346	0.983	0.990
IL2	Interleukin 2	Pro-inflammatory cytokine	F: TACATGCCCAAGCAGGCTAC R: TTTAGCACTCCCTCCAGAGC	3.487	0.882	0.940
NLRP3	NLR family pyrin domain containing 3	PRRs	F: GACTTTCCAGGAGTTCTTTGCTG R: CCTGGTTTACAAGGCCAAAG	3.124	0.964	1.090
TLR3	Toll-like receptor 3	PRRs	F: ATTGTGCAAAAGATTCAAGGTG R: TCTTCGCAAACAGAGTGCAT	2.801	0.861	1.280
TLR7	Toll-like receptor 7	PRRs	F: AGAAGCCCCTTCAGAAGTCC R: GGTGAGCCTGTGGATTTGTT	3.417	0.962	0.960

TLR8	Toll-like receptor 8	PRRs	F: GCAAAGACCACCACCAACTT R: ATCCGTCAGTCTGGGAATTG	3.656	0.891	0.880
TLR9	Toll-like receptor 9	PRRs	F: CCTGTTCTATGATGCCTTCGTG R: GGTACCCAGTCTCGCTCCTC	3.745	0.951	0.850
NLRP6	NLR family pyrin domain containing 6	PRRs	F: CGCGTCCGAGTACAAGAAG R: AATGAGCACCTTGGTGAAGC	3.381	0.840	0.980
RIG-I/DDX58	RNA helicase retinoic acid-inducible gene I	PRRs	F: TTGCTCAGTGCAATCTGGTC R: CTTCCTCTGCCTCTGGTTTG	3.057	0.985	0.930
IFIH1/MDA5	Interferon induced with helicase C domain 1	PRRs	F: TCGGATTTTGGAACTCAACC R: TCTTTGCGATTTCCGTCTCT	3.710	0.993	0.860
RPL13A	Ribosomal protein L13a (HK)	Normalizer gene	F: ATTGTGGCCAAGCAGGTACT R: AATTGCCAGAAATGTTGATGC	3.421	0.994	0.96
YWHAZ	Tyrosine 3-monooxygenase/tryptophan 5-monooxygenase (HK)	Normalizer gene	F: GCTGCTGGTGATGATAAGAAGG R: AGTTAAGGGCCAGACCCAAT	3.523	0.994	0.920
HPRT1	Hypoxanthine-Guanine Phosphoribosyltransferase	Normalizer gene	F: ACACTGGCAAAACAATGCAA R: TGCAACCTTGACCATCTTTG	3.386	0.975	0.97
GAPDH	Glyceraldehyde-3-phosphate dehydrogenase (HK)	Normalizer gene	F: ACCCAGAAGACTGTGGATGG R: AAGCAGGGATGATGTTCTGG	3.367	0.995	0.98
PPIA	peptidylprolyl isomerase A	Normalizer gene	F: CAAGACTGAGTGGTTGGATGG R: TGTCCACAGTCAGCAATGGT	3.368	0.992	0.98
LCN2	Lipocalin2	Sign Pathw	F: CAGTTCCAGGGGAAGTGGTA R: GAGCTCGTAGGTGGTGGTGT	3.602	0.904	0.900
MAPK9	Mitogen-activated protein kinase 9	Sign Pathw	F: CGCCACCACCTCAGATTT R: TGTTTCTTTCTTCCCAATCCA	3.237	0.907	1.040
STAT2	Ssignal transducer and activator of transcription 2	Sign Pathw	F: GCTGGTGAGACTCCAGGAAG R: TTGAACTTCCGGAAACCTTG	3.291	0.966	1.010
SOCS1	Suppressor of cytokine signaling 1	Sign Pathw	F: CCAGCGCATTGTGGCTAC R: GCGGCCGATCATATCTGGAA	3.712	0.901	0.860
STAT3	Signal transducer and activator of transcription 3	Sign Pathw	F: GAAGCTGACCCAGGTAGTGC R: GGCAGGTCAATGGTATTGCT	3.556	0.992	0.910

STAT1	Signal Transducer And Activator Of Transcription 1	Sign Pathw	F: CCTTGCAGAATAGAGAACATGATAC R: CCTTTCTCTTGTTGTCAAGCATT	3.623	0.993	0.890
ZO-1	Zonula Occludens-1	Struct MB prot	F: ATGACTCCTGACGGTTGGTC R: TGCCAGGTTTTAGGATCACC	2.874	0.884	1.230
OCLN	Occludin	Struct MB prot	F: GACGAGCTGGAGGAAGACTG R: GTACTCCTGCAGGCCACTGT	3.447	0.982	0.950
NFKBIA	Nuclear Factor Of Kappa Light Polypeptide Gene Enhancer In B-Cells Inhibitor, Alpha	TFs	F: GAGGATGAGCTGCCCTATGAC R: CCATGGTCTTTTAGACACTTTCC	3.572	0.992	0.910
FOS	proto-oncogene c-Fos	TFs	F: CTCCAAGCGGAGACAGACC R: CTTCTCCTTCAGCAGGTTGG	3.485	0.902	0.940
JUN	c-jun	TFs	F: AGTGAAAACCTTGAAAGCGCAG R: TGGCACCCACTGTTAACGTG	3.362	0.996	0.980
IRF1	Interferon regulatory factor 1	TFs	F: TGAAGCTGCAACAGATGAGG R: CTTCCCATCCACGTTTGTCT	3.809	0.978	0.830
IRF3	Interferon regulatory factor 3	TFs	F: GCTACACCCTCTGGTTCTGC R: GAGACACATGGGGACAACCT	3.730	0.908	0.850
IRF7	Interferon regulatory factor 7	TFs	F: GTGTGCTCCTGTACGGGTCT R: CTGCAGCAGCTTCTCTGTGT	3.314	0.979	1.000
NFKB1	Nuclear factor kappa B subunit 1	TFs	F: CCCTGTGAAGACCACCTCTC R: ATCCCGGAGCTCGTCTATTT	3.043	0.972	1.130
IRF5	Interferon regulatory factor 5	TFs	F: TCTTCAGCCTGGAGCATTTT R: CTCCCCAAAGCAGAAGAAGA	2.956	0.876	1.180
IRF9	Interferon regulatory factor 9	TFs	F: CATTCAGACTTGGGGAGCAG R: AAAGGGGCCTCAGTGGTAAC	3.409	0.975	0.960
PEDV N	PEDV Nucleoprotein gene	Virus	F: TCGTGAGCTAGCGGACTCTTACGAGATTAC R: GCTGCAGCGTGGTTTCACGCTTGTTCTTCT	3.727	0.991	0.85

Results

Newborn piglets experienced more severe disease than weaned piglets, but neither PEDV strain caused fever or mortality after acute infection

By 48 hpi, weight loss was observed in all piglets from the PEDV CALAF 5d and PEDV USA 5d groups compared to their initial weight. This reduction was statistically significant only in the PEDV CALAF 5d group. Specifically, piglets in this group experienced nearly double weight loss compared to those in the PEDV USA 5d group, with reductions of approximately 10% and less than 5%, respectively. In contrast, piglets in both the PEDV CALAF 5w and PEDV USA 5w groups exhibited statistically significant weight gains ranging from 5 to 10% at 48hpi, similar to the weight gain observed in both CNEG groups (Figure 4.1A).

At 24 hpi, pasty diarrhea was observed in piglets from the PEDV CALAF 5d and PEDV USA 5d groups. However, in the PEDV USA 5d group, diarrhea progressed rapidly to a liquid form by 36 hpi, while in the PEDV CALAF 5d group, liquid diarrhea appeared later, at 48 hpi, in only 2 out of 4 piglets. Among the weaned piglets, pasty feces were observed in the PEDV USA 5w group by 36 hpi in 2 of 4 animals, but no diarrhea was recorded in any animal from the PEDV CALAF 5w group throughout the study period (Figure 4.1B). Although no statistically significant differences were detected between the groups at any specific time point, a trend toward more severe diarrhea was noted in the PEDV USA 5d group at 36 hpi and in both PEDV USA 5d and PEDV CALAF 5d groups at 48 hpi compared to the CNEG 5d group.

No fever was recorded in any animal throughout the study period.

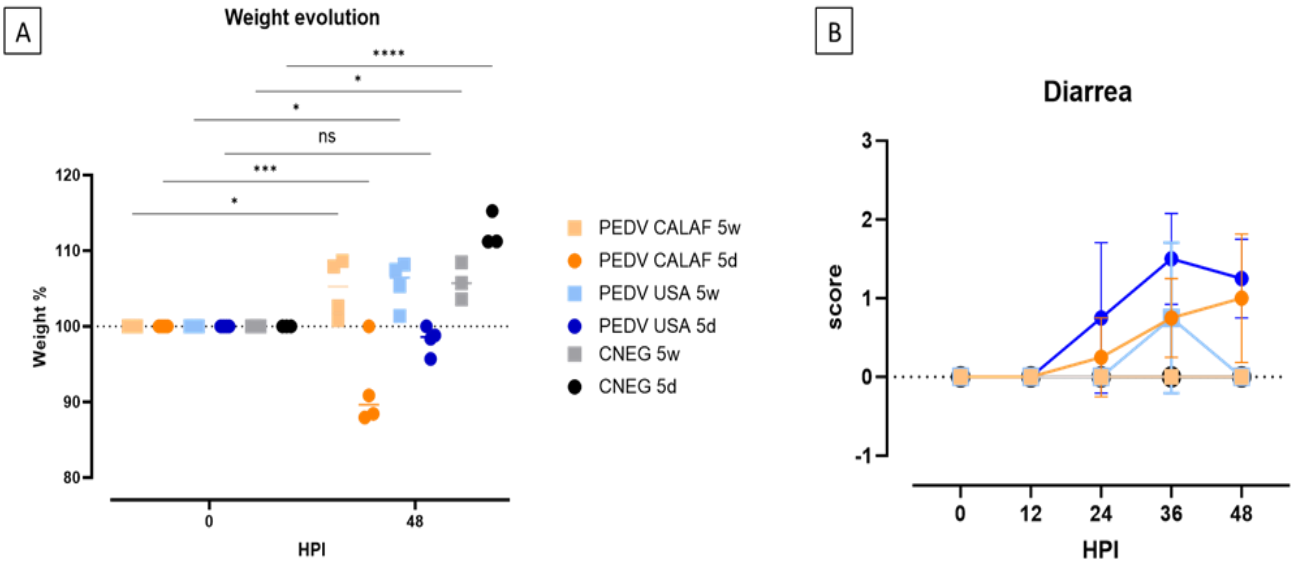

Figure 4.1. (A) Individual and average weight changes (expressed as a percentage of increase or decrease relative to the initial weight) of the experimental groups from 0 to 48 hpi. (B) Diarrhea evolution over 48 hpi. Diarrhea was scored as no diarrhea (0); pasty (1) and liquid (2) diarrhea. No significant differences between study groups were detected at any HPI. (*, *p*-value < 0.05; ***, *p*-value < 0.001; ****, *p*-value < 0.0001; ns: non-significant).

Age and strain independence in PEDV-induced small intestinal damage

The summary of individual scores concerning the intestinal wall damage and digestive contents is illustrated in Figure 4.2.

At 48 hpi, all newborn piglets in both the PEDV CALAF 5d and PEDV USA 5d groups exhibited thin intestinal walls, gas distension, and liquid contents in the jejunum. In the colon, the PEDV CALAF 5d group showed thin intestinal walls, with 3 out of 4 piglets presenting this condition alone, while 1 piglet exhibited both thin walls and gas distension. Liquid contents in the colon were observed in only 2 piglets from this group. In contrast, only one piglet from the PEDV USA 5d group demonstrated both a thin intestinal wall and gas distension in the colon; nevertheless, 3 out of 4 piglets in this group displayed liquid contents. The remaining animals of both study groups had pasty intestinal contents.

In the PEDV USA 5w group, all piglets exhibited a thin wall and liquid content in the jejunum. Although none of the piglets from this group displayed changes in the colon, three had pasty contents, and one had liquid content. No notable intestinal abnormalities were observed in the PEDV CALAF 5w group; however, two out of four piglets had pasty intestinal contents. Although clear differences observed in intestinal lesions and contents among the groups, these observations did not reach statistical significance.

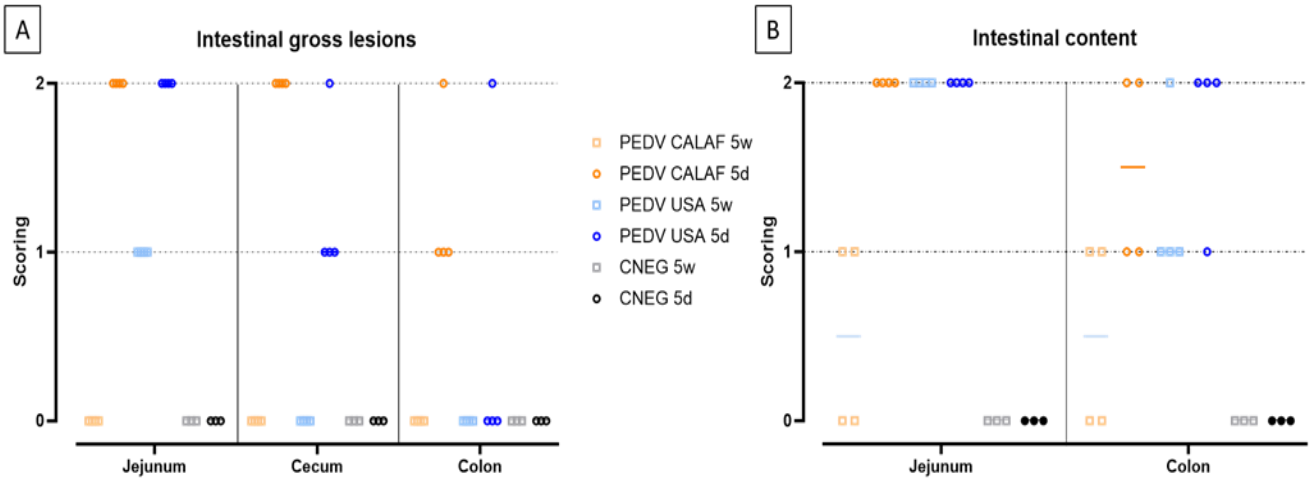

Figure 4.2. Intestinal lesions (A) and contents (B) in 5-day-old and 5-week-old piglets at 48 hours post-inoculation (hpi) with both strains of PEDV. Intestinal lesion was scored as 0, normal; 1, thin-walled or gas-distended; 2, presence of both. Intestinal content was scored as 0, normal; 1, pasty; or 2, watery content.

Histological analysis of jejunum and ileum sections revealed severe, diffuse villus atrophy and fusion in all piglets inoculated with either the PEDV USA or PEDV CALAF strains, irrespective of age (Figure 4.3A). Enterocytes exhibited vacuolization, cellular hypereosinophilia, and epithelial attenuation, with no evidence of inflammation. These abnormalities were absent in animals administered with PBS. At 48 hpi, intestinal atrophy and fusion were characterized by a notable decrease in villus height (VH), resulting in a reduced VH:CD ratio, which ranged from 1.8 in the PEDV CALAF 5w, PEDV USA 5d, and PEDV USA 5w groups to 2.5 in the PEDV CALAF 5d (Figure 4.3B). This decrease in VH:CD was statistically significant when compared to the negative controls, which had VH:CD ratios of 4 and 6 in the CNEG 5w and CNEG 5d groups, respectively. No lesions were identified in the colon, nasal turbinates, or lungs of any piglet inoculated with either PEDV isolate or in the negative control piglets.

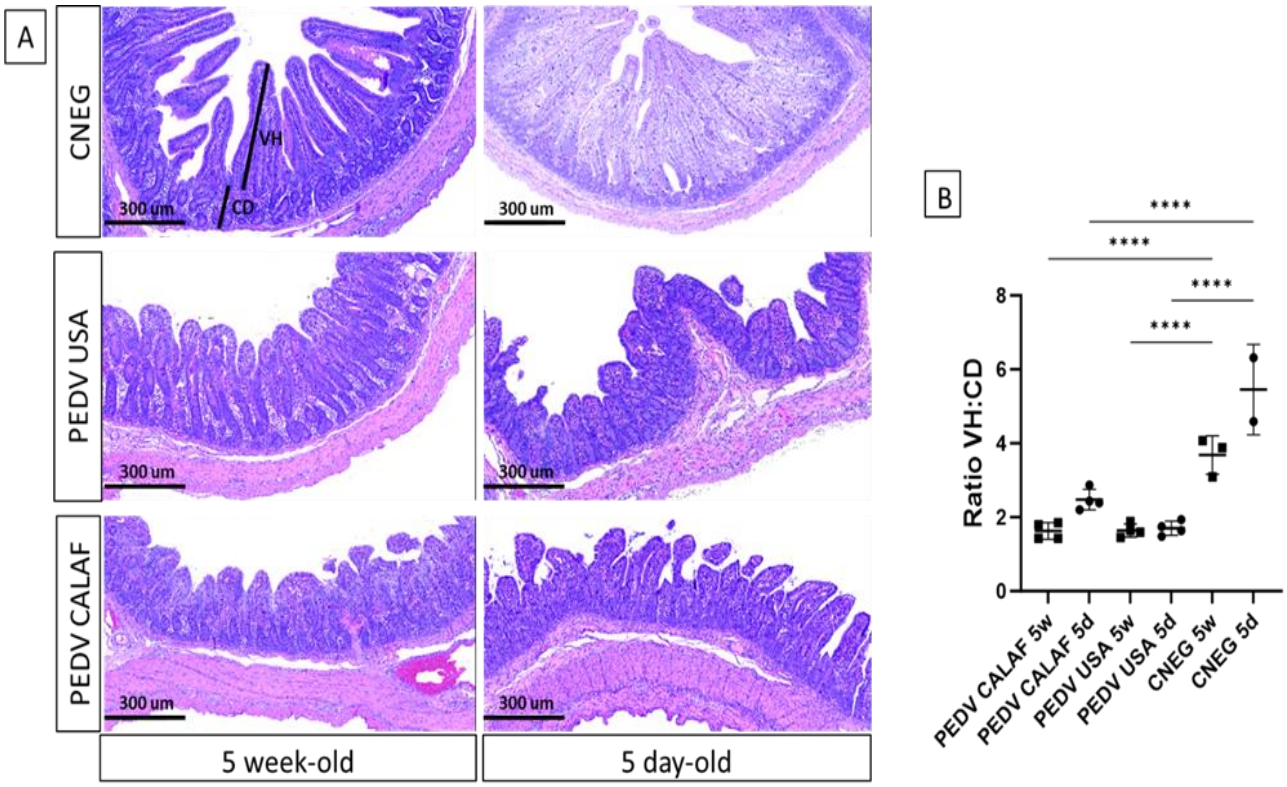

Figure 4.3. (A) Jejunum at 48 hpi from 5-day-old and 5-week-old piglets from the negative control (CNEG), PEDV USA and PEDV CALAF groups stained with Hematoxylin and Eosin (H&E). Similar severe villous atrophy and fusion was observed in both PEDV groups regardless of age

compared to their respective CNEG. (B) The extent of intestinal damage was assessed using the villus- height-to-crypt-depth ratio (VH:CD) (**, *p*-value < 0.01; ****, *p*-value < 0.0001).

PEDV antigen, detected by IHC, exhibited diffuse and granular staining patterns, primarily located within the enterocytes of the jejunum and ileum in all PEDV-inoculated piglets, regardless of PEDV strain and age (Figure 4.4A). Viral antigen was widely distributed in the apical portion of the intestinal villi, corresponding to areas of villus atrophy and fusion, and occasionally observed in the crypts of Lieberkühn and in interstitial mononuclear cells dispersed throughout the lamina propria (Figure 4.4A, indicated by arrows and arrowhead). While the jejunum contained the highest amount of PEDV antigen in all animals from inoculated groups, PEDV antigen in the colon was sparsely detected in a few enterocytes in only 2 out of 4 piglets from the PEDV CALAF 5d group and in 1 out of 4 piglets from the PEDV USA 5d group (Figure 4.4B). Additionally, PEDV antigen was detected in dendritic-like cells within the MLN. The detection levels in these cells were comparable between the PEDV CALAF 5d and PEDV USA 5d groups, with both showing a higher amount antigen presence compared to that of 5-week-old piglets. Among the latter, a higher amount of PEDV antigen was observed in the PEDV USA 5w group compared to the PEDV CALAF 5w one. Statistical analysis, however, did not reveal significant differences among the study groups.

No PEDV antigen was identified in sections of the nasal turbinate or lungs in any PEDV-inoculated piglet inoculated, or in intestinal segments of PBS-administered piglets.

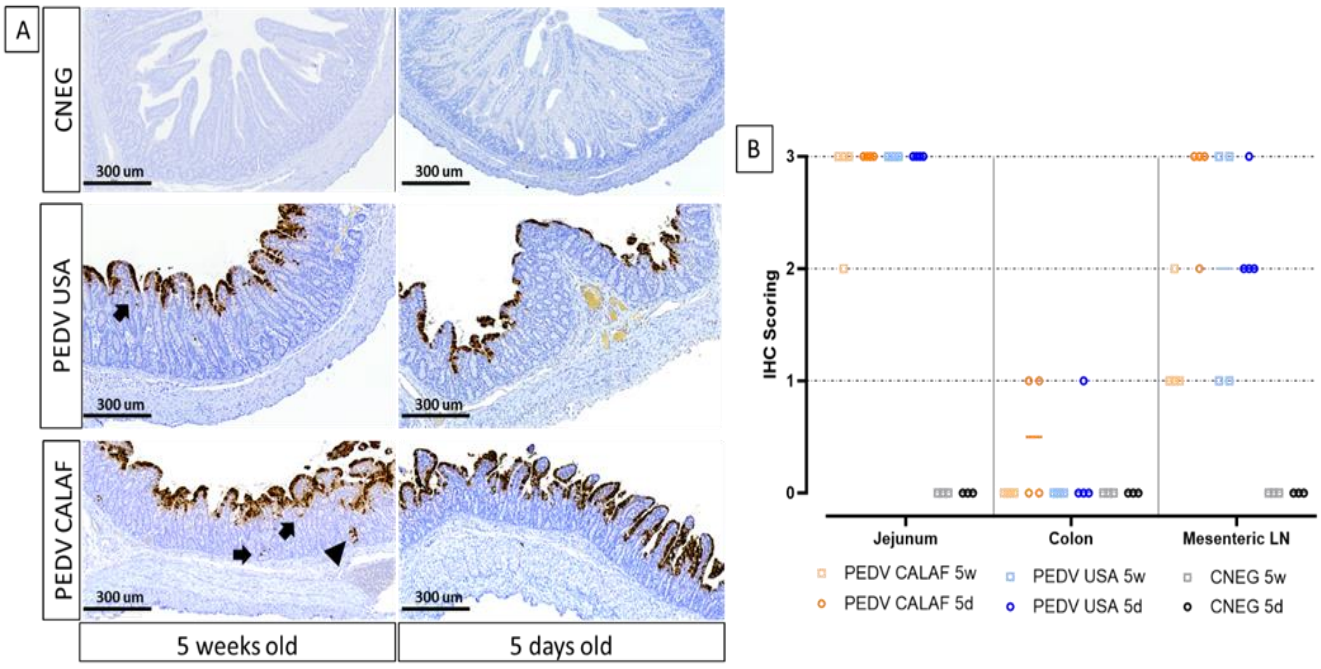

Figure 4.4. (A) Detection of PEDV by IHC in sections of jejunum of 5-day-old and 5-week-old piglets at 48 hpi. PEDV was similarly detected in the jejunum of the different study groups, regardless of age. PEDV antigen was distributed widely in the cytoplasm of enterocytes from the apical part of atrophic and fused villi. IHC for PEDV detection, hematoxylin counterstain. Detection of PEDV in occasional intestinal crypts (arrowhead) and mononuclear cells of the lamina propria (arrow). (B) Individual IHC scoring of PEDV in jejunum, colon, and MLN at 48 hpi.

Non-S INDEL and S INDEL PEDV isolates had similar loads in small intestine and feces in newborn and weaned piglets

The amount of PEDV RNA was analyzed by RT-qPCR in RS at 0 and 48 hpi, as well as in samples from jejunal and colon mucosa, jejunal content, nasal turbinate, and lung macerates at 48 hpi from all piglets.

At 0 hpi, RS from all groups tested negative for PEDV. However, by 48 hpi, viral RNA was detected in fecal samples (Figure 4.5A), intestinal wall sections (Figures 4.5B and 4.5C), and jejunal content (Figure 4.5D) in all PEDV-inoculated piglets, with comparable levels of viral RNA across groups. No viral RNA was detected in the CNEG groups. The differences in viral RNA levels observed between the PEDV-inoculated groups were not statistically significant. Additionally, all inoculated piglets shed infectious virus, as evidenced by viral titration in the jejunal content (Figure 4.5E). The levels of infectious PEDV were similar between 5-day-old and 5-week-old piglets for each PEDV isolate. However, a higher viral titer was observed in both PEDV USA age groups (10^4 $TCID_{50}$/mL) compared to both PEDV CALAF age groups ($10^{2.5}$ $TCID_{50}$/mL), although the difference was not statistically significant.

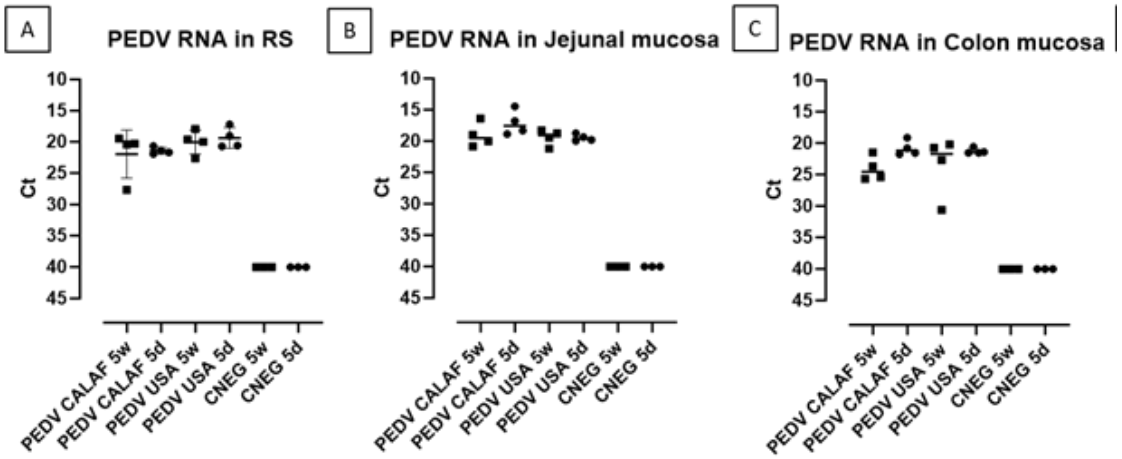

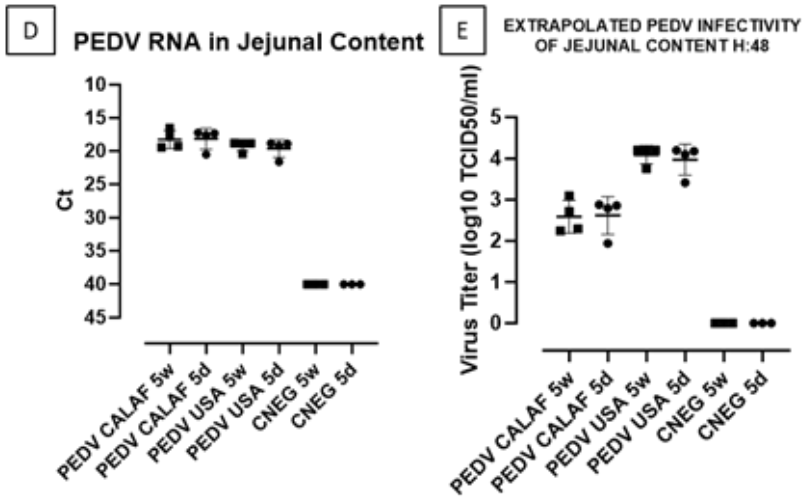

Figure 4.5. PEDV loads detected in rectal swabs (RS) (A), jejunal (B), and colonic (C) mucosa, and jejunal content (D) at 48 hpi. Fecal viral infectious titer (VT), expressed as inferred log10 $TCID_{50}$/ml, was calculated from Ct values of jejunal content at 48hpi (E).

PEDV RNA was detected in the nasal turbinates of all animals in the PEDV CALAF 5w group, but only in a few animals from the other groups, with Ct values ranging from 33 to 38 (Figure 4.6A). Also, in the lungs (Figure 4.6B), PEDV RNA was found in all piglets from the PEDV CALAF 5w group and in only one piglet from the PEDV USA 5w group. Interestingly, no PEDV RNA was detected in the lungs of 5-day-old piglets inoculated with either PEDV isolate or in those from the control groups. Nonetheless, no statistically significant differences were observed between the study groups or their respective negative controls.

All viral inocula and all samples tested negative for TGEV and PRV-A, as determined by RT-qPCR. The detection limit for all RT-qPCR was set at a Ct value of 40.

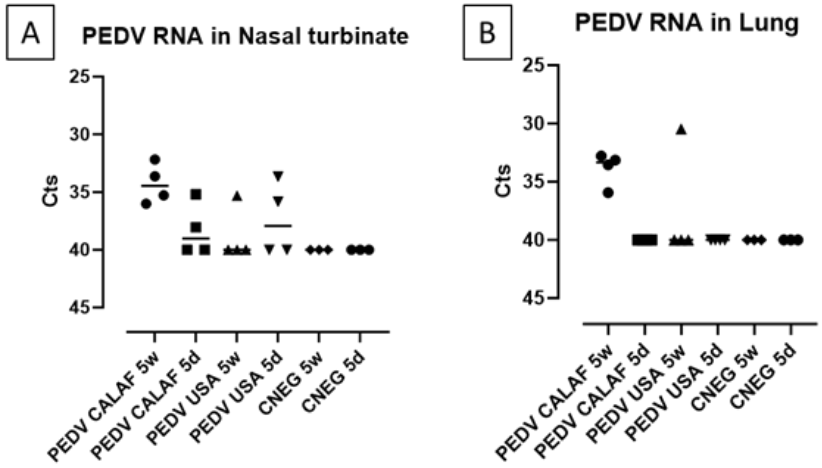

Figure 4.6. PEDV loads (measured as Ct values) detected in nasal turbinate (A) and lung (B) at 48 hpi of suckling (5d) and weaned (5w) piglets inoculated with PEDV CALAF and PEDV USA strains.

Both PEDV strains actively replicated in the jejunum of newborn and weaned piglets

PEDV loads in enterocytes from micro-dissected MFPE intestinal samples were quantified using specific primers for the N protein employing a microfluidic quantitative PCR assay. The limit of detection for the PEDV N gene was set at Ct = 25.26, ensuring accurate quantification with an average Tm value of 79.45, which confirmed the specificity of the amplification. Notably, the amount of PEDV N RNA levels in the jejunal sections were twice as abundant in the CALAF 5d group (NQ: 2.55) compared to the other groups, which had an average NQ of 0.5. This observation contrasted with the PEDV viral load from the jejunal mucosa macerates and the IHC results, which did not show such a pronounced difference.

Weaned piglets mount a stronger antiviral (IFN I/III and ISGs) jejunal response against PEDV USA and PEDV CALAF isolates compared to newborn piglets

NQ values for each assay were converted into Z-scores and presented in a heatmap (Figure 4.7) to illustrate gene regulation patterns in the intestinal mucosa of suckling and weaned piglets. Overall, at 5 days of age the PEDV USA group showed upregulation at 48 hpi in jejunal tissue of more IFN and ISG related genes than the PEDV CALAF group (Figure 4.7). When infected at weaning, both groups showed significant upregulation of both antiviral and proinflammatory gene expression.

Overexpressed genes in suckling and weaned pigs at 48 hpi exhibited a relative expression increase of more than two-Fc compared to the CNEG animals (Figure 4.8). Although numerous differences in gene transcription profiles between age groups achieved statistical significance ($p<0.05$), others did not, possibly because of the limited sample size and substantial individual variability in gene expression levels within the groups.

A consistent pattern of jejunal gene expression was observed across all levels of innate immune-related downstream pathways, from PRRs to IFNs and ISGs, in response to infection with PEDV (Figure 4.8).

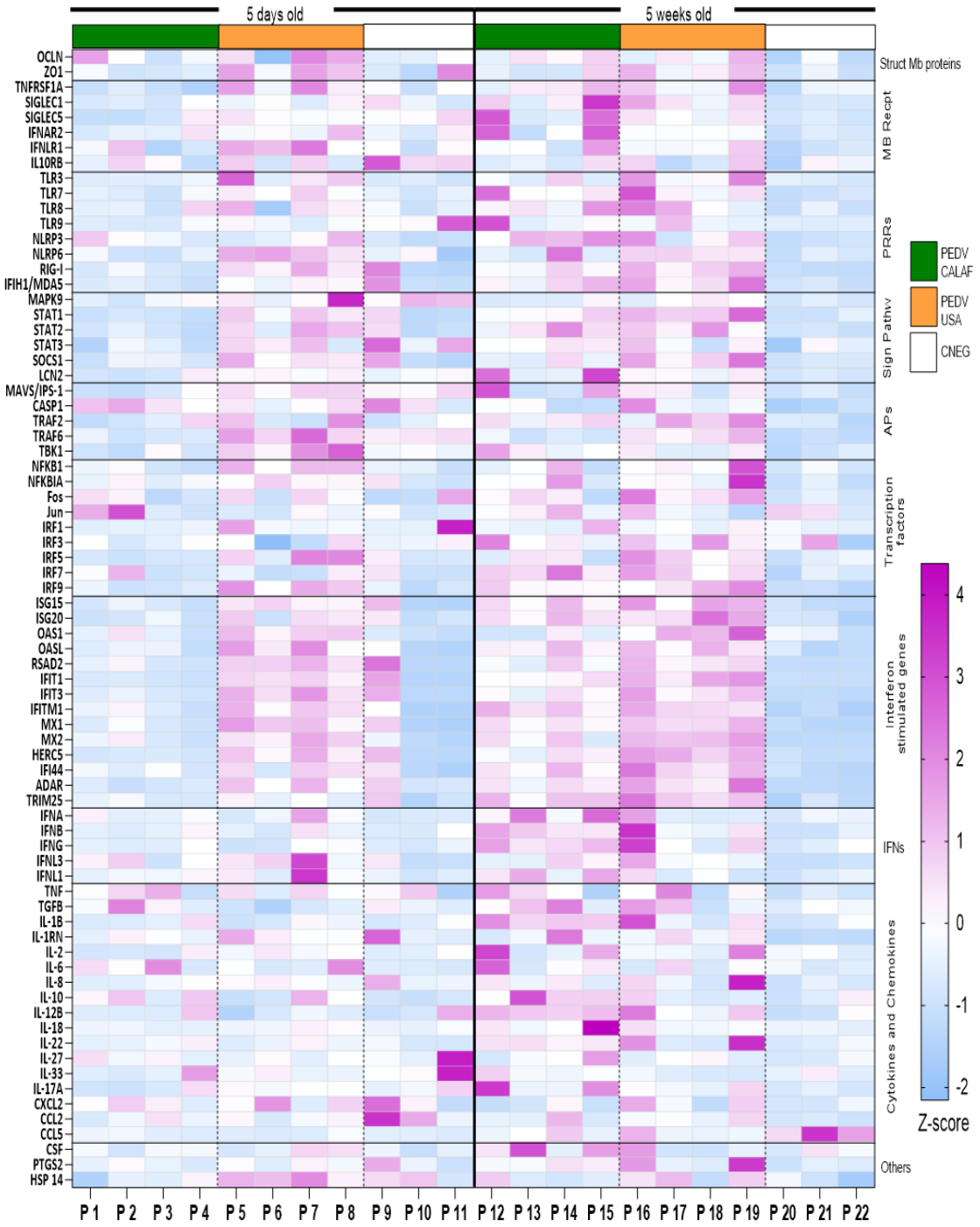

Figure 4.7. Transcriptional expression of innate immune response-related genes in the jejunum at 48 hours after PEDV CALAF and PEDV USA infection in 5-day-old and 5-week-old piglets, respectively. Each column represents an individual piglet (P1 to P22) within the different age (right and left) and inoculation group (PEDV CALAF, green color; PEDV USA, orange color; CNEG, white color). The resulting heatmap shows color variations corresponding to Z-score; blue indicates decreased gene expression, while pink represents increased expression, relative to piglets in the CNEG groups. Mb Recpt: Membrane receptors; PRRs: Pattern recognition receptors; Sign Pathw: Signaling pathways; APs, adaptor proteins; IFNs: Interferons.

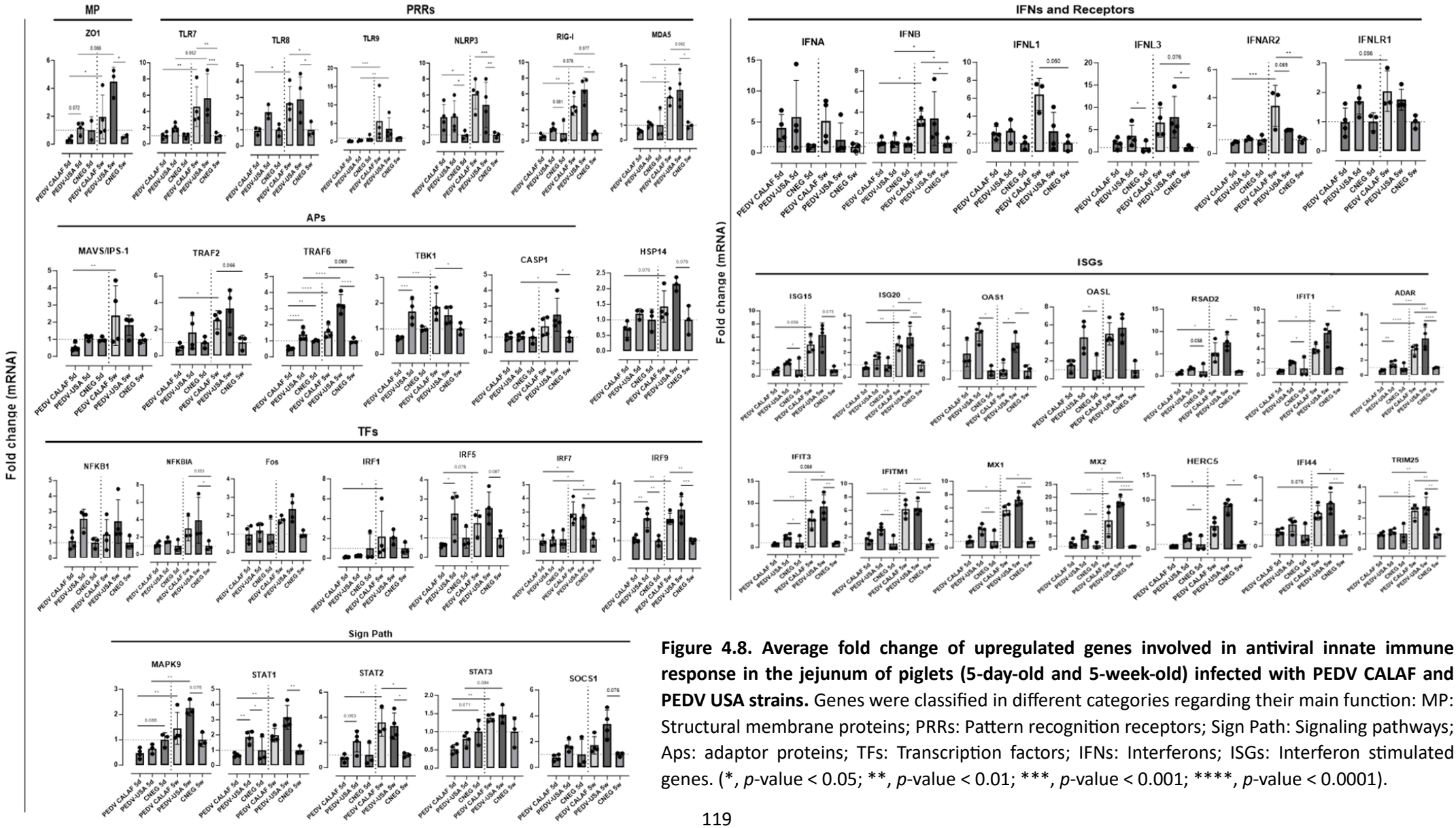

Figure 4.8. Average fold change of upregulated genes involved in antiviral innate immune response in the jejunum of piglets (5-day-old and 5-week-old) infected with PEDV CALAF and PEDV USA strains. Genes were classified in different categories regarding their main function: MP: Structural membrane proteins; PRRs: Pattern recognition receptors; Sign Path: Signaling pathways; Aps: adaptor proteins; TFs: Transcription factors; IFNs: Interferons; ISGs: Interferon stimulated genes. (*, *p*-value < 0.05; **, *p*-value < 0.01; ***, *p*-value < 0.001; ****, *p*-value < 0.0001).

Genes coding for IFN-β, IFN-λ1, and particularly IFN-λ3 were significantly upregulated in all piglets from PEDV CALAF 5w and PEDV USA 5w groups relative to piglets in the CNEG groups. In contrast, in 5-day-old piglets, IFN-λ1 and IFN-λ3 were slightly although not significantly upregulated in response to the PEDV USA isolate, and to a lesser extent to the PEDV CALAF strain. Notably, IFN-β remained unaltered in newborn piglets compared to both groups of weaned piglets. In contrast, IFN-α showed similar upregulation across all study groups compared to the CNEG groups, with no significant differences between them (Figure 4.9).

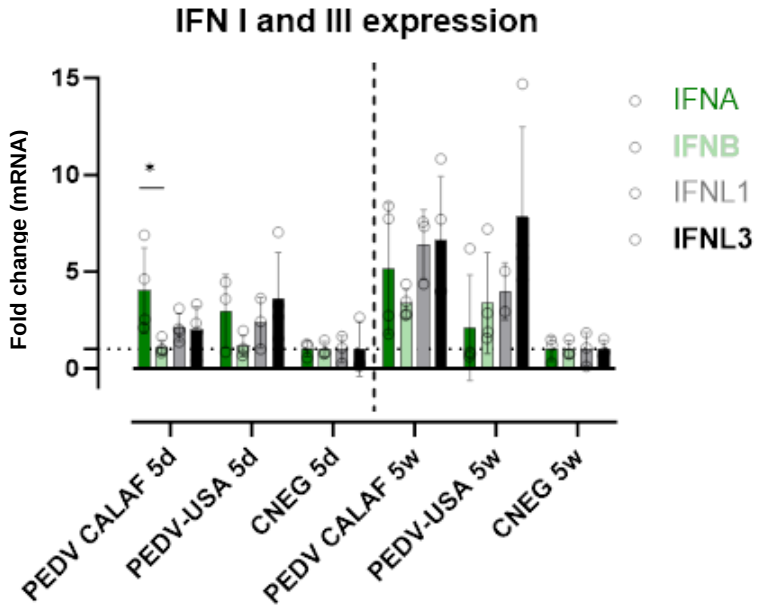

Figure 4.9. Comparative IFN I and III intestinal gene expression in suckling (5d) and weaned (5w) piglets inoculated with PEDV CALAF and PEDV USA strains. (*, *p*-value < 0.05)

A similar transcription profile was noted for most PRRs, such as cytoplasmic RNA sensors (RIG-I, MDA5, and NLR, particularly NLRP3), viral endosome double- and single-stranded RNA sensors (TLR3 and TLR7/8, respectively), and cytoplasmic DNA sensors (TLR9). This pattern extended to most PRR-related APs (such as TRIM25, MAVS/IPS-1, TRAF2/6 and TBK1) and TFs (such as IRF1, IRF7 and NF-κB). However, unlike the other TFs, IRF3, which is crucial for the induction of type I IFNs (IFN-α and IFN-β), showed no change in transcription in any of the infected groups. In addition, the relative expression of genes encoding IFN receptors (IFNAR2 and IFNLR1), TFs involved in ISG synthesis (IRF9, STAT1 and STAT2), antiviral ISGs (ISG15, ISG20, OASL, radical S-adenosyl methionine domain containing 2 (RSAD2), MX1, MX2, Interferon-induced protein with tetratricopeptide repeats (IFIT)1, IFIT3, IFITM1, HECT and RLD domain containing E3 ubiquitin protein ligase 5 (HERC5), IFI44 and adenosine deaminases acting on RNA (ADAR)) and IFNs/ISGs and proinflammatory regulators (STAT3 and suppressor of cytokine

signaling (SOCS1)) increased similarly in the PEDV CALAF 5w and PEDV USA 5w groups. In 5 day-old-piglets the expression of none of these genes was induced by CALAF PEDV infection while they were moderately induced by PEDV USA.

Furthermore, HSP14 was significantly upregulated in piglets from PEDV USA 5w group and moderately in those from the PEDV CALAF 5w group compared to 5-day-old piglets. Nevertheless, the relative expression of HSP14 in the PEDV USA 5d group was similar to that of the control group, while it was downregulated in the PEDV CALAF 5d one.

Overall, weaned piglets exhibited a pronounced intestinal antiviral response against both non-S INDEL (PEDV USA) and S INDEL (PEDV CALAF) strains of PEDV, contrasting with the relatively weak response in newborn piglets. Interestingly, newborn piglets exposed to the non-S INDEL PEDV strain showed higher levels of gene transcription compared to the S INDEL one.

In all control non-infected animals, except for one piglet (P9), all gene transcripts were at baseline levels and the mean expression of the three pigs were used as calibrator values to determine the NQ value for each assay (Supplementary table 4.1). In that particular piglet, the relative expression of most antiviral and proinflammatory genes was similar to that of PEDV USA 5d group, although no evidence of PEDV infection based on RT-qPCR or IHC. This suggests that observed response was unrelated to PEDV infection.

Both non-S INDEL and S INDEL PEDV strains modulated the MAPK signaling pathway in weaned piglets but not in newborn piglets

At 48 hpi, five-week-old piglets from the PEDV CALAF and PEDV USA groups exhibited a significant increase in the expression of genes involved in cell survival such as the MAPK9 and proto-oncogene c-Fos (Fos) (a subunits of the MAPK-dependent activator protein 1 (AP-1) complex) gene compared to the response of infected 5-day-old piglets (Figure 8). This transcriptional pattern correlated with the expression of TRAF6 and TRAF2, APs critical for activating both the NF-κB and MAPK-JNK/p38 signaling pathways. Although the increase following infection in MAPK9 gene expression was statistically significant when comparing 5-day-old and 5-week-old piglets, the difference in Fos gene expression did not reach statistical significance.

Junctional membrane and pyroptosis-related genes were upregulated in weaned piglets but not in newborn piglets inoculated with both PEDV strains

To evaluate putative cellular changes following PEDV infection, we examined the gene expression of junctional membrane proteins that are critical for enterocyte membrane integrity, such as ZO-1 and OCLN. In weaned piglets from both PEDV groups, there was a slight increase in OCLN transcriptional expression, while the ZO-1 gene was significantly upregulated post-infection (Figure 4.8). These responses were not observed in newborn piglets. Additionally, the expression pattern of caspase (CASP)-1 gene, associated with pyroptosis, mirrored the significant upregulation observed in ZO-1 in weaned piglets.

Weaned piglets mounted a proinflammatory intestinal response mediated by Th1 and Th17 cytokines, and prostaglandins against both PEDV strains, whereas this response was suppressed in newborn piglets

In response to PEDV infection, the pro-inflammatory transcription factor NF-κB was slightly upregulated across all study groups, particularly in piglets inoculated with the PEDV USA strain, regardless of age (Figure 4.8), though this difference was not statistically significant. Conversely, the NF-κB inhibitor (NFκBIA or IκBα) was notably upregulated in PEDV CALAF and PEDV USA-inoculated weaned pigs compared to newborn piglets, where no changes were observed in comparison to CNEG 5d group.

Most genes coding for pro-inflammatory cytokines (IFN-γ, TNF-α, IL-27, colony stimulating factor (CSF), and IL-17A) produced by Th1 and Th17 responses were similarly upregulated in weaned piglets inoculated with either PEDV CALAF or PEDV USA (Figure 4.10). Similarly, the intestinal expression of the immune regulators IL-2 and TGF-β were increased in weaned piglets from both PEDV groups. In contrast, these cytokines remained at baseline levels in newborn piglets, similar to the CNEG 5d group. Other pro-inflammatory factors like IRF5, IL-12B, IL-1RN, IL-22, IL-8, and IL-33 significantly increased at 48 hpi in weaned piglets compared to newborn piglets after infection. Notably, the expression of IL-1RN was remarkably high and restricted to all 5-week-old piglets. Moreover, CASP-1, IL-1β, and IL-18, key components of the NLRP3 inflammasome and NK cells and CD8+ CTLs promoters (IL-18), exhibited significant mRNA upregulation in weaned piglets compared to newborn piglets. Furthermore, the prostaglandin E2 gene (PTGS2) was upregulated in PEDV CALAF 5w and PEDV USA 5w groups, with no transcriptional activity observed in newborn piglets.

The chemokine CCL2 was similarly upregulated in 5-week-old piglets from both PEDV CALAF and PEDV USA groups, while CXCL2 was only overexpressed in the PEDV USA 5w group (Figure 4.10). None of these chemokines showed altered gene expression in 5-day-old piglets from any group. Conversely, CCL5 gene expression was induced in newborn piglets from both PEDV CALAF and PEDV USA groups, compared to weaned piglets, in which its expression was downregulated relative to the control.

Similar to CCL5, Th2-related cytokines such as IL-6 and the pro-inflammatory antagonist IL-10 exhibited higher expression levels in 5-day-old piglets inoculated with both PEDV CALAF and PEDV USA, whereas their expression was marginal in all weaned piglets (Figure 4.10).

Discussion

The impact of PEDV infection depends on host factors like age, innate immune response, and cellular pathways related to cell damage and survival (182,354,368). Virus-specific factors such as PEDV strain type (non-S INDEL or S INDEL), inoculum dose, and herd immunity status also play key roles in disease outcome (182,301,304,305). The present study compared the transcriptomic responses between newborn (5-days-old) and weaned (5-week-old) piglets after inoculation with either the European S INDEL (CALAF) or North American non-S INDEL (USA) PEDV isolates to explore age-dependent immune and inflammatory responses.

In line with previous literature (2,182), the clinical outcomes in the present study were age and PEDV strain-dependent. Newborn piglets suffered from severe diarrhea, weight loss, and pronounced intestinal lesions, whereas weaned piglets developed less severe symptoms, with moderate to severe gross intestinal lesions and pasty diarrhea. Although the non-S INDEL strain caused earlier onset and more severe diarrhea in newborn piglets compared to the S INDEL strain, as previously reported (301,305,309), the S INDEL group experienced more significant body weight loss. However, contrary to expectations, no mortality was observed, even among newborn piglets infected with the more virulent non-S INDEL strain—a surprising deviation from established literature (2).

Furthermore, pathological and virological outcomes, including intestinal damage (villi atrophy and fusion), PEDV distribution in the jejunum, replication, and virus shedding in feces were similar across all groups. These findings contradict earlier literature, which suggested that these parameters are more pronounced in newborn piglets, especially when infected with the non-S INDEL strain (301,305,309).

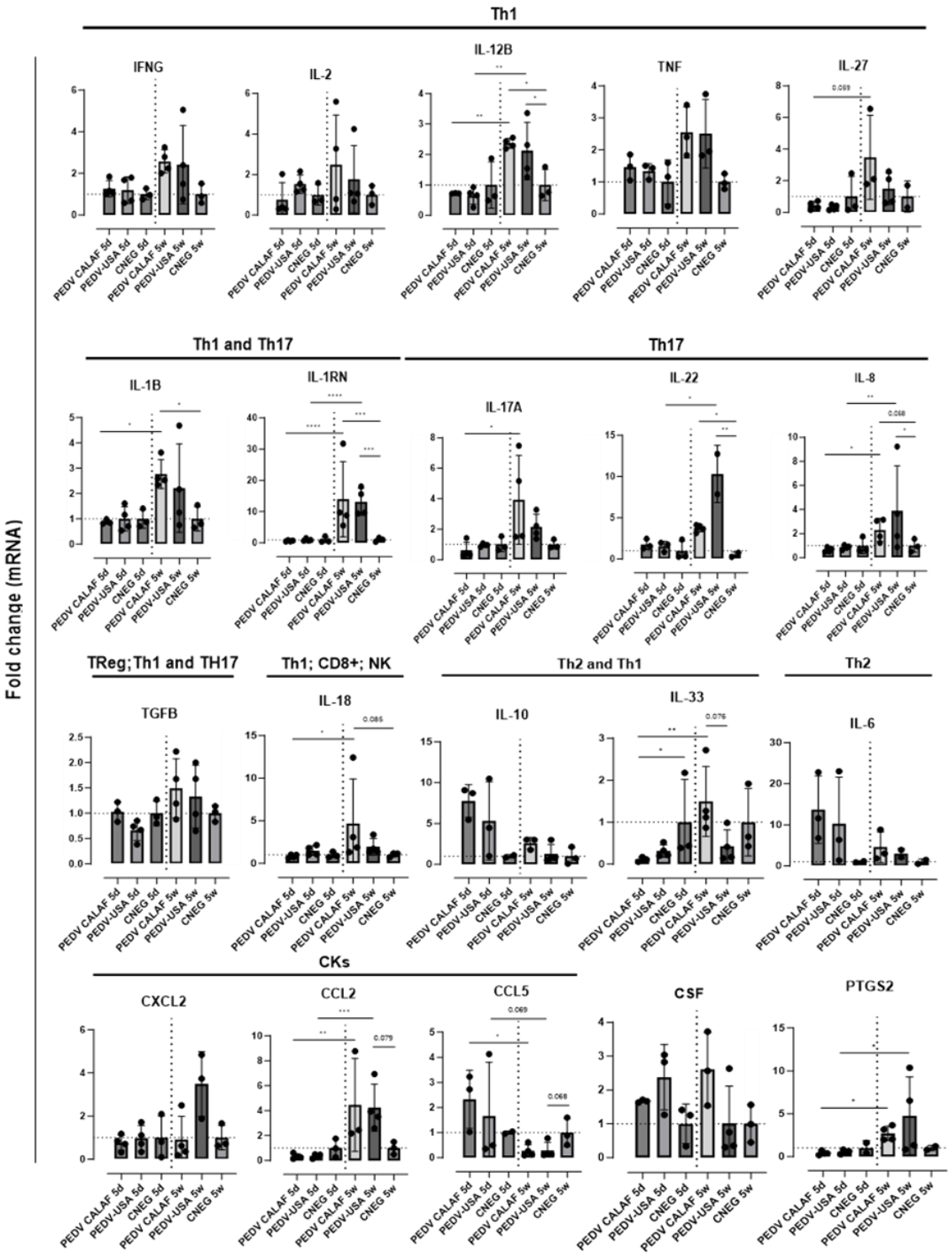

Figure 4.10. Average fold change of genes upregulated after infection involved in the inflammatory response in the jejunum of piglets (5-day-old and 5-week-old) infected with PEDV CALAF and PEDV USA strains. Genes were classified in Th1, Th2 and Th17 phenotypes as well as involved in Treg, natural killer (NK) cells and CD8+ (cytotoxic T-Lymphocytes) cell activation. CKs: Chemokines; CSF: Colony Stimulating Factor; PTGS: prostaglandin. (*, *p*-value < 0.05; **, *p*-value < 0.01; *** > *p*-value < 0.001; ****, *p*-value < 0.0001). Dashed lines represent baseline expression levels from negative control animals, used as calibrators to calculate the NQ values for each assay.

These observations suggest different explanations for the lack of evident clinical signs in weaned piglets despite viral replication, excretion, and intestinal damage. First, clinical signs in weaned piglets may appear later than in newborns (182), suggesting that diarrhea might have developed if the study would have been extended. Additionally, resistance to PEDV infection may be affected by differences in intestinal development between newborn and weaned piglets, as noted in previous studies on the small intestine (305,306). In addition to the small intestine, this study also found gross lesions and PEDV antigen in the large intestine, but only in newborn piglets. Therefore, the more developed, lesion-free colon in weaned piglets may help mitigating small intestinal diarrhea, preventing overt clinical signs. However, further studies are needed to explore other factors influencing PEDV pathogenesis, such as differences in intestinal microbiota and anatomical or physiological factors, including key functional membrane receptors in small and large enterocytes across different piglet ages.

Moreover, the upregulation of junctional membrane protein genes (ZO-1) in jejunal enterocytes from weaned piglets after PEDV inoculation indicates an adequate response to cellular disruption, aligning with previous studies (356,360). This suggests that weaned piglets have better intestinal regeneration capabilities, which mitigate PEDV-induced enterocyte damage and explain the lack of evident clinical signs. Conversely, newborn piglets show unchanged ZO-1 gene expression, suggesting either limited intestinal regeneration or PEDV-mediated transcriptional inhibition, as previously reported (305,354). While the upregulation of ZO-1 in weaned piglets may imply enhanced intestinal regeneration, additional markers of epithelial repair and barrier function would be needed to confirm this hypothesis.

The efficiency of the innate immune response is a key factor in determining clinical outcomes of PEDV infection in newborn versus older piglets (306). In this context, the integrity of the mucosal barrier, a vital component of innate immunity, is crucial for defense against pathogens such as PCoVs (162,163,354). Therefore, special attention was given here to characterize innate immune responses in the jejunum during the acute phase of PEDV infection (48 hpi). Microfluidic qPCR analysis on LCM-derived jejunal enterocytes with high viral loads showed distinct gene transcription patterns for antiviral and inflammatory responses between neonatal and weaned piglets, correlating with the observed age-dependent clinical outcomes. These findings underscore that in this study the development of effective innate immune and inflammatory responses is influenced by age rather than by the specific strain of PEDV.

Regarding the antiviral response, weaned piglets similarly upregulated the intestinal gene expression of IFNs and ISGs against both PEDV strains at 48 hpi. Conversely, these genes

were less expressed in newborn piglets, a fact apparently associated with severe clinical outcomes. However, antiviral IFNs and ISGs were more upregulated in newborn piglets inoculated with the more virulent non-S INDEL strain compared to the S INDEL strain. This suggests that the S INDEL strain may modulate the expression of these genes to evade the host immune response, promoting viral replication, which aligns with the higher viral load (PEDV N mRNA) observed in the PEDV CALAF 5d group (75,366). Additionally, the resultant gene transcription pattern in newborn piglets infected with non-S INDEL PEDV strains may explain the lack of mortality, highlighting the antiviral role of IFNs and ISGs in controlling PEDV replication.

Based on the obtained results, Figure 4.11 illustrates a proposed model for PEDV-induced immune responses, highlighting the overexpressed PRRs, APs, TFs, and IFN receptor-related genes that activate IFN and ISG signaling pathways in weaned piglets. Consistent with previous studies (368,398,405,406), type III IFNs, particularly IFN-λ3, and their receptor (IFNLR1), were generally expressed at higher levels than type I IFNs in all piglets. This result underscores the importance of type III IFNs in intestinal immunity and their antiviral role against PEDV compared to type I IFNs. Regardless, both IFNs lead to the production of various ISGs. Some of them, such as RIG-I/MDA5, TRIM25, IRF7, and STAT1, act as regulators of IFN signaling. The remaining ISGs function as antiviral effectors, obstructing viral replication by preventing viral entry and degrading viral ssRNA (363,365,412).

Based on our findings, HSP 14 may play an antiviral role in protecting weaned piglets against PEDV, aligning with the antiviral effects previously observed for other HSPs (HSP 27, HSP 70, and HSP 90) against PCoVs (415–419). These results indicate a potential avenue for developing novel antiviral therapies.

Weaned piglets exhibited a proinflammatory reaction to both PEDV strains, highlighted by a significant upregulation of Th1 and Th17 cytokines at 48 hpi. Conversely, newborn piglets had elevated levels of Th2 cytokines, including the anti-inflammatory IL-10. This result suggest that Th1 and Th17 responses (such as IL-22) may favor clinical protection during the acute phase in weaned piglets, while an anti-inflammatory response dominates in newborns (502). Additionally, this study also shows a negative correlation between IL-10 and IFNs expression and clinical outcome. In this context, it is tempting to hypothesize that the lack of an effective inflammatory response in newborns, driven by IL-10, contributes to the more severe clinical outcome. Despite its known antiviral and mucosal protective role in promoting IL-22 overexpression (502,520), it is possible to speculate that STAT3 may also be involved in a negative feedback loop between IL-10 and IFN signaling. Considering this, the synergistic role of STAT3, IL-

10, and IL-22 could offer a novel therapeutic approach to managing severe viral diarrhea in piglets. However, this hypothesis requires validation through more in-depth studies.

Based on obtained results, NF-κB is likely crucial in initiating the antiviral proinflammatory response. However, the overexpression of inflammasome-related IL-1β and IL-18 as well as IRF5, a critical transcription factor for M1 macrophage polarization and Th1-Th17 responses (521,522), indicates a more complex response against PEDV in weaned piglets. IL-18 activates and recruits CTLs, NK cells, and macrophages, leading to increased levels of INF-γ and NF-κB (523,524). The observed overexpression of IL-18 and INF-γ as well as IL-2 and TNF-α, in this study suggests that these cells play a crucial role in virus clearance in weaned piglets exposed to both PEDV strains, supporting the assertion that a cytotoxic inflammatory response plays a key role in countering PEDV during the acute phase of infection. In contrast, the absence of IL-18 in newborns following PEDV infection correlates with their limited presence of CTLs and NK cells in the intestinal mucosa (306). Although further studies are needed, IL-18 synthesis may also be associated with STAT3/IL-22 activation (502). Interestingly, NF-κB and IL-1β were expressed in weaned piglets at levels comparable to their main inhibitors, NFKBIA and interleukin 1 receptor antagonist (IL-1RA) (encoded by IL-1RN), respectively. These data suggest critical simultaneous regulation of inflammatory and anti-inflammatory pathways to prevent the progression of inflammatory disease (525,526).

Furthermore, the increased PTGS2 expression in weaned piglets suggests that proinflammatory eicosanoids play a key role in defense against PEDV, similar to their role in immune responses to other coronaviruses like SARS-CoV-2 (527–531). These results also propose potential new therapeutic targets for disease control. Additionally, chemokines like CCL2 seem to strongly counteract both PEDV strains as previously observed (247). However, the expression of CCL5 differs from earlier findings (516), suggesting the need for further research to clarify its role in disease protection.

Consistent with previous reports (348,364,532), our findings suggest that PEDV may use kinase-dependent pathways (MAPK/AP-1 and JNK/p38) via TRAF2, TRAF6, and TBK1 to enhance viral replication in weaned piglets during acute infection, unlike in newborns. This could explain the similar viral loads observed in both weaned and newborn piglets. Additionally, the current study provides evidence that PEDV can regulate cellular surveillance and key programmed cell death pathways (apoptosis and pyroptosis), by modulating STAT3 as previously reported (449,533). We also found that the overexpression of pyroptosis-related genes (NLRP3 and CASP-1) in weaned piglets indicates that the inflammasome regulates PEDV-infected enterocyte death

via GSDMD-mediated pyroptosis (419,455,534). In contrast, the lack of this response in newborn piglets suggests that both PEDV strains suppress pyroptosis, potentially aiding viral replication as an immune evasion strategy (455). Additionally, CASP-1 may trigger other cell death pathways, such as apoptosis (535). Given that PEDV can influence apoptosis, ER stress, the UPR, and autophagy (354), further research is needed to investigate these pathways and their role in disease pathogenesis.

Conclusion

The present study enhances our understanding of age- and strain-dependent PEDV pathogenesis and early clinical outcomes, emphasizing the critical roles of IFNs and ISGs in innate antiviral immunity and Th1-Th17 mediated inflammatory response during acute phases, which protect weaned piglets in contrast to newborn animals that suffer from a more severe overt disease.

Supplementary material

The following supporting information can be downloaded at: Cts and Nq (normalized- Fc) values of innate immune response genes induced at the micro-dissected intestinal epithelia.xlsx

Supplementary table 4.1: Ct, NQ values and Mean fold change (Fc) of each selected gene

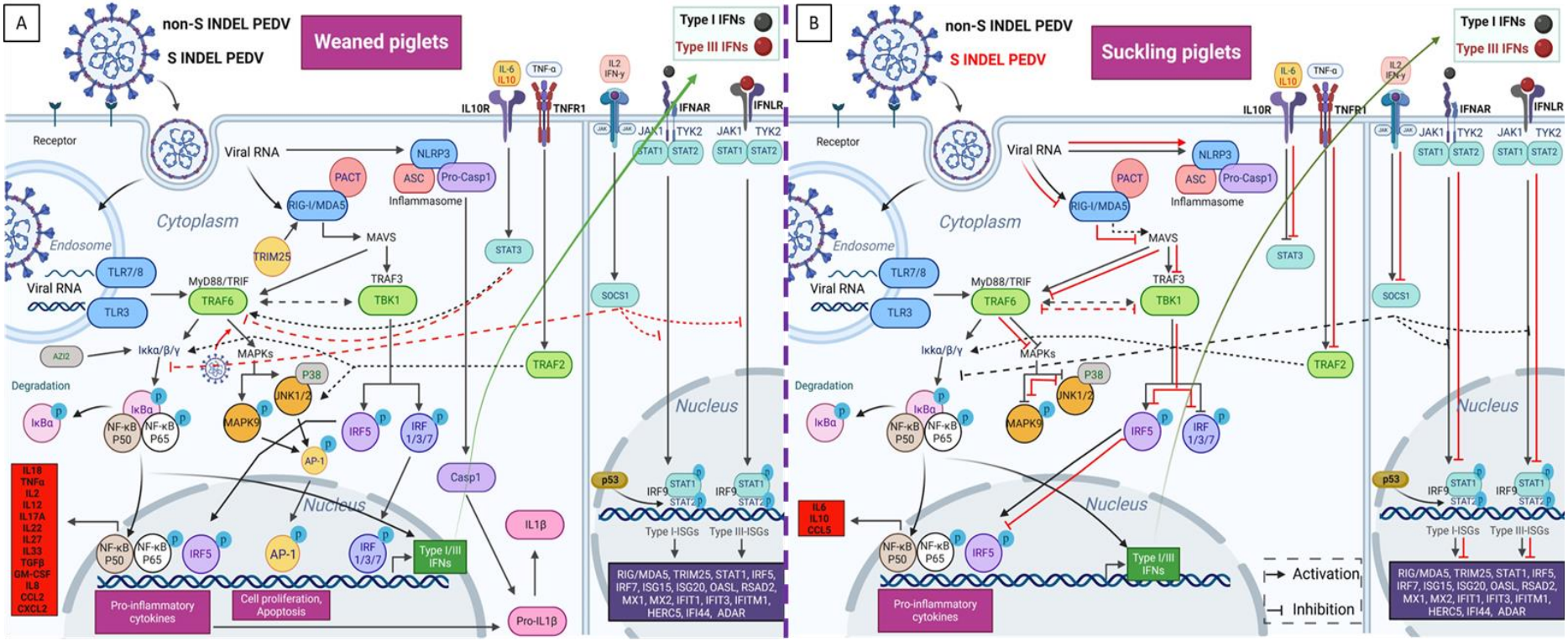

Figure 4.11. Diverse intestinal innate immune pathway responses induced by non-S INDEL and S INDEL PEDV strain in weaned (A) and suckling (B) piglets. In weaned piglets (A), the PRRs involved in PEDV recognition include TLR3, TLR7/8, RIG-I/MDA5, and NLRP3 which activate the following APs: TRIM25/MAVS/IPS-1, TRAF6, and TBK1. These APs activate key TFs like IRFs and NF-κB, which drive the transcription of antiviral genes and proinflammatory cytokines. IFN I and III synthesis in response to PEDV infection is mainly controlled by IRF7, IRF1, and NF-κB, with minimal involvement from IRF3, a crucial early regulator of type I IFNs. As a result, numerous ISGs are overexpressed through the JAK-STAT/IRF9 signaling pathway, along with other key ISGs and proinflammatory regulators like STAT3 and SOCS1. The primary drivers of proinflammatory responses to PEDV are NF-κB, IRF5, and IL-1β-mediated NLRP3 inflammasome activation, which also control the pyroptosis cell death pathway via CASP-1 overexpression. Key regulators of cell survival, including MAPKs and the transcription factor AP-1, are also overexpressed following PEDV infection. Most of these pathways are activated in infected enterocytes of suckling piglets (B) exposed to the non-S INDEL strain (black arrows), whereas they are suppressed in response to the S INDEL strain (red lines). Created with BioRender.com

CHAPTER 5

Study III

Porcine alveolar macrophages and nasal epithelial cells internalize porcine epidemic diarrhea virus (PEDV) but do not support its replication *in vitro*.

Submitted for publication

Introduction

The respiratory tract serves as the primary route of entry for a variety of respiratory pathogens. Consequently, the nasal mucosa plays a pivotal role as the initial line of defense against the intrusion of microorganisms (504). In addition, there is growing evidence of the airborne transmission of various gastrointestinal pathogens, such as noroviruses and rotaviruses (220,536,537). However, the interactions between gastrointestinal pathogens and nasal epithelial cells (NECs) remain relatively understudied. Nevertheless, enteric pathogen interaction with NECs could trigger proinflammatory and antiviral responses following the recognition of these infectious agents by pattern recognition membrane receptors (504).

Within the *Coronaviridae* family, certain viruses, such as MERS-CoV, SARS-CoV, and SARS-CoV-2, are known to infect the respiratory tract leading to severe disease. In pigs, TGEV, a highly virulent gastrointestinal pathogen, is also capable of replicating in respiratory tissues, although it does not induce primary respiratory disease (2). Additionally, PRCV, a naturally occurring TGEV variant, exhibits more extensive replication in the respiratory tract, targeting alveolar, bronchiolar, and bronchial epithelial cells as well as bronchoalveolar macrophages, resulting in subclinical infections with worldwide distribution (26,222,538). Recent studies have demonstrated that the primary receptor utilized by some PCoVs, the APN, is found in the respiratory epithelium, particularly in the nasal turbinates, as well as in the bronchiolar epithelium, pneumocytes, and lung alveolar macrophages (Fabian Z.X, personal communication). These findings, based on IHC, help explaining the tropism of these PCoVs for the respiratory tract.

While the fecal-oral route has traditionally been regarded as the primary mode of PEDV transmission, recent research has suggested the fecal-nasal route as an alternative transmission pathway, involving airborne aerosolized PEDV particles (220,504). These studies provided evidence that PEDV caused intestinal infection in piglets by intranasal inoculation indicating systemic spread of PEDV from the nasal cavity. While the exact mechanisms of PEDV interaction with nasal mucosa remain unclear, emerging evidence suggests a potential affinity between PEDV, NECs and nasal DCs (220,241,504). Consistent with these studies, these cells can internalize PEDV and trigger the production of antiviral and proinflammatory cytokines, subsequently presenting the virus to subepithelial CD3+ T lymphocytes. Consequently, virus-loaded CD3+ T cells may act as systemic carriers of PEDV through the bloodstream to the intestinal mucosa (220,504). Additionally, it has recently been demonstrated that PEDV can disrupt the nasal endothelial barrier to facilitate viral dissemination (505). These findings, along

with the fact that PEDV also uses APN as a main receptor, suggest that PEDV replication may take place in extra-intestinal tissues. Consequently, respiratory infections might affect the enteric disease following systemic spread, similar to observations made with other coronaviruses such as SARS-CoV-2 (539).

Additionally, PEDV has been detected in macrophages within the intestinal lamina propria, as well as in PAMs and continuous porcine alveolar macrophage cell lines like 3D4 (222,540). Although the specific role of these cells in PEDV pathogenesis is still unknown, sequencing analyses suggest that the PEDV S glycoprotein may play a crucial role in adapting to new host cells such as PAMs and establishing respiratory infections (222).

Therefore, the aim of the present study was to explore a potential alternative route of PEDV infection by examining the susceptibility of PAMs and 3D4 cells to viral replication and their eventual innate antiviral and anti-inflammatory responses upon exposure to a Vero cell-adapted non-S INDEL USA PEDV strain. Furthermore, we investigated the susceptibility of nasal turbinate epithelial organoids (NTO) as a potential alternative model for PEDV infection.

Materials and Methods

Cells and virus

African green monkey kidney cells (Vero cells, ATCC CCL-81) were cultured in Dulbecco's Modified Eagle Medium (DMEM, Corning). Porcine monomyeloid 3D4/21 cells (ATCC- CRL-2843) were maintained in Roswell Park Memorial Institute (RPMI) 1640 Medium (Gibco-BRL). PAMs were maintained in minimum essential medium (MEM, Gibco-BRL). The DMEM and MEM media were supplemented with 10% fetal bovine serum (FBS, Corning), 1% penicillin/streptomycin (Thermo Fisher Scientific), 1% glutamine (L-Glutamina 200 mM, Gibco-BRL), 0.5% nystatin (Merck), 0.3% tryptone phosphate broth (Merck) and 0.02% yeast extract (Thermo Fisher Scientific). RPMI was supplemented with 1% non-essential aa (MEM Non-Essential Amino Acids Solution (100X), Gibco-BRL), 10 mM HEPES (Gibco-BRL), and 1 mM sodium pyruvate (Gibco-BRL) in addition to 10% FBS, 1% penicillin/streptomycin, 0.3% tryptone phosphate broth, and 0.02% yeast extract. All cell cultures tested negative for *Mycoplasma spp*. contamination (Mycoplasma Gel Detection Kit, BIOTOOLS B & M LABS S.A). Subsequently, cells were cultured in 75 cm^2 flasks at 37ºC with 5% CO_2, with unvented caps specifically for the 3D4 cells.

The USA PEDV isolate USA/NC49469/2013 (GenBank accession number KM975737) has been characterized elsewhere and is described in the M&M section from the previous study I.

Sequencing analysis of the inocula

The genome encoding the S glycoprotein of PEDV USA/NC49469/2013 (KM975737) was sequenced and compared with sequences from Park and Shin (222). The sequencing procedure was carried out as described in the M&M section from the previous study I. The graphical representations were generated using the Geneious Prime software by Dotmatics (version 2023.1.2).

Isolation of PAMs

PAMs were obtained from healthy piglets via bronchoalveolar lavage (BAL), performed following tracheal cannulation and infusion with PBS containing 1% gentamicin (Sigma-Aldrich). The BAL fluid was then centrifuged at 600 × g for 10 minutes at 4ºC to isolate the PAMs which were resuspended in 90% FBS and 10% DMSO and cryopreserved in liquid nitrogen.

Infection of CCL-81, 3D4 and PAMs to PEDV

CCL-81, 3D4 and PAMs were seeded in 48-well plates at densities of 90,000, 150,000, and 500,000 cells/well, respectively, 72, 48 and 24 hours prior to infection with 1% trypsin-treated PEDV (USA/NC49469/2013 strain) at a multiplicity of infection (MOI) of 1. Following 2.5-hours of adsorption, cells were washed with PBS and incubated for 4 days at 37ºC with 5% CO_2 in serum-free DMEM, RPMI or MEM for CCL-81, 3D4, and PAMs, respectively. Media were supplemented with 5 µg/mL trypsin (trypsin solution from porcine pancreas, T4549 Sigma-Aldrich) and other required factors as described above.

PEDV presence was assessed in cells and supernatants using RT-qPCR (VetMAX 25XSwine Enteric Panel TGEV/PEDV/PRV-A Quantification, Thermo Fisher Scientific) at various post-inoculation time-points (0, 6, 12, 24, 48, 72, and 96 hpi). PEDV immunofluorescence (IF) (Medgene Labs SD6-29) was performed on ethanol-fixed cells at 24 and 48 hpi. Viral titers in the supernatants were determined on Vero cells using the Reed-Muench method (measured as $TCID_{50}$/mL) and confirmed by IF. Furthermore, viral internalization and replication were studied through IF and electron microscopy examination of infected cells at 24 and 48 hpi. Additionally, the proinflammatory and antiviral responses were assessed by ELISA on the supernatants.

NTO obtention and culture

Porcine NTOs were isolated from piglet nasal turbinates, as described in Bonillo-López et al. (541). Briefly, samples were cut in small pieces, processed mechanically and enzymatically with collagenase IV and 0.25% EDTA-trypsin, strained through a 100-µm strainer and the cell pellet resuspended in Matrigel (Corning 356231). Nasal organoids were cultured at 37ºC with 500 µL of Pneumacult-Ex Medium (Stemcell) supplemented with penicillin/streptomycin and Amphotericin B and passaged every 7-10 days, changing the medium every 2 days.

Susceptibility of nasal turbinate organoids to PEDV

NTOs were maintained as 3D airway organoids in Matrigel and 2D cultures were prepared for the infection experiments (541). Briefly, 3D NTOs were dissociated with 0.05% trypsin-EDTA (Gibco). Once trypsin was inactivated, the organoids were vigorously repeated pipetted up and down to dissociate into single cells that were filtered through a 40-µm cell strainer (352340; Corning), centrifuged and resuspended in PneumaCult-Ex Medium with 10 µM rock inhibitor (Y-27632). These cells were seeded at $3x10^5$ into a 96-well plate pre-coated with Matrigel and incubated at 37ºC for 5 days. The PneumaCult-Ex Medium was then changed to Differentiation Medium (Complete PneumaCult Airway Organoid Basal Medium, Stemcell) and replaced every 2 days for 7 more days of incubation. After 12-14 days differentiated monolayers were ready for the infections.

ALI (Air-Liquid Interface) cultures were also prepared using 0.4 µm pore size transwells (Costar) following the same procedure mentioned above, but with different incubation times after seeding. Cells were cultured with PneumaCult-Ex Medium for 3-4 days, then switched to differentiation medium for 7 days and then cultured with PneumaCult-ALI Medium for 7-10 days more only in the basal compartment (21 days in total approximately). TransEpithelial Electrical Resistance (TEER) was regularly measured to check the monolayer barrier integrity.

Subsequently, the NTOs were infected with 1% trypsin-treated PEDV (USA/NC49469/2013 strain) at an MOI of 1.5, following the same procedure described above. Finally, the presence of PEDV in cells and supernatants was detected using RT-qPCR and IF of fixed cells at 24 and 48 hpi. Images were obtained using a confocal microscope (LEICA Stellaris 8).

Nucleic acid extration and detection of PEDV using RT-qPCR

Viral RNA was extracted from cells and supernatants using the IndiMag RNA/DNA Kit (INDICAL) and MagMAX Pathogen RNA/DNA kit (Thermo Fisher Scientific), respectively, according to the manufacturer's instructions. The detection and quantification of PEDV, TGEV and PRV-A were performed using commercial kits as described in the M&M section from the previous study I. The results were expressed as Ct values in both cells and supernatants.

Virus titration in cell culture

Viral titration in cell culture involved assessing infectious virus in supernatant samples collected at designated times points. The titration assay was conducted in duplicate using CCL-81 Vero cells. Samples were subjected to seven serial dilutions, starting with a 1:10 dilution, and were transferred to CCL-81 cells in a final volume of 50 µL/well. Following virus adsorption for 2.5 hours, the plates were incubated for 5 days at 37ºC with 5% CO_2 in 100 µL/well of serum-free DMEM containing 10 µg/mL of trypsin. Plates were monitored daily under a light microscope to evaluate the presence of cytopathic effect (CPE) until 5 dpi. The infectious virus concentration was quantified by determining the dilution at which 50% CPE was observed in the cell cultures ($TCID_{50}$/mL). Additionally, the presence of PEDV antigen in 3D4 and PAM supernatants was confirmed by IF (Medgene Labs SD6-29).

PEDV IF

PEDV nucleoprotein antigen detection was carried out on infected PAMs and 3D4 cells at 24 and 48 hpi using IF. Cells were washed with PBS and fixed in 96% ethanol before being frozen overnight at -20ºC. Upon thawing, three consecutive washes with PBS-1% FBS were performed; then, directly FITC-labelled anti-PEDV rabbit monoclonal antibody (Medgene Labs SD6-29) diluted at 1:200 was added. After 1 hour of incubation at 37ºC in darkness, cells underwent six washes with PBS, the initial three of which supplemented with 1% FBS. Subsequently, 100 µL of Hoechst (Hoechst 33342 Invitrogen- H3570) diluted at 1:2,000 was added and incubated for 5 minutes at RT in darkness. Finally, two PBS washes were performed before examination using an inverted fluorescence microscope (Motic AE31E).

For 2D NTO, cells were fixed with 96% ethanol following the same procedure as described above. On the other hand, ALI organoids on transwells were fixed using 4%

paraformaldehyde (PFA 4%). Briefly, after removing the PneumaCult-Ex Medium from the transwells, the cells were fixed with 100 µL of PFA 4% and incubated for 2 hours at RT followed by overnight incubation at 4ºC. Subsequent steps involved permeabilizing the cell membranes with 0.5% Triton-X/3% BSA for 1 hour at RT, followed by a wash with PBS supplemented with 0.1% BSA. Anti-PEDV antibody and Hoechst were added following the same procedure as previously described above. The membrane was then cut and carefully positioned cell-side up on a drop of mounting medium (ProLong Invitrogen-P36982) on a slide. After covering the surface with mounting liquid, a coverslip was placed, and the slide was left overnight in the dark at RT. Confocal images were acquired using a Leica Stellaris 8 microscope (Leica Microsystems, Wetzlar, Germany) equipped with HyD detectors and a 63×/1.40 NA oil immersion objective (HC PL APO CS2, Leica). The refractive index of the immersion medium was 1.518. A z-stack consisting of 77 optical sections, separated by 130 nm, covered a total axial volume of 10 µm. Excitation was performed using a 405 nm diode laser (2.45% power) and a white light laser tuned to 501 nm (6.42%). Emission was detected in two sequentially acquired channels: 420–506 nm (blue, gain = 2.5) and 509–557 nm (green, gain = 29.3). 1024 × 1024-pixel images were acquired at a 400 Hz scanning speed, with bidirectional scanning and a zoom factor of 5. Each image was the result of averaging 2 scanned lines, with the pinhole set to 95.5 µm (1 Airy unit for 580 nm emission). The acquisition system was controlled by Leica LAS X software (version 4.6.1), and images were saved in .lif format with embedded metadata.

Transmission electron microscopy

Cells with >90% confluence were fixed with 4% PFA and 1% glutaraldehyde diluted in PBS (fixation buffer). Then, cells were mechanically detached using a cell scraper and transferred to a 50 mL tube. After centrifugation at 500g for 10 minutes at 4ºC, the supernatant was discarded, and the pellet was treated with 1.5 mL of fixation buffer. The sample was then stored at 4ºC until processed for embedding in resin, ultramicrotomy, and transmission electron microscopy (TEM).

Briefly, cells were fixed with 2.5% glutaraldehyde in PBS for 2 hours at 4ºC, post-fixed with 1% osmium tetroxide with 0.8% potassium ferrocyanide for 2 hours and dehydrated in increasing concentrations of ethanol. Cell pellets were then embedded in epon resin (EMS, Hatfield, PA, USA) and polymerized at 60ºC for 48 hours. Sections of 70 nm were stained with 2% uranyl acetate and Reynold's solution (0.2% sodium citrate and 0.2% lead nitrate) and imaged using a JEM-1400 TEM (JEOL, Akishima, Tokyo, Japan), at 120 kV. All chemicals and reagents used were purchased from Sigma Chemical Co. (St. Louis, Mo, USA) unless otherwise stated.

Cytokine profiling

Cytokines in supernatants at designated time points (0–96 hpi) were measured by Luminex and ELISA assays. Concentrations of TNF-α, IL-4, IL-6, IL-8 (CXCL8), IL-10, IL-12/IL-23p40, IL-1β, IFN-α, and IFN-γ were quantified using a Luminex assay following the manufacturer's protocol (ProcartaPlex Porcine Cytokine & Chemokine Panel 1 9-Plex, Thermo Fisher Scientific #EPX090-60829-901). The lower limits of detection for each cytokine were: TNFα 199.42 pg/mL, IL-4 1.44 pg/mL, IL-6 171.04 pg/mL, IL-8 (CXCL8) 277.50 pg/mL, IL-10 14.77 pg/mL, IL-12/IL-23p40 255.70 pg/mL, IL-1β 29.16 pg/mL, IFN-α 3.43 pg/mL and IFN-γ 19.15 pg/mL. Additionally, ELISAs were performed to analyze the levels of IFN-β (Thermo Fisher Scientific, #ES8RB); IFN L3 (IL-28b) (Krishgen #KLP0471), IL-1α (GENLISA, #KLP0115), IL-11 (R&D SYSTEM, #D1100), IL-18 (GENLISA, #KLP0114), IL-22 (GENLISA, #KLP0518), TGF-β (GENLISA, #KLP0376), CXCL10 (GENLISA, #KLP0554), CCL5 (PIG RANTES #ABX154995-96) and IL-17 (Kingfisher Biotech, #DIY0730S-003) in accordance with the manufacturer's instructions. A 1:2 dilution was performed prior to the ELISAs for IFN-β, IL-1α, IL-18, IL-22, TGF-β, and CCL5.

Statistical analyses

Statistical analyses and graphs were conducted using GraphPad Prism 10. PEDV load in cells and supernatants across time points was analyzed using a mixed model analysis with Šídák's multiple comparisons test, while comparisons among cell types and ELISA results used Tukey's multiple comparisons test.

Results

The PEDV-USA inoculum S protein shared a high homology with PEDV strains that replicate in alveolar macrophages

The similarities between the S protein nucleotide and aa sequences between PEDV isolates are described in Figure 5.1. Analysis of the S gene sequences revealed a conserved sequence length of 4172 nucleotides encoding a 1386-aa protein. The S protein from the inoculum exhibited high homology with CNU-091222 PEDV strains, showing 97.1% nucleotide and 96.4% aa sequence similarity. These strains, obtained from intestinal homogenates, were found to be capable of replicating in PAMs, as suggested by Park and Shin (222). Conversely, the similarity of the S protein from the viral inoculum with PEDV strains that only exhibit affinity for

intestinal enterocytes, such as the CV777 reference strain, was lower, with identities ranging from 93.6% to 94.9% in nucleotide sequences and 91.5% to 94.2% in aa sequences. Analysis of variations within the S-protein aa sequence of the inoculum revealed differences in the S1 and S2 regions (55% and 45%, respectively of the total mutations of the S protein) compared to the consensus sequence, including key regions such as the HR regions (25%), S1/S2 cleavage site (10%) and FP (10%).

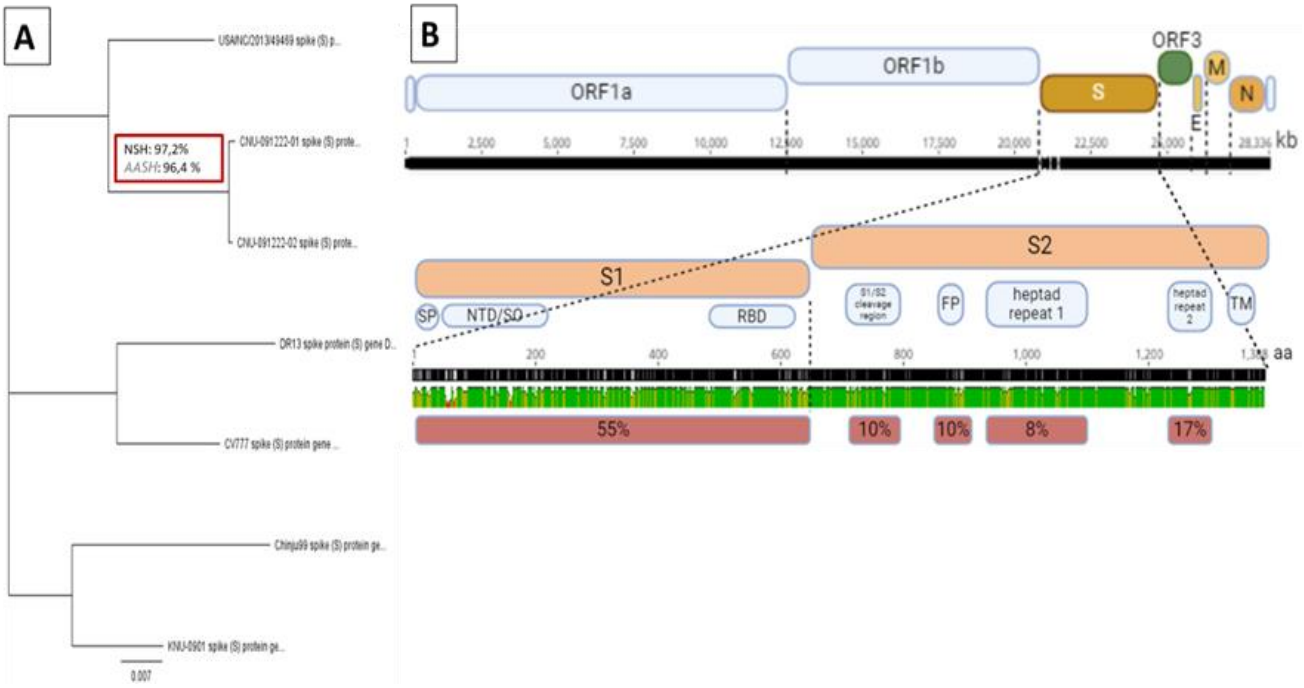

Figure 5.1. Phylogenetic and sequencing analysis of the Inoculum (USA/NC49469/2013). The inoculum is most closely related to the CNU-091222 strains, with 97.2% nucleotide sequence homology (NSH) and 96.4% aa sequence homology (AASH). Compared to strictly intestinal strains, variations in the aa sequence of the inoculum were identified in S1 (55%), the S1/S2 cleavage region (10%), the fusion peptide (FP) (10%), heptad repeat 1 (HR1) (8%), and HR2 (17%).

Despite PEDV internalization, PAMs and 3D4 cells exhibited limited susceptibility to the virus leading to nonproductive infection *in vitro*

CCL-81, PAMs and 3D4 cells were susceptible to PEDV infection, as indicated by the detection of PEDV RNA in all cell types from 6 hpi onwards (Figure 5.2A and B). While CCL-81 cells were able to sustain viral replication, peaking at 48 hpi (Ct=16 in both cells and supernatant), 3D4 cells harbored a higher amount of PEDV RNA than PAMs, but no viral replication occurred in either, as indicated by stable Ct values in the supernatant up to 96 hpi (Ct average around 23).

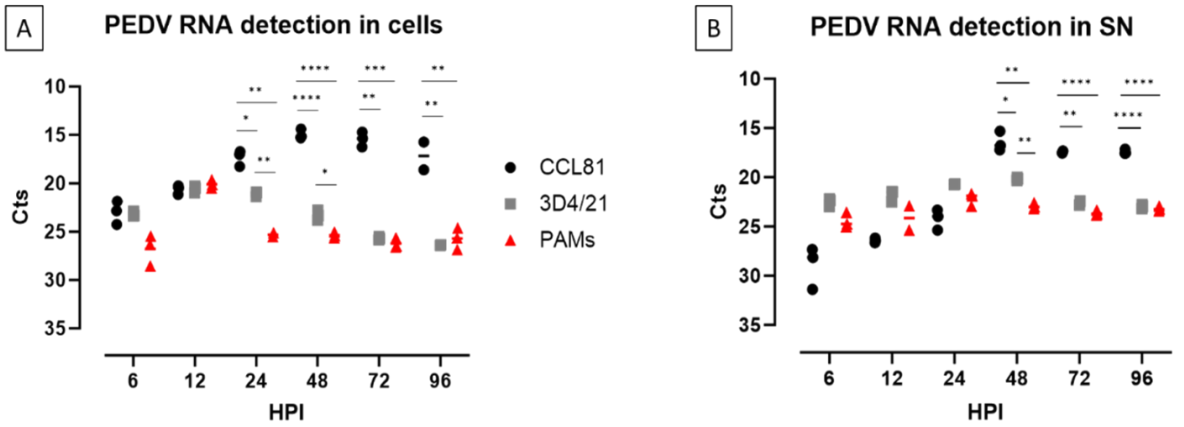

Figure 5.2. Detection of PEDV RNA in CCL8, 3D4/21 and PAMs by RT-qPCR in cells (A) and supernatant (B) from 6 to 96 hpi. HPI: hours post infection; PAMs: porcine primary alveolar macrophages; * (p<0.05); ** (*p*<0.01); *** (*p*<0.001); **** (*p*<0.0001). The bars show the mean + standard deviation. SN: supernatant.

IF analysis confirmed the presence of PEDV antigen within the cytoplasm of CCL-81, PAMs, and 3D4 cells at 24 and 48 hpi. However, large aggregates of PEDV-immunolabeling cells were predominantly observed in CCL-81 cells (80% and 95% at 24 and 48 hpi, respectively), while PAMs and 3D4 cells showed minimal numbers of PEDV-positive cells (below 5% at 24 hpi, with no increase at 48 hpi) (Figure 5.3A, B and C).

Furthermore, supernatants from CCL-81, PAMs, and 3D4 induced the formation of cellular syncytia in CCL-81 cells, indicating their infectious potential (Figure 5.3D, E and F). The amount of infectious virus titers was significantly lower in supernatants from PAMs and 3D4 compared to CCL-81 cells (Figure 5.3G) with viral infectivity declining over time in PAMs and 3D4 cells, although with significant differences from 72 hpi onwards between the later cell types.

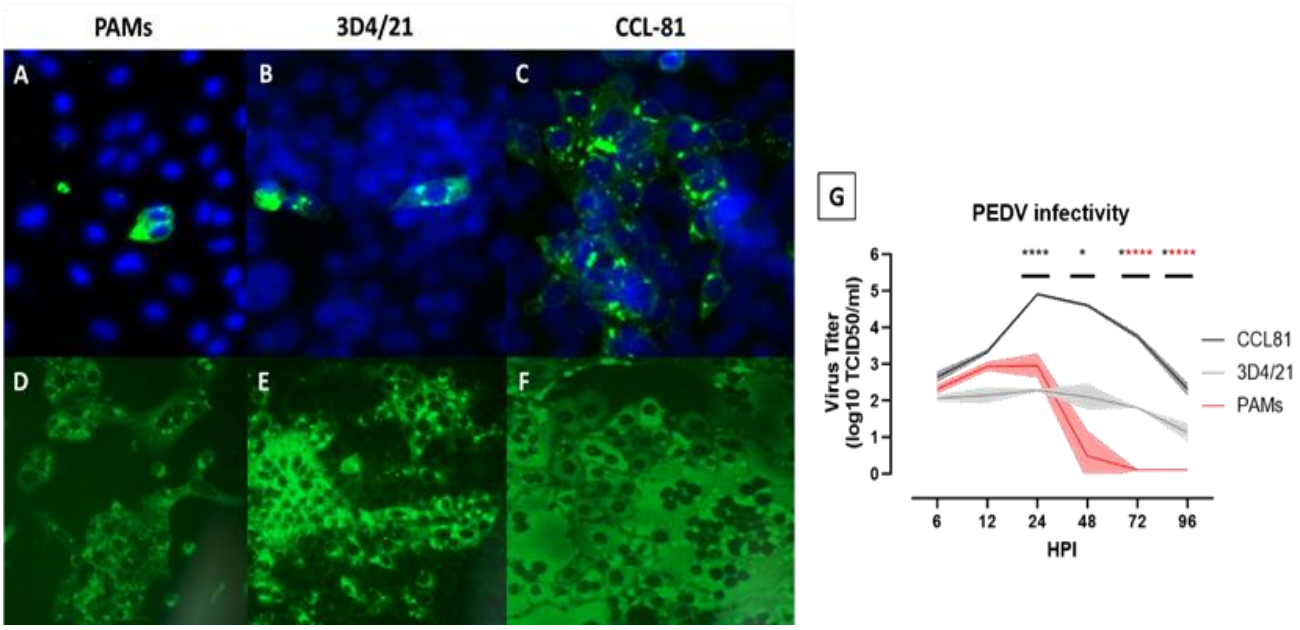

Figure 5.3. Localization of PEDV antigen in the cytoplasm of PAMs (A), 3D4 (B), and CCL-81 (C) examined through immunofluorescence. Presence of individualized PEDV-loaded macrophages unlike large aggregates of PEDV-immunolabeled VERO cells. PEDV infectivity from the supernatant of PAMs (D), 3D4 (E), and CCL-81 (F) in VERO cell culture (CCL-81). Presence of PEDV antigen in syncytial cells (cytopathic effect) by immunofluorescence in the three different cell lines. G: Comparison of infectious virus (measured by $TCID_{50}$/ml) in the supernatant of PAMs, 3D4, and CCL-81 at different time points. Significant differences between groups are shown as asterisks above each time point. Black asterisks show differences between CCL-81 and both PAMs and 3D4 while red asterisks show differences between PAMs and 3D4. The bars show the mean + standard deviation.

Ultrastructural changes confirm CCL-81 cells support PEDV replication unlike PAMs and 3D4 cells

To investigate the ultrastructural changes induced by PEDV in PAMs and 3D4, CCL-81 cells were used as control cells at both 24 and 48 hpi.

As observed in Figure 5.4, unexposed CCL-81 cells exhibited typical cellular characteristics, including cell size and well-preserved organelles, cytosol, and nucleus. Conversely, 24 hours after exposure to PEDV, CCL-81 cells showed morphological alterations indicative of cellular damage, such as mitochondrial and lysosomal swelling, and chromatin condensation. Large vacuoles containing virions were also observed throughout the cytoplasm, confirming the reorganization of host cell membranes and evidence of PEDV replication (Figure 5.4B arrows). These vacuoles may correspond to large virion-containing vacuoles (LVCVs), but their specific membrane origin could not be confirmed. Ultra-thin sections at 24 hpi revealed other PEDV-related structures, such as double-membrane vesicles (DMVs) and dilated single-

membrane transport vesicles containing numerous mature virions (Figure 5.4C arrowhead). Some DMVs were individualized, while others were within irregular vesicle clusters (IVCs). In general terms, these vesicles were found near the rough ER, suggesting they may correspond to dilated ERGIC; however, they could also be secretion vesicles (SV) due to their proximity to the plasma membrane. The Golgi apparatus was not well-preserved at 24 hpi, hindering its identification. At 48 hours post-PEDV exposure, most cells exhibited an increase in the size and number of LVCVs throughout the cytoplasm (Figure 5.4D), highlighting ongoing PEDV replication between 24 and 48 hpi in CCL-81 cells. The virion-filled transport vesicles described at 24 hpi were still present at 48 hpi (Figure 5.4E), along with two other structures: single-membrane vacuoles containing virions, compact membrane whorls, and amorphous material, consistent with endolysosomal compartments (ELS) (Figure 5.4E and 5.4F); and large cytoplasmic inclusions connected to the ER, exhibiting a dense inner core with a geometric appearance (Figure 5.4G star). This structure could not be precisely identified but may be consistent with either ER bodies (ERBs) or convoluted membranes (CMs). At 48 hours post-PEDV exposure, most cells exhibited marked chromatin condensation and the presence of abundant cellular debris and mature virions extracellularly, indicating cell death and lysis (Figure 5.5).

No ultrastructural membrane rearrangements were observed in PAMs or 3D4 cells at 24 or 48 hpi. Considering the limited number of PAMs and 3D4 cells expressing PEDV antigen as detected by IF, TEM was not a suitable technique for analyzing virus internalization, replication, or degradation in these cell lines. Nevertheless, these cells did not exhibit morphological differences from their negative controls (data not shown), suggesting no apparent signs of cellular damage at the ultrastructural level after PEDV exposure.

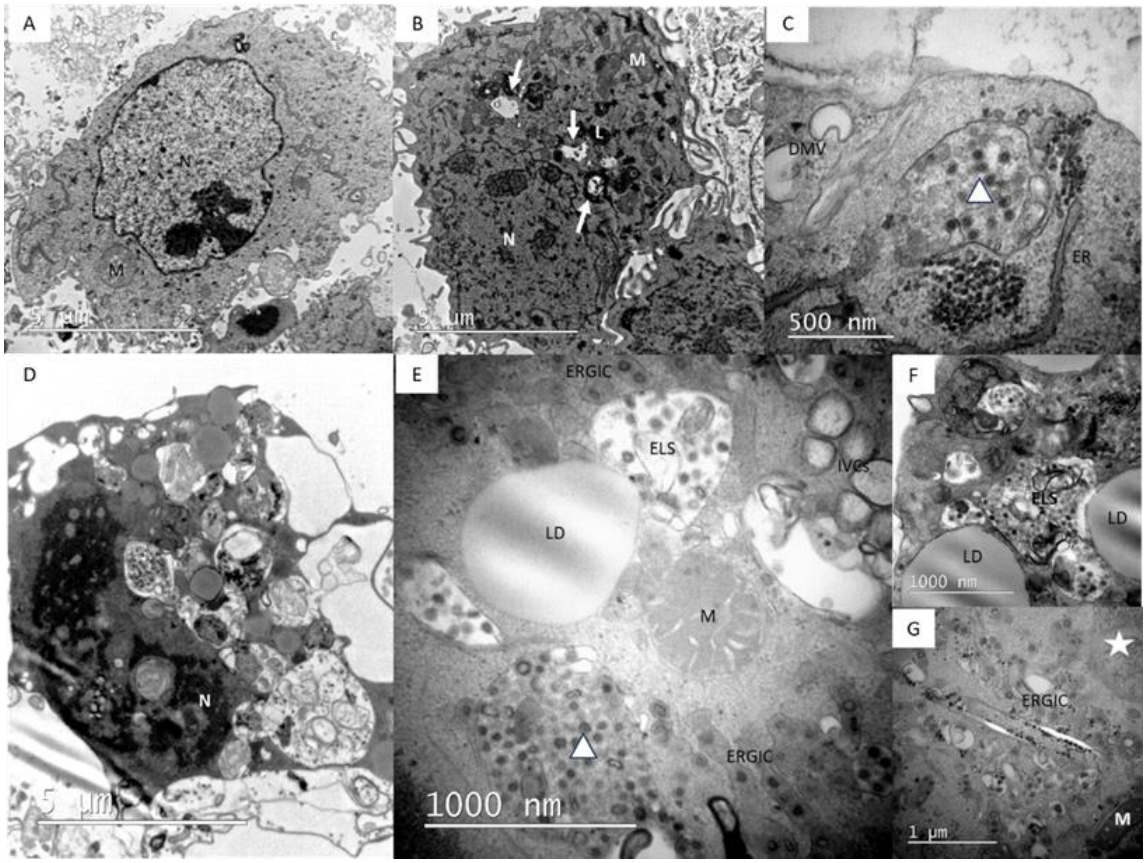

Figure 5.4. Ultrastructural features of untreated CCL-81 cells (A) and PEDV exposed CCL-81 (B-C: 24 hpi; D-G: 48hpi). B: Presence of large vesicles containing virions (arrows) in the cytoplasm of a CCL-81 cell at 24 hpi. C: CCL-81 at higher magnification: Mature virions inside a single-membrane vesicle (arrowhead) between the endoplasmic reticulum (ER) and the cell membrane. Presence of double-membrane vesicles (DMVs). D: Degenerated CCL-81 cells at 48 hpi with condensed and fragmented nucleus and presence of abundant large vacuoles filled with virions and cell debris in the cytoplasm; E: Higher magnification of CCL-81 at 48 hpi showing different cellular structures filled with mature virions (arrowhead) including dilated ER-Golgi intermediate compartment (ERGIC) and single-membrane vesicle filled with cell debris compatible with endolysosomal compartment (ELS). Double-membrane vesicle (DMV) within Irregular vesicle clusters (IVCs). Higher magnification image of a CCL-81 at 48 hpi showing the ultrastructural characteristics of an ELS filled with mature virions (F) and ERGIC close to the endoplasmic reticulum (G). Presence of cytoplasmic inclusions with a dense inner core and a geometric appearance (star) compatible with Convoluted membranes or ER body. N: Nucleus; M: Mitochondria; L: Lysosome; LD: Lipid droplet.

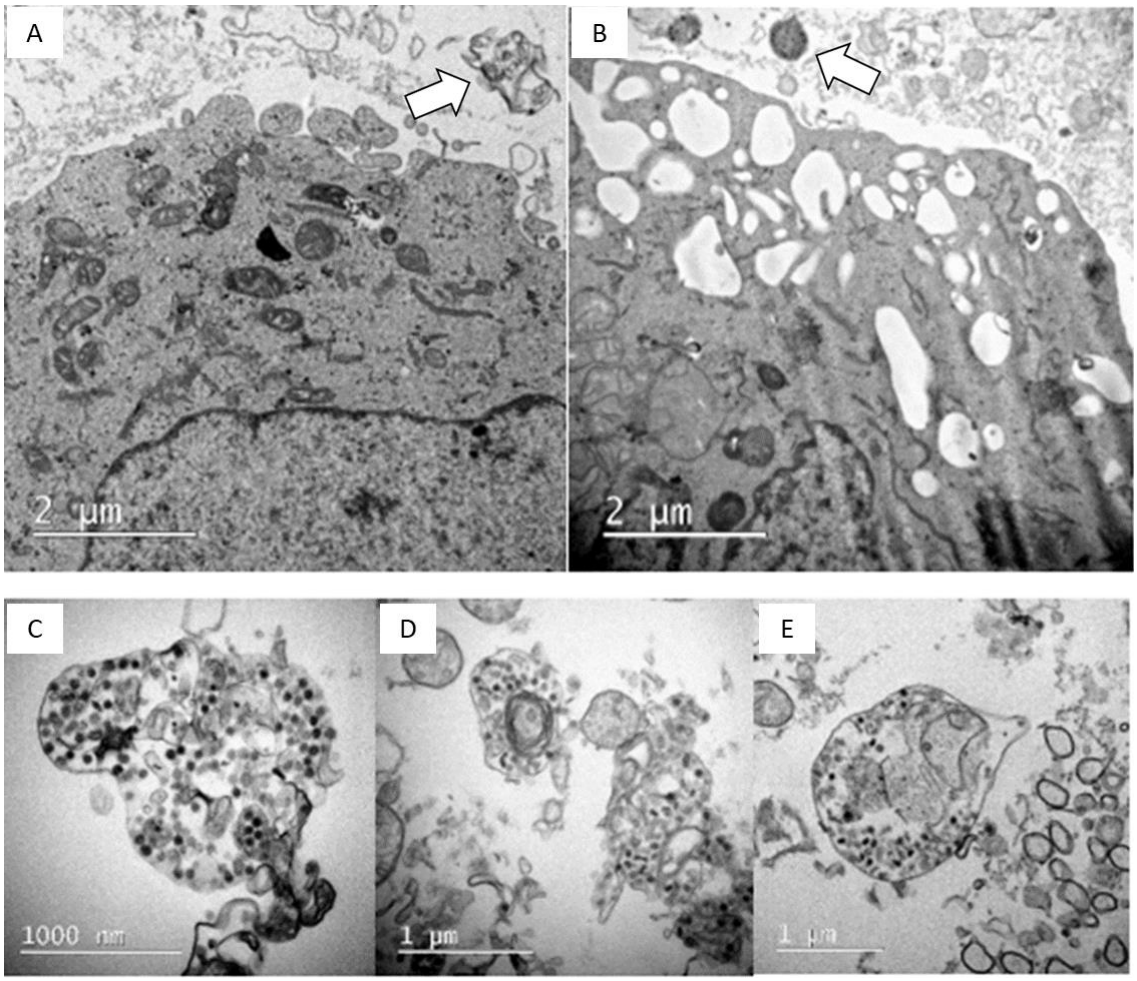

Figure 5.5. Ultrastructural images of CCL-81 at 48 hpi of PEDV exposure. A-B: Presence of cellular debris and remnants of vacuoles filled with virions at the extracellular level (arrow), indicative of cell lysis. C-E: Ultrastructural images at higher magnifications of vacuoles filled with virions at the extracellular level.

Lack of proinflammatory or antiviral responses in PAMs and 3D4 cells post-PEDV exposure

Cytokines analysis in PEDV-exposed PAMs, 3D4, and CCL-81 cells revealed no statistically significant differences compared to mock-treated cells at different time points ($p<0.05$). Specifically, CXCL10, IL-11, and IL-28 remained stable across all cell lines before and after PEDV exposure. IL-22, TNF- α, and IL-18 expression was limited to PAMs, showing a decrease over time. While IL-6 was upregulated in 3D4 cells at 24 hpi and IL-8 in both PAMs and 3D4 cells from 6 hpi, levels did not increase post-PEDV exposure and were comparable to mock-treated cells, indicating that their upregulation was independent of PEDV exposure.

Additionally, no expression of TGF- β, IL-1 (α or β), CCL5, IL-4, IL-10, IL-12, or interferons (IFN) type I (IFN-α and β) and II (IFN-γ) was observed throughout the study in any cell line

following PEDV exposure. These results indicate a lack of proinflammatory or antiviral response in alveolar macrophages following PEDV exposure.

NTOs successfully captured and internalized PEDV within 24 hpi, serving as an alternative model for studying PEDV pathogenesis

PEDV RNA was detected in nasal turbinate epithelial cells and SN at 24 hpi. Viral load was higher in the respiratory epithelium cultured in ALI (transwells) compared to 2D monolayer culture, as indicated by lower Ct values (28.07 versus 31.3, respectively). No significant differences in Ct values were observed in the SN collected from both culture methods (Figure 5.6A). To demonstrate the internalization of PEDV in the nasal epithelium, PEDV antigens were labeled using IF. Few NTOs obtained from both the 2D monolayer and ALI culture showed PEDV in the cytoplasm by widefield and confocal microscopy (Figure 5.6B and C, respectively). However, less than 5% of cells were found to be PEDV-immunolabeled in both cases. Due to the low number of PEDV-infected epithelial cells, viral titration was not feasible, making it impossible to assess the infective capacity of PEDV in this model.

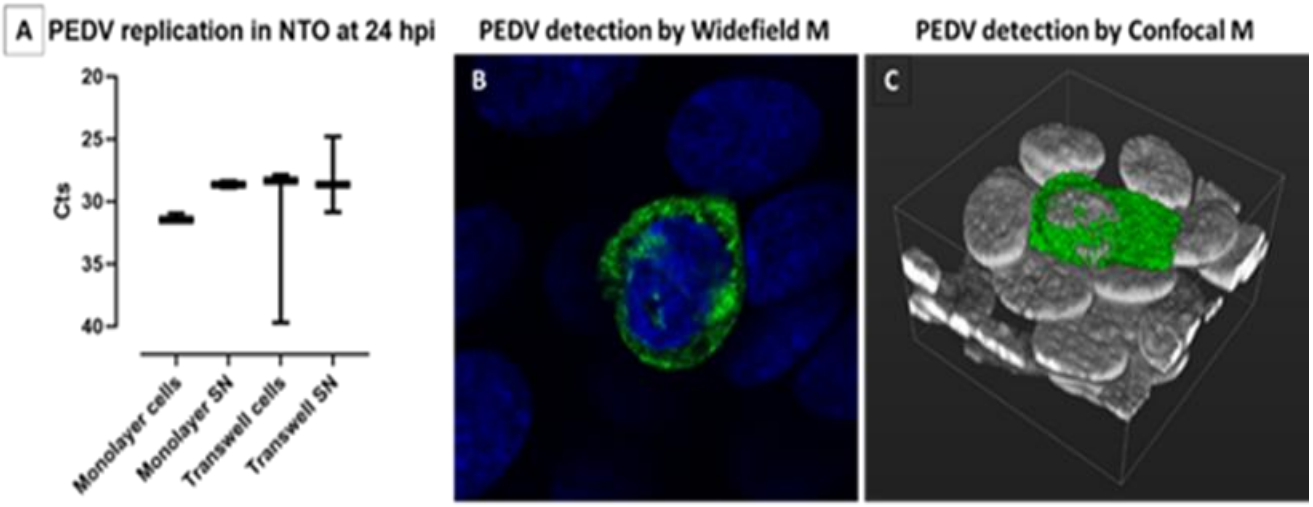

Figure 5.6. Viral load of PEDV assessed by RT-qPCR (A) in cells and supernatant of nasal turbinate organoids (2D-Monolayer and ALI culture) at 24 hpi. PEDV antigen localization in the cytoplasm of nasal turbinate organoids cultured in ALI technique detected by widefield (B) and confocal microscopy (C).

Discussion

PED is a severe gastrointestinal disease that results in high mortality rates in piglets, mainly due to severe diarrhea. PEDV primarily replicates in mature enterocytes of the small

intestine and colon (182), leading to significant atrophy and fusion of microvilli. Despite this major tropism, studies have indicated that PEDV can also infect other cell types, including macrophages in the intestinal lamina propria, DCs, respiratory epithelial cells, and alveolar macrophages (220,222,241,504,505,540). These studies suggest the possibility of systemic spread of PEDV through an aerogenic route of entry. Several CoVs, including TGEV, can replicate in respiratory tract tissues (2), while MERS-CoV can also be captured and internalized by llama alveolar macrophages (542). However, in both cases, alveolar macrophages did not allow effective viral replication, thus preventing lower respiratory tract disease. Similarly, Park and Shin (222) suggested that PAMs may not be the primary target for PEDV replication, though they could still play a role in its survival and potential persistence infection. Therefore, the present study aimed at investigating the involvement of primary PAMs in the pathogenesis of PEDV by analyzing ultrastructural changes in inoculated cells and evaluating potential anti-inflammatory and antiviral responses upon viral sensing.

Here, PEDV was demonstrated to be internalized by both 3D4 cells and PAMs via IF analysis. However, the number of PEDV-labeled cells remained consistently low, even after 48 hpi with no significant increase observed between 24 and 48 hpi. Additionally, RT-qPCR analysis confirmed the presence of PEDV in both PAMs and 3D4 cells, but no significant increase in RNA copies or viral particles was detected in the supernatant of these macrophagic cells. Moreover, the supernatants of these PEDV inoculated-cells showed low viral titers, indicating a lack of infectious capacity compared to Vero cells. Overall, these results suggested that while PEDV can be captured by PAMs, it may not replicate efficiently in these cells compared to Vero cells, as previously reported (222). Nevertheless, these results contradict those observed in other studies (243). The reasons behind this discrepancy are uncertain and remain speculative. However, Park and Shin (222) observed that wild-type strains of PEDV capable of replicating in alveolar macrophages displayed certain degree of heterogeneity in the S glycoprotein compared to other PEDV strains that primarily cause enteric diseases, as indicated by sequencing analysis. This observation led researchers to propose that natural mutations in the S protein could potentially determine auxiliary targets for PEDV, allowing its entry and replication in other cells such as PAMs and facilitating its ability to replicate in extraintestinal tissues.

Sequencing analysis of the inoculum (USA/NC49469/2013) revealed a higher degree of similarity to PEDV strains claiming their replication in alveolar macrophages compared to those replicating exclusively in intestinal enterocytes (222). Consistent with these results, most aa variations in our inoculum were identified in the S1 subunit, particularly in the RBD, followed by the HR 1 and HR2 of the S2. These viral proteins play a crucial role in mediating viral entry into

host cells through the 6-HB mechanism, leading to fusion between the viral envelope and the host cell membrane (166). Although the present study does not confirm whether these S protein variations facilitate PEDV replication in PAMs, the findings align with Park and colleagues' hypothesis that mutations in the S may contribute to the tropism shift of PEDV.

The present study also revealed that PAMs did not exhibit significant antiviral or pro-inflammatory responses upon PEDV internalization, unlike what has been observed in DCs and other monocyte-derived antigen-presenting cells (241). Consequently, our findings suggest that PEDV-infected piglets do not develop respiratory disease despite PAMs harboring the virus. However, this observation should be interpreted with caution, as other studies have reported differing results, highlighting the need for further investigation into the relationship between PAMs and disease pathogenesis. The reason for the lack of a robust immune or inflammatory response in PAMs upon virus sensing remains unclear. One possibility is that the low number of PEDV-positive cells detected by IF might result in subtle, undetectable overexpression of cytokines in infected cells, potentially due to limitations in the techniques used for protein expression analysis. Another possibility is that PEDV may employ mechanisms to modulate or evade the innate immune response of host cells, as reported in both *in vitro* and *in vivo* studies (75,388). Another proposed hypothesis is that PAMs have a reduced capacity to recognize PAMPs compared to other DCs, which could impair their ability to enhance antigen presentation and cytokine production following PEDV infection (241).

At the ultrastructural level, PEDV induced significant reorganization of Vero cell membranes and organelles, as previously described (83). PEDV virions were observed in DMVs, the ERGIC, and in large single-membrane vacuoles compatible with LVCVs. These observations suggest that PEDV assembles in both the ER and Golgi, a phenomenon also noted in other coronaviruses such as SARS-CoV, MERS-CoV, infectious bronchitis virus (IBV), mouse hepatitis virus (MHV), and human CoV NL63 (HCoV-NL63) (83). These cellular compartments likely serve as platforms for viral replication and transcription, underscoring the utility of Vero cells as an *ex vivo* model for PEDV studies, except for pathogenicity studies due to their lack of IFN. At 48 hpi, single-membrane vesicles resembling lysosomal compartments containing virions were noteworthy, suggesting that while PEDV replicates in Vero cells, there is also evidence of cellular degradation of viral particles. Additionally, the presence of abundant degenerated cellular material and free virions extracellularly suggests that the mechanism of PEDV-induced cell damage in Vero cells may occur through cellular necrosis. Notably, these findings were not observed in 3D4 cells or PAMs exposed to PEDV, possibly due to the limited number of PEDV-

positive cells in these cell lines, leading to negative results in TEM analysis. Therefore, TEM may not be the optimal technique for analyzing PEDV internalization in alveolar macrophages.

In accordance with previous studies (220,504), PEDV has been detected in NECs at 24 hpi by both RT-qPCR and IF assays. However, it remains inconclusive whether this cellular model supports viral replication *in vitro*.

Conclusion

Our findings suggest that PAMs can capture and internalize PEDV; however, they do not appear to support productive viral replication, based on the data obtained. We hypothesize that PEDV may persist in these cells undetected by the immune system, as PAMs do not trigger an inflammatory or antiviral response. Future research into this alternative pathway should include *in vivo* studies with intranasal infection, kinetic analyses using NTOs at various time points, and comprehensive transcriptional and proteomic analyses as well as flow cytometry to assess whether these cells activate innate immune and inflammatory responses upon PEDV internalization. In this case, PEDV-susceptible cells other than CCL-81, such as IPEC-J2, would be more useful for this purpose, as Vero cells are IFN-deficient. Additionally, studies using cellular markers for necrosis, apoptosis, and other programmed cell death pathways are needed to clarify the mechanisms of PEDV-induced cell death in sensitized cells.

PART III

General discussion and conclusions

CHAPTER 6

General discussion

PED is a gastrointestinal disease that causes significant economic losses to the global swine industry (4). Its impact is more pronounced in the Americas and Asia, where highly pathogenic non-S INDEL and S INDEL strains co-circulate. In contrast, Europe predominantly contends with S INDEL strains (2,4). The emergence of highly virulent genotypes highlights the urgent need for in-depth research to better control and prevent the disease. Over the past decade, the number of studies related to PEDV has grown significantly, and deepened our understanding of viral dynamics, genetics, and factors contributing to more severe outbreaks. Building on these findings, this PhD project aimed to investigate key factors influencing PEDV pathogenesis, including PEDV strain (non-S INDEL vs. S INDEL), piglet age, and the intestinal innate immune response. The general objective was to identify potential gaps and open new avenues for future research in the development of preventive treatments.

Prior to the start of this PhD project, several *in vivo* and *in vitro* studies demonstrated that clinical outbreaks caused by non-S INDEL strains were generally more severe than those caused by S INDEL strains. This increased severity was attributed to higher intestinal replication, increased fecal shedding, and more extensive intestinal damage, resulting in higher mortality rates especially in newborn piglets (182,207,301,307–312). Moreover, these effects tend to manifest earlier in infections with non-S INDEL strains. However, when both PEDV strains were adapted to Vero cells, their virulence was significantly reduced (316–320). Despite this observation, the mechanism underlying the loss of virulence remained unknown at the start of this PhD thesis. To address this, we analyzed genomic variations across the entire genome of wild-type and cell-adapted non-S INDEL and S INDEL strains, comparing clinical, pathological, and virological outcomes in 5-day-old suckling piglets inoculated orogastrically (*Study I*). As expected, the virulence of cell-adapted PEDV strains was significantly lower compared to wild-type strains and decreased inversely with the number of cell passages. This was illustrated by the partially attenuated PEDV-USA strain (8 cell passages) and the non-pathogenic PEDV-CALAF strain (22 cell passages). However, despite this attenuation, the cell-adapted PEDV S INDEL strain retained the ability to replicate in the intestine and was shed by feces, albeit at lower levels, compared to wild-type strains. This phenomenon was also observed in both PEDV strains after substantially more cell passages, as previously reported (316–320). These findings suggest that while PEDV adaptation to cells could serve as an attenuation methodology, it would not adequately reduce viral pressure on unimmunized farms if these strains were used as live-attenuated vaccines. Interestingly, when comparing the results from suckling piglets inoculated with the cell-adapted non-S INDEL strain (*Study I*) to those inoculated with the wild-type non-S INDEL strain (*Study II*), similar outcomes were observed across all analyzed parameters, including clinical, pathological,

and virological aspects, demonstrating that complete loss of virulence requires a high number of cell passages.

Sequencing analysis identified mutations in the S protein, several nsp, and the ORF3 gene of the cell-adapted S INDEL strain. Similar alterations were observed when comparing the more virulent non-S INDEL strain with the less virulent wild-type S INDEL strain. These findings underscore the significance of these genomic differences in contributing to the loss of virulence in cell-adapted strains and establish a potential genetic basis for the clinical differences between non-S INDEL and S INDEL strains. Based on the sequencing analysis results, we can speculate that observed differences between all PEDV strains may be associated with the production of IFN antagonists (regulated by nsp-2, 3, 4, 12 and 15) or with the inhibition of viral entry and fusion. This phenomenon may occur either due to alterations in the RBD within the S1 domain or due to abnormal formation of the 6-HB structure, regulated by HR1 and HR2 in the S2 domain. Additionally, in line with previous studies, ORF3 is prone to deletion or mutations during continuous *in vitro* passage, leading to attenuation *in vivo* due to premature translation terminations and a frameshift in the reading frame (102,543). Also, truncated ORF3 has been linked to increased virulence, resulting in severe clinical signs and elevated mortality rates, as observed with Chinese PEDV field strains (544,545). Similarly, genomic variations in both S and ORF3 proteins can contribute to interferon resistance and evasion of neutralizing antibodies (244). These findings suggest that genetic modifications in ORF3 identified in all PEDV inocula may be pivotal in the virulence differences between S INDEL and non-S INDEL strains, as well as in the attenuation of virulence after adaptation (96,100). While these variations could serve as potential therapeutic targets for disease control, further research are necessary to validate this correlation. Interestingly, the E protein remained highly conserved across different PEDV strains, showing no alterations even after multiple cell passages. This finding represents a significant step forward in developing new preventive treatments for PEDV, such as creating pan-PEDV vaccines.

The absence of overt disease in piglets inoculated with the cell-adapted S INDEL strain was associated with a lack of intestinal villi fusion and atrophy, suggesting a strong correlation between intestinal damage and clinical outcome. However, intestinal damage caused by cell-adapted non-S INDEL and wild-type S INDEL strains was similar, despite more severe diarrhea and weight loss was observed in piglets inoculated with the non-S INDEL strain. Similarly, villous atrophy and the amount of PEDV antigen in the damaged intestine were comparable when suckling and weaned piglets were exposed to both S INDEL and non-S INDEL strains (*Study II*). These findings indicate that the age-dependent clinical outcome was not directly proportional to intestinal damage and suggests the involvement of factors other than strain type and viral

load in the intestine, contrary to prior assertions (301,305,309). Similarly, this study demonstrated that both S INDEL and non-S INDEL PEDV strains exhibit a similar ability to replicate in the intestine and fecal shedding in both suckling and weaned piglets, as indicated by the viral load in the intestine and its contents, challenging previous reports (*Study II*). Despite all these results, weaned piglets exhibited resistance during the acute phase of the disease, while suckling piglets were highly susceptible. The absence of PEDV antigen in the colon of weaned piglets, compared to suckling piglets enables us to propose that the intact colon in weaned piglets may have reabsorbed watery content from the atrophic small intestines, thereby preventing the onset of diarrhea at 48 hpi. Additionally, the intestinal transcriptional pattern (*Study II*) revealed a greater ability for intestinal regeneration in weaned piglets due to the upregulation of tight and adherens junction proteins compared to suckling piglets, which aligns with previous studies (305). Alternatively, diarrhea might have appeared later in weaned piglets if the study duration would have been extended, as reported in other studies (219,233,302). Nevertheless, the involvement of other factors, such as microbiota composition and intestinal morphological or physiological differences, like the expression of aquaporin receptors, could be of interest for future studies to explore age-related differences among piglets. On the other hand, despite the significant intestinal damage observed in weaned piglets exposed to both PEDV strains, the absence of clinical disease was correlated with the activation of the innate antiviral immune response, as shown by intestinal transcription results (*Study II*). This study highlights the role of type I and, especially, type III IFNs, along with various Th1-Th17 proinflammatory cytokines in the intestinal mucosa, as the primary protective mechanism against both PEDV strains in weaned piglets during the acute phase of the infection. In contrast, the absence of IFNs and the overexpression of IL-10 were identified as risk factors for more severe disease in suckling piglets. Interestingly, the overexpression of several genes involved in IFN and ISGs could explain the unexpectedly low mortality in suckling piglets exposed to the non-S INDEL strain, emphasizing the protective antiviral role of these innate immune effectors against PEDV.

Furthermore, the activation of numerous ISGs, prostaglandins, HSP, STAT3, and inflammasome-related mediators underscored the establishment of a robust antiviral state in weaned piglets. Furthermore, this study also corroborated previous findings (306), emphasizing the critical role of NK cells and CTLs as key effectors of intestinal innate immunity during the acute phase of viral infections, particularly in weaned piglets compared to suckling ones (*Study II*). Collectively, the present PhD thesis provides valuable insights into potential therapeutic targets for combating the disease. However, while the upregulation of mRNA for several genes

involved in IFN and proinflammatory signaling pathways was demonstrated, drawing definitive conclusions requires confirmation at the protein level. Techniques like specific ELISAs or other protein detection methods would be essential, since many PCoVs, including PEDV, have evolved mechanisms to evade innate immune responses, such as directly antagonizing IFNs or inhibiting their translation (75,363,546).

Earlier research widely assumed that PEDV infection leads to enterocyte necrosis and detachment, resulting in the atrophy and fusion of intestinal villi (2,182). However, the exact mechanism of cell death caused by PEDV was unclear at the start of this PhD project. The findings from the three studies conducted in this PhD have confirmed that PEDV-infected cells, including enterocytes (*Studies I and II*) and CCL-81 cells (*Study III*), exhibited signs of damage and cell death. While TEM suggested necrosis in CCL-81 cells at 48 hpi, histopathological analysis revealed damage to enterocytes without clear evidence of necrosis. The transcriptional profile of PEDV-damaged enterocytes during the acute phase of infection demonstrated that PEDV modifies several cellular signaling pathways related to programmed cell death mechanisms, such as pyroptosis and apoptosis, for its own benefit, as previously reported (354). Interestingly, transcriptional patterns linked to these pathways differed between weaned and suckling piglets (*Study II*), underscoring their potential role in the age-dependent clinical presentation of PEDV. Nonetheless, further in-depth studies using techniques such as immunofluorescence and confocal microscopy, along with specific cellular markers for apoptosis, pyroptosis, necroptosis, ER stress, and autophagy, are needed to substantiate this hypothesis.

Historically, PEDV has been regarded as a gastrointestinal virus due to its exclusive tropism for intestinal enterocytes. However, emerging evidence suggested that PEDV may spread systemically after replicating in extraintestinal tissues, such as the respiratory system, particularly in the nasal epithelium and pulmonary macrophages (220–222). Despite these findings, the mechanisms of infection, pathological consequences, and the involvement of these cells in the pathogenesis of PED remained largely unexplored prior to this PhD project. In consequence, to investigate this potential alternative pathway, we conducted an *in vitro* study using PAMs and an *in vivo* experiment to evaluate the effects of intranasal infection on the manifestation of gastrointestinal signs.

As detailed in *Study III* of this PhD thesis, PAMs and NECs internalized PEDV but did not support viral replication. Therefore, the role of these cells in disease pathogenesis remains unclear. Nevertheless, we confirmed that despite detecting the virus in the nasal turbinates and lungs following intranasal inoculation of PEDV in both suckling and weaned piglets (*Study II*), this

alternative route of infection did not worsen the clinical presentation. When compared to the results from *Study I*, where only intragastric inoculation was performed, the intranasal inoculation did not increase diarrhea or mortality. Future studies on this line of research aimed at comparing the onset and severity of gastrointestinal signs between groups exposed exclusively to intranasal inoculation and those receiving only intragastric inoculation would be advisable. Addressing this direct comparison, which was not the objective of this PhD, could significantly enhance our understanding of the role of intranasal infection in PEDV pathogenesis.

In the absence of protein expression analysis, enterocytes from weaned piglets following acute PEDV infection showed overexpression of IFNs, pro-inflammatory cytokines, and NK and CTL promoters, triggered by recognition of PRRs such as TLR3, TLR7, RIG-1, and NLR3. However, PAMs did not contribute to inflammatory or antiviral responses during the acute infection, as no overexpression of pro-inflammatory or antiviral cytokines was detected. Furthermore, transcriptional analysis of PAMs could provide insight into whether there is overexpression of IFNs and/or pro-inflammatory cytokine mRNA, or if PEDV induces post-transcriptional inhibition as an immune evasion strategy, as observed in Vero cells, IPEC, IEC and PAMs (75,363,388,546). Nonetheless, the lack of an antiviral response in these infected myeloid cells may be due to insufficient PRRs sensitization to PEDV, representing another important area for future investigation. A limitation of this study was the lack of investigation into whether these myeloid cells express pAPN, although it has been suggested (Fabian Z.X, personal communication). However, detection of PEDV antigen in PAMs suggested the presence of another membrane receptor that can be recognized and utilized by PEDV for entry. While this PhD project did not provide specific information on this topic, interactions between PEDV and membrane glycoproteins, such as Siglecs, could play a significant role, as documented in other CoVs like SARS-CoV-2 (547,548).

This project strongly corroborates previous literature on the critical role of the S protein in adaptation of PEDV to new cells and tissues, as shown by the sequencing results in *Study III*. Furthermore, phylogenetic analysis presented in *Study I* highlighted the role of PEDV recombination processes in the emergence of new genotypes, which complicates the global epidemiological situation and poses challenges to the global swine industry. For instance, the NC/2013/49469 inoculum clustered with other USA non-S INDEL strains within the GIIa genotype (e.g., Wisconsin74 and Minnesota100), alongside Asian non-S INDEL strains (e.g., SK/KNU1305). This suggests that its origin likely involves recombination events with re-emerging Asian strains from that period. Similarly, the 2014 outbreak in Ukraine involved a non-S INDEL strain closely related to non-S INDEL strains from both the USA and Asia (eg., NC35140; Texas31; Minnesota94

and JPN/OKN1), indicating a potential origin from these regions. Additionally, emerging European S INDEL strains from 2014 to 2016, such as ESP/Calaf-1/2014, were introduced into Europe through recombination events involving S INDEL strains from the GIb genotype, originating in either the USA (e.g., OH851, Minnesota58, and Indiana12.83) or Asia (e.g., SK/KNU-1406-1). Moreover, the development of new Chinese GIIc genotypes may have potentially resulted from the recombination of GIIa and GIIb Asian strains, differing from previous hypotheses (209,218).

The S protein not only influences the evolutionary development of new PEDV strains with expanded tissue tropism but also contributes to the emergence of more pathogenic strains. These findings underscore the significant challenge posed by new strains for disease control and their potential risk for cross-species transmission and public health. Given the rising severity and prevalence of PEDV, there is an urgent need for further investigation into the genetic diversity and molecular characteristics of the S gene in PEDV field strains.

Overall, in this PhD project, we investigated the molecular mechanisms behind the attenuation and loss of virulence in PEDV, identifying certain viral proteins associated with PEDV pathogenicity (*Study I*). Additionally, we proposed that, contrary to previous understanding, the severity of digestive clinical signs is not directly linked to the extent of intestinal damage caused by PEDV. To understand the cause of this age- and strain-dependent clinical outcome, we examined the intestinal innate immune response in detail against both PEDV strains, highlighting a crucial role in disease control by weaned piglets as opposed to suckling ones. Lastly, we demonstrated that PEDV may exhibit tropism for different cells beyond enterocytes, with this ability specifically depending on the S protein. However, the role of these other cells in PED pathogenesis remains unclear.

CHAPTER 7

Conclusions

1) Suckling piglets were susceptible to both wild-type and cell-adapted S INDEL and non-S INDEL PEDV strains. However, virulence decreased with increasing cell passages (at least 22 passages). The S INDEL strain adapted to cell culture did not cause clinical disease but replicated in enterocytes and was shed in feces, although to a much lower extent than the non-S INDEL strain.

2) The reduction in virulence of cell-adapted PEDV strains was linked to the absence of villous atrophy and fusion, potentially driven by specific amino acid variations in the Nsp, S protein, and ORF3 regions of the PEDV genome. Similar genomic variations could explain the different clinical outcomes between S INDEL and non-S INDEL strains.

3) The E protein exhibited the most conserved sequence within the genome across PEDV strains, remaining unchanged after multiple cell passages (at least 22 passages).

4) Pigs of 5 days and 5 weeks of age were susceptible to both PEDV strains, with non-S INDEL PEDV causing more severe disease in suckling and weaned piglets. However, PEDV replication, shedding, intestinal damage, and the amount of PEDV antigen in affected intestinal areas were similar across piglets of all ages, regardless of the viral strain. Therefore, the clinical outcome was not proportional to intestinal damage.

5) Intestinal innate immunity, particularly type III IFN and Th1-Th17 proinflammatory cytokines, played a key role in determining the age-dependent clinical outcomes, providing similar protection to weaned piglets against both PEDV strains.

6) Prostaglandins, HSPs, STAT3, inflammasome-related mediators along with NK cells or CTLs inductors, supported a protective antiviral state against PEDV in weaned pigs. Conversely, an IL-10–induced anti-inflammatory state promoted disease progression in suckling piglets.

7) Weaned piglets showed a greater capacity to regenerate intestinal tissue after infection compared to suckling piglets. Enhanced expression of tight junction and adhesion molecules restored membrane integrity, highlighting age-related differences in recovery mechanisms.

8) PEDV, particularly the non-S INDEL strain, modulated the expression of MAPK and programmed cell death pathways, such as pyroptosis, indicating that these cellular signaling pathways were crucial for promoting a proviral state.

9) Alveolar macrophages and nasal epithelial cells allowed the internalization of non-S INDEL PEDV. However, these cells did not support evident viral replication, likely not contributing to PEDV pathogenesis.

REFERENCES

1. Cavanagh D. Nidovirales: a new order comprising Coronaviridae and Arteriviridae. Arch Virol. 1997;142(3):629–33.

2. Saif LJ, Wang Q, Vlasova AN, Jung K, Xiao S. Coronaviruses. In: Zimmerman JJ, Karriker LA, Ramirez A, Schwartz KJ, Stevenson GW, Zhang J, editors. Diseases of Swine. 1st ed. Wiley; 2019. p. 488–523.

3. Yan Q, Liu X, Sun Y, Zeng W, Li Y, Zhao F, et al. Swine Enteric Coronavirus: Diverse Pathogen–Host Interactions. Int J Mol Sci. 2022;23(7):3953.

4. Turlewicz-Podbielska H, Pomorska-Mól M. Porcine Coronaviruses: Overview of the State of the Art. Virol Sin. 2021;36(5):833–51.

5. Doyle LP, Hutchings LM. A transmissible gastroenteritis in pigs. J Am Vet Med Assoc. 1946 Apr;108:257–9.

6. Enjuanes L, van der Zeijst BAM. Molecular Basis of Transmissible Gastroenteritis Virus Epidemiology. In: Stuart G. Siddell, editor. The Coronaviridae. Boston, MA: Springer US; 1995. p. 337–76.

7. Magtoto R, Poonsuk K, Baum D, Zhang J, Chen Q, Ji J, et al. Evaluation of the Serologic Cross-Reactivity between Transmissible Gastroenteritis Coronavirus and Porcine Respiratory Coronavirus Using Commercial Blocking Enzyme-Linked Immunosorbent Assay Kits. mSphere. 2019;4(2):e00017-19.

8. Pensaert M, Callebaut P, Vergote J. Isolation of a porcine respiratory, non-enteric coronavirus related to transmissible gastroenteritis. Vet Q. 1986;8(3):257–61.

9. Pensaert M, Cox E. Porcine Respiratory Coronavirus Related to Transmissible Gastroenteritis Virus. Agri-practice--Gastroenterology. 1989;10:17–21.

10. Guo R, Fan B, Chang X, Zhou J, Zhao Y, Shi D, et al. Characterization and evaluation of the pathogenicity of a natural recombinant transmissible gastroenteritis virus in China. Virology. 2020;545:24–32.

11. Yuan D, Yan Z, Li M, Wang Y, Su M, Sun D. Isolation and Characterization of a Porcine Transmissible Gastroenteritis Coronavirus in Northeast China. Front Vet Sci. 2021;8.

12. Alexander TJ, Richards WP, Roe CK. An Encephalomyelitis Of Suckling Pigs In Ontario. Can J Comp Med Vet Sci. 1959;23(10):316–9.

13. Greig AS, Mitchell D, Corner AH, Bannister GL, Meads EB, Julian RJ. A Hemagglutinating Virus Producing Encepkalomyelitis in Baby Pigs. Can J Comp Med Vet Sci. 1962;26(3):49–56.

14. Mitchell D, Corner AH, Bannister GL, Greig AS. Studies on Pathogenic Porcine Enteroviruses. Can J Comp Med Vet Sci. 1961;25(4):85–93.

15. Alexander TJ, Saunders CN. Vomiting and wasting disease of piglets. Vet Rec. 1969;84(7):178.

16. Cartwright SF, Lucas M, Cavill JP, Gush AF, Blandford TB. Vomiting and wasting disease of piglets. Vet Rec. 1969;84(7):175–6.

17. Kershaw GF. Vomiting and wasting disease of piglets. Vet Rec. 1969;84(7):178–9.

18. Mora-Díaz JC, Magtoto R, Houston E, Baum D, Carrillo-Ávila JA, Temeeyasen G, et al. Detecting and Monitoring Porcine Hemagglutinating Encephalomyelitis Virus, an Underresearched Betacoronavirus. Frieman MB, editor. mSphere. 2020;5(3):e00199-20.

19. Mora-Díaz JC, Piñeyro PE, Houston E, Zimmerman J, Giménez-Lirola LG. Porcine Hemagglutinating Encephalomyelitis Virus: A Review. Front Vet Sci. 2019;6:53.

20. Domingo E, Escarmís C, Sevilla N, Moya A, Elena SF, Quer J, et al. Basic concepts in RNA virus evolution. FASEB J. 1996;10(8):859–64.

21. Xiao Y, Rouzine IM, Bianco S, Acevedo A, Goldstein EF, Farkov M, et al. RNA Recombination Enhances Adaptability and Is Required for Virus Spread and Virulence. Cell Host & Microbe. 2016;19(4):493–503.

22. Elena SF, Sanjuán R. Adaptive value of high mutation rates of RNA viruses: separating causes from consequences. J Virol. 2005;79(18):11555–8.

23. Holmes EC. The Evolutionary Genetics of Emerging Viruses. Annu Rev Ecol Evol Syst. 2009;40(1):353–72.

24. Domingo E, Holland JJ. RNA virus mutations and fitness for survival. Annu Rev Microbiol. 1997;51:151–78.

25. Thakor JC, Dinesh M, Manikandan R, Bindu S, Sahoo M, Sahoo D, et al. Swine coronaviruses (SCoVs) and their emerging threats to swine population, inter-species transmission, exploring the susceptibility of pigs for SARS-CoV-2 and zoonotic concerns. Vet Q. 2022;42(1):125–47.

26. Cox E, Hooyberghs J, Pensaert MB. Sites of replication of a porcine respiratory coronavirus related to transmissible gastroenteritis virus. Res Vet Sci. 1990;48(2):165–9.

27. Saif LJ, Jung K. Comparative Pathogenesis of Bovine and Porcine Respiratory Coronaviruses in the Animal Host Species and SARS-CoV-2 in Humans. J Clin Microbiol. 2020;58(8):e01355-20.

28. Sánchez CM, Izeta A, Sánchez-Morgado JM, Alonso S, Sola I, Balasch M, et al. Targeted Recombination Demonstrates that the Spike Gene of Transmissible Gastroenteritis Coronavirus Is a Determinant of Its Enteric Tropism and Virulence. J Virol. 1999;73(9):7607–18.

29. De Nova PJG, Cortey M, Díaz I, Puente H, Rubio P, Martín M, et al. A retrospective study of porcine epidemic diarrhoea virus (PEDV) reveals the presence of swine enteric coronavirus (SeCoV) since 1993 and the recent introduction of a recombinant PEDV-SeCoV in Spain. Transbound Emerg Dis. 2020;67(6):2911–22.

30. Akimkin V, Beer M, Blome S, Hanke D, Höper D, Jenckel M, et al. New Chimeric Porcine Coronavirus in Swine Feces, Germany, 2012. Emerg Infect Dis. 2016;22(7):1314–5.

31. Belsham GJ, Rasmussen TB, Normann P, Vaclavek P, Strandbygaard B, Bøtner A. Characterization of a Novel Chimeric Swine Enteric Coronavirus from Diseased Pigs in Central Eastern Europe in 2016. Transbound Emerg Dis. 2016;63(6):595–601.

32. Boniotti MB, Papetti A, Lavazza A, Alborali G, Sozzi E, Chiapponi C, et al. Porcine Epidemic Diarrhea Virus and Discovery of a Recombinant Swine Enteric Coronavirus, Italy. Emerg Infect Dis. 2016;22(1):83–7.

33. Gong L, Li J, Zhou Q, Xu Z, Chen L, Zhang Y, et al. A New Bat-HKU2–like Coronavirus in Swine, China, 2017. Emerg Infect Dis. 2017;23(9):1607–9.

34. Pan Y, Tian X, Qin P, Wang B, Zhao P, Yang YL, et al. Discovery of a novel swine enteric alphacoronavirus (SeACoV) in southern China. Vet Microbiol. 2017;211:15–21.

35. Zhou P, Fan H, Lan T, Yang XL, Shi WF, Zhang W, et al. Fatal swine acute diarrhoea syndrome caused by an HKU2-related coronavirus of bat origin. Nature. 2018;556(7700):255–8.

36. Yang YL, Yu JQ, Huang YW. Swine enteric alphacoronavirus (swine acute diarrhea syndrome coronavirus): An update three years after its discovery. Virus Res. 2020;285:198024.

37. Sun Y, Xing J, Xu Z ying, Gao H, Xu S jia, Liu J, et al. Re-emergence of Severe Acute Diarrhea Syndrome Coronavirus (SADS-CoV) in Guangxi, China, 2021. J Infect. 2022;85(5):e130–3.

38. Zhou L, Li Q, Su J, Chen G, Wu Z, Luo Y, et al. The re-emerging of SADS-CoV infection in pig herds in Southern China. Transbound Emerg Dis. 2019;66:2180–3.

39. Marthaler D, Raymond L, Jiang Y, Collins J, Rossow K, Rovira A. Rapid Detection, Complete Genome Sequencing, and Phylogenetic Analysis of Porcine Deltacoronavirus. Emerg Infect Dis. 2014;20(8):1347–50.

40. Wang L, Byrum B, Zhang Y. Detection and Genetic Characterization of Deltacoronavirus in Pigs, Ohio, USA, 2014. Emerg Infect Dis. 2014;20(7):1227–30.

41. Wang L, Byrum B, Zhang Y. Porcine Coronavirus HKU15 Detected in 9 US States, 2014. Emerg Infect Dis. 2014;20(9):1594–5.

42. Woo PCY, Lau SKP, Lam CSF, Lau CCY, Tsang AKL, Lau JHN, et al. Discovery of Seven Novel Mammalian and Avian Coronaviruses in the Genus Deltacoronavirus Supports Bat Coronaviruses as the Gene Source of Alphacoronavirus and Betacoronavirus and Avian Coronaviruses as the Gene Source of Gammacoronavirus and Deltacoronavirus. J Virol. 2012;86(7):3995–4008.

43. Duan C. An Updated Review of Porcine Deltacoronavirus in Terms of Prevalence, Pathogenicity, Pathogenesis and Antiviral Strategy. Front Vet Sci. 2022;8:811187.

44. More-Bayona JA, Ramirez-Velasquez M, Hause B, Nelson E, Rivera-Geronimo H. First isolation and whole genome characterization of porcine deltacoronavirus from pigs in Peru. Transbound Emerg Dis. 2022;69(5):e1561–73.

45. Wang B, Liu Y, Ji CM, Yang YL, Liang QZ, Zhao P, et al. Porcine Deltacoronavirus Engages the Transmissible Gastroenteritis Virus Functional Receptor Porcine Aminopeptidase N for Infectious Cellular Entry. Gallagher T, editor. J Virol. 2018;92(12):e00318-18.

46. Chen Q, Gauger P, Stafne M, Thomas J, Arruda P, Burrough E, et al. Pathogenicity and pathogenesis of a United States porcine deltacoronavirus cell culture isolate in 5-day-old neonatal piglets. Virology. 2015;482:51–9.

47. Jung K, Hu H, Eyerly B, Lu Z, Chepngeno J, Saif LJ. Pathogenicity of 2 Porcine Deltacoronavirus Strains in Gnotobiotic Pigs. Emerg Infect Dis. 2015;21(4):650–4.

48. Zhang H, Han F, Shu X, Li Q, Ding Q, Hao C, et al. Co-infection of porcine epidemic diarrhoea virus and porcine deltacoronavirus enhances the disease severity in piglets. Transbound Emerg Dis. 2022;69(4):1715–26.

49. Li K, Li H, Bi Z, Gu J, Gong W, Luo S, et al. Complete Genome Sequence of a Novel Swine Acute Diarrhea Syndrome Coronavirus, CH/FJWT/2018, Isolated in Fujian, China, in 2018. Microbiol Resour Announc. 2018;7(22):e01259-18.

50. Wesseling JG, Vennema H, Godeke GJ, Horzinek MC, Rottier PJ. Nucleotide sequence and expression of the spike (S) gene of canine coronavirus and comparison with the S proteins of feline and porcine coronaviruses. J Gen Virol. 1994;75:1789–94.

51. McClurkin AW, Stark SL, Norman JO. Transmissible Gastroenteritis (TGE) of Swine: The Possible Role of Dogs in the Epizootiology of TGE. Can J Comp Med. 1970;34(4):347–9.

52. Reynolds D, Garwes D. Virus isolation and serum antibody responses after infection of cats with transmissible gastroenteritis virus. Brief report. Arch Virol. 1979;60(2):161–6.

53. Kocherhans R, Bridgen A, Ackermann M, Tobler K. Completion of the porcine epidemic diarrhoea coronavirus (PEDV) genome sequence. Virus Genes. 2001;23(2):137–44.

54. Huang YW, Dickerman AW, Piñeyro P, Li L, Fang L, Kiehne R, et al. Origin, Evolution, and Genotyping of Emergent Porcine Epidemic Diarrhea Virus Strains in the United States. Griffin DE, editor. mBio. 2013;4(5):e00737-13.

55. Liu C, Tang J, Ma Y, Liang X, Yang Y, Peng G, et al. Receptor Usage and Cell Entry of Porcine Epidemic Diarrhea Coronavirus. J Virol. 2015;89(11):6121–5.

56. Niu Z, Zhang S, Xu S, Wang J, Wang S, Hu X, et al. Porcine Epidemic Diarrhea Virus Replication in Human Intestinal Cells Reveals Potential Susceptibility to Cross-Species Infection. Viruses. 2023;15(4):956.

57. Luo Y, Chen Y, Geng R, Li B, Chen J, Zhao K, et al. Broad Cell Tropism of SADS-CoV In Vitro Implies Its Potential Cross-Species Infection Risk. Virol Sin. 2021;36(3):559–63.

58. Yang YL, Qin P, Wang B, Liu Y, Xu GH, Peng L, et al. Broad Cross-Species Infection of Cultured Cells by Bat HKU2-Related Swine Acute Diarrhea Syndrome Coronavirus and Identification of Its Replication in Murine Dendritic Cells In Vivo Highlight Its Potential for Diverse Interspecies Transmission. J Virol. 2019;93(24):e01448-19.

59. Edwards CE, Yount BL, Graham RL, Leist SR, Hou YJ, Dinnon KH, et al. Swine acute diarrhea syndrome coronavirus replication in primary human cells reveals potential susceptibility to infection. Proc Natl Acad Sci USA. 2020;117(43):26915–25.

60. Li W, Hulswit RJG, Kenney SP, Widjaja I, Jung K, Alhamo MA, et al. Broad receptor engagement of an emerging global coronavirus may potentiate its diverse cross-species transmissibility. PNAS. 2018;115(22):E5135–43.

61. Boley PA, Alhamo MA, Lossie G, Yadav KK, Vasquez-Lee M, Saif LJ, et al. Porcine Deltacoronavirus Infection and Transmission in Poultry, United States1. Emerg Infect Dis. 2020;26(2):255–65.

62. Jung K, Hu H, Saif LJ. Calves are susceptible to infection with the newly emerged porcine deltacoronavirus, but not with the swine enteric alphacoronavirus, porcine epidemic diarrhea virus. Arch Virol. 2017;162(8):2357–62.

63. Liang Q, Zhang H, Li B, Ding Q, Wang Y, Gao W, et al. Susceptibility of Chickens to Porcine Deltacoronavirus Infection. Viruses. 2019;11(6):573.

64. Lednicky JA, Tagliamonte MS, White SK, Elbadry MA, Alam MdM, Stephenson CJ, et al. Independent infections of porcine deltacoronavirus among Haitian children. Nature. 2021;600(7887):133–7.

65. Pensaert MB, de Bouck P. A new coronavirus-like particle associated with diarrhea in swine. Arch Virol. 1978;58(3):243–7.

66. Bosch BJ, van der Zee R, de Haan CAM, Rottier PJM. The Coronavirus Spike Protein Is a Class I Virus Fusion Protein: Structural and Functional Characterization of the Fusion Core Complex. J Virol. 2003;77(16):8801–11.

67. Deng F, Ye G, Liu Q, Navid MT, Zhong X, Li Y, et al. Identification and Comparison of Receptor Binding Characteristics of the Spike Protein of Two Porcine Epidemic Diarrhea Virus Strains. Viruses. 2016;8(3):55.

68. Kirchdoerfer RN, Bhandari M, Martini O, Sewall LM, Bangaru S, Yoon KJ, et al. Structure and immune recognition of the porcine epidemic diarrhea virus spike protein. Structure. 2021;29(4):385-392.e5.

69. Li W, Van Kuppeveld FJM, He Q, Rottier PJM, Bosch BJ. Cellular entry of the porcine epidemic diarrhea virus. Virus Res. 2016;226:117–27.

70. Shirato K, Matsuyama S, Ujike M, Taguchi F. Role of Proteases in the Release of Porcine Epidemic Diarrhea Virus from Infected Cells. J Virol. 2011;85(15):7872–80.

71. Li F. Structure, Function, and Evolution of Coronavirus Spike Proteins. Annu Rev Virol. 2016;3(1):237–61.

72. Liu C, Ma Y, Yang Y, Zheng Y, Shang J, Zhou Y, et al. Cell Entry of Porcine Epidemic Diarrhea Coronavirus Is Activated by Lysosomal Proteases. J Biol Chem. 2016;291(47):24779–86.

73. Reguera J, Santiago C, Mudgal G, Ordoño D, Enjuanes L, Casasnovas JM. Structural Bases of Coronavirus Attachment to Host Aminopeptidase N and Its Inhibition by Neutralizing Antibodies. Baric RS, editor. PLoS Pathog. 2012;8(8):e1002859.

74. Su Y, Hou Y, Wang Q. The enhanced replication of an S-intact PEDV during coinfection with an S1 NTD-del PEDV in piglets. Vet Microbiol. 2019;228:202–12.

75. Li S, Yang J, Zhu Z, Zheng H. Porcine Epidemic Diarrhea Virus and the Host Innate Immune Response. Pathogens. 2020;9(5):367.

76. Jang G, Lee D, Shin S, Lim J, Won H, Eo Y, et al. Porcine epidemic diarrhea virus: an update overview of virus epidemiology, vaccines, and control strategies in South Korea. J Vet Sci. 2023;24(4):e58.

77. Chen B, Dong S, Yu L, Si F, Li C, Xie C, et al. Three Amino Acid Substitutions in the Spike Protein Enable the Coronavirus Porcine Epidemic Diarrhea Virus To Infect Vero Cells. Microbiol Spectr. 2022;11(1):e03872-22.

78. Chen J, Liu X, Shi D, Shi H, Zhang X, Li C, et al. Detection and Molecular Diversity of Spike Gene of Porcine Epidemic Diarrhea Virus in China. Viruses. 2013;5(10):2601–13.

79. Hou Y, Meulia T, Gao X, Saif LJ, Wang Q. Deletion of both the Tyrosine-Based Endocytosis Signal and the Endoplasmic Reticulum Retrieval Signal in the Cytoplasmic Tail of Spike Protein Attenuates Porcine Epidemic Diarrhea Virus in Pigs. J Virol. 2019;93(2):e01758-18.

80. Li Z, Ma Z, Li Y, Gao S, Xiao S. Porcine epidemic diarrhea virus: Molecular mechanisms of attenuation and vaccines. Microb Pathog. 2020;149:104553.

81. Tan Y, Sun L, Wang G, Shi Y, Dong W, Fu Y, et al. Trypsin-Enhanced Infection with Porcine Epidemic Diarrhea Virus Is Determined by the S2 Subunit of the Spike Glycoprotein. J Virol. 2021;95(11):e02453-20.

82. Tang T, Bidon M, Jaimes JA, Whittaker GR, Daniel S. Coronavirus membrane fusion mechanism offers a potential target for antiviral development. Antiviral Res. 2020;178:104792.

83. Zhou X, Cong Y, Veenendaal T, Klumperman J, Shi D, Mari M, et al. Ultrastructural Characterization of Membrane Rearrangements Induced by Porcine Epidemic Diarrhea Virus Infection. Viruses. 2017;9(9):251.

84. Lei XM, Yang YL, He YQ, Peng L, Zhao P, Xu SY, et al. Specific recombinant proteins of porcine epidemic diarrhea virus are immunogenic, revealing their potential use as diagnostic markers. Vet Microbiol. 2019;236:108387.

85. Li X, Wu Y, Yan Z, Li G, Luo J, Huang S, et al. A Comprehensive View on the Protein Functions of Porcine Epidemic Diarrhea Virus. Genes. 2024;15(2):165.

86. Raamsman MJ, Locker JK, de Hooge A, de Vries AA, Griffiths G, Vennema H, et al. Characterization of the coronavirus mouse hepatitis virus strain A59 small membrane protein E. J Virol. 2000;74(5):2333–42.

87. Fan JH, Zuo YZ, Shen XQ, Gu WY, Di JM. Development of an enzyme-linked immunosorbent assay for the monitoring and surveillance of antibodies to porcine epidemic diarrhea virus based on a recombinant membrane protein. J Virol Methods. 2015;225:90–4.

88. Ren X, Suo S, Jang YS. Development of a porcine epidemic diarrhea virus M protein-based ELISA for virus detection. Biotechnol Lett. 2011;33(2):215–20.

89. Xu XG, Zhang HL, Zhang Q, Dong J, Huang Y, Tong DW. Porcine epidemic diarrhea virus M protein blocks cell cycle progression at S-phase and its subcellular localization in the porcine intestinal epithelial cells. Acta Virol. 2015;59(3):265–75.

90. Hurst KR, Koetzner CA, Masters PS. Characterization of a Critical Interaction between the Coronavirus Nucleocapsid Protein and Nonstructural Protein 3 of the Viral Replicase-Transcriptase Complex. J Virol. 2013;87(16):9159–72.

91. Narayanan K, Maeda A, Maeda J, Makino S. Characterization of the Coronavirus M Protein and Nucleocapsid Interaction in Infected Cells. J Virol. 2000;74(17):8127–34.

92. Su M, Shi D, Xing X, Qi S, Yang D, Zhang J, et al. Coronavirus Porcine Epidemic Diarrhea Virus Nucleocapsid Protein Interacts with p53 To Induce Cell Cycle Arrest in S-Phase and Promotes Viral Replication. Gallagher T, editor. J Virol. 2021;95(16):e00187-21.

93. Tan YW, Fang S, Fan H, Lescar J, Liu DX. Amino acid residues critical for RNA-binding in the N-terminal domain of the nucleocapsid protein are essential determinants for the infectivity of coronavirus in cultured cells. Nucleic Acids Res. 2006;34(17):4816–25.

94. Xu X, Zhang H, Zhang Q, Huang Y, Dong J, Liang Y, et al. Porcine epidemic diarrhea virus N protein prolongs S-phase cell cycle, induces endoplasmic reticulum stress, and up-regulates interleukin-8 expression. Veterinary Microbiology. 2013 Jun;164(3–4):212–21.

95. Zhai H, Qin W, Dong S, Yang X, Zhai X, Tong W, et al. PEDV N protein capture protein translation element PABPC1 and eIF4F to promote viral replication. Vet Microbiol. 2023;284:109844.

96. Beall A, Yount B, Lin CM, Hou Y, Wang Q, Saif L, et al. Characterization of a Pathogenic Full-Length cDNA Clone and Transmission Model for Porcine Epidemic Diarrhea Virus Strain PC22A. Lipkin WI, editor. mBio. 2016;7(1):e01451-15.

97. Kaewborisuth C, Yingchutrakul Y, Roytrakul S, Jongkaewwattana A. Porcine Epidemic Diarrhea Virus (PEDV) ORF3 Interactome Reveals Inhibition of Virus Replication by Cellular VPS36 Protein. Viruses. 2019;11(4):382.

98. Kaewborisuth C, He Q, Jongkaewwattana A. The Accessory Protein ORF3 Contributes to Porcine Epidemic Diarrhea Virus Replication by Direct Binding to the Spike Protein. Viruses. 2018;10(8):399.

99. Kristen-Burmann C, Rogger P, Veiga IB, Riebesehl S, Rappe J, Ebert N, et al. Reverse Genetic Assessment of the Roles Played by the Spike Protein and ORF3 in Porcine Epidemic Diarrhea Virus Pathogenicity. Gallagher T, editor. J Virol. 2023;97(7):e01964-22.

100. Lee S, Son KY, Noh YH, Lee SC, Choi HW, Yoon IJ, et al. Genetic characteristics, pathogenicity, and immunogenicity associated with cell adaptation of a virulent genotype 2b porcine epidemic diarrhea virus. Vet Microbiol. 2017;207:248–58.

101. Song DS, Yang JS, Oh JS, Han JH, Park BK. Differentiation of a Vero cell adapted porcine epidemic diarrhea virus from Korean field strains by restriction fragment length polymorphism analysis of ORF 3. Vaccine. 2003;21(17):1833–42.

102. Wang K, Lu W, Chen J, Xie S, Shi H, Hsu H, et al. PEDV ORF3 encodes an ion channel protein and regulates virus production. FEBS Letters. 2012;586(4):384–91.

103. Wongthida P, Liwnaree B, Wanasen N, Narkpuk J, Jongkaewwattana A. The role of ORF3 accessory protein in replication of cell-adapted porcine epidemic diarrhea virus (PEDV). Arch Virol. 2017;162(9):2553–63.

104. Richard A, Tulasne D. Caspase cleavage of viral proteins, another way for viruses to make the best of apoptosis. Cell Death Dis. 2012;3(3):e277–e277.

105. St John SE, Anson BJ, Mesecar AD. X-Ray Structure and Inhibition of 3C-like Protease from Porcine Epidemic Diarrhea Virus. Sci Rep. 2016;6:25961.

106. Tomar S, Johnston ML, St John SE, Osswald HL, Nyalapatla PR, Paul LN, et al. Ligand-induced Dimerization of Middle East Respiratory Syndrome (MERS) Coronavirus nsp5 Protease (3CLpro): IMPLICATIONS FOR nsp5 REGULATION AND THE DEVELOPMENT OF ANTIVIRALS. J Biol Chem. 2015;290(32):19403–22.

107. Snijder EJ, Decroly E, Ziebuhr J. The Nonstructural Proteins Directing Coronavirus RNA Synthesis and Processing. Adv Virus Res. 2016;96:59–126.

108. Zeng Z, Deng F, Shi K, Ye G, Wang G, Fang L, et al. Dimerization of Coronavirus nsp9 with Diverse Modes Enhances Its Nucleic Acid Binding Affinity. J Virol. 2018;92(17):e00692-18.

109. Sexton NR, Smith EC, Blanc H, Vignuzzi M, Peersen OB, Denison MR. Homology-Based Identification of a Mutation in the Coronavirus RNA-Dependent RNA Polymerase That Confers Resistance to Multiple Mutagens. J Virol. 2016;90(16):7415–28.

110. Chen Y, Cai H, Pan J, Xiang N, Tien P, Ahola T, et al. Functional screen reveals SARS coronavirus nonstructural protein nsp14 as a novel cap N7 methyltransferase. PNAS. 2009;106(9):3484–9.

111. Denison MR, Graham RL, Donaldson EF, Eckerle LD, Baric RS. Coronaviruses: An RNA proofreading machine regulates replication fidelity and diversity. RNA Biol. 2011;8(2):270–9.

112. Niu X, Kong F, Hou YJ, Wang Q. Crucial mutation in the exoribonuclease domain of nsp14 of PEDV leads to high genetic instability during viral replication. Cell Biosci. 2021;11(1):106.

113. Kindler E, Gil-Cruz C, Spanier J, Li Y, Wilhelm J, Rabouw HH, et al. Early endonuclease-mediated evasion of RNA sensing ensures efficient coronavirus replication. Perlman S, editor. PLoS Pathog. 2017;13(2):e1006195.

114. Decroly E, Imbert I, Coutard B, Bouvet M, Selisko B, Alvarez K, et al. Coronavirus Nonstructural Protein 16 Is a Cap-0 Binding Enzyme Possessing (Nucleoside-2′ *O*)-Methyltransferase Activity. J Virol. 2008;82(16):8071–84.

115. Hu Y, Xie X, Yang L, Wang A. A Comprehensive View on the Host Factors and Viral Proteins Associated With Porcine Epidemic Diarrhea Virus Infection. Front Microbiol. 2021;12:762358.

116. Li Z, Ma Z, Dong L, Yang T, Li Y, Jiao D, et al. Molecular Mechanism of Porcine Epidemic Diarrhea Virus Cell Tropism. mBio. 2022;13(2):e03739-21.

117. Li BX, Ge JW, Li YJ. Porcine aminopeptidase N is a functional receptor for the PEDV coronavirus. Virology. 2007;365(1):166–72.

118. Nam E, Lee C. Contribution of the porcine aminopeptidase N (CD13) receptor density to porcine epidemic diarrhea virus infection. Vet Microbiol. 2010;144(1):41–50.

119. Mina-Osorio P. The moonlighting enzyme CD13: old and new functions to target. Trends Mol Med. 2008;14(8):361–71.

120. Oh JS, Song DS, Park BK. Identification of a putative cellular receptor 150 kDa polypeptide for porcine epidemic diarrhea virus in porcine enterocytes. J Vet Sci. 2003;4(3):269–75.

121. Meng F, Suo S, Zarlenga DS, Cong Y, Ma X, Zhao Q, et al. A phage-displayed peptide recognizing porcine aminopeptidase N is a potent small molecule inhibitor of PEDV entry. Virology. 2014;456–457:20–7.

122. Park JE, Park ES, Yu JE, Rho J, Paudel S, Hyun BH, et al. Development of transgenic mouse model expressing porcine aminopeptidase N and its susceptibility to porcine epidemic diarrhea virus. Virus Res. 2015;197:108–15.

123. Teeravechyan S, Frantz PN, Wongthida P, Chailangkarn T, Jaru-ampornpan P, Koonpaew S, et al. Deciphering the biology of porcine epidemic diarrhea virus in the era of reverse genetics. Virus Res. 2016;226:152–71.

124. Ji CM, Wang B, Zhou J, Huang YW. Aminopeptidase-N-independent entry of porcine epidemic diarrhea virus into Vero or porcine small intestine epithelial cells. Virology. 2018;517:16–23.

125. Li W, Luo R, He Q, van Kuppeveld FJM, Rottier PJM, Bosch BJ. Aminopeptidase N is not required for porcine epidemic diarrhea virus cell entry. Virus Res. 2017;235:6–13.

126. Whitworth KM, Rowland RRR, Petrovan V, Sheahan M, Cino-Ozuna AG, Fang Y, et al. Resistance to coronavirus infection in amino peptidase N-deficient pigs. Transgenic Res. 2019;28(1):21–32.

127. Zhang J, Wu Z, Yang H. Aminopeptidase N Knockout Pigs Are Not Resistant to Porcine Epidemic Diarrhea Virus Infection. Virol Sin. 2019;34(5):592–5.

128. Shirato K, Maejima M, Islam MdT, Miyazaki A, Kawase M, Matsuyama S, et al. Porcine aminopeptidase N is not a cellular receptor of porcine epidemic diarrhea virus, but promotes its infectivity via aminopeptidase activity. J Gen Virol. 2016;97(10):2528–39.

129. Delmas B, Gelfi J, Kut E, Sjöström H, Noren O, Laude H. Determinants essential for the transmissible gastroenteritis virus-receptor interaction reside within a domain of aminopeptidase-N that is distinct from the enzymatic site. J Virol. 1994;68(8):5216–24.

130. Delmas B, Gelfi J, Sjöström H, Noren O, Laude H. Further characterization of aminopeptidase-N as a receptor for coronaviruses. Adv Exp Med Biol. 1993;342:293–8.

131. Wrapp D, McLellan JS. The 3.1-Angstrom Cryo-electron Microscopy Structure of the Porcine Epidemic Diarrhea Virus Spike Protein in the Prefusion Conformation. J Virol. 2019;93(23).

132. Lin F, Zhang H, Li L, Yang Y, Zou X, Chen J, et al. PEDV: Insights and Advances into Types, Function, Structure, and Receptor Recognition. Viruses. 2022;14(8):1744.

133. Wang J huai. Protein recognition by cell surface receptors: physiological receptors versus virus interactions. Trends Biochem Sci. 2002;27(3):122–6.

134. Chen Y, Liu X, Zheng JN, Yang LJ, Luo Y, Yao YL, et al. N-linked glycoproteins and host proteases are involved in swine acute diarrhea syndrome coronavirus entry. J Virol. 2023;97(10):e00916-23.

135. Hu S, Zhao K, Lan Y, Shi J, Guan J, Lu H, et al. Cell-surface glycans act as attachment factors for porcine hemagglutinating encephalomyelitis virus. Vet Microbiol. 2022;265:109315.

136. Schwegmann-Weßels C, Bauer S, Winter C, Enjuanes L, Laude H, Herrler G. The sialic acid binding activity of the S protein facilitates infection by porcine transmissible gastroenteritis coronavirus. Virol J. 2011;8(1):435.

137. Wang X, Jin Q, Xiao W, Fang P, Lai L, Xiao S, et al. Genome-Wide CRISPR/Cas9 Screen Reveals a Role for SLC35A1 in the Adsorption of Porcine Deltacoronavirus. J Virol. 2022;96(24):e01626-22.

138. Yang YL, Wang B, Li W, Cai HL, Qian QY, Qin Y, et al. Functional dissection of the spike glycoprotein S1 subunit and identification of cellular cofactors for regulation of swine acute diarrhea syndrome coronavirus entry. J Virol. 2024;98(4):e00139-24.

139. Zhao Y, Tang T, Zhao W, Fu W, Li T. Inhibition of PEDV viral entry upon blocking N-glycan elaboration. Virology. 2024;594:110039.

140. Wang HM, Qiao YY, Liu YG, Cai BY, Yang YL, Lu H, et al. The N-glycosylation at positions 652 and 661 of viral spike protein negatively modulates porcine deltacoronavirus entry. Front Vet Sci. 2024;11.

141. Xiong M, Liu X, Liang T, Ban Y, Liu Y, Zhang L, et al. The Alpha-1 Subunit of the Na+/K+-ATPase (ATP1A1) Is a Host Factor Involved in the Attachment of Porcine Epidemic Diarrhea Virus. IJMS. 2023;24(4):4000.

142. Zhang Y, Zhang S, Sun Z, Liu X, Liao G, Niu Z, et al. Porcine epidemic diarrhea virus causes diarrhea by activating EGFR to regulates NHE3 activity and mobility on plasma membrane. Front Microbiol. 2023;14.

143. Hu W, Zhang S, Shen Y, Yang Q. Epidermal growth factor receptor is a co-factor for transmissible gastroenteritis virus entry. Virology. 2018;521:33–43.

144. Hu W, Zhu L, Yang X, Lin J, Yang Q. The epidermal growth factor receptor regulates cofilin activity and promotes transmissible gastroenteritis virus entry into intestinal epithelial cells. Oncotarget. 2016;7(11):12206.

145. Li M, Zhang L, Zhou P, Zhang Z, Yu R, Zhang Y, et al. Porcine deltacoronavirus nucleocapsid protein interacts with the Grb2 through its proline-rich motifs to induce activation of the Raf-MEK-ERK signal pathway and promote virus replication. J Gen Virol. 2024;105(8):002014.

146. Zhou L, Li C, Zhang R, Li Q, Sun Y, Feng Y, et al. Identification of a receptor tyrosine kinase inhibitor CP-724714 inhibits SADS-CoV related swine diarrhea coronaviruses infection *in vitro*. Virol Sin. 2023;38(5):778–86.

147. Zhang Y, Buckles E, Whittaker GR. Expression of the C-type lectins DC-SIGN or L-SIGN alters host cell susceptibility for the avian coronavirus, infectious bronchitis virus. Vet Microbiol. 2012;157(3):285–93.

148. Zhao P, Xu LD, Zhang Y, Cao H, Chen R, Wang B, et al. Expression of the human or porcine C-type lectins DC-SIGN/L-SIGN confers susceptibility to porcine epidemic diarrhea virus entry and infection in otherwise refractory cell lines. Microb Pathog. 2021;157:104956.

149. Huan C chao, Wang Y, Ni B, Wang R, Huang L, Ren X feng, et al. Porcine epidemic diarrhea virus uses cell-surface heparan sulfate as an attachment factor. Arch Virol. 2015;160(7):1621–8.

150. Zhou Y, Jiang X, Tong T, Fang L, Wu Y, Liang J, et al. High antiviral activity of mercaptoethane sulfonate functionalized Te/BSA nanostars against arterivirus and coronavirus. RSC Adv. 2020;10(24):14161–9.

151. Xiao W, Chen C, Xia S, Li Z, Ding T, Zhou J, et al. Cell-surface d-glucuronyl C5-epimerase binds to porcine deltacoronavirus spike protein facilitating viral entry. J Virol. 2024;98(8):e00880-24.

152. Xiao W, Huang W, Chen C, Wang X, Liao S, Xia S, et al. Porcine deltacoronavirus uses heparan sulfate as an attachment receptor. Vet Microbiol. 2023;276:109616.

153. Park JE, Cruz DJM, Shin HJ. Clathrin- and serine proteases-dependent uptake of porcine epidemic diarrhea virus into Vero cells. Virus Res. 2014;191:21–9.

154. Shi W, Fan W, Bai J, Tang Y, Wang L, Jiang Y, et al. TMPRSS2 and MSPL Facilitate Trypsin-Independent Porcine Epidemic Diarrhea Virus Replication in Vero Cells. Viruses. 2017;9(5):114.

155. Zhang J, Chen J, Shi D, Shi H, Zhang X, Liu J, et al. Porcine deltacoronavirus enters cells via two pathways: A protease-mediated one at the cell surface and another facilitated by cathepsins in the endosome. J Biol Chem. 2019;294(25):9830–43.

156. Zhou C, Liu Y, Wei Q, Chen Y, Yang S, Cheng A, et al. HSPA5 Promotes Attachment and Internalization of Porcine Epidemic Diarrhea Virus through Interaction with the Spike Protein and the Endo-/Lysosomal Pathway. J Virol. 2023;97(6):e00549-23.

157. Zhang S, Cao Y, Yang Q. Transferrin receptor 1 levels at the cell surface influence the susceptibility of newborn piglets to PEDV infection. Baric RS, editor. PLoS Pathog. 2020;16(7):e1008682.

158. Zhang S, Hu W, Yuan L, Yang Q. Transferrin receptor 1 is a supplementary receptor that assists transmissible gastroenteritis virus entry into porcine intestinal epithelium. Cell Commun Signal. 2018;16(1):69.

159. Zhang XZ, Tian WJ, Wang J, You JL, Wang XJ. Death Receptor DR5 as a Proviral Factor for Viral Entry and Replication of Coronavirus PEDV. Viruses. 2022;14(12):2724.

160. Sun D, Shi H, Guo D, Chen J, Shi D, Zhu Q, et al. Analysis of protein expression changes of the Vero E6 cells infected with classic PEDV strain CV777 by using quantitative proteomic technique. J Virol Methods. 2015;218:27–39.

161. Li C, Su M, Yin B, Guo D, Wei S, Kong F, et al. Integrin αvβ3 enhances replication of porcine epidemic diarrhea virus on Vero E6 and porcine intestinal epithelial cells. Vet Microbiol. 2019;237:108400.

162. Luo X, Guo L, Zhang J, Xu Y, Gu W, Feng L, et al. Tight Junction Protein Occludin Is a Porcine Epidemic Diarrhea Virus Entry Factor. J Virol. 2017;91(10):e00202-17.

163. Zhao S, Gao J, Zhu L, Yang Q. Transmissible gastroenteritis virus and porcine epidemic diarrhoea virus infection induces dramatic changes in the tight junctions and microfilaments of polarized IPEC-J2 cells. Virus Res. 2014;192:34–45.

164. Li Y, Wang J, Hou W, Shan Y, Wang S, Liu F. Dynamic Dissection of the Endocytosis of Porcine Epidemic Diarrhea Coronavirus Cooperatively Mediated by Clathrin and Caveolae as Visualized by Single-Virus Tracking. mBio. 2021;12(2).

165. V'kovski P, Kratzel A, Steiner S, Stalder H, Thiel V. Coronavirus biology and replication: implications for SARS-CoV-2. Nat Rev Microbiol. 2021;19(3):155–70.

166. Chan WE, Chuang CK, Yeh SH, Chang MS, Chen SSL. Functional characterization of heptad repeat 1 and 2 mutants of the spike protein of severe acute respiratory syndrome coronavirus. J Virol. 2006;80(7):3225–37.

167. Zhang Q, Xiang R, Huo S, Zhou Y, Jiang S, Wang Q, et al. Molecular mechanism of interaction between SARS-CoV-2 and host cells and interventional therapy. Sig Transduct Target Ther. 2021;6(1):1–19.

168. Lee C. Porcine epidemic diarrhea virus: An emerging and re-emerging epizootic swine virus. Virol J. 2015;12(1):193.

169. Fehr AR, Perlman S. Coronaviruses: An Overview of Their Replication and Pathogenesis. Coronaviruses. 2015 Feb 12;1282:1–23.

170. Wood EN. An apparently new syndrome of porcine epidemic diarrhoea. Vet Rec. 1977;100(12):243–4.

171. Carvajal A, Lanza I, Diego R, Rubio P, Cármenes P. Seroprevalence of porcine epidemic diarrhea virus infection among different types of breeding swine farms in Spain. Prev Vet Med. 1995;23(1–2):33–40.

172. Van Reeth K, Pensaert M. Prevalence of infections with enzootic respiratory and enteric viruses in feeder pigs entering fattening herds. Vet Rec. 1994;135(25):594–7.

173. Pijpers A, van Nieuwstadt AP, Terpstra C, Verheijden JH. Porcine epidemic diarrhoea virus as a cause of persistent diarrhoea in a herd of breeding and finishing pigs. Vet Rec. 1993;132(6):129–31.

174. Nagy B, Nagy G, Meder M, Mocsári E. Enterotoxigenic Escherichia coli, rotavirus, porcine epidemic diarrhoea virus, adenovirus and calici-like virus in porcine postweaning diarrhoea in Hungary. Acta Vet Hung. 1996;44(1):9–19.

175. Smíd B, Valícek L, Rodák L, Kudrna J, Musilová J. [Detection of porcine epidemic diarrhea virus using electron microscopy in the Czech Republic]. Vet Med (Praha). 1993;38(6):333–41.

176. Pritchard GC, Paton DJ, Wibberley G, Ibata G. Transmissible gastroenteritis and porcine epidemic diarrhoea in Britain. Vet Rec. 1999;144(22):616–8.

177. Martelli P, Lavazza A, Nigrelli AD, Merialdi G, Alborali LG, Pensaert MB. Epidemic of diarrhoea caused by porcine epidemic diarrhoea virus in Italy. Vet Rec. 2008;162(10):307–10.

178. Jung K, Saif LJ. Porcine epidemic diarrhea virus infection: Etiology, epidemiology, pathogenesis and immunoprophylaxis. TVJ. 2015;204(2):134–43.

179. Song D, Park B. Porcine epidemic diarrhoea virus: a comprehensive review of molecular epidemiology, diagnosis, and vaccines. Virus Genes. 2012;44(2):167–75.

180. Kusanagi K ichi, Kuwahara H, Katoh T, Nunoya T, Ishikawa Y, Samejima T, et al. Isolation and Serial Propagation of Porcine Epidemic Diarrhea Virus in Cell Cultures and Partial Characterization of the Isolate. J Vet Med Sci. 1992;54(2):313–8.

181. Takahashi K, Okada K, Ohshima K. An outbreak of swine diarrhea of a new-type associated with coronavirus-like particles in Japan. Jpn J Vet Sci. 1983;45(6):829–32.

182. Jung K, Saif LJ, Wang Q. Porcine epidemic diarrhea virus (PEDV): An update on etiology, transmission, pathogenesis, and prevention and control. Virus Res. 2020;286:198045.

183. Vlasova AN, Marthaler D, Wang Q, Culhane MR, Rossow KD, Rovira A, et al. Distinct Characteristics and Complex Evolution of PEDV Strains, North America, May 2013–February 2014. Emerg Infect Dis. 2014;20(10):1620–8.

184. Li W, Li H, Liu Y, Pan Y, Deng F, Song Y, et al. New Variants of Porcine Epidemic Diarrhea Virus, China, 2011. Emerg Infect Dis. 2012;18(8):1350.

185. Sun RQ, Cai RJ, Chen YQ, Liang PS, Chen DK, Song CX. Outbreak of Porcine Epidemic Diarrhea in Suckling Piglets, China. Emerg Infect Dis. 2012;18(1):161.

186. Chen F, Pan Y, Zhang X, Tian X, Wang D, Zhou Q, et al. Complete genome sequence of a variant porcine epidemic diarrhea virus strain isolated in China. J Virol. 2012;86(22):12448.

187. Lee DK, Park CK, Kim SH, Lee C. Heterogeneity in spike protein genes of porcine epidemic diarrhea viruses isolated in Korea. Virus Res. 2010;149(2):175–82.

188. Luo Y, Zhang J, Deng X, Ye Y, Liao M, Fan H. Complete genome sequence of a highly prevalent isolate of porcine epidemic diarrhea virus in South China. J Virol. 2012;86(17):9551.

189. Wang J, Zhao P, Guo L, Liu Y, Du Y, Ren S, et al. Porcine Epidemic Diarrhea Virus Variants with High Pathogenicity, China. Emerg Infect Dis. 2013;19(12):2048–9.

190. Sasaki Y, Alvarez J, Sekiguchi S, Sueyoshi M, Otake S, Perez A. Epidemiological factors associated to spread of porcine epidemic diarrhea in Japan. Prev Vet Med. 2016;123:161–7.

191. Sun M, Ma J, Wang Y, Wang M, Song W, Zhang W, et al. Genomic and Epidemiological Characteristics Provide New Insights into the Phylogeographical and Spatiotemporal Spread of Porcine Epidemic Diarrhea Virus in Asia. J Clin Microbiol. 2015;53(5):1484–92.

192. Vui DT, Thanh TL, Tung N, Srijangwad A, Tripipat T, Chuanasa T, et al. Complete genome characterization of porcine epidemic diarrhea virus in Vietnam. Arch Virol. 2015;160(8):1931–8.

193. EFSA. Scientific Opinion on porcine epidemic diarrhoea and emerging porcine deltacoronavirus. EFSA Journal. 2014;12(11):3877.

194. Stevenson GW, Hoang H, Schwartz KJ, Burrough ER, Sun D, Madson D, et al. Emergence of Porcine epidemic diarrhea virus in the United States: clinical signs, lesions, and viral genomic sequences. J Vet Diagn Invest. 2013;25(5):649–54.

195. Cima G. Viral disease affects U.S. pigs: porcine epidemic diarrhea found in at least 11 states. J Am Vet Med Assoc. 2013;243(1):30-1.

196. Kochhar HS. Canada: Porcine epidemic diarrhea in Canada: an emerging disease case study. Can Vet J. 2014;55(11):1048–9.

197. Lara-Romero R, Gómez-Núñez L, Cerriteño-Sánchez JL, Márquez-Valdelamar L, Mendoza-Elvira S, Ramírez-Mendoza H, et al. Molecular characterization of the spike gene of the porcine epidemic diarrhea virus in Mexico, 2013–2016. Virus Genes. 2018;54(2):215–24.

198. Mole B. Deadly pig virus slips through US borders. Nature. 2013;499(7459):388–388.

199. Chen Q, Li G, Stasko J, Thomas JT, Stensland WR, Pillatzki AE, et al. Isolation and characterization of porcine epidemic diarrhea viruses associated with the 2013 disease outbreak among swine in the United States. J Clin Microbiol. 2014;52(1):234–43.

200. Ojkic D, Hazlett M, Fairles J, Marom A, Slavic D, Maxie G, et al. The first case of porcine epidemic diarrhea in Canada. Can Vet J. 2015;56:149–52.

201. Wang L, Byrum B, Zhang Y. New Variant of Porcine Epidemic Diarrhea Virus, United States, 2014. Emerg Infect Dis. 2014;20(5):917–9.

202. Dastjerdi A, Carr J, Ellis RJ, Steinbach F, Williamson S. Porcine Epidemic Diarrhea Virus among Farmed Pigs, Ukraine. Emerg Infect Dis. 2015;21(12):2235–7.

203. Grasland B, Bigault L, Bernard C, Quenault H, Toulouse O, Fablet C, et al. Complete genome sequence of a porcine epidemic diarrhea s gene indel strain isolated in france in december 2014. Genome Announc. 2015;3(3):e00535-15.

204. Hanke D, Jenckel M, Petrov A, Ritzmann M, Stadler J, Akimkin V, et al. Comparison of Porcine Epidemic Diarrhea Viruses from Germany and the United States, 2014. Emerg Infect Dis. 2015;21(3):493–6.

205. Steinrigl A, Fernández SR, Stoiber F, Pikalo J, Sattler T, Schmoll F. First detection, clinical presentation and phylogenetic characterization of Porcine epidemic diarrhea virus in Austria. BMC Vet Res. 2015;11:310.

206. Theuns S, Conceição-Neto N, Christiaens I, Zeller M, Desmarets LMB, Roukaerts IDM, et al. Complete genome sequence of a porcine epidemic diarrhea virus from a novel outbreak in belgium, january 2015. Genome Announc. 2015;3(3):e00506-15.

207. Lin CM, Saif LJ, Marthaler D, Wang Q. Evolution, antigenicity and pathogenicity of global porcine epidemic diarrhea virus strains. Virus Res. 2016;226:20–39.

208. Antas M, Olech M, Szczotka-Bochniarz A. Molecular characterization of porcine epidemic diarrhoea virus (PEDV) in Poland reveals the presence of swine enteric coronavirus (SeCoV) sequence in S gene. PLoS One. 2021;16(10):e0258318.

209. Guo J, Fang L, Ye X, Chen J, Xu S, Zhu X, et al. Evolutionary and genotypic analyses of global porcine epidemic diarrhea virus strains. Transbound Emerg Dis. 2019;66(1):111–8.

210. Hsueh FC, Lin CN, Chiou HY, Chia MY, Chiou MT, Haga T, et al. Updated phylogenetic analysis of the spike gene and identification of a novel recombinant porcine epidemic diarrhoea virus strain in Taiwan. Transbound Emerg Dis. 2020;67(1):417–30.

211. Tian Y, Yang X, Li H, Ma B, Guan R, Yang J, et al. Molecular characterization of porcine epidemic diarrhea virus associated with outbreaks in southwest China during 2014-2018. Transbound Emerg Dis. 2021;68(6):3482–97.

212. Kim SJ, Nguyen VG, Huynh TML, Park YH, Park BK, Chung HC. Molecular Characterization of Porcine Epidemic Diarrhea Virus and Its New Genetic Classification Based on the Nucleocapsid Gene. Viruses. 2020;12(8):790.

213. Liu Q, Wang HY. Porcine enteric coronaviruses: an updated overview of the pathogenesis, prevalence, and diagnosis. Vet Res Commun. 2021;45(2–3):75–86.

214. Antas M, Woźniakowski G. Current status of porcine epidemic diarrhoea (PED) in European pigs. J Vet Res. 2019;63(4):465–70.

215. Stadler J, Zoels S, Fux R, Hanke D, Pohlmann A, Blome S, et al. Emergence of porcine epidemic diarrhea virus in southern Germany. BMC Vet Res. 2015;11(1):142.

216. Zhang Y, Chen Y, Zhou J, Wang X, Ma L, Li J, et al. Porcine Epidemic Diarrhea Virus: An Updated Overview of Virus Epidemiology, Virulence Variation Patterns and Virus–Host Interactions. Viruses. 2022;14(11):2434.

217. Hanke D, Pohlmann A, Sauter-Louis C, Höper D, Stadler J, Ritzmann M, et al. Porcine Epidemic Diarrhea in Europe: In-Detail Analyses of Disease Dynamics and Molecular Epidemiology. Viruses. 2017;9(7):177.

218. Han X, Liu Y, Wang Y, Wang T, Li N, Hao F, et al. Isolation and characterization of porcine epidemic diarrhea virus with a novel continuous mutation in the S10 domain. Front Microbiol. 2023;14:1203893.

219. Gallien S, Andraud M, Moro A, Lediguerher G, Morin N, Gauger PC, et al. Better horizontal transmission of a US non-InDel strain compared with a French InDel strain of porcine epidemic diarrhoea virus. Transbound Emerg Dis. 2018;65(6):1720–32.

220. Li Y, Wu Q, Huang L, Yuan C, Wang J, Yang Q. An alternative pathway of enteric PEDV dissemination from nasal cavity to intestinal mucosa in swine. Nat Commun. 2018;9(1):3811.

221. Niederwerder MC, Nietfeld JC, Bai J, Peddireddi L, Breazeale B, Anderson J, et al. Tissue localization, shedding, virus carriage, antibody response, and aerosol transmission of Porcine epidemic diarrhea virus following inoculation of 4-week-old feeder pigs. J Vet Diagn Invest. 2016;28(6):671–8.

222. Park JE, Shin HJ. Porcine epidemic diarrhea virus infects and replicates in porcine alveolar macrophages. Virus Res. 2014;191:143–52.

223. Yuan C, Zhang P, Liu P, Li Y, Li J, Zhang E, et al. A Novel Pathway for Porcine Epidemic Diarrhea Virus Transmission from Sows to Neonatal Piglets Mediated by Colostrum. Gallagher T, editor. J Virol. 2022;96(14):e00477-22.

224. Ryu J, Kang GJ, Kim O, Park JY, Shin HJ. Transplacental Transmission of Porcine Epidemic Diarrhea Virus. Front Vet Sci. 2022;8.

225. Gallien S, Moro A, Lediguerher G, Catinot V, Paboeuf F, Bigault L, et al. Limited shedding of an S-InDel strain of porcine epidemic diarrhea virus (PEDV) in semen and questions regarding the infectivity of the detected virus. Vet Microbiol. 2019;228:20–5.

226. Gallien S, Moro A, Lediguerher G, Catinot V, Paboeuf F, Bigault L, et al. Evidence of porcine epidemic diarrhea virus (PEDV) shedding in semen from infected specific pathogen-free boars. Vet Res. 2018;49(1):7.

227. Lowe J, Gauger P, Harmon K, Zhang J, Connor J, Yeske P, et al. Role of Transportation in Spread of Porcine Epidemic Diarrhea Virus Infection, United States. Emerg Infect Dis. 2014;20(5):872–4.

228. Kim Y, Yang M, Goyal SM, Cheeran MCJ, Torremorell M. Evaluation of biosecurity measures to prevent indirect transmission of porcine epidemic diarrhea virus. BMC Vet Res. 2017;13(1):89.

229. Pasick J, Berhane Y, Ojkic D, Maxie G, Embury-Hyatt C, Swekla K, et al. Investigation into the Role of Potentially Contaminated Feed as a Source of the First-Detected Outbreaks of Porcine Epidemic Diarrhea in Canada. Transbound Emerg Dis. 2014;61(5):397–410.

230. Perri AM, Poljak Z, Dewey C, Harding JCS, O'Sullivan TL. An epidemiological investigation of the early phase of the porcine epidemic diarrhea (PED) outbreak in Canadian swine herds in 2014: A case-control study. Prev Vet Med. 2018;150:101–9.

231. Scott A, McCluskey B, Brown-Reid M, Grear D, Pitcher P, Ramos G, et al. Porcine epidemic diarrhea virus introduction into the United States: Root cause investigation. Prev Vet Med. 2016;123:192–201.

232. Alonso C, Goede DP, Morrison RB, Davies PR, Rovira A, Marthaler DG, et al. Evidence of infectivity of airborne porcine epidemic diarrhea virus and detection of airborne viral RNA at long distances from infected herds. Vet Res. 2014;45(1):73.

233. Crawford K, Lager K, Miller L, Opriessnig T, Gerber P, Hesse R. Evaluation of porcine epidemic diarrhea virus transmission and the immune response in growing pigs. Vet Res. 2015;46(1):49.

234. Lee DU, Kwon T, Je SH, Yoo SJ, Seo SW, Sunwoo SY, et al. Wild boars harboring porcine epidemic diarrhea virus (PEDV) may play an important role as a PEDV reservoir. Vet Microbiol. 2016;192:90–4.

235. Hofmann M, Wyler R. Propagation of the virus of porcine epidemic diarrhea in cell culture. J Clin Microbiol. 1988;26(11):2235–9.

236. Desmyter J, Melnick JL, Rawls WE. Defectiveness of Interferon Production and of Rubella Virus Interference in a Line of African Green Monkey Kidney Cells (Vero). J Virol. 1968;2(10):955–61.

237. Osada N, Kohara A, Yamaji T, Hirayama N, Kasai F, Sekizuka T, et al. The Genome Landscape of the African Green Monkey Kidney-Derived Vero Cell Line. DNA Res. 2014;21(6):673–83.

238. Li L, Fu F, Guo S, Wang H, He X, Xue M, et al. Porcine Intestinal Enteroids: a New Model for Studying Enteric Coronavirus Porcine Epidemic Diarrhea Virus Infection and the Host Innate Response. J Virol. 2019;93(5):e01682-18.

239. Mao J, Huang X, Shan Y, Xu J, Gao Q, Xu X, et al. Transcriptome analysis revealed inhibition of lipid metabolism in 2-D porcine enteroids by infection with porcine epidemic diarrhea virus. Vet Microbiol. 2022;273:109525.

240. Yin L, Liu X, Hu D, Luo Y, Zhang G, Liu P. Swine Enteric Coronaviruses (PEDV, TGEV, and PDCoV) Induce Divergent Interferon-Stimulated Gene Responses and Antigen Presentation in Porcine Intestinal Enteroids. Front Immunol. 2022;12:826882.

241. Gao Q, Zhao S, Qin T, Yin Y, Yang Q. Effects of porcine epidemic diarrhea virus on porcine monocyte-derived dendritic cells and intestinal dendritic cells. Vet Microbiol. 2015;179(3–4):131–41.

242. Wang J, Wang Y, Liu B, He Y, Li Z, Zhao Q, et al. Porcine Epidemic Diarrhea Virus Envelope Protein Blocks SLA-DR Expression in Barrow-Derived Dendritic Cells by Inhibiting Promoters Activation. Front Immunol. 2021;12:741425.

243. Jin J, Xu C, Wu S, Wu Z, Wu S, Sun M, et al. m6A Demethylase ALKBH5 Restrains PEDV Infection by Regulating GAS6 Expression in Porcine Alveolar Macrophages. Int J Mol Sci. 2022;23(11):6191.

244. Shin HJ. characterization of newly isolated porcine epidemic diarrhea virus (PEDV) and its resistance to interferon and neutralizing antibody. The Journal of Immunology. 2020 May 1;204(1_Supplement):92.17.

245. Wang XY, Zhao TQ, Xu DP, Zhang X, Ji CJ, Zhang DL. The influence of porcine epidemic diarrhea virus on pig small intestine mucosal epithelial cell function. Arch Virol. 2019;164(1):83–90.

246. Xu X, Wang J, Zhang Y, Yan Y, Liu Y, Shi X, et al. Inhibition of DDX6 enhances autophagy and alleviates endoplasmic reticulum stress in Vero cells under PEDV infection. Vet Microbiol. 2022;266:109350.

247. Yuan C, Sun L, Chen L, Li L, Yao Z, Wang Y, et al. Differences in cytokines expression between Vero cells and IPEC-J2 cells infected with porcine epidemic diarrhea virus. Front Microbiol. 2022;13:1002349.

248. Zeng W, Ren J, Yang G, Jiang C, Dong L, Sun Q, et al. Porcine Epidemic Diarrhea Virus and Its nsp14 Suppress ER Stress Induced GRP78. Int J Mol Sci. 2023;24(5):4936.

249. Cao L, Gao Y, Ren X, Ren Y, Ge X, Li G. Porcine epidemic diarrhea virus infection induces NF-κB activation through the TLR2, TLR3 and TLR9 pathways in porcine intestinal epithelial cells. J Gen Virol. 2015;96(7):1757–67.

250. Cao L, Ge X, Gao Y, Herrler G, Ren Y, Ren X, et al. Porcine epidemic diarrhea virus inhibits dsRNA-induced interferon-β production in porcine intestinal epithelial cells by blockade of the RIG-I-mediated pathway. Virol J. 2015 Aug 18;12:127.

251. Cong Y, Li X, Bai Y, Lv X, Herrler G, Enjuanes L, et al. Porcine aminopeptidase N mediated polarized infection by porcine epidemic diarrhea virus in target cells. Virology. 2015;478:1–8.

252. Dong W, Cheng Y, Zhou Y, Zhang J, Yu X, Guan H, et al. The nucleocapsid protein facilitates p53 ubiquitination-dependent proteasomal degradation via recruiting host ubiquitin ligase COP1 in PEDV infection. J Biol Chem. 2024;300(4).

253. Hao Z, Fu F, Cao L, Guo L, Liu J, Xue M, et al. Tumor suppressor p53 inhibits porcine epidemic diarrhea virus infection via interferon-mediated antiviral immunity. Mol Immunol. 2019;108:68–74.

254. Ko S, Gu MJ, Kim CG, Kye YC, Lim Y, Lee JE, et al. Rapamycin-induced autophagy restricts porcine epidemic diarrhea virus infectivity in porcine intestinal epithelial cells. Antiviral Res. 2017;146:86–95.

255. Liwnaree B, Narkpuk J, Sungsuwan S, Jongkaewwattana A, Jaru-Ampornpan P. Growth enhancement of porcine epidemic diarrhea virus (PEDV) in Vero E6 cells expressing PEDV nucleocapsid protein. PLoS One. 2019;14(3):e0212632.

256. Peng O, Wu Y, Hu F, Xia Y, Geng R, Huang Y, et al. Transcriptome Profiling of Vero E6 Cells during Original Parental or Cell-Attenuated Porcine Epidemic Diarrhea Virus Infection. Viruses. 2023;15(7):1426.

257. Zhou Y, Zhang Y, Dong W, Gan S, Du J, Zhou X, et al. Porcine epidemic diarrhea virus activates PERK-ROS axis to benefit its replication in Vero E6 cells. Vet Res. 2023;54(1):9.

258. Wang X, Qiao X, Sui L, Zhao H, Li F, Tang YD, et al. Establishment of stable Vero cell lines expressing TMPRSS2 and MSPL: A useful tool for propagating porcine epidemic diarrhea virus in the absence of exogenous trypsin. Virulence. 2020;11(1):669–85.

259. Lazov CM, Lohse L, Belsham GJ, Rasmussen TB, Bøtner A. Experimental Infection of Pigs with Recent European Porcine Epidemic Diarrhea Viruses. Viruses. 2022;14(12):2751.

260. Luo M, Ma J, Pan X, Zhang X, Yao H. AEN Suppresses the Replication of Porcine Epidemic Diarrhea Virus by Inducing the Expression of Type I IFN and ISGs in MARC-145 Cells. Pathogens. 2024;13(1):24.

261. Xu X, Ma M, Shi X, Yan Y, Liu Y, Yang N, et al. The novel Nsp9-interacting host factor H2BE promotes PEDV replication by inhibiting endoplasmic reticulum stress-mediated apoptosis. Vet Res. 2023;54(1):27.

262. Xu X, Wang L, Liu Y, Shi X, Yan Y, Zhang S, et al. TRIM56 overexpression restricts porcine epidemic diarrhoea virus replication in Marc-145 cells by enhancing TLR3-TRAF3-mediated IFN-β antiviral response. J Gen Virol. 2022;103(5).

263. Zhang Q, Ke H, Blikslager A, Fujita T, Yoo D. Type III Interferon Restriction by Porcine Epidemic Diarrhea Virus and the Role of Viral Protein nsp1 in IRF1 Signaling. Gallagher T, editor. J Virol. 2018;92(4):e01677-17.

264. Zhang Q, Shi K, Yoo D. Suppression of type I interferon production by porcine epidemic diarrhea virus and degradation of CREB-binding protein by nsp1. Virology. 2016;489:252–68.

265. Zhou H, Zhang Y, Wang J, Yan Y, Liu Y, Shi X, et al. The CREB and AP-1–Dependent Cell Communication Network Factor 1 Regulates Porcine Epidemic Diarrhea Virus-Induced Cell Apoptosis Inhibiting Virus Replication Through the p53 Pathway. Front Microbiol. 2022;13:831852.

266. Cheng J, Tao J, Li B, Shi Y, Liu H. Coinfection with PEDV and BVDV induces inflammatory bowel disease pathway highly enriched in PK-15 cells. Virol J. 2022;19:119.

267. Jin D, Xinna G, Jun H, Lei Z, Ning ZY, Xin G, et al. Proteomics Analysis of Porcine Kidney Cell Lines LLC-PK1 and PK15 with Different PEDV Infectivity. Advance. 2023;

268. Lv Y, Shao Y, Jiang C, Wang Y, Li Y, Li Y, et al. Quantitative proteomics based on TMT revealed the response of PK15 cells infected PEDV wild strain. Microb Pathog. 2024;186:106503.

269. Wang D, Fang L, Shi Y, Zhang H, Gao L, Peng G, et al. Porcine Epidemic Diarrhea Virus 3C-Like Protease Regulates Its Interferon Antagonism by Cleaving NEMO. J Virol. 2016;90(4):2090–101.

270. Weingartl HM, Derbyshire JB. Antiviral activity against transmissible gastroenteritis virus, and cytotoxicity, of natural porcine interferons alpha and beta. Can J Vet Res. 1991;55(2):143–9.

271. Lu Y, Yu R, Tong L, Zhang L, Zhang Z, Pan L, et al. Transcriptome Analysis of LLC-PK Cells Single or Coinfected with Porcine Epidemic Diarrhea Virus and Porcine Deltacoronavirus. Viruses. 2023;16(1):74.

272. Zhang Q, Ma J, Yoo D. Inhibition of NF-κB activity by the porcine epidemic diarrhea virus nonstructural protein 1 for innate immune evasion. Virology. 2017;510:111–26.

273. Kadoi K, Sugioka H, Satoh T, Kadoi BK. The propagation of a porcine epidemic diarrhea virus in swine cell lines. New Microbiol. 2002;25(3):285–90.

274. Shi W, Jia S, Zhao H, Yin J, Wang X, Yu M, et al. Novel Approach for Isolation and Identification of Porcine Epidemic Diarrhea Virus (PEDV) Strain NJ Using Porcine Intestinal Epithelial Cells. Viruses. 2017;9(1):19.

275. Xu X, Zhang H, Zhang Q, Dong J, Liang Y, Huang Y, et al. Porcine epidemic diarrhea virus E protein causes endoplasmic reticulum stress and up-regulates interleukin-8 expression. Virol J. 2013;10(1):26.

276. Altawaty T, Liu L, Zhang H, Tao C, Hou S, Li K, et al. Lack of LTβR Increases Susceptibility of IPEC-J2 Cells to Porcine Epidemic Diarrhea Virus. Cells. 2018;7(11):222.

277. Cui J, Li X, Kang Y, Li P, Guo X, Zhao W, et al. Integrating network pharmacology with pharmacological research to elucidate the mechanism of modified Gegen Qinlian Decoction in treating porcine epidemic diarrhea. Sci Rep. 2024;14(1):18929.

278. Hu Z, Li Y, Du H, Ren J, Zheng X, Wei K, et al. Transcriptome analysis reveals modulation of the STAT family in PEDV-infected IPEC-J2 cells. BMC Genomics. 2020;21(1):891.

279. Lin H, Li B, Chen L, Ma Z, He K, Fan H. Differential Protein Analysis of IPEC-J2 Cells Infected with Porcine Epidemic Diarrhea Virus Pandemic and Classical Strains Elucidates the Pathogenesis of Infection. J Proteome Res. 2017;16(6):2113–20.

280. Ouyang T, Yang Z, Wan J, Zhang Y, Wang X, Kong L, et al. Transcriptome analysis of host response to porcine epidemic diarrhea virus nsp15 in IPEC-J2 cells. Microb Pathog. 2022;162:105195.

281. Song L, Chen J, Hao P, Jiang Y, Xu W, Li L, et al. Differential Transcriptomics Analysis of IPEC-J2 Cells Single or Coinfected With Porcine Epidemic Diarrhea Virus and Transmissible Gastroenteritis Virus. Front Immunol. 2022;13:844657.

282. Zhang J, Guo L, Yang L, Xu J, Zhang L, Feng L, et al. Metalloprotease ADAM17 regulates porcine epidemic diarrhea virus infection by modifying aminopeptidase N. Virology. 2018;517:24–9.

283. Li X, Sun J, Prinz RA, Liu X, Xu X. Inhibition of porcine epidemic diarrhea virus (PEDV) replication by A77 1726 through targeting JAK and Src tyrosine kinases. Virology. 2020;551:75–83.

284. Lu Y, Cai H, Lu M, Ma Y, Li A, Gao Y, et al. Porcine Epidemic Diarrhea Virus Deficient in RNA Cap Guanine-N-7 Methylation Is Attenuated and Induces Higher Type I and III Interferon Responses. Dutch RE, editor. J Virol. 2020;94(16):e00447-20.

285. Wang J, Kan X, Li X, Sun J, Xu X. Porcine epidemic diarrhoea virus (PEDV) infection activates AMPK and JNK through TAK1 to induce autophagy and enhance virus replication. Virulence. 2022;13(1):1697–712.

286. Zhou J, Qiu Y, Zhao J, Wang Y, Zhu N, Wang D, et al. The Network of Interactions between the Porcine Epidemic Diarrhea Virus Nucleocapsid and Host Cellular Proteins. Viruses. 2022;14(10):2269.

287. Wang X, Fang L, Liu S, Ke W, Wang D, Peng G, et al. Susceptibility of porcine IPI-2I intestinal epithelial cells to infection with swine enteric coronaviruses. Vet Microbiol. 2019;233:21–7.

288. Zhang X, Li C, Zhang B, Li Z, Zeng W, Luo R, et al. Differential expression and correlation analysis of miRNA–mRNA profiles in swine testicular cells infected with porcine epidemic diarrhea virus. Sci Rep. 2021;11(1):1868.

289. Jung K, Vasquez-Lee M, Saif LJ. Replicative capacity of porcine deltacoronavirus and porcine epidemic diarrhea virus in primary bovine mesenchymal cells. Vet Microbiol. 2020;244:108660.

290. Khatri M. Porcine Epidemic Diarrhea Virus Replication in Duck Intestinal Cell Line. Emerg Infect Dis. 2015;21(3):549–50.

291. Chen J, Cui Y, Wang Z, Liu G. Identification and characterization of PEDV infection in rat crypt epithelial cells. Vet Microbiol. 2020;249:108848.

292. Si F, Hu X, Wang C, Chen B, Wang R, Dong S, et al. Porcine Epidemic Diarrhea Virus (PEDV) ORF3 Enhances Viral Proliferation by Inhibiting Apoptosis of Infected Cells. Viruses. 2020;12(2):214.

293. Si F, Chen B, Hu X, Yu R, Dong S, Wang R, et al. Porcine Epidemic Diarrhea Virus ORF3 Protein Is Transported through the Exocytic Pathway. J Virol. 2020;94(17).

294. Zhou J, Feng Z, Lv D, Wang D, Sang K, Liu Z, et al. Unveiling the Role of Protein Kinase C θ in Porcine Epidemic Diarrhea Virus Replication: Insights from Genome-Wide CRISPR/Cas9 Library Screening. Int J Mol Sci. 2024;25(6):3096.

295. Lv L, Luo H, Yu L, Tong W, Jiang Y, Li G, et al. Identification and Characterization of Cell Lines HepG2, Hep3B217 and SNU387 as Models for Porcine Epidemic Diarrhea Coronavirus Infection. Viruses. 2022;14(12):2754.

296. Zhang J, Guo L, Xu Y, Yang L, Shi H, Feng L, et al. Characterization of porcine epidemic diarrhea virus infectivity in human embryonic kidney cells. Arch Virol. 2017;162(8):2415–9.

297. Madson DM, Arruda PHE, Magstadt DR, Burrough ER, Hoang H, Sun D, et al. Characterization of Porcine Epidemic Diarrhea Virus Isolate US/Iowa/18984/2013 Infection in 1-Day-Old Cesarean-Derived Colostrum-Deprived Piglets. Vet Pathol. 2016;53(1):44–52.

298. Jung K, Wang Q, Scheuer KA, Lu Z, Zhang Y, Saif LJ. Pathology of US porcine epidemic diarrhea virus strain PC21A in gnotobiotic pigs. Emerg Infect Dis. 2014;20(4):662–5.

299. Jung K, Miyazaki A, Saif LJ. Immunohistochemical detection of the vomiting-inducing monoamine neurotransmitter serotonin and enterochromaffin cells in the intestines of conventional or gnotobiotic (Gn) pigs infected with porcine epidemic diarrhea virus (PEDV) and serum cytokine responses of Gn pigs to acute PEDV infection. Res Vet Sci. 2018;119:99–108.

300. Shibata I, Tsuda T, Mori M, Ono M, Sueyoshi M, Uruno K. Isolation of porcine epidemic diarrhea virus in porcine cell cultures and experimental infection of pigs of different ages. Vet Microbiol. 2000;72(3):173–82.

301. Chen Q, Gauger PC, Stafne MR, Thomas JT, Madson DM, Huang H, et al. Pathogenesis comparison between the United States porcine epidemic diarrhoea virus prototype and S-INDEL-variant strains in conventional neonatal piglets. J Gen Virol. 2016;97(5):1107–21.

302. Gerber PF, Xiao CT, Lager K, Crawford K, Kulshreshtha V, Cao D, et al. Increased frequency of porcine epidemic diarrhea virus shedding and lesions in suckling pigs compared to nursery pigs and protective immunity in nursery pigs after homologous re-challenge. Vet Res. 2016;47:118.

303. Liu X, Lin CM, Annamalai T, Gao X, Lu Z, Esseili MA, et al. Determination of the infectious titer and virulence of an original US porcine epidemic diarrhea virus PC22A strain. Vet Res. 2015;46(1):109.

304. Thomas JT, Chen Q, Gauger PC, Giménez-Lirola LG, Sinha A, Harmon KM, et al. Effect of Porcine Epidemic Diarrhea Virus Infectious Doses on Infection Outcomes in Naïve Conventional Neonatal and Weaned Pigs. PLoS One. 2015;10(10):e0139266.

305. Jung K, Annamalai T, Lu Z, Saif LJ. Comparative pathogenesis of US porcine epidemic diarrhea virus (PEDV) strain PC21A in conventional 9-day-old nursing piglets vs. 26-day-old weaned pigs. Vet Microbiol. 2015;178(1–2):31–40.

306. Annamalai T, Saif LJ, Lu Z, Jung K. Age-dependent variation in innate immune responses to porcine epidemic diarrhea virus infection in suckling versus weaned pigs. Vet Immunol Immunopathol. 2015;168(3):193–202.

307. Hou Y, Lin CM, Yokoyama M, Yount BL, Marthaler D, Douglas AL, et al. Deletion of a 197-Amino-Acid Region in the N-Terminal Domain of Spike Protein Attenuates Porcine Epidemic Diarrhea Virus in Piglets. J Virol. 2017;91(14).

308. Lin CM, Annamalai T, Liu X, Gao X, Lu Z, El-Tholoth M, et al. Experimental infection of a US spike-insertion deletion porcine epidemic diarrhea virus in conventional nursing piglets and cross-protection to the original US PEDV infection. Vet Res. 2015;46(1):134.

309. Lohse L, Krog JS, Strandbygaard B, Rasmussen TB, Kjær J, Belsham GJ, et al. Experimental Infection of Young Pigs with an Early European Strain of Porcine Epidemic Diarrhoea Virus and a Recent US Strain. Transbound Emerg Dis. 2017;64(5):1380–6.

310. Madson DM, Magstadt DR, Arruda PHE, Hoang H, Sun D, Bower LP, et al. Pathogenesis of porcine epidemic diarrhea virus isolate (US/Iowa/18984/2013) in 3-week-old weaned pigs. Vet Microbiol. 2014;174(1–2):60–8.

311. Masuda T, Murakami S, Takahashi O, Miyazaki A, Ohashi S, Yamasato H, et al. New porcine epidemic diarrhoea virus variant with a large deletion in the spike gene identified in domestic pigs. Arch Virol. 2015;160(10):2565–8.

312. Suzuki T, Shibahara T, Yamaguchi R, Nakade K, Yamamoto T, Miyazaki A, et al. Pig epidemic diarrhoea virus S gene variant with a large deletion non-lethal to colostrum-deprived newborn piglets. J Gen Virol. 2016;97(8):1823–8.

313. Leidenberger S, Schröder C, Zani L, Auste A, Pinette M, Ambagala A, et al. Virulence of current German PEDV strains in suckling pigs and investigation of protective effects of maternally derived antibodies. Sci Rep. 2017;7(1):10825.

314. Jermsutjarit P, Mebumroong S, Watcharavongtip P, Lin H, Tantituvanont A, Kaeoket K, et al. Evolution and virulence of porcine epidemic diarrhea virus following in vitro and in vivo propagation. Sci Rep. 2024;14(1):12279.

315. Hou Y, Wang Q. Emerging Highly Virulent Porcine Epidemic Diarrhea Virus: Molecular Mechanisms of Attenuation and Rational Design of Live Attenuated Vaccines. Int J Mol Sci. 2019;20(21):5478.

316. Kim Y, Oh C, Shivanna V, Hesse RA, Chang KO. Trypsin-independent porcine epidemic diarrhea virus US strain with altered virus entry mechanism. BMC Vet Res. 2017;13(1):356.

317. Lin CM, Hou Y, Marthaler DG, Gao X, Liu X, Zheng L, et al. Attenuation of an original US porcine epidemic diarrhea virus strain PC22A *via* serial cell culture passage. Vet Microbiol. 2017;201:62–71.

318. Wu Y, Li W, Zhou Q, Li Q, Xu Z, Shen H, et al. Characterization and pathogenicity of Vero cell-attenuated porcine epidemic diarrhea virus CT strain. Virol J. 2019;16(1):121.

319. Chen F, Zhu Y, Wu M, Ku X, Ye S, Li Z, et al. Comparative Genomic Analysis of Classical and Variant Virulent Parental/Attenuated Strains of Porcine Epidemic Diarrhea Virus. Viruses. 2015;7(10):5525–38.

320. Sato T, Takeyama N, Katsumata A, Tuchiya K, Kodama T, Kusanagi K ichi. Mutations in the spike gene of porcine epidemic diarrhea virus associated with growth adaptation in vitro and attenuation of virulence in vivo. Virus Genes. 2011;43(1):72–8.

321. Dong W, Ding N, Zhang Y, Tan Z, Ding X, Zhang Q, et al. Alterations of Suckling Piglet Jejunal Microbiota Due to Infection With Porcine Epidemic Diarrhea Virus and Protection Against Infection by Lactobacillus salivarius. Front Vet Sci. 2021;8.

322. Huang A, Cai R, Wang Q, Shi L, Li C, Yan H. Dynamic Change of Gut Microbiota During Porcine Epidemic Diarrhea Virus Infection in Suckling Piglets. Front Microbiol. 2019;10.

323. Huang MZ, Wang SY, Wang H, Cui DA, Yang YJ, Liu XW, et al. Differences in the intestinal microbiota between uninfected piglets and piglets infected with porcine epidemic diarrhea virus. PLoS One. 2018;13(2):e0192992.

324. Koh HW, Kim MS, Lee JS, Kim H, Park SJ. Changes in the Swine Gut Microbiota in Response to Porcine Epidemic Diarrhea Infection. Microbes Environ. 2015;30(3):284–7.

325. Li Z, Zhang W, Su L, Huang Z, Zhang W, Ma L, et al. Difference analysis of intestinal microbiota and metabolites in piglets of different breeds exposed to porcine epidemic diarrhea virus infection. Front Microbiol. 2022;13.

326. Song D, Peng Q, Chen Y, Zhou X, Zhang F, Li A, et al. Altered Gut Microbiota Profiles in Sows and Neonatal Piglets Associated with Porcine Epidemic Diarrhea Virus Infection. Sci Rep. 2017;7(1):17439.

327. Tan Z, Dong W, Ding Y, Ding X, Zhang Q, Jiang L. Porcine Epidemic Diarrhea Altered Colonic Microbiota Communities in Suckling Piglets. Genes. 2020;11(1):44.

328. Tan Z, Dong W, Ding Y, Ding X, Zhang Q, Jiang L. Changes in cecal microbiota community of suckling piglets infected with porcine epidemic diarrhea virus. PLoS One. 2019;14(7):e0219868.

329. Xing JH, Niu TM, Zou BS, Yang GL, Shi CW, Yan QS, et al. Gut microbiota-derived LCA mediates the protective effect of PEDV infection in piglets. Microbiome. 2024;12(1):20.

330. Yang S, Li Y, Wang B, Yang N, Huang X, Chen Q, et al. Acute porcine epidemic diarrhea virus infection reshapes the intestinal microbiota. Virology. 2020;548:200–12.

331. Yang S, Liu G, Savelkoul HFJ, Jansen CA, Li B. Mini-review: microbiota have potential to prevent PEDV infection by improved intestinal barrier. Front Immunol. 2023;14.

332. Shu X, Han F, Hu Y, Hao C, Li Z, Wei Z, et al. Co-infection of porcine deltacoronavirus and porcine epidemic diarrhoea virus alters gut microbiota diversity and composition in the colon of piglets. Virus Res. 2022;322:198954.

333. Shi D, Shi H, Sun D, Chen J, Zhang X, Wang X, et al. Nucleocapsid Interacts with NPM1 and Protects it from Proteolytic Cleavage, Enhancing Cell Survival, and is Involved in PEDV Growth. Sci Rep. 2017;7(1):39700.

334. Li Z, Zeng W, Ye S, Lv J, Nie A, Zhang B, et al. Cellular hnRNP A1 Interacts with Nucleocapsid Protein of Porcine Epidemic Diarrhea Virus and Impairs Viral Replication. Viruses. 2018;10(3):127.

335. Zhai X, Kong N, Zhang Y, Song Y, Qin W, Yang X, et al. N protein of PEDV plays chess game with host proteins by selective autophagy. Autophagy. 2023;19(8):2338–52.

336. Wang H, Kong N, Jiao Y, Dong S, Sun D, Chen X, et al. EGR1 Suppresses Porcine Epidemic Diarrhea Virus Replication by Regulating IRAV To Degrade Viral Nucleocapsid Protein. J Virol. 2021;95(19).

337. Dong S, Kong N, Wang C, Li Y, Sun D, Qin W, et al. FUBP3 Degrades the Porcine Epidemic Diarrhea Virus Nucleocapsid Protein and Induces the Production of Type I Interferon. J Virol. 2022;96(13):e00618-22.

338. Dong S, Kong N, Zhang Y, Li Y, Sun D, Qin W, et al. TARDBP Inhibits Porcine Epidemic Diarrhea Virus Replication through Degrading Viral Nucleocapsid Protein and Activating Type I Interferon Signaling. J Virol. 2022;96(10):e00070-22.

339. Qin W, Kong N, Zhang Y, Wang C, Dong S, Zhai H, et al. PTBP1 suppresses porcine epidemic diarrhea virus replication via inducing protein degradation and IFN production. J Biol Chem. 2023;299(8).

340. Zhai X, Kong N, Wang C, Qin W, Dong S, Zhai H, et al. PRPF19 Limits Porcine Epidemic Diarrhea Virus Replication through Targeting and Degrading Viral Capsid Protein. Gallagher T, editor. J Virol. 2023;97(1):e01614-22.

341. Kong N, Shan T, Wang H, Jiao Y, Zuo Y, Li L, et al. BST2 suppresses porcine epidemic diarrhea virus replication by targeting and degrading virus nucleocapsid protein with selective autophagy. Autophagy. 2020;16(10):1737–52.

342. Xu J, Mao J, Han X, Shi F, Gao Q, Wang T, et al. Porcine Epidemic Diarrhea Virus Inhibits HDAC1 Expression To Facilitate Its Replication via Binding of Its Nucleocapsid Protein to Host Transcription Factor Sp1. Williams BRG, editor. J Virol. 2021;95(18):e00853-21.

343. Wang R, Yu R, Chen B, Si F, Wang J, Xie C, et al. Identification of host cell proteins that interact with the M protein of porcine epidemic diarrhea virus. Vet Microbiol. 2020;246:108729.

344. Dong S, Wang R, Yu R, Chen B, Si F, Xie C, et al. Identification of cellular proteins interacting with PEDV M protein through APEX2 labeling. J Proteomics. 2021;240:104191.

345. Song Z, Yan T, Ran L, Niu Z, Zhang Y, Kan Z, et al. Reduced activity of intestinal surface Na+/H+ exchanger NHE3 is a key factor for induction of diarrhea after PEDV infection in neonatal piglets. Virology. 2021;563:64–73.

346. Niu Z, Zhang Y, Kan Z, Ran L, Yan T, Xu S, et al. Decreased NHE3 activity in intestinal epithelial cells in TGEV and PEDV-induced piglet diarrhea. Vet Microbiol. 2021;263:109263.

347. Chen J, Zhang C, Zhang N, Liu G. Porcine endemic diarrhea virus infection regulates long noncoding RNA expression. Virology. 2019;527:89–97.

348. Kim Y, Lee C. Extracellular signal-regulated kinase (ERK) activation is required for porcine epidemic diarrhea virus replication. Virology. 2015;484:181–93.

349. Shen X, Yin L, Pan X, Zhao R, Zhang D. Porcine epidemic diarrhea virus infection blocks cell cycle and induces apoptosis in pig intestinal epithelial cells. Microb Pathog. 2020;147:104378.

350. Sun P, Fahd Q, Li Y, Sun Y, Li J, Qaria MA, et al. Transcriptomic analysis of small intestinal mucosa from porcine epidemic diarrhea virus infected piglets. Microb Pathog. 2019;132:73–9.

351. Zeng S, Zhang H, Ding Z, Luo R, An K, Liu L, et al. Proteome analysis of porcine epidemic diarrhea virus (PEDV)-infected Vero cells. PROTEOMICS. 2015;15(11):1819–28.

352. Zhang H, Liu Q, Su W, Wang J, Sun Y, Zhang J, et al. Genome-wide analysis of differentially expressed genes and the modulation of PEDV infection in Vero E6 cells. Microb Pathog. 2018;117:247–54.

353. Chen YM, Gabler NK, Burrough ER. Porcine epidemic diarrhea virus infection induces endoplasmic reticulum stress and unfolded protein response in jejunal epithelial cells of weaned pigs. Vet Pathol. 2022;59(1):82–90.

354. Chen YM, Burrough E. The Effects of Swine Coronaviruses on ER Stress, Autophagy, Apoptosis, and Alterations in Cell Morphology. Pathogens. 2022;11(8):940.

355. Chen YM, Helm ET, Groeltz-Thrush JM, Gabler NK, Burrough ER. Epithelial-mesenchymal transition of absorptive enterocytes and depletion of Peyer's patch M cells after PEDV infection. Virology. 2021;552:43–51.

356. Jung K, Eyerly B, Annamalai T, Lu Z, Saif LJ. Structural alteration of tight and adherens junctions in villous and crypt epithelium of the small and large intestine of conventional nursing piglets infected with porcine epidemic diarrhea virus. Vet Microbiol. 2015;177(3):373–8.

357. Jung K, Saif LJ. Goblet cell depletion in small intestinal villous and crypt epithelium of conventional nursing and weaned pigs infected with porcine epidemic diarrhea virus. Res Vet Sci. 2017;110:12–5.

358. Wei X, Li J, Zhang Y, Gong L, Xue C, Cao Y. Profiling of alternative polyadenylation and gene expression in PEDV-infected IPEC-J2 cells. Virus Genes. 2021;57(2):181–93.

359. Zhao H, Yang J, Wang Q, Cui Z, Li D, Niu J, et al. Exosomal miRNA-328-3p targets ZO-3 and inhibits porcine epidemic diarrhea virus proliferation. Arch Virol. 2022;167(3):901–10.

360. Zong QF, Huang YJ, Wu LS, Wu ZC, Wu SL, Bao WB. Effects of porcine epidemic diarrhea virus infection on tight junction protein gene expression and morphology of the intestinal mucosa in pigs. Pol J Vet Sci. 2019;22(2):345–53.

361. Hou W, Kang W, Li Y, Shan Y, Wang S, Liu F. Dynamic Dissection of Dynein and Kinesin-1 Cooperatively Mediated Intercellular Transport of Porcine Epidemic Diarrhea Coronavirus along Microtubule Using Single Virus Tracking. Virulence. 2021;12(1):615–29.

362. Hou W, Li Y, Kang W, Wang X, Wu X, Wang S, et al. Real-time analysis of quantum dot labeled single porcine epidemic diarrhea virus moving along the microtubules using single particle tracking. Sci Rep. 2019;9(1):1307.

363. Zhang K, Lin S, Li J, Deng S, Zhang J, Wang S. Modulation of Innate Antiviral Immune Response by Porcine Enteric Coronavirus. Front Microbiol. 2022;13:845137.

364. Du J, Luo J, Yu J, Mao X, Luo Y, Zheng P, et al. Manipulation of Intestinal Antiviral Innate Immunity and Immune Evasion Strategies of Porcine Epidemic Diarrhea Virus. Biomed Res Int. 2019;2019:1862531.

365. Koonpaew S, Teeravechyan S, Frantz PN, Chailangkarn T, Jongkaewwattana A. PEDV and PDCoV Pathogenesis: The Interplay Between Host Innate Immune Responses and Porcine Enteric Coronaviruses. Front Vet Sci. 2019;6:34.

366. Orosco FL. Immune evasion mechanisms of porcine epidemic diarrhea virus: A comprehensive review. Vet Integr Sci. 2024;22(1):171–92.

367. Yuan P, Yang Z, Yang Y, Wang K, Dong W, Song H, et al. Structural and non-structural proteins of porcine epidemic diarrhea virus against congenital immunity of host cells. Gastroenterol Hepatol Endosc. 2018;3(2).

368. Zhang Q, Yoo D. Immune evasion of porcine enteric coronaviruses and viral modulation of antiviral innate signaling. Virus Res. 2016;226:128–41.

369. Carpenter S, O'Neill LAJ. From periphery to center stage: 50 years of advancements in innate immunity. Cell. 2024;187(9):2030–51.

370. Takeuchi O, Akira S. Innate immunity to virus infection. Immunol Rev. 2009;227(1):75–86.

371. Kawai T, Akira S. Toll-like receptors and their crosstalk with other innate receptors in infection and immunity. Immunity. 2011;34(5):637–50.

372. Nicholson LB. The immune system. Essays Biochem. 2016;60(3):275–301.

373. Mair KH, Sedlak C, Käser T, Pasternak A, Levast B, Gerner W, et al. The porcine innate immune system: An update. Dev Comp Immunol. 2014;45(2):321–43.

374. Ohto U. Activation and regulation mechanisms of NOD-like receptors based on structural biology. Front Immunol. 2022;13:953530.

375. Ishikawa H, Barber GN. STING is an endoplasmic reticulum adaptor that facilitates innate immune signalling. Nature. 2008;455(7213):674–8.

376. Sun L, Wu J, Du F, Chen X, Chen ZJ. Cyclic GMP-AMP synthase is a cytosolic DNA sensor that activates the type I interferon pathway. Science. 2013;339(6121):786–91.

377. Wu J, Sun L, Chen X, Du F, Shi H, Chen C, et al. Cyclic GMP-AMP is an endogenous second messenger in innate immune signaling by cytosolic DNA. Science. 2013;339(6121):826–30.

378. Almeida-da-Silva CLC, Savio LEB, Coutinho-Silva R, Ojcius DM. The role of NOD-like receptors in innate immunity. Front Immunol. 2023;14.

379. Te N, Rodon J, Ballester M, Pérez M, Pailler-García L, Segalés J, et al. Type I and III IFNs produced by the nasal epithelia and dimmed inflammation are features of alpacas resolving MERS-CoV infection. PLoS Pathog. 2021;17(5):e1009229.

380. Wang P, Zhu S, Yang L, Cui S, Pan W, Jackson R, et al. Nlrp6 regulates intestinal antiviral innate immunity. Science. 2015;350(6262):826–30.

381. Rawling DC, Pyle AM. Parts, assembly and operation of the RIG-I family of motors. Curr Opin Struct Biol. 2014;25:25–33.

382. Yoneyama M, Kikuchi M, Natsukawa T, Shinobu N, Imaizumi T, Miyagishi M, et al. The RNA helicase RIG-I has an essential function in double-stranded RNA-induced innate antiviral responses. Nat Immunol. 2004;5(7):730–7.

383. Liu HM, Loo YM, Horner SM, Zornetzer GA, Katze MG, Gale M. The mitochondrial targeting chaperone 14-3-3ε regulates a RIG-I translocon that mediates membrane association and innate antiviral immunity. Cell Host Microbe. 2012;11(5):528–37.

384. Fang R, Jiang Q, Zhou X, Wang C, Guan Y, Tao J, et al. MAVS activates TBK1 and IKKε through TRAFs in NEMO dependent and independent manner. PLOS Pathogens. 2017;13(11):e1006720.

385. Odendall C, Dixit E, Stavru F, Bierne H, Franz KM, Durbin AF, et al. Diverse intracellular pathogens activate type III interferon expression from peroxisomes. Nat Immunol. 2014;15(8):717–26.

386. Gao R, Zhang Y, Kang Y, Xu W, Jiang L, Guo T, et al. Glycyrrhizin Inhibits PEDV Infection and Proinflammatory Cytokine Secretion via the HMGB1/TLR4-MAPK p38 Pathway. Int J Mol Sci. 2020;21(8):2961.

387. Huan C chao, Wang H xia, Sheng X xiang, Wang R, Wang X, Mao X. Glycyrrhizin inhibits porcine epidemic diarrhea virus infection and attenuates the proinflammatory responses by inhibition of high mobility group box-1 protein. Arch Virol. 2017;162(6):1467–76.

388. Liu D, Wang Q, He W, Ge L, Huang K. Deoxynivalenol aggravates the immunosuppression in piglets and PAMs under the condition of PEDV infection through inhibiting TLR4/NLRP3 signaling pathway. Ecotoxicol Environ Saf. 2022;231:113209.

389. Temeeyasen G, Sinha A, Gimenez-Lirola LG, Zhang JQ, Piñeyro PE. Differential gene modulation of pattern-recognition receptor TLR and RIG-I-like and downstream mediators on intestinal mucosa of pigs infected with PEDV non S-INDEL and PEDV S-INDEL strains. Virology. 2018;517:188–98.

390. Wang F, Wang SQ, Wang HF, Wu ZC, Bao WB, Wu SL. Effects of porcine epidemic diarrhea virus infection on Toll-like receptor expression and cytokine levels in porcine intestinal epithelial cells. Pol J Vet Sci. 2020;119–26.

391. Kawai T, Akira S. The role of pattern-recognition receptors in innate immunity: update on Toll-like receptors. Nat Immunol. 2010;11(5):373–84.

392. Liu L, Botos I, Wang Y, Leonard JN, Shiloach J, Segal DM, et al. Structural basis of toll-like receptor 3 signaling with double-stranded RNA. Science. 2008;320(5874):379–81.

393. Kotenko SV. IFN-λs. Curr Opin Immunol. 2011;23(5):583–90.

394. Kotenko SV, Gallagher G, Baurin VV, Lewis-Antes A, Shen M, Shah NK, et al. IFN-lambdas mediate antiviral protection through a distinct class II cytokine receptor complex. Nat Immunol. 2003;4(1):69–77.

395. Prokunina-Olsson L, Muchmore B, Tang W, Pfeiffer RM, Park H, Dickensheets H, et al. A variant upstream of IFNL3 (IL28B) creating a new interferon gene IFNL4 is associated with impaired clearance of hepatitis C virus. Nat Genet. 2013;45(2):164–71.

396. Sheppard P, Kindsvogel W, Xu W, Henderson K, Schlutsmeyer S, Whitmore TE, et al. IL-28, IL-29 and their class II cytokine receptor IL-28R. Nat Immunol. 2003;4(1):63–8.

397. Li L, Xue M, Fu F, Yin L, Feng L, Liu P. IFN-Lambda 3 Mediates Antiviral Protection Against Porcine Epidemic Diarrhea Virus by Inducing a Distinct Antiviral Transcript Profile in Porcine Intestinal Epithelia. Front Immunol. 2019;10:2394.

398. Li L, Fu F, Xue M, Chen W, Liu J, Shi H, et al. IFN-lambda preferably inhibits PEDV infection of porcine intestinal epithelial cells compared with IFN-alpha. Antiviral Res. 2017;140:76–82.

399. Dixit E, Boulant S, Zhang Y, Lee ASY, Odendall C, Shum B, et al. Peroxisomes are signaling platforms for antiviral innate immunity. Cell. 2010;141(4):668–81.

400. Honda K, Taniguchi T. IRFs: master regulators of signalling by Toll-like receptors and cytosolic pattern-recognition receptors. Nat Rev Immunol. 2006;6(9):644–58.

401. Napetschnig J, Wu H. Molecular basis of NF-κB signaling. Annu Rev Biophys. 2013;42:443–68.

402. Ingle H, Peterson ST, Baldridge MT. Distinct Effects of Type I and III Interferons on Enteric Viruses. Viruses. 2018;10(1):46.

403. Jewell NA, Cline T, Mertz SE, Smirnov SV, Flaño E, Schindler C, et al. Lambda interferon is the predominant interferon induced by influenza A virus infection in vivo. J Virol. 2010;84(21):11515–22.

404. Nakagawa S ichiro, Hirata Y, Kameyama T, Tokunaga Y, Nishito Y, Hirabayashi K, et al. Targeted induction of interferon-λ in humanized chimeric mouse liver abrogates hepatotropic virus infection. PLoS One. 2013;8(3):e59611.

405. Li L, Xue M, Fu F, Yin L, Feng L, Liu P. IFN-Lambda 3 Mediates Antiviral Protection Against Porcine Epidemic Diarrhea Virus by Inducing a Distinct Antiviral Transcript Profile in Porcine Intestinal Epithelia. Front Immunol. 2019;10:2394.

406. Mahlakõiv T, Hernandez P, Gronke K, Diefenbach A, Staeheli P. Leukocyte-derived IFN-α/β and epithelial IFN-λ constitute a compartmentalized mucosal defense system that restricts enteric virus infections. PLoS Pathog. 2015;11(4):e1004782.

407. Pott J, Mahlakõiv T, Mordstein M, Duerr CU, Michiels T, Stockinger S, et al. IFN-lambda determines the intestinal epithelial antiviral host defense. PNAS. 2011;108(19):7944–9.

408. Schneider WM, Chevillotte MD, Rice CM. Interferon-Stimulated Genes: A Complex Web of Host Defenses. Annu Rev Immunol. 2014;32(Volume 32, 2014):513–45.

409. Hoffmann HH, Schneider WM, Rice CM. Interferons and viruses: an evolutionary arms race of molecular interactions. Trends Immunol. 2015;36(3):124–38.

410. Mendoza JL, Schneider WM, Hoffmann HH, Vercauteren K, Jude KM, Xiong A, et al. The IFN-λ-IFN-λR1-IL-10Rβ Complex Reveals Structural Features Underlying Type III IFN Functional Plasticity. Immunity. 2017;46(3):379–92.

411. Guo L, Luo X, Li R, Xu Y, Zhang J, Ge J, et al. Porcine Epidemic Diarrhea Virus Infection Inhibits Interferon Signaling by Targeted Degradation of STAT1. Perlman S, editor. J Virol. 2016;90(18):8281–92.

412. Schoggins JW, Rice CM. Interferon-stimulated genes and their antiviral effector functions. Curr Opin Virol. 2011;1(6):519–25.

413. Lazear HM, Schoggins JW, Diamond MS. Shared and Distinct Functions of Type I and Type III Interferons. Immunity. 2019;50(4):907–23.

414. Li Z, Chen F, Ye S, Guo X, Muhanmmad Memon A, Wu M, et al. Comparative Proteome Analysis of Porcine Jejunum Tissues in Response to a Virulent Strain of Porcine Epidemic Diarrhea Virus and Its Attenuated Strain. Viruses. 2016;8(12):323.

415. Zhang X, Yu W. Heat shock proteins and viral infection. Front Immunol. 2022;13:947789.

416. Kong F, Xu Y, Ran W, Yin B, Feng L, Sun D. Cold Exposure-Induced Up-Regulation of Hsp70 Positively Regulates PEDV mRNA Synthesis and Protein Expression In Vitro. Pathogens. 2020;9(4):246.

417. Park JY, Ryu J, Park JE, Hong EJ, Shin HJ. Heat shock protein 70 could enhance porcine epidemic diarrhoea virus replication by interacting with membrane proteins. Vet Res. 2021;52(1):138.

418. Sun M, Yu Z, Ma J, Pan Z, Lu C, Yao H. Down-regulating heat shock protein 27 is involved in porcine epidemic diarrhea virus escaping from host antiviral mechanism. Veterinary Microbiology. 2017 Jun 1;205:6–13.

419. Zhao Z, Zhang YQ, Xu LD, Xiao L, Feng Y, Wang B, et al. Role of heat shock protein 90 as an antiviral target for swine enteric coronaviruses. Virus Res. 2023;329:199103.

420. Chen X, Wang K, Xing Y, Tu J, Yang X, Zhao Q, et al. Coronavirus membrane-associated papain-like proteases induce autophagy through interacting with Beclin1 to negatively regulate antiviral innate immunity. Protein Cell. 2014;5(12):912–27.

421. Kong N, Shan T, Wang H, Jiao Y, Zuo Y, Li L, et al. BST2 suppresses porcine epidemic diarrhea virus replication by targeting and degrading virus nucleocapsid protein with selective autophagy. Autophagy. 2020;16(10):1737–52.

422. Lin H, Li B, Liu M, Zhou H, He K, Fan H. Nonstructural protein 6 of porcine epidemic diarrhea virus induces autophagy to promote viral replication via the PI3K/Akt/mTOR axis. Vet Microbiol. 2020;244:108684.

423. Park JY, Ryu J, Hong EJ, Shin HJ. Porcine Epidemic Diarrhea Virus Infection Induces Autophagosome Formation but Inhibits Autolysosome Formation during Replication. Viruses. 2022;14(5):1050.

424. Yang L, Xu J, Guo L, Guo T, Zhang L, Feng L, et al. Porcine Epidemic Diarrhea Virus-Induced Epidermal Growth Factor Receptor Activation Impairs the Antiviral Activity of Type I Interferon. J Virol. 2018;92(8):e02095-17.

425. Chen Y, Zhang Z, Li J, Gao Y, Zhou L, Ge X, et al. Porcine epidemic diarrhea virus S1 protein is the critical inducer of apoptosis. Virol J. 2018;15:170.

426. Li S, Zhu Z, Yang F, Cao W, Yang J, Ma C, et al. Porcine Epidemic Diarrhea Virus Membrane Protein Interacted with IRF7 to Inhibit Type I IFN Production during Viral Infection. J Immunol. 2021;206(12):2909–23.

427. Ding Z, Fang L, Jing H, Zeng S, Wang D, Liu L, et al. Porcine Epidemic Diarrhea Virus Nucleocapsid Protein Antagonizes Beta Interferon Production by Sequestering the Interaction between IRF3 and TBK1. J Virol. 2014 Aug 15;88(16):8936–45.

428. Shan Y, Liu Z qi, Li G wei, Chen C, Luo H, Liu Y jie, et al. Nucleocapsid protein from porcine epidemic diarrhea virus isolates can antagonize interferon-λ production by blocking the nuclear factor-κB nuclear translocation. J Zhejiang Univ-Sci B. 2018;19(7):570.

429. Qin W, Kong N, Wang C, Dong S, Zhai H, Zhai X, et al. hnRNP K Degrades Viral Nucleocapsid Protein and Induces Type I IFN Production to Inhibit Porcine Epidemic Diarrhea Virus Replication. J Virol. 2022;96(22):e01555-22.

430. Wang H, Chen X, Kong N, Jiao Y, Sun D, Dong S, et al. TRIM21 inhibits porcine epidemic diarrhea virus proliferation by proteasomal degradation of the nucleocapsid protein. Arch Virol. 2021;166(7):1903–11.

431. Li X, Yan Z, Ma J, Li G, Liu X, Peng Z, et al. TRIM28 promotes porcine epidemic diarrhea virus replication by mitophagy-mediated inhibition of the JAK-STAT1 pathway. Int J Biol Macromol. 2024;254(Pt 1):127722.

432. Qin W, Kong N, Zhang Y, Dong S, Zhai H, Zhai X, et al. Nuclear ribonucleoprotein RALY targets virus nucleocapsid protein and induces autophagy to restrict porcine epidemic diarrhea virus replication. J Biol Chem. 2022;298(8).

433. Li Z, Ma Z, Han W, Chang C, Li Y, Guo X, et al. Deletion of a 7-amino-acid region in the porcine epidemic diarrhea virus envelope protein induces higher type I and III interferon responses and results in attenuation in vivo. J Virol. 2023;97(9):e0084723.

434. Zheng L, Wang X, Guo D, Cao J, Cheng L, Li X, et al. Porcine epidemic diarrhea virus E protein suppresses RIG-I signaling-mediated interferon-β production. Vet Microbiol. 2021;254:108994.

435. Zheng L, Liu H, Tian Z, Kay M, Wang H, Wang X, et al. Porcine epidemic diarrhea virus E protein inhibits type I interferon production through endoplasmic reticulum stress response (ERS)-mediated suppression of antiviral proteins translation. Res Vet Sci. 2022;152:236–44.

436. Zheng L, Yang Y, Ma M, Hu Q, Wu Z, Kay M, et al. Porcine epidemic diarrhea virus E protein induces unfolded protein response through activating both PERK and ATF6 rather than IRE1 signaling pathway. Virus Genes. 2024;60(6):652–66.

437. Gao Q, Weng Z, Feng Y, Gong T, Zheng X, Zhang G, et al. KPNA2 suppresses porcine epidemic diarrhea virus replication by targeting and degrading virus envelope protein through selective autophagy. J Virol. 2023;97(12):e0011523.

438. Kaewborisuth C, Koonpaew S, Srisutthisamphan K, Viriyakitkosol R, Jaru-Ampornpan P, Jongkaewwattana A. PEDV ORF3 Independently Regulates IκB Kinase β-Mediated NF-κB and IFN-β Promoter Activities. Pathogens. 2020;9(5):376.

439. Wu Z, Cheng L, Xu J, Li P, Li X, Zou D, et al. The accessory protein ORF3 of porcine epidemic diarrhea virus inhibits cellular interleukin-6 and interleukin-8 productions by blocking the nuclear factor-κB p65 activation. Vet Microbiol. 2020;251:108892.

440. Zheng L, Liu H, Tian Z, Kay M, Wang H, Cheng L, et al. Porcine epidemic diarrhea virus (PEDV) ORF3 protein inhibits cellular type I interferon signaling through down-regulating proteins expression in RLRs-mediated pathway. Res J Vet Sci. 2023;159:146–59.

441. Ye S, Li Z, Chen F, Li W, Guo X, Hu H, et al. Porcine epidemic diarrhea virus ORF3 gene prolongs S-phase, facilitates formation of vesicles and promotes the proliferation of attenuated PEDV. Virus Genes. 2015;51(3):385–92.

442. Guo X, Zhang M, Zhang X, Tan X, Guo H, Zeng W, et al. Porcine Epidemic Diarrhea Virus Induces Autophagy to Benefit Its Replication. Viruses. 2017;9(3):53.

443. Zou D, Xu J, Duan X, Xu X, Li P, Cheng L, et al. Porcine epidemic diarrhea virus ORF3 protein causes endoplasmic reticulum stress to facilitate autophagy. Vet Microbiol. 2019;235:209–19.

444. Shen Z, Yang Y, Yang S, Zhang G, Xiao S, Fu ZF, et al. Structural and Biological Basis of Alphacoronavirus nsp1 Associated with Host Proliferation and Immune Evasion. Viruses. 2020;12(8):812.

445. Fan B, Peng Q, Song S, Shi D, Zhang X, Guo W, et al. Nonstructural Protein 1 of Variant PEDV Plays a Key Role in Escaping Replication Restriction by Complement C3. J Virol. 2022;96(18):e01024.

446. Li M, Wu Y, Chen J, Shi H, Ji Z, Zhang X, et al. Innate Immune Evasion of Porcine Epidemic Diarrhea Virus through Degradation of the FBXW7 Protein via the Ubiquitin-Proteasome Pathway. J Virol. 2022;96(5):e00889-21.

447. Xing Y, Chen J, Tu J, Zhang B, Chen X, Shi H, et al. The papain-like protease of porcine epidemic diarrhea virus negatively regulates type I interferon pathway by acting as a viral deubiquitinase. J Gen Virol. 2013;94(Pt 7):1554–67.

448. Zhang P, Yu L, Dong J, Liu Y, Zhang L, Liang P, et al. Cellular poly(C) binding protein 2 interacts with porcine epidemic diarrhea virus papain-like protease 1 and supports viral replication. Vet Microbiol. 2020;247:108793.

449. Fu X, Xu W, Yang Y, Li D, Shi W, Li X, et al. Diverse Strategies Utilized by Coronaviruses to Evade Antiviral Responses and Suppress Pyroptosis. bioRxiv; 2024. p. 2022.07.29.502014.

450. Yuan L, Chen Z, Song S, Wang S, Tian C, Xing G, et al. p53 Degradation by a Coronavirus Papain-like Protease Suppresses Type I Interferon Signaling. J Biol Chem. 2015;290(5):3172–82.

451. Yu L, Dong J, Wang Y, Zhang P, Liu Y, Zhang L, et al. Porcine epidemic diarrhea virus nsp4 induces pro-inflammatory cytokine and chemokine expression inhibiting viral replication in vitro. Arch Virol. 2019;164(4):1147–57.

452. Zhu X, Fang L, Wang D, Yang Y, Chen J, Ye X, et al. Porcine deltacoronavirus nsp5 inhibits interferon-β production through the cleavage of NEMO. Virology. 2017;502:33–8.

453. Zhu X, Wang D, Zhou J, Pan T, Chen J, Yang Y, et al. Porcine Deltacoronavirus nsp5 Antagonizes Type I Interferon Signaling by Cleaving STAT2. J Virol. 2017;91(10):e00003-17.

454. Liang R, Song H, Wang K, Ding F, Xuan D, Miao J, et al. Porcine epidemic diarrhea virus 3CLpro causes apoptosis and collapse of mitochondrial membrane potential requiring its protease activity and signaling through MAVS. Vet Microbiol. 2022;275:109596.

455. Shi F, Lv Q, Wang T, Xu J, Xu W, Shi Y, et al. Coronaviruses Nsp5 Antagonizes Porcine Gasdermin D-Mediated Pyroptosis by Cleaving Pore-Forming p30 Fragment. mBio. 2022;13(1):e02739-21.

456. Zhang J, Yuan S, Peng Q, Ding Z, Hao W, Peng G, et al. Porcine Epidemic Diarrhea Virus nsp7 Inhibits Interferon-Induced JAK-STAT Signaling through Sequestering the Interaction between KPNA1 and STAT1. J Virol. 2022;96(9):e00400-22.

457. Zhang J, Fang P, Ren J, Xia S, Zhang H, Zhu X, et al. Porcine Epidemic Diarrhea Virus nsp7 Inhibits MDA5 Dephosphorylation to Antagonize Type I Interferon Production. Microbiol Spectr. 2023;11(2):e05017.

458. Shi P, Su Y, Li R, Liang Z, Dong S, Huang J. PEDV nsp16 negatively regulates innate immunity to promote viral proliferation. Virus Res. 2019;265:57–66.

459. Zhu L, Liu S, Zhuo Z, Lin Y, Zhang Y, Wang X, et al. Expression and immunogenicity of nsp10 protein of porcine epidemic diarrhea virus. Res Vet Sci. 2022;144:34–43.

460. Yang N, Zhang Q, Wang Q, Zhang Y, Li S, Zhao Y, et al. Nsp10-interacting host protein SAP18 restricts PEDV replication in Marc-145 cells via enhancing dephosphorylation of RIG-I. Vet Microbiol. 2024;294:110124.

461. Jia X, Chen J, Qiao C, Li C, Yang K, Zhang Y, et al. Porcine Epidemic Diarrhea Virus nsp13 Protein Downregulates Neonatal Fc Receptor Expression by Causing Promoter Hypermethylation through the NF-κB Signaling Pathway. J Immunol. 2023;210(4):475–85.

462. Li S, Yang F, Ma C, Cao W, Yang J, Zhao Z, et al. Porcine epidemic diarrhea virus nsp14 inhibits NF-κB pathway activation by targeting the IKK complex and p65. Animal Diseases. 2021;1(1):24.

463. Deng X, van Geelen A, Buckley AC, O'Brien A, Pillatzki A, Lager KM, et al. Coronavirus Endoribonuclease Activity in Porcine Epidemic Diarrhea Virus Suppresses Type I and Type III Interferon Responses. J Virol. 2019;93(8):e02000-18.

464. Wu Y, Zhang H, Shi Z, Chen J, Li M, Shi H, et al. Porcine Epidemic Diarrhea Virus nsp15 Antagonizes Interferon Signaling by RNA Degradation of TBK1 and IRF3. Viruses. 2020;12(6):599.

465. Gao B, Gong X, Fang S, Weng W, Wang H, Chu H, et al. Inhibition of anti-viral stress granule formation by coronavirus endoribonuclease nsp15 ensures efficient virus replication. PLoS Pathog. 2021;17(2):e1008690.

466. Annamalai T, Lin CM, Gao X, Liu X, Lu Z, Saif LJ, et al. Cross protective immune responses in nursing piglets infected with a US spike-insertion deletion porcine epidemic diarrhea virus strain and challenged with an original US PEDV strain. Vet Res. 2017;48(1):61.

467. de Arriba M, Carvajal A, Pozo J, Rubio P. Mucosal and systemic isotype-specific antibody responses and protection in conventional pigs exposed to virulent or attenuated porcine epidemic diarrhoea virus. Vet immunol immunopathol. 2002;85(1–2):85–97.

468. Chen Q, Thomas JT, Giménez-Lirola LG, Hardham JM, Gao Q, Gerber PF, et al. Evaluation of serological cross-reactivity and cross-neutralization between the United States porcine

epidemic diarrhea virus prototype and S-INDEL-variant strains. BMC Vet Res. 2016;12(1):70.

469. Krishna VD, Kim Y, Yang M, Vannucci F, Molitor T, Torremorell M, et al. Immune responses to porcine epidemic diarrhea virus (PEDV) in swine and protection against subsequent infection. PLoS One. 2020;15(4):e0231723.

470. Okda F, Liu X, Singrey A, Clement T, Nelson J, Christopher-Hennings J, et al. Development of an indirect ELISA, blocking ELISA, fluorescent microsphere immunoassay and fluorescent focus neutralization assay for serologic evaluation of exposure to North American strains of Porcine Epidemic Diarrhea Virus. BMC Vet Res. 2015;11(1):180.

471. Gimenez-Lirola LG, Zhang J, Carrillo-Avila JA, Chen Q, Poonsuk K, Baum DH, et al. Reactivity of Porcine Epidemic Diarrhea Virus Structural Proteins to Antibodies against Porcine Enteric Coronaviruses: Diagnostic Implications. J Clin Microbiol. 2017;55(5):1426–36.

472. Díaz I, Pujols J, Cano E, Cortey M, Navarro N, Vidal A, et al. Immune response does not prevent homologous Porcine epidemic diarrhoea virus reinfection five months after the initial challenge. Transbound Emerg Dis. 2022;69(3):997–1009.

473. Ouyang K, Shyu DL, Dhakal S, Hiremath J, Binjawadagi B, Lakshmanappa YS, et al. Evaluation of humoral immune status in porcine epidemic diarrhea virus (PEDV) infected sows under field conditions. Vet Res. 2015;46(1):140.

474. Chen Q. Porcine epidemic diarrhea virus in the United States: Cell culture isolation, genetic phylogeny, pathogenesis, and immunity. Iowa State University, Digital Repository; 2016.

475. Goede D, Murtaugh MP, Nerem J, Yeske P, Rossow K, Morrison R. Previous infection of sows with a “mild” strain of porcine epidemic diarrhea virus confers protection against infection with a “severe” strain. Vet Microbiol. 2015;176(1):161–4.

476. Bohl E, Gupta R, Olquin M, Saif L. Antibody responses in serum, colostrum, and milk of swine after infection or vaccination with transmissible gastroenteritis virus. Infect Immun. 1972;6(3).

477. Roux M, McWilliams M, Phillips-Quagliata J, Weisz-Carrington P, Lamm M. Origin of IgA-secreting plasma cells in the mammary gland. J Exp Med. 1977;146(5).

478. Saif LJ. Enteric Viral Infections of Pigs and Strategies for Induction of Mucosal Immunity. Adv Vet Med. 1999;41:429–46.

479. Rooke JA, Bland IM. The acquisition of passive immunity in the new-born piglet. Livest Prod Sci. 2002;78(1):13–23.

480. Amimo JO, Michael H, Chepngeno J, Jung K, Raev SA, Paim FC, et al. Maternal immunization and vitamin A sufficiency impact sow primary adaptive immunity and passive protection to nursing piglets against porcine epidemic diarrhea virus infection. Front Immunol. 2024;15.

481. Langel SN, Wang Q, Vlasova AN, Saif LJ. Host Factors Affecting Generation of Immunity Against Porcine Epidemic Diarrhea Virus in Pregnant and Lactating Swine and Passive Protection of Neonates. Pathogens. 2020;9(2):130.

482. Langel SN, Paim FC, Lager KM, Vlasova AN, Saif LJ. Lactogenic immunity and vaccines for porcine epidemic diarrhea virus (PEDV): Historical and current concepts. Virus Research. 2016;226:93–107.

483. Poonsuk K, Zhang J, Chen Q, Gonzalez W, da Silva Carrion LC, Sun Y, et al. Quantifying the effect of lactogenic antibody on porcine epidemic diarrhea virus infection in neonatal piglets. Vet Microbiol. 2016;197:83–92.

484. Zheng D, Wang X, Ju N, Wang Z, Sui L, Wang L, et al. Immune Responses in Pregnant Sows Induced by Recombinant Lactobacillus johnsonii Expressing the COE Protein of Porcine Epidemic Diarrhea Virus Provide Protection for Piglets against PEDV Infection. Viruses. 2022;14(1):7.

485. Song DS, Oh JS, Kang BK, Yang JS, Moon HJ, Yoo HS, et al. Oral efficacy of Vero cell attenuated porcine epidemic diarrhea virus DR13 strain. Res Vet Sci. 2007;82(1):134–40.

486. Zhou Y, Chen C, Chen Y, Liu Z, Zheng J, Wang T, et al. Effect of route of inoculation on innate and adaptive immune responses to porcine epidemic diarrhea virus infection in suckling pigs. Vet Microbiol. 2019;228:83–92.

487. Langel SN, Paim FC, Alhamo MA, Buckley A, Van Geelen A, Lager KM, et al. Stage of Gestation at Porcine Epidemic Diarrhea Virus Infection of Pregnant Swine Impacts Maternal Immunity and Lactogenic Immune Protection of Neonatal Suckling Piglets. Front Immunol. 2019;10:727.

488. Clement T, Singrey A, Lawson S, Okda F, Nelson J, Diel D, et al. Measurement of neutralizing antibodies against porcine epidemic diarrhea virus in sow serum, colostrum, and milk samples and in piglet serum samples after feedback. J Swine Health Prod. 2016;24(3).

489. Song Q, Stone S, Drebes D, Greiner LL, Dvorak CMT, Murtaugh MP. Characterization of anti-porcine epidemic diarrhea virus neutralizing activity in mammary secretions. Virus Res. 2016;226:85–92.

490. Langel SN, Paim FC, Alhamo MA, Lager KM, Vlasova AN, Saif LJ. Oral vitamin A supplementation of porcine epidemic diarrhea virus infected gilts enhances IgA and lactogenic immune protection of nursing piglets. Vet Res. 2019;50(1):101.

491. Gillespie T, Song Q, Inskeep M, Stone S, Murtaugh MP. Effect of Booster Vaccination with Inactivated Porcine Epidemic Diarrhea Virus on Neutralizing Antibody Response in Mammary Secretions. Viral Immunol. 2018;31(1):62–8.

492. Bowman AS, Nolting JM, Nelson SW, Bliss N, Stull JW, Wang Q, et al. Effects of disinfection on the molecular detection of porcine epidemic diarrhea virus. Vet Microbiol. 2015;179(3–4):213–8.

493. Chen J, Zhang C, Liu Y, Liu G. Super-oxidized water inactivates major viruses circulating in swine farms. J Virol Methods. 2017;242:27–9.

494. Baker KL, Thomas PR, Karriker LA, Ramirez A, Zhang J, Wang C, et al. Evaluation of an accelerated hydrogen peroxide disinfectant to inactivate porcine epidemic diarrhea virus in swine feces on aluminum surfaces under freezing conditions. BMC Vet Res. 2017;13(1):372.

495. Baker KL, Mowrer CL, Zhang J, Chen Q, Ramirez A, Wang C, et al. Evaluation of a peroxygen-based disinfectant for inactivation of porcine epidemic diarrhea virus at low temperatures on metal surfaces. Vet Microbiol. 2018;214:99–107.

496. Jung K, Ha Y, Ha SK, Kim J, Choi C, Park HK, et al. Identification of porcine circovirus type 2 in retrospective cases of pigs naturally infected with porcine epidemic diarrhoea virus. Vet J. 2006;171(1):166–8.

497. Park JE. Porcine Epidemic Diarrhea: Insights and Progress on Vaccines. Vaccines. 2024;12(2):212.

498. Lee S, Lee C. Outbreak-related porcine epidemic diarrhea virus strains similar to US strains, South Korea, 2013. Emerg Infect Dis. 2014;20(7):1223–6.

499. Oh J, Lee KW, Choi HW, Lee C. Immunogenicity and protective efficacy of recombinant S1 domain of the porcine epidemic diarrhea virus spike protein. Arch Virol. 2014;159(11):2977–87.

500. Lee S, Kim Y, Lee C. Isolation and characterization of a Korean porcine epidemic diarrhea virus strain KNU-141112. Virus Res. 2015;208:215–24.

501. Kim SH, Lee JM, Jung J, Kim IJ, Hyun BH, Kim HI, et al. Genetic characterization of porcine epidemic diarrhea virus in Korea from 1998 to 2013. Arch Virol. 2015;160(4):1055–64.

502. Xue M, Zhao J, Ying L, Fu F, Li L, Ma Y, et al. IL-22 suppresses the infection of porcine enteric coronaviruses and rotavirus by activating STAT3 signal pathway. Antiviral Res. 2017;142:68–75.

503. Li Y, Wu Q, Jin Y, Yang Q. Antiviral activity of interleukin-11 as a response to porcine epidemic diarrhea virus infection. Vet Res. 2019;50(1):111.

504. Yuan C, Jin Y, Li Y, Zhang E, Zhang P, Yang Q. PEDV infection in neonatal piglets through the nasal cavity is mediated by subepithelial CD3+ T cells. Vet Res. 2021;52(1):26.

505. Li J, Li Y, Liu P, Wang X, Ma Y, Zhong Q, et al. Porcine Epidemic Diarrhea Virus Infection Disrupts the Nasal Endothelial Barrier To Favor Viral Dissemination. J Virol. 2022;96(9):e00380-22.

506. Okonechnikov K, Golosova O, Fursov M, UGENE team. Unipro UGENE: a unified bioinformatics toolkit. Bioinformatics. 2012;28(8):1166–7.

507. Anisimova M, Gascuel O. Approximate likelihood-ratio test for branches: A fast, accurate, and powerful alternative. Syst Biol. 2006;55(4):539–52.

508. Wen F, Yang J, Li A, Gong Z, Yang L, Cheng Q, et al. Genetic characterization and phylogenetic analysis of porcine epidemic diarrhea virus in Guangdong, China, between 2018 and 2019. PLoS One. 2021;16(6):e0253622.

509. Karte C, Platje N, Bullermann J, Beer M, Höper D, Blome S. Re-emergence of porcine epidemic diarrhea virus in a piglet-producing farm in northwestern Germany in 2019. BMC Vet Res. 2020;16(1):329.

510. Blázquez E, Pujols J, Segalés J, Rodríguez C, Campbell J, Russell L, et al. Estimated quantity of swine virus genomes based on quantitative PCR analysis in spray-dried porcine plasma samples collected from multiple manufacturing plants. PLoS One. 2022;17(5):e0259613.

511. Uzal FA, Plattner BL, Hostetter JM. Alimentary System. Jubb, Kennedy & Palmer's Pathology of Domestic Animals. 2016;2:1–257.

512. Stadler J, Moser L, Numberger J, Rieger A, Strutzberg-Minder K, Stellberger T, et al. Investigation of three outbreaks of Porcine Epidemic Diarrhea in Germany in 2016 demonstrates age dependent differences in the development of humoral immune response. Prev Vet Med. 2018;150:93–100.

513. López-Figueroa C, Cano E, Navarro N, Pérez-Maíllo M, Pujols J, Núñez JI, et al. Clinical, Pathological and Virological Outcomes of Tissue-Homogenate-Derived and Cell-Adapted Strains of Porcine Epidemic Diarrhea Virus (PEDV) in a Neonatal Pig Model. Viruses. 2024;16(1):44.

514. Wang S, Wu J, Wang F, Wang H, Wu Z, Wu S, et al. Expression Pattern Analysis of Antiviral Genes and Inflammatory Cytokines in PEDV-Infected Porcine Intestinal Epithelial Cells. Front Vet Sci. 2020;7:75.

515. Xu X, Zhang H, Zhang Q, Huang Y, Dong J, Liang Y, et al. Porcine epidemic diarrhea virus N protein prolongs S-phase cell cycle, induces endoplasmic reticulum stress, and up-regulates interleukin-8 expression. Vet Microbiol. 2013;164(3):212–21.

516. Zhang Y, Chen H, Yu J, Feng R, Chen Z, Zhang X, et al. Comparative transcriptomic analysis of porcine epidemic diarrhea virus epidemic and classical strains in IPEC-J2 cells. Vet Microbiol. 2022;273:109540.

517. Dotti I, Bonin S, Basili G, Nardon E, Balani A, Siracusano S, et al. Effects of formalin, methacarn, and fineFIX fixatives on RNA preservation. Diagn Mol Pathol. 2010;19(2):112–22.

518. Wang Z, Li X, Shang Y, Wu J, Dong Z, Cao X, et al. Rapid differentiation of PEDV wild-type strains and classical attenuated vaccine strains by fluorescent probe-based reverse transcription recombinase polymerase amplification assay. BMC Vet Res. 2020;16(1):208.

519. Ballester M, Cordón R, Folch JM. DAG Expression: High-Throughput Gene Expression Analysis of Real-Time PCR Data Using Standard Curves for Relative Quantification. PLoS One. 2013;8(11):e80385.

520. Liu S, Liu S, Yu Z, Zhou W, Zheng M, Gu R, et al. STAT3 regulates antiviral immunity by suppressing excessive interferon signaling. Cell Rep. 2023;42(7):112806.

521. Krausgruber T, Blazek K, Smallie T, Alzabin S, Lockstone H, Sahgal N, et al. IRF5 promotes inflammatory macrophage polarization and TH1-TH17 responses. Nat Immunol. 2011;12(3):231–8.

522. Weiss M, Blazek K, Byrne AJ, Perocheau DP, Udalova IA. IRF5 is a specific marker of inflammatory macrophages in vivo. Mediators Inflamm. 2013;2013:245804.

523. Pirhonen J. Regulation of IL-18 Expression in Virus Infection. Scand J Immunol. 2001;53(6):533–9.

524. Rex DAB, Agarwal N, Prasad TSK, Kandasamy RK, Subbannayya Y, Pinto SM. A comprehensive pathway map of IL-18-mediated signalling. J Cell Commun Signal. 2020;14(2):257–66.

525. Arend WP, Guthridge CJ. Biological role of interleukin 1 receptor antagonist isoforms. Ann Rheum Dis. 2000;59(suppl 1):i60–4.

526. Neila-Ibáñez C, Brogaard L, Pailler-García L, Martínez J, Segalés J, Segura M, et al. Piglet innate immune response to Streptococcus suis colonization is modulated by the virulence of the strain. Vet Res. 2021;52(1):145.

527. Chen JS, Alfajaro MM, Chow RD, Wei J, Filler RB, Eisenbarth SC, et al. Nonsteroidal Anti-inflammatory Drugs Dampen the Cytokine and Antibody Response to SARS-CoV-2 Infection. J Virol. 2021;95(7).

528. Mohammed A, Kalle AM, Reddanna P. Managing SARS-CoV2 Infections Through Resolution of Inflammation by Eicosanoids: A Review. J Inflamm Res. 2022;15:4349–58.

529. Rahman MS, Hossain MS. Eicosanoids Signals in SARS-CoV-2 Infection: A Foe or Friend. Mol Biotechnol. 2023;66(11):3025–41.

530. Ricke-Hoch M, Stelling E, Lasswitz L, Gunesch AP, Kasten M, Zapatero-Belinchón FJ, et al. Impaired immune response mediated by prostaglandin E2 promotes severe COVID-19 disease. PLoS One. 2021;16(8):e0255335.

531. Wong LYR, Zheng J, Wilhelmsen K, Li K, Ortiz ME, Schnicker NJ, et al. Eicosanoid signalling blockade protects middle-aged mice from severe COVID-19. Nature. 2022;605(7908):146–51.

532. Lee C, Kim Y, Jeon JH. JNK and p38 mitogen-activated protein kinase pathways contribute to porcine epidemic diarrhea virus infection. Virus Research. 2016;222:1–12.

533. Battle TE, Frank DA. The Role of STATs in Apoptosis. Curr Mol Med. 2002;2(4):381–92.

534. Dai Z, Liu WC, Chen XY, Wang X, Li JL, Zhang X. Gasdermin D-mediated pyroptosis: mechanisms, diseases, and inhibitors. Front Immunol. 2023;14:1178662.

535. Tsuchiya K, Nakajima S, Hosojima S, Thi Nguyen D, Hattori T, Manh Le T, et al. Caspase-1 initiates apoptosis in the absence of gasdermin D. Nat Commun. 2019;10(1):2091.

536. Alsved M, Fraenkel CJ, Bohgard M, Widell A, Söderlund-Strand A, Lanbeck P, et al. Sources of Airborne Norovirus in Hospital Outbreaks. Clin Infect Dis. 2020;70(10):2023–8.

537. Obregon-Gutierrez P, Bonillo-Lopez L, Correa-Fiz F, Sibila M, Segalés J, Kochanowski K, et al. Gut-associated microbes are present and active in the pig nasal cavity. Sci Rep. 2024;14(1):8470.

538. Keep S, Carr BV, Lean FZX, Fones A, Newman J, Dowgier G, et al. Porcine Respiratory Coronavirus as a Model for Acute Respiratory Coronavirus Disease. Front Immunol. 2022;13:867707.

539. Deshmukh V, Motwani R, Kumar A, Kumari C, Raza K. Histopathological observations in COVID-19: a systematic review. J Clin Pathol. 2021;74(2):76–83.

540. Lee HM, Lee BJ, Tae JH, Kweon CH, Lee YS, Park JH. Detection of porcine epidemic diarrhea virus by immunohistochemistry with recombinant antibody produced in phages. J Vet Med Sci. 2000;62(3):333–7.

541. Bonillo-Lopez L, Carmona-Vicente N, Tarrés-Freixas F, Kochanowski K, Martínez J, Perez M, et al. Porcine Nasal Organoids as a model to study the interactions between the swine nasal microbiota and the host. bioRxiv. 2024;606910.

542. Rodon J, Sachse M, Te N, Segalés J, Bensaid A, Risco C, et al. Middle East respiratory coronavirus (MERS-CoV) internalized by llama alveolar macrophages does not result in virus replication or induction of pro-inflammatory cytokines. Microbes Infect. 2024;26(3):105252.

543. Park SJ, Moon HJ, Luo Y, Kim HK, Kim EM, Yang JS, et al. Cloning and further sequence analysis of the ORF3 gene of wild- and attenuated-type porcine epidemic diarrhea viruses. Virus Genes. 2008;36(1):95–104.

544. Zhang YH, Li HX, Chen XM, Zhang LH, Zhao YY, Luo AF, et al. Genetic Characteristics and Pathogenicity of a Novel Porcine Epidemic Diarrhea Virus with a Naturally Occurring Truncated ORF3 Gene. Viruses. 2022;14(3):487.

545. Lu Y, Huang W, Zhong L, Qin Y, Liu X, Yang C, et al. Comparative Characterization and Pathogenicity of a Novel Porcine Epidemic Diarrhea Virus (PEDV) with a Naturally Occurring Truncated ORF3 Gene Coinfected with PEDVs Possessing an Intact ORF3 Gene in Piglets. Viruses. 2021;13(8):1562.

546. Li M, Guo L, Feng L. Interplay between swine enteric coronaviruses and host innate immune. Front Vet Sci. 2022;9:1083605.

547. Murch SH SH. Common determinants of severe Covid-19 infection are explicable by SARS-CoV-2 secreted glycoprotein interaction with the CD33-related Siglecs, Siglec-3 and Siglec-5/14. Med Hypotheses. 2020;144:110168.

548. Perez-Zsolt D, Muñoz-Basagoiti J, Rodon J, Elosua-Bayes M, Raïch-Regué D, Risco C, et al. SARS-CoV-2 interaction with Siglec-1 mediates trans-infection by dendritic cells. Cell Mol Immunol. 2021;18(12):2676–8.

SUPPLEMENTARY MATERIAL

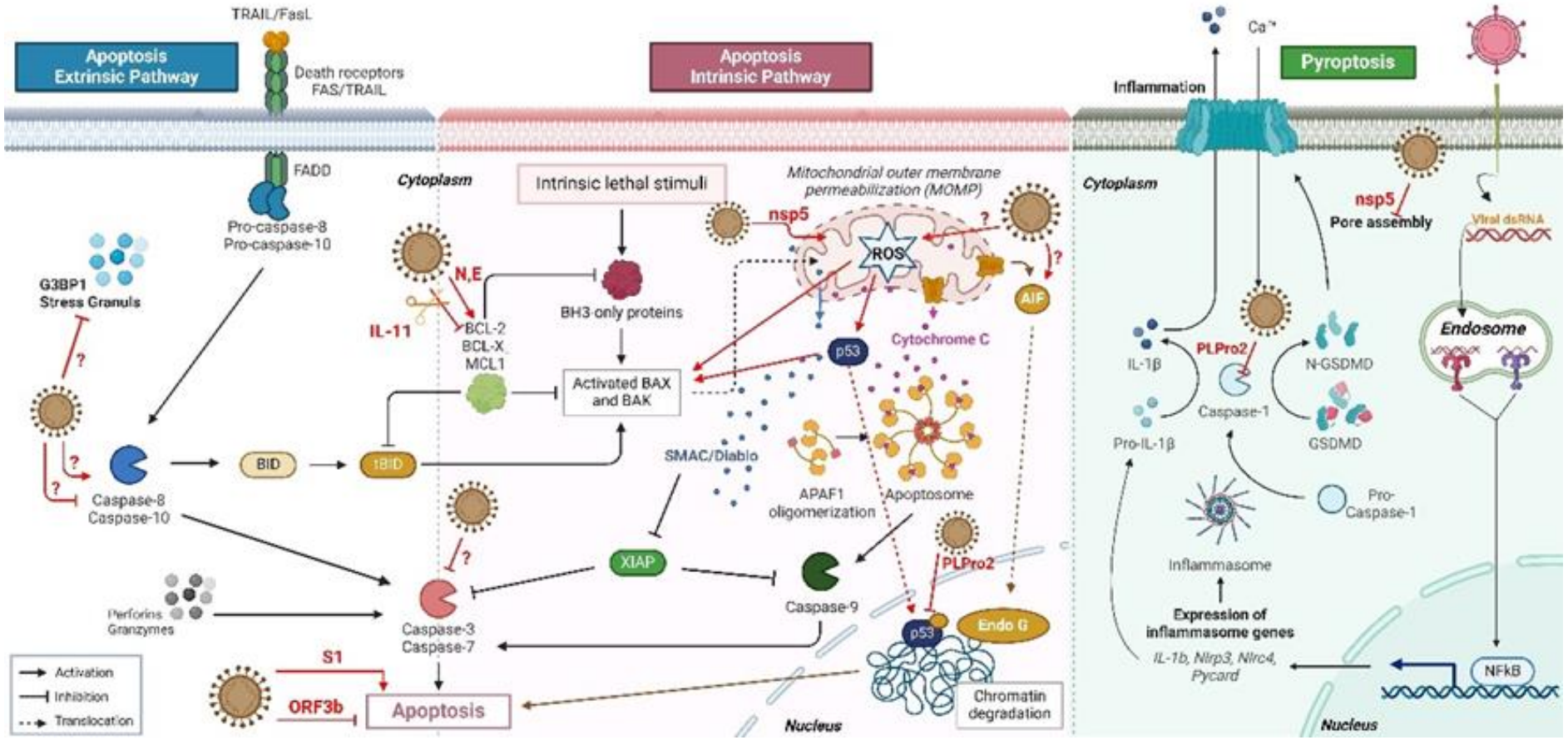

Supplementary Figure 1. Mechanisms employed by PEDV to regulate apoptosis and pyroptosis. Both mechanisms of programmed cell death can promote viral release and spread in the late stages of infection, while their inhibition during the early phase prevents premature cell death, allowing PEDV to replicate. PEDV utilizes various mechanisms (highlighted in red) to modulate intrinsic and extrinsic apoptosis, as well as pyroptosis, at different stages of infection to ensure efficient viral proliferation. These strategies are primarily governed by structural proteins (S1, N, E), ORF3, and nsp 3 and 5, while some remain linked to unknown mechanisms (indicated by a question mark). The anti-apoptotic function triggered by IL-11 is mediated through the IL-11/STAT3 signaling pathway, counteracting (represented by scissors) one of the mechanisms PEDV has developed to induce apoptosis. Created with BioRender.com

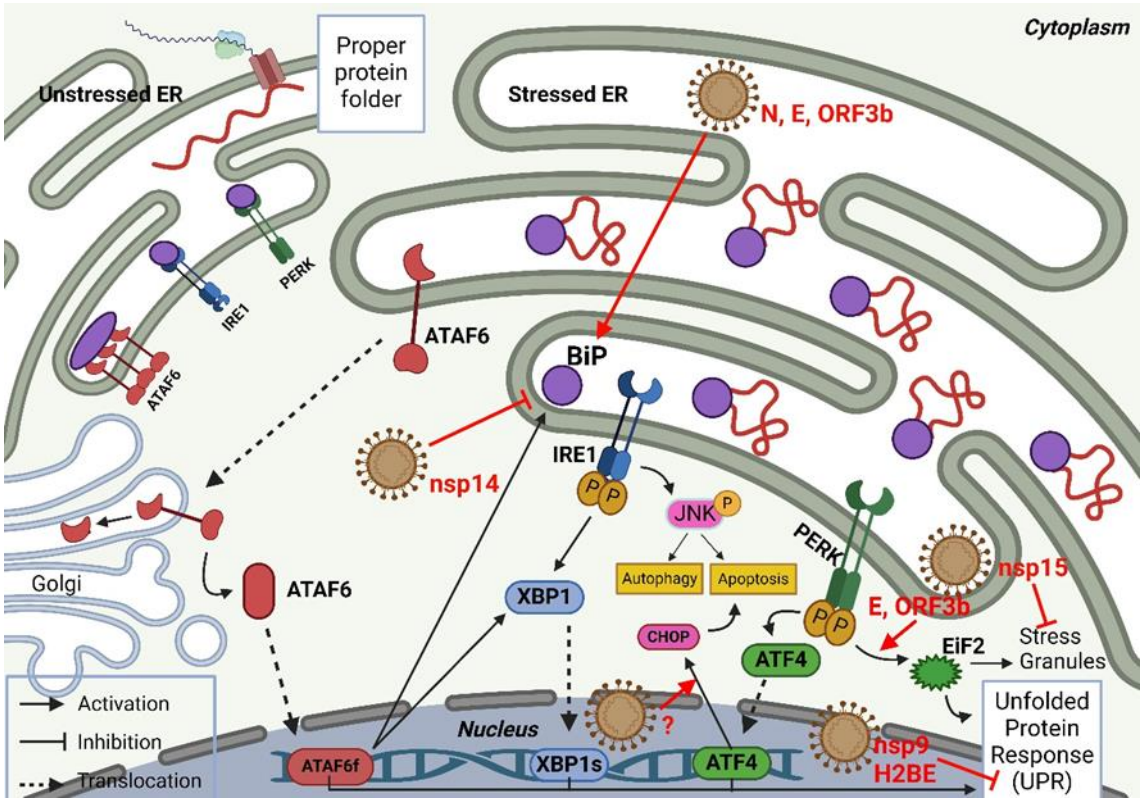

Supplementary Figure 2. Mechanisms employed by PEDV to modulate endoplasmic reticulum stress (ER stress). During the PEDV life cycle, the ER membrane becomes progressively depleted, leading to disruptions in its morphology and function. This depletion causes increased ER stress, which triggers a series of coordinated responses collectively referred to as the UPR to restore ER homeostasis. However, if the damage persists and remains unresolved, the cell may undergo death by apoptosis or autophagy. PEDV has developed multiple strategies to regulate these processes of cell death at different stages of infection by modulating key sensors of ER stress, including PERK/eIF2α, ATF6, and inositol-requiring transmembrane kinase/endonuclease 1 (IRE1), along with the GRP78 or BiP. These mechanisms (indicated in red) are regulated by structural proteins (N, E), ORF3, and nsp 9, 14, and 15. Created with BioRender.com

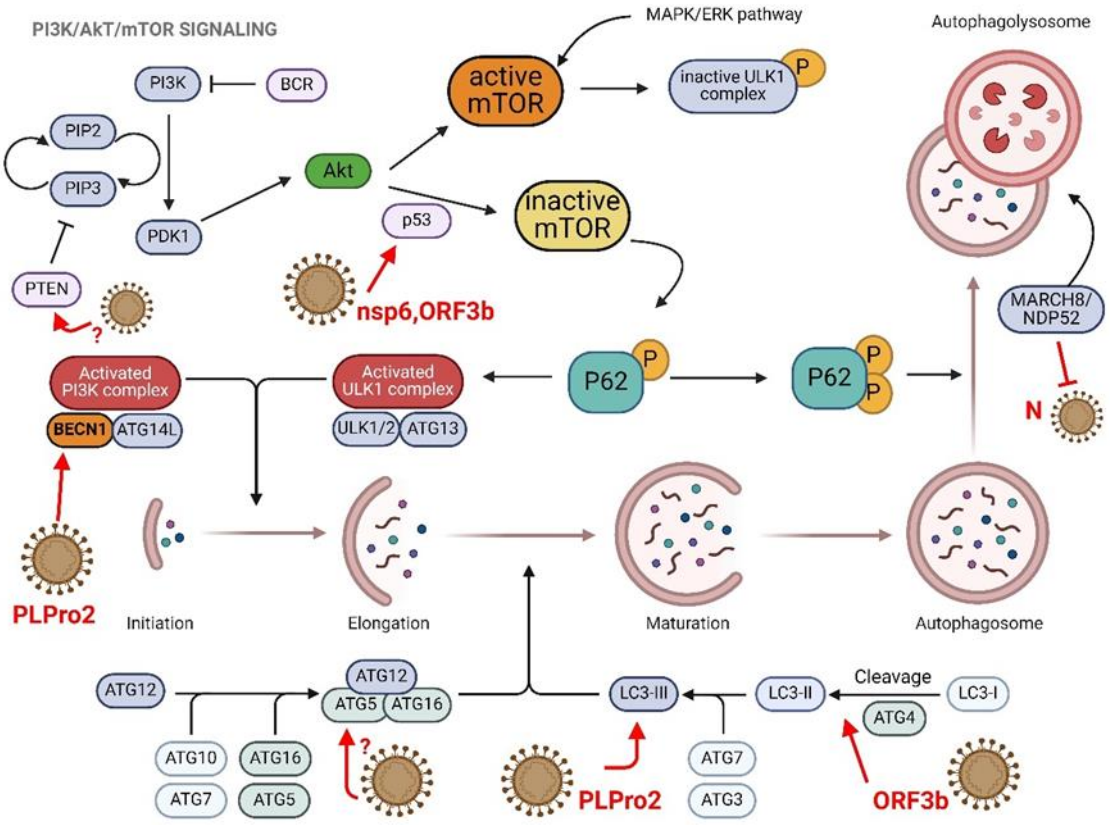

Supplementary Figure 3. Mechanisms employed by PEDV to modulate Autophagy. Autophagy is essential for maintaining cellular homeostasis and plays a vital role in the immune response against viral infections by preventing viral replication and promoting the death of infected cells. PEDV has developed various strategies (indicated in red) to modulate autophagy to enhance viral replication. This is achieved through the regulation of the PI3K/Akt/mTOR signaling pathway and key autophagy markers, including ATGs, ULK1 protein kinase, the LC3 conjugation system, the adapter protein p62/SQSTM1, ubiquitinated proteins, and BECN1. These mechanisms are primarily regulated by structural proteins (N), ORF3, and nsp 3, and 6, while some remain linked to unknown mechanisms (indicated by a question mark). Created with BioRender.com

Acknowledgments

La primera vez que puse un pie en el CReSA fue en julio de 2017, hace ya ocho años. Mi tesis doctoral ha ocupado los últimos cuatro años de mi vida, por lo que con estas páginas no solo concluyo un trabajo enorme, sino que también pongo fin a una etapa muy importante de mi vida. Podéis imaginar la cantidad de personas que han formado parte de este proceso a lo largo de todos estos años. Así que, si me olvido de mencionar a alguien, os pido disculpas de antemano. Seas quien seas, estoy seguro de que sabes cuánto te lo agradezco, incluso si tu nombre no aparece aquí.

Para empezar, no podría hacerlo de otra forma que agradeciéndotelo a ti, **Sergio**. Resulta irónico lo poco que coincidimos y lo mucho que dejaste en mí. Fuiste mi primer jefe, y eso es algo que nunca se olvida. De ti me llevo muchas cosas, pero sobre todo un recuerdo imborrable y un agradecimiento que no tiene límites. Jamás supiste decir que no a mis propuestas, y eso te llevó a darme la oportunidad que más deseaba: me apoyaste cuando te pedí abrir una plaza de residencia en patología veterinaria en colaboración con la UAB. En ese momento me demostraste lo que significa ser un buen jefe y, aún más importante, un gran compañero. Simplemente, gracias por permitirme cumplir mi sueño profesional.

Aquí también debo mencionar a **Toni Ramis**, la otra pieza clave del acuerdo por parte de la UAB, que hizo posible el inicio del mejor viaje que he vivido hasta ahora. Gracias por tenderme la mano y enseñarme tanto. Os lo debo todo a los dos.

Los siguientes cuatro años de mi vida transcurrieron de forma maravillosa. ¡Qué buenos años, jolines! Para empezar, tuve la suerte de compartir mi día a día con el mejor equipo de trabajo que jamás podría existir: **Estudis de Camp**. Cuando pienso en vosotros, me viene a la mente una nube de azúcar, por supuesto rosa… ¡vaya fantasía y qué chute de energía sois para mi vida! Necesitaría un libro entero para explicar lo que significáis para mí y cuánto bien habéis aportado a mi despertar "adulto". Gema, Rosa, Diego y Patri, os elegiría una y otra vez como compañeros de vida, de trabajo, de granjas, pero, sobre todo, de despacho. Gracias por convertir esas cuatro paredes en un lugar seguro, una segunda casa a la que siempre querer volver cada mañana con una sonrisa enorme.

Gema, eres una líder excepcional: organizada, proactiva y con una capacidad innata para hacer que gestionar un equipo parezca tarea sencilla. **Patri**, ay, si fueras un hombre… Creo sinceramente que muchas de las cosas que he logrado han sido gracias a tu inagotable ayuda.

Podría decir, sin miedo a equivocarme, que eres la mejor compañera que nadie podría soñar. No cambies nunca, por favor. No tienes idea de cuánto te recordaré allá donde esté y necesite un apoyo externo. **Diego**, sinceramente, me has hecho mejor en todos los aspectos. Dicen que una imagen vale más que mil palabras, y quiero que sepas que me llevo miles de recuerdos compartidos contigo. Espero que todas esas imágenes y estas dos palabras te demuestren lo que significas para mí: Te quiero. **Rosa**, si tuviera que escribir mi vida, tú tendrías un capítulo propio. Empezaría explicando cuánto valoro tu apoyo constante, continuaría agradeciéndote nuestras tertulias interminables y terminaría recordando las miles de horas que pasaste al teléfono cuando más necesité ayuda. Eso eres tú: una fuente infinita de bondad y compañerismo. Me hace inmensamente feliz verte sonreír. No sabes lo afortunados que somos los que podemos tenerte cerca.

Durante esta etapa, otras personas dejaron una huella profunda, tanto que su impacto en mi vida es imborrable. **Montse Ordoñez**, jamás imaginé que alguien lograría poner orden en mi descontrolada manera de hacer y organizarme. Mucho menos que esa persona me haría ver lo valioso que es tener a alguien que te ayude en ese proceso. Créeme, te recuerdo mucho, especialmente cuando no sé cómo abordar algo. Siempre pienso: ¿Cómo lo haría Montse? Gracias de corazón, tanto de mi parte como de la de mi madre, que está encantada de que aparecieras en mi vida, jajaja. **Miquel Nofrarias, Rosa Valle, Marina Sibila, Cristina (Bisbal)** y todos los técnicos con los que compartí mi etapa en Estudis de Camp, gracias por todo. Y a ti, **Mónica**, un agradecimiento muy especial… eres puro oro. Si pudiera, te llevaría conmigo allá donde fuera, incluso te clonaría. Tu perfección te define, tanto como persona como profesional. Me has malacostumbrado tanto que no sé cómo me las arreglaré sin ti. Cuánto voy a echarte de menos.

Jamás podría olvidarme de agradecéroslo a vosotros, los grandes protagonistas de mi primera etapa en el CReSA. Me refiero a cada uno de los miembros que formáis el **SDPV** (Servei de Diagnòstic de Patologia Veterinària - UAB). Empezando, por supuesto, por mis compañeros: **Canturri, Gina, Isabel, mi Mary, Berni, Ester, Jaume, Elisa y Álex**. Que quede algo muy claro: soy quien soy gracias a vosotros. Me llena de felicidad ver en lo grandes profesionales en los que os habéis convertido. No cabe más orgullo en mi cuerpo. Siguiendo por MIS NIÑAS MARAVILLOSAS, **Lola, Mar, Aida, y Blanquilla**… Madre mía cuánto os quiero. Dejemos otra cosa bien clara: Vosotras sois el corazón del SDPV. Y finalizando por vosotros, el cerebro del SDPV. **Toni**, ja t'he dit abans com d'important has estat en la meva vida. Sense tu, no sé què seria de mi ara mateix. Que sàpigues que algun dia portaré un grup d'estudiants i tinc molt clar que repetiré el teu procediment de formació fil per randa. L'èxit de la residència de la UAB és, principalment, mèrit

teu. **Alberto**, contra todo pronóstico, puedo asegurarte que eres quien más me ha enseñado. Tu manera de explicar es como recitar un poema; todo lo que sale de tu boca es arte, y ese arte deja huella. **Mariano**, si pudiera elegir revivir un único día en el departamento, sería uno en el que tú estuvieras como responsable de necropsias. Es un auténtico placer escucharte. Ya fuiste un gran profesor durante mi etapa como estudiante, pero no imaginas cuánto influyeron tus horas de formación en mi curva de aprendizaje durante la residencia. **Jorge**, nunca te conté el motivo por el que decidí dedicarme a la patología, pero tu nombre tiene mucho que ver en esa decisión.

Quim... buf, Quim... un altre personatge de la meva història que es mereix un parell de capítols. Quan penso en tu, m'adono de la influència que poden tenir certes persones en la vida dels altres. És evident com m'has influït i tot el que m'has ofert, les portes que m'has ajudat a obrir... i les que encara queden per obrir. Però no em refereixo només a aquest tipus d'influència.

Quan vaig començar el meu camí en patologia, no et coneixia. Molta gent em parlava de tu, però com que mai m'havies fet classe (en aquell moment eres el cap del CReSA), no sabia ni tan sols quina cara feies... tot i que això no va durar gaire, jajaja. Entre totes les teves virtuts, mai deixarà de sorprendre'm el teu poder d'influència sobre els altres. Saps entrar en una habitació i, en menys de vint segons, fer que tothom sàpiga que ja has arribat, com si fossis l'amfitrió de totes les festes.

Hi ha qui t'admira pel teu caràcter, i d'altres ho fan per la teva feina i l'herència que deixes en el món de la sanitat animal. Però jo no t'admiro per cap d'aquests motius. T'admiro per la teva part humana dins del món elitista en què t'has col·locat. És un fet: com més es té, més es vol. Només cal mirar certs grans investigadors, on el més gran que posseeixen és el seu ego i la dificultat de tractar amb ells. Però tu no ets així. Ets tan humà com qualsevol altre. Dones oportunitats a tots aquells joves aspirants que truquen a la teva porta, i els ensenyes a ser la millor versió d'ells mateixos. Sense cap dubte, aquesta és la teva característica més admirable, i és a la que aspiro més en aquesta vida.

Gràcies per ensenyar-m'ho tot i per fer-ho com ho has fet. Ets el millor company i "jefe" que podria haver somiat mai. És curiós, quan analitzo la meva trajectòria, adonar-me del poder que has tingut en ella. El 2017, quan vaig començar, tenia claríssim que volia acabar fent oncopatologia de petits animals. Però després de conèixer-te, he acabat fent infeccioses de porcí... Això és la influència de la qual et parlava, el teu gran poder. No canviïs mai per res del món. Això és el que et diferencia de la resta d'investigadors i el que fa que, any rere any, més estudiants et triïn a tu com a model a seguir.

Finalment, **Natàlia**. A tu et dedicaria el pròleg del meu llibre. O potser series la protagonista si mai escrivís una preqüela sobre la meva vida. Ser veterinari era el meu somni des que vaig descobrir Disney, i es va acabar de confirmar després de conviure amb les meves dues primeres gosses. Però, un cop a la carrera, vaig tenir la meva primera crisi existencial cap a tercer. Ja havia decidit que deixaria els estudis, però llavors vas aparèixer tu.

Aquell any, en què jo estava molt perdut, cursàvem l'assignatura d'anatomia patològica general, on tu ens vas donar oncopatologia. Sempre recordaré aquell dia en què em vas fer canviar per sempre. Em vas donar l'oportunitat de tornar a interessar-me per alguna cosa, em vas donar un motiu per voler continuar. Aquell dia, Natàlia, gràcies a tu, vaig decidir que volia ser professor d'universitat per poder ajudar els estudiants, com un dia tu vas fer amb mi. No sé què seria de mi si aquell dia no haguessis donat aquella classe. Sincerament, vaig ser molt afortunat de tenir-te com a professora.

És curiós com, en la decisió de convertir-me en patòleg, també vas ser fonamental, juntament amb en Jorge. Imagino que no ho recordaràs, però en una de les meves setmanes de necropsies, tu eres la responsable. Aquell dia ens va tocar un poltre que havia mort causant molts maldecaps al departament d'èquids. Encara recordo com, només mirant el múscul del cavall, ja tenies claríssim de què havia mort, sense cap altra prova més que els teus ulls. Em vas semblar una mena de divinitat rossa… quina fantasia de persona amb aquella melena! Jo ja només volia ser com tu. En algunes coses, a poc a poc, ho estic aconseguint, però pel que fa al cabell... bé, en una altra vida, jajaja.

Gràcies, Natàlia, per inspirar-me, per donar-me un objectiu, per ensenyar-me tot el que sé de patologia, però sobretot, per mostrar-me el camí que vull seguir. Mai a la vida podré agrair-te prou el teu suport infinit durant els mesos d'estudi de l'examen… gràcies per agafar-me el telèfon i calmar-me. Era l'únic que necessitava, i tu sempre hi eres. Ets el meu gran referent a la vida.

Finalmente, doy paso a mi última etapa en el CReSA, la tesis doctoral. Vaya añitos, Maricarmeeen. ¿Pero en qué momento? Jaja. Siendo consciente de que era algo necesario para alcanzar mi objetivo, he de admitir que, a veces, la vida resulta realmente injusta. Sin embargo, incluso en esos momentos "duros", la vida te ofrece un pequeño dulce que hace que el camino sea más llevadero. En esta etapa, me quedo con todos aquellos que habéis aparecido para endulzarme estos años, y que, sin vosotros, NO HABRÍA PODIDO TERMINAR, NI DE BROMA. Si bien es cierto que he aprendido mucho sobre ciencia, la lección más valiosa que me llevo de esta etapa es mucho más profunda y tiene que ver con lo esencial que es rodearte de las personas adecuadas cuando realmente lo necesitas.

La primera lección: escoge bien a tu equipo, porque no sabes ni cuándo ni cómo podrán ayudarte. Este equipo tiene dos grandes protagonistas que han sido los motores de todo este proyecto, y sin ellas, esto no habría sido más que una ilusión frustrada. **Esmeralda y Nuria Navarro**, necesitaría varias vidas para encontrar las palabras que os hagan justicia. Habéis sido mi pilar en esta carrera a contraviento. Gracias por abrigarme y, sobre todo, por aguantarme. Esta tesis es tan vuestra como mía. Os quiero de una forma incondicional.

La segunda lección: ándate acompañado. Juntos, la luz al final del túnel se hace visible mucho más rápido. Si algo agradezco de esta etapa es de haber coincidido con vosotros: **María, Carla Usai, Carla Ruiz, Albert Burgas, Laura, Judith, David, Nuria Roca, Cris Lorca**. Es hermoso ver cómo las personas somos capaces de transmitirnos fortaleza e incluso seguridad cuando más lo necesitamos. Me hace tremendamente feliz haberos encontrado y haber compartido este camino a vuestro lado. A algunos de vosotros os considero amigos realmente importantes, y, a pesar de todo, solo por haberos conocido ya ha valido la pena.

Com no podia ser d'altra manera, no puc acabar aquests agraïments sense dedicar-te unes paraules, **my lady princess, la bichota**, jajaja. Quan penso en tu, m'adono que la vida no deixa de sorprendre'm. Ens pensem que, pel fet d'haver rebut una educació determinada o haver crescut en un entorn concret, estem destinats a conviure amb certes persones i que amb altres no tenim res en comú. La nostra relació m'ha ensenyat que, si deixéssim que els judicis de valor que fem de les persones d'entrada determinessin qui pot o no compartir el nostre camí, tu i jo segurament no hauríem pogut conviure i m'hauria perdut l'oportunitat de tenir una gran amiga. Mira que som diferents, mare mevaaaa… Tot i així, cada dia dono gràcies per aquestes diferències i per com han consolidat una relació tan bonica i sana com la nostra. **Leira**, la vida em va fer un regal posant-te com a companya d'equip. Un regal que no té preu i que, si en tingués, seria incalculable. No saps com anyoro cada dia que vam conviure.

Per últim, i no per això menys important, la gran protagonista d'aquesta última etapa: **Júlia**. Com ja has pogut veure, durant aquests últims 8 anys he estat envoltat de gent increïble, però tu vas aparèixer per sorpresa en els darrers 4, just al final. Per això puc assegurar que, com bé diuen els refranys, el millor sempre arriba al final. No només m'has ensenyat tot el que sé sobre la part molecular del diagnòstic, sinó que també m'has mostrat què significa ser un bon referent: com respectar, com parlar i com dirigir-se a aquells que depenen de tu. Però, sobretot, m'has deixat opinar i prendre decisions. M'has donat l'espai per créixer a través de les meves pròpies hipòtesis i, quan he fracassat, m'has recollit i hem refet el camí junts, deixant-me sempre ser jo qui fes el primer pas. De tu extrec la tercera i última lliçó d'aquesta etapa: si vols que la gent aprengui de

veritat, deixa'ls provar. Un bon líder no imposa. Gràcies per deixar-me fer ciència, per escoltar les meves propostes, per donar-me l'espai que he necessitat, per atendre'm quan necessitava parlar i per posar-te la bata quan he necessitat ajuda.

M'encanta la relació que hem construït, basada en el respecte mutu i l'admiració. Però el que més valoro és que m'hagis permès accedir a tu i m'hagis donat l'oportunitat de considerar-te molt més que la meva cap. Estic segur que, en un futur, la nostra relació perdurarà. Sé que aquesta no acabarà amb la tesi, i això és el que em fa més feliç d'aquesta última etapa.

Para finalizar, quiero expresar mi más profundo agradecimiento a los de siempre, mi fortaleza. **Papás**, qué suerte tengo de teneros. Sé que no debe haber sido fácil, pero dejadme deciros algo: habéis hecho un trabajo increíble. Solo aspiro a hacerlo un 5% tan bien como lo hicisteis vosotros, y con eso ya sería un éxito rotundo. Sin vuestro apoyo, estos últimos años hubieran sido imposibles de sobrellevar. Los padres sois quienes hacen posible que los jóvenes investigadores puedan seguir haciendo ciencia en este país. Gracias por vuestra ayuda y vuestro amor incondicional. **Herman**, me inspiras cada día. Me encanta verte crecer. Si cuidas de los tuyos como lo haces conmigo, sé que les ofrecerás un lugar seguro, lleno de protección y cariño. **Laia**, quan penso en l'amor, el sentiment que més s'hi assembla té la teva essència. Si algú creu que l'amistat és només un premi de consolació, s'equivoca; és la forma més pura i sincera d'amor. No sé si algun dia viuré un amor diferent, però puc assegurar que tu has estat el gran amor de la meva vida. **Àlex, Octavi, Isaac, Goñi, Gala, Memé** i tots els altres amics de la universitat (vosaltres sabeu qui sou), gràcies per ser-hi sempre, per sostenir-me en els moments difícils i compartir amb mi els bons. Us estimo infinitament.